National Library of Canada
Bibliothèque nationale du Canada

Canadian Theses Service
Service des thèses canadiennes

Ottawa, Canada
K1A 0N4

NOTICE

The quality of this microform is heavily dependent upon the quality of the original thesis submitted for microfilming. Every effort has been made to ensure the highest quality of reproduction possible.

If pages are missing, contact the university which granted the degree.

Some pages may have indistinct print especially if the original pages were typed with a poor typewriter ribbon or if the university sent us an inferior photocopy.

Previously copyrighted materials (journal articles, published tests, etc.) are not filmed.

Reproduction in full or in part of this microform is governed by the Canadian Copyright Act, R.S.C. 1970, c. C-30.

AVIS

La qualité de cette microforme dépend grandement de la qualité de la thèse soumise au microfilmage. Nous avons tout fait pour assurer une qualité supérieure de reproduction.

S'il manque des pages, veuillez communiquer avec l'université qui a conféré le grade.

La qualité d'impression de certaines pages peut laisser à désirer, surtout si les pages originales ont été dactylographiées à l'aide d'un ruban usé ou si l'université nous a fait parvenir une photocopie de qualité inférieure.

Les documents qui font déjà l'objet d'un droit d'auteur (articles de revue, tests publiés, etc.) ne sont pas microfilmés.

La reproduction, même partielle, de cette microforme est soumise à la Loi canadienne sur le droit d'auteur, SRC 1970, c. C-30.

NL-339 (r. 88/04)

Canadä

THE UNIVERSITY OF ALBERTA

A HYDROGEOLOGICAL INVESTIGATION OF THE ORIGIN OF SALINE SOILS AT BLACKSPRING RIDGE, SOUTHERN ALBERTA

BY

RICHARD STEIN

A THESIS

SUBMITTED TO THE FACULTY OF GRADUATE STUDIES AND RESEARCH

IN PARTIAL FULFILMENT OF THE REQUIREMENTS FOR THE DEGREE

OF MASTER OF SCIENCE

DEPARTMENT OF GEOLOGY

EDMONTON, ALBERTA

FALL, 1987

Permission has been granted to the National Library of Canada to microfilm this thesis and to lend or sell copies of the film.

The author (copyright owner) has reserved other publication rights, and neither the thesis nor extensive extracts from it may be printed or otherwise reproduced without his/her written permission.

L'autorisation a été accordée à la Bibliothèque nationale du Canada de microfilmer cette thèse et de prêter ou de vendre des exemplaires du film.

L'auteur (titulaire du droit d'auteur) se réserve les autres droits de publication; ni la thèse ni de longs extraits de celle-ci ne doivent être imprimés ou autrement reproduits sans son autorisation écrite.

ISBN 0-315-41007-8

THE UNIVERSITY OF ALBERTA

RELEASE FORM

NAME OF AUTHOR: Richard Stein

TITLE OF THESIS: A Hydrogeological Investigation of the Origin of Saline Soils at Blackspring Ridge, Southern Alberta

DEGREE: Master of Science

YEAR THIS DEGREE GRANTED: Fall, 1987

Permission is hereby granted to THE UNIVERSITY OF ALBERTA LIBRARY to reproduce single copies of this thesis and to lend or sell such copies for private, scholarly or scientific research purposes only.

The author reserves other publication rights, and neither the thesis nor extensive extracts from it may be printed or otherwise reproduced without the author's written permission.

(signed) Richard Stein

(permanent address) 736 - Lee Ridge Rd.
Edmonton, Alberta
T6K 0P2

Date: Oct. 13 / 87

THE UNIVERSITY OF ALBERTA

FACULTY OF GRADUATE STUDIES AND RESEARCH

The undersigned certify that they have read, and recommend to the Faculty of Graduate Studies and Research for acceptance, a thesis entitled A HYDROGEOLOGICAL INVESTIGATION OF THE ORIGIN OF SALINE SOILS AT BLACKSPRING RIDGE, SOUTHERN ALBERTA submitted by Richard Stein in partial fulfilment of the requirements for the degree of MASTER OF SCIENCE.

....
(Supervisor)

....

....

....

Date: Sept 28, 1987

ABSTRACT

Soil salinity occurs in a variety of topographic settings and has a broad range of severity in the Blackspring Ridge area of Southern Alberta. Blackspring Ridge is a structural bedrock high that is underlain by upper Cretaceous sediment of the Horseshoe Canyon Formation. Bedrock is overlain by stratified, till, lacustrine, and aeolean sediment whose thickness ranges from about 2 m on top of the ridge to 110 m within buried valleys located west and north of the ridge.

Piezometric data indicate that groundwater is recharged on and along upper flanks of Blackspring Ridge and discharges in southern parts of a lacustrine plain that surrounds the ridge. Regional groundwater flow is strongly influenced by basal sandstone of the Horseshoe Canyon Formation and by highly permeable sand and gravel sediment in the buried valleys. The bedrock valleys act as line sinks, transmit most groundwater along their axes, and cause predominantly downward flow in northern parts of the lacustrine plain.

Local groundwater flow is strongly influenced by bedrock fracturing to a depth of about 30 m along the west flank of the ridge. Hydraulic conductivity data, water-level fluctuations, stable isotopes, and hydrochemical data indicate that the fractured near-surface bedrock and overlying thin drift sediment constitutes a zone of active groundwater flow within which salts are generated and transported, and from which they eventually discharge to saline areas at the base of the ridge. The zone of active flow contains by far the dominant salt load, and has a TDS content from 6000 to more than 50 000 mg/L. Salt fluxes that exceed

2 kg/m^2/year exist in areas where groundwater from the active-flow zone discharges to the water table.

High water tables in saline areas are maintained by infiltration from runoff of snowmelt, rain, and groundwater discharge. Surface runoff water of the spring-melt event assimilates up to 500 mg/L of salt as it traverses saline groundwater discharge areas along the flanks and base of Blackspring Ridge. This water and dissolved salt is the primary cause of salinity in low-lying portions of the lacustrine plain.

ACKNOWLEDGEMENTS

The author extends sincere appreciation to Dr. F.W. Schwartz for his patience, constructive criticism, and helpful suggestions. The suggestions for improvement and constructive criticism of the examination committee are also gratefully acknowledged. Dr. S. Moran of the Alberta Reserach Council reviewed a draft version of this thesis; his effort and thoughtful suggestions are much appreciated. The concept to study the hydrogeology associated with soil salinity has long been a favorite idea of Dr. J. Toth. His years of leadership by example provided motivation and inspiration for which the author will always be indebted.

I thank Dr. L.D. Arnold and staff of the Alberta Environment, Environmental Research Centre for pore water extraction and tritium analyses. To Dr. H.R. Krouse and staff of the University of Calgary Stable Isotope Laboratory I extend thanks for stable isotope analyses. Appreciation is also extended to Canadian Occidental Petroleum Limited for providing confidential seismic data.

The cooperation and interest of landowners in the study area is sincerely appreciated. In this regard I thank the Hutterian Brethren Church of Carmangay, Hugh and Barb Crawford, Allan Kittleson, Randal Lyckman, Barry McFarland, John McFarland, Roy McLeod, John Ostero, Albert Ross, and George Sevko. Special thanks are extended to Barry McFarland for his keen interest, generous donation of storage facilities, and for keeping a watchful eye on instrumentation and equipment.

Mr. Grant Sjostrom provided conscientious and extremely competent field and office support. His generous help and long working hours, often under severe weather conditions, are much appreciated. I thank B. Balakrishna, and D. Cheel for manipulation of hydrochemical data, A. Howard for numerous helpful discussions and for his work with the EM38 data, and G. Jean and S. MacKenzie for their competent office and field assistance. The fine draftsmanship of L. Bradley, J. Dlask, W. Hutniak, and J. Mathie and photographic expertise of L. Lorinczi are also much appreciated. The typing services of K. Gates, L. Fudge, and N. Luck, are gratefully acknowledged.

This work was jointly funded by the Alberta Agriculture Farming for the Future Program and the Alberta Research Council. Gratitude is expressed to Dr. R.J. Fessenden of the Terrain Sciences Department, for generous allowance of time and operational support.

TABLE OF CONTENTS

Cont'd ...

TABLE OF CONTENTS CONT'D

LIST OF TABLES

LIST OF FIGURES

Cont'd ...

Page

Cont'd...

LIST OF FIGURES CONT'D

LIST OF PLATES

1. INTRODUCTION

Dryland salinity is a serious problem affecting agriculture in the southern parts of the Prairie Provinces and northern Great Plains of the United States. It has been estimated that more than 800 000 ha of dryland are affected and that the problem is increasing (Vander Pluym, 1978). In addition to the loss of soil productivity, seeding delays, poor soil trafficability, and contamination of surface and subsurface water resources have resulted.

The causes of dryland salinity are reasonably well understood in general terms (Vander Pluym, 1978; Hendry and Schwartz, 1982; Brown, et al., 1983). Essentially, soil salinization occurs in areas where groundwater carrying dissolved salts discharges at or near the soil surface. The salts originate from chemical weathering of carbonaceous, sulfur-bearing Cretaceous bedrock and associated glacial till deposits (Hendry et al., 1986; Wallick, in preparation). Oxidation of organic sulfur derived from lignite and from organics disseminated in shale is shown to be the primary source of sulfate in weathered till of Southern Alberta (Hendry et al., 1986). Oxidation is postulated to have occurred [illegible] a relatively thick unsaturated zone that existed during the drier and warmer climate of the Altithermal Period (11 000 to 3000 years B.P.).

The location and intensity of groundwater discharge is controlled and influenced by configuration of the water table (major and minor topographic lows, breaks in slope), relative position of geologic units and their permeability contrasts, shapes, and slopes (Freeze, 1969). Because many different combinations of these factors are possible in nature, it is apparent that the contribution of groundwater flow to soil salinity may be difficult to evaluate.

The important role of groundwater in forming saline soils has been clearly established. Meyboom (1966) related major areas of saline soil occurrences in south-central Saskatchewan to both regional and local groundwater discharge from artesian aquifers. He presented evidence that flowing wells and strong upward hydraulic gradients are associated with the occurrences. Doering and Benz (1972) showed that discharge of saline water from the Dakota Sandstone is responsible for soil salinization in North Dakota. Brown et al. (1983) identified seven distinct types of saline seeps resulting from the interplay of several combinations of hydrologic, geologic, and topographic features in Alberta, Saskatchewan, and the northern Great Plains of the United States. Henry et al. (1985) implicated upward hydraulic gradients and groundwater discharge in soil salinization at 15 sites in Saskatchewan. They calculated that observed soil salt loads could have accumulated by upward movement from underlying aquifers in 500 to 5300 years.

Recent increases in area affected by dryland salinity are attributed to farming and other cultural practices (Ballantyne, 1963; Doering and Sandoval, 1975; Brown and Miller, 1978; Hendry and Schwartz, 1982; Brown et al., 1983). Of particular importance in this respect are plowing of native grasses, planting cereal or other crops that make less efficient use of available soil moisture, summer fallowing, and widespread use of effective herbicides. All of these factors result in increased availability of soil moisture to the groundwater system, a general raising of the water table, and an increased water and salt flux through the system.

Control measures are aimed at reducing the amounts of water available to the groundwater system. These measures are most effective if applied at the source - the areas of groundwater recharge (Brown et al., 1983; Vander Pluym, 1982). Methods to intercept water before it can reach the water table in recharge areas include:

(a) mechanically draining depressions and dugouts;

(b) planting deep-rooted, high water consuming crops such as alfalfa that will use soil water; and,

(c) increasing the efficiency of water use by flex cropping, or by growing crops every year when spring soil moisture is sufficient for seed germination.

Control measures useful in areas of groundwater discharge all involve lowering the water table. This can be accomplished by intercepting laterally flowing groundwater before it reaches saline soil areas, tile drainage of the affected areas, or by lowering of piezometric heads in relatively permeable units below saline soil areas.

A clear understanding of the various underlying processes and the groundwater flow regime is essential for the successful management of soil salinity. In particular, many investigators feel that it is important to identify the location and relative importance of areas of recharge that contribute to the development of saline soils, how changes in land management practices will affect the amount of water entering the landscape in those recharge areas, and how that will affect the amount and quality of discharge water.

The goal of this study is to develop a quantitative understanding of the dynamics of water and salt movement in an area with an identified salinity problem. While much is known about the general factors that cause salinity, the number of site-specific studies is limited.

Detailed studies are needed to examine the role of groundwater and other water sources in dissolving, transporting, and eventually depositing salts in the soil zone. The objectives of this study are to determine the rates of recharge and discharge, where these processes occur, factors that control the groundwater chemistry and flow distribution between the areas of recharge and discharge, and factors that are responsible for high water tables, groundwater discharge, and salt accumulation at specific sites.

The Blackspring Ridge area offers a unique opportunity to study the relative importance of these factors because salinity is developed in a variety of topographic settings and to different degrees of severity. Salinity thus is likely to have a number of different causes or combinations of causes. Results of the research should therefore be representative of a broad range of salinity types and can hopefully be extrapolated to other geographic areas.

2. PHYSICAL SETTING

2.1 Location, Physiography, and Drainage

The Blackspring Ridge area is located in southwestern Alberta near the Town of Carmangay, approximately midway between the Cities of Calgary and Lethbridge (Figure 1). The dominant topographic feature of the area is Blackspring Ridge, a till-covered bedrock ridge trending approximately north to south, about 20 km long and 9 km wide. It rises about 50 m above a surrounding lacustrine plain that gently slopes to the west and northwest toward the Little Bow River (Figure 2). The river is incised about 50 m into this plain and is superimposed on a major preglacial bedrock valley - the Carmangay Valley.

Figure 1. Location of the Blackspring Ridge study area.

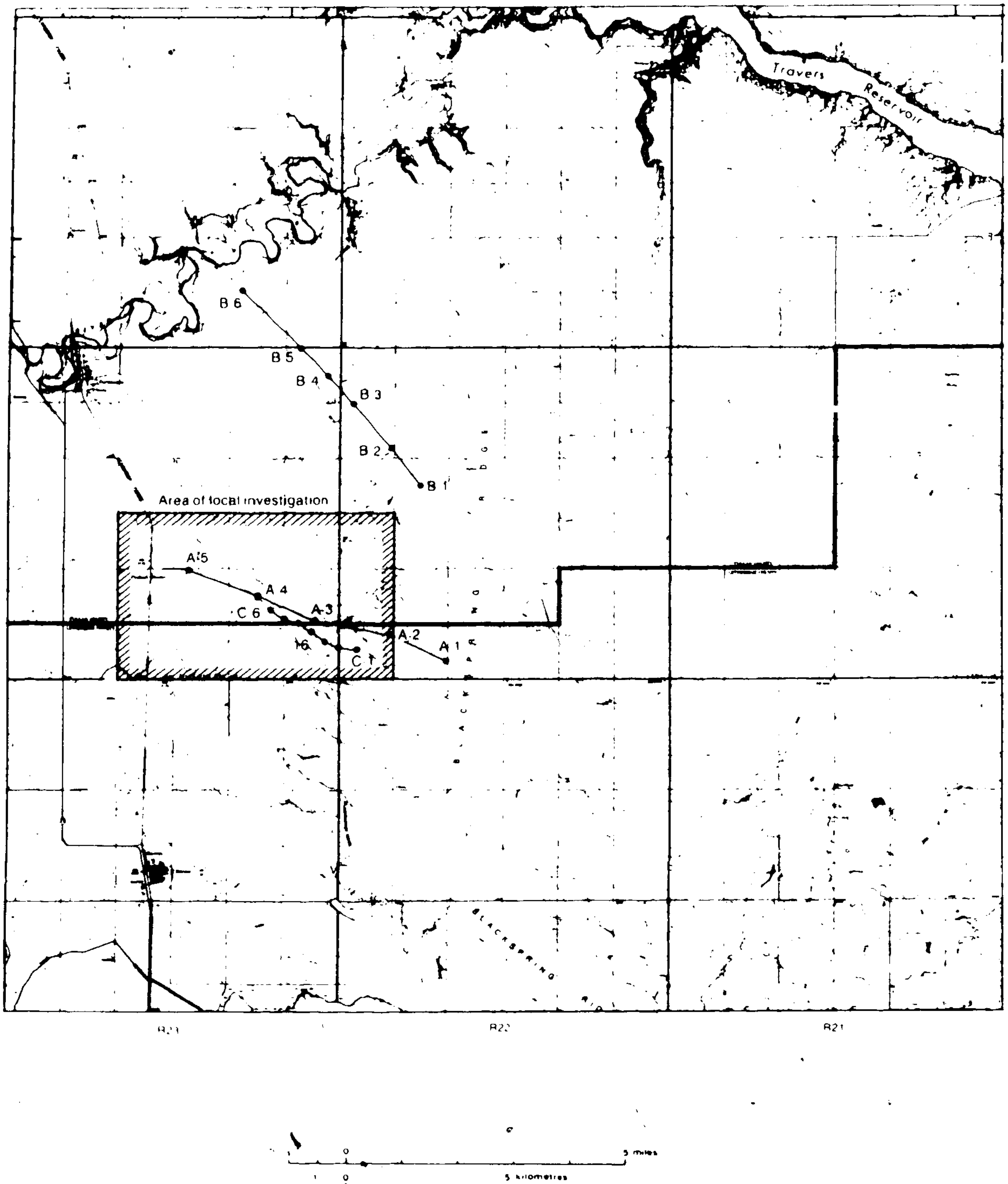

Figure 2. Topography and drainage.

Local relief on the ridge is about 5 to 8 m. Drainage is poorly integrated and a significant number of closed depressions exist. A number of steep-sided coulees originate on the west flank of the ridge and terminate at about the uppermost limit of the lacustrine plain. The coulees are dry for most of the year, but carry large volumes of snowmelt water for short periods of time in the spring and occasionally runoff from summer rains, when these are of sufficient intensity and duration.

Except for the northernmost tip of the ridge, no surface drainage originating from the west ridge flank leaves the lacustrine plain, but follows a series of road and field ditches and minor natural depressions to low portions of the plain. Drainage is somewhat better integrated on the east flank and reaches Travers Reservoir and the Little Bow River to the north and east via intermittent streams.

Distinct lineations exist in the southern and northern boundaries of the ridge, in coulees, and in other drainage channels originating from the ridge. Although no rigorous statistical analysis was performed, lineations are oriented at about 127° and 55° azimuth. These directions are close to those reported by Babcock (1974) for southern Alberta and indicate that strong structural control of bedrock morphology exists.

The area receives about 380 mm of precipitation annually, of which about 255 mm falls from April to September (Longley, 1968). Potential evapotranspiration is about 585 mm (Government and University of Alberta, 1969). The years 1984 and 1985 had below normal summer precipitation, with 105 and 194 mm recorded at the study site, respectively.

Soils are Dark Brown chernozemic (Agriculture Canada, unpublished information) and farming consists almost entirely of dryland cereal crop production.

The investigation proceeded in two phases. An initial regional investigation focused along two regional cross-sections, A-A' and B-B', whose location is shown on Figure 2. A detailed study was then conducted in a smaller area shown on the figure where severe soil salinization was noted. Section C-C' is located in this local area (Figure 2).

2.2 Soil Salinity

The main occurrences of saline soils are shown regionally and for the local investigation in Figures 3 and 4, respectively. Both are probably underestimates because only areas with actual white salt crusts on the ground surface are shown. Salinity, as determined by EM38 traverses (Appendix 1), is shown above each hydrogeologic cross section (Figures 5, 6, 11 and 24). Saturation paste extract results and depth profiles are given in Appendix 2 and 3, respectively.

These surveys show that the salinity occurs in several distinct topographic settings:

a) from 5 to 10 m below the first major decline in slope from the top of the ridge;

b) near the base of the ridge;

c) from bedrock outcrops along coulee sides; and,

d) as diffuse saline occurrences on the lacustrine plain.

Those on the lacustrine plain appear as more concentrated linear occurrences where thin aeolian sediment overlies lacustrine deposits

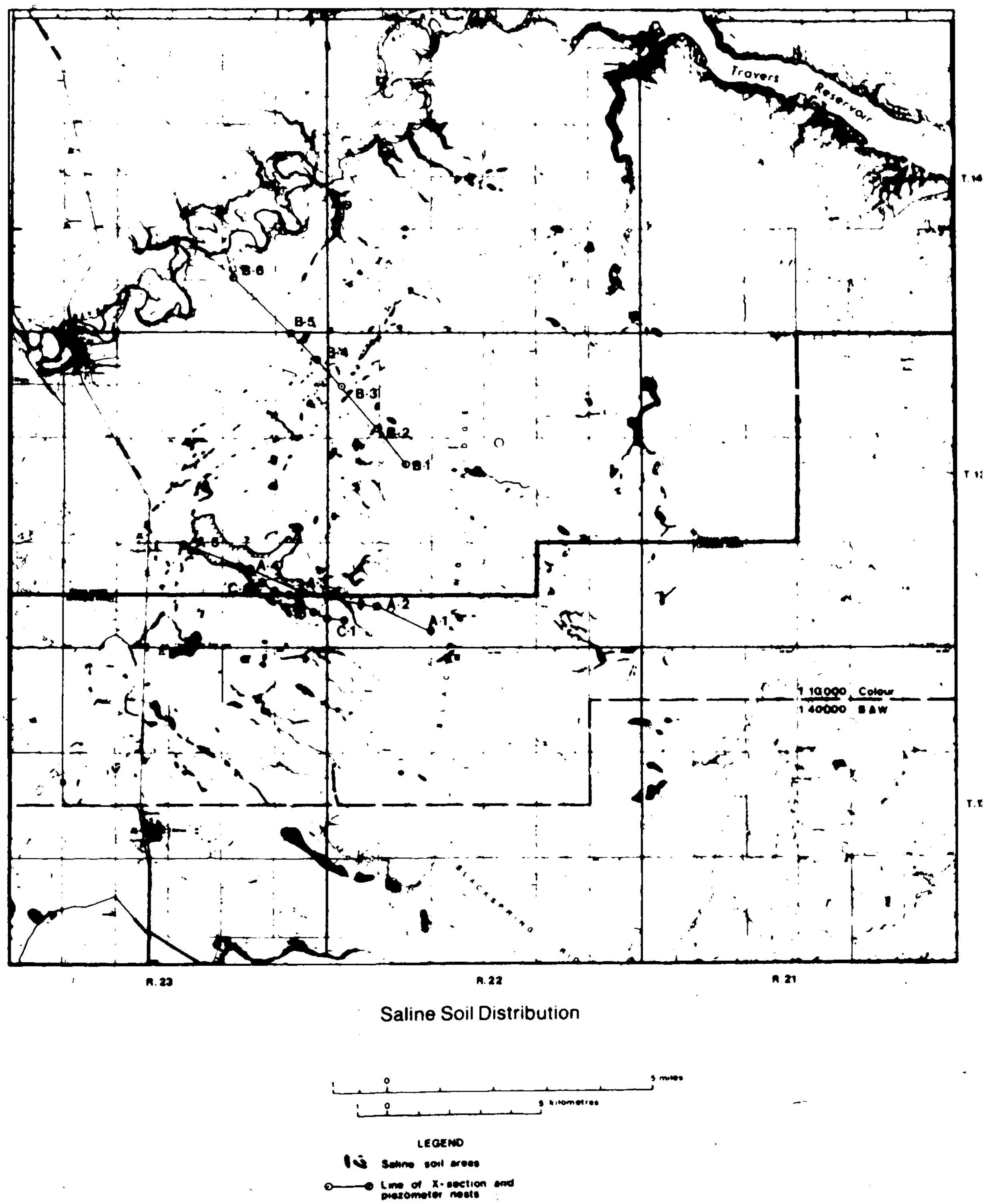

Figure 3. Saline soil distribution.

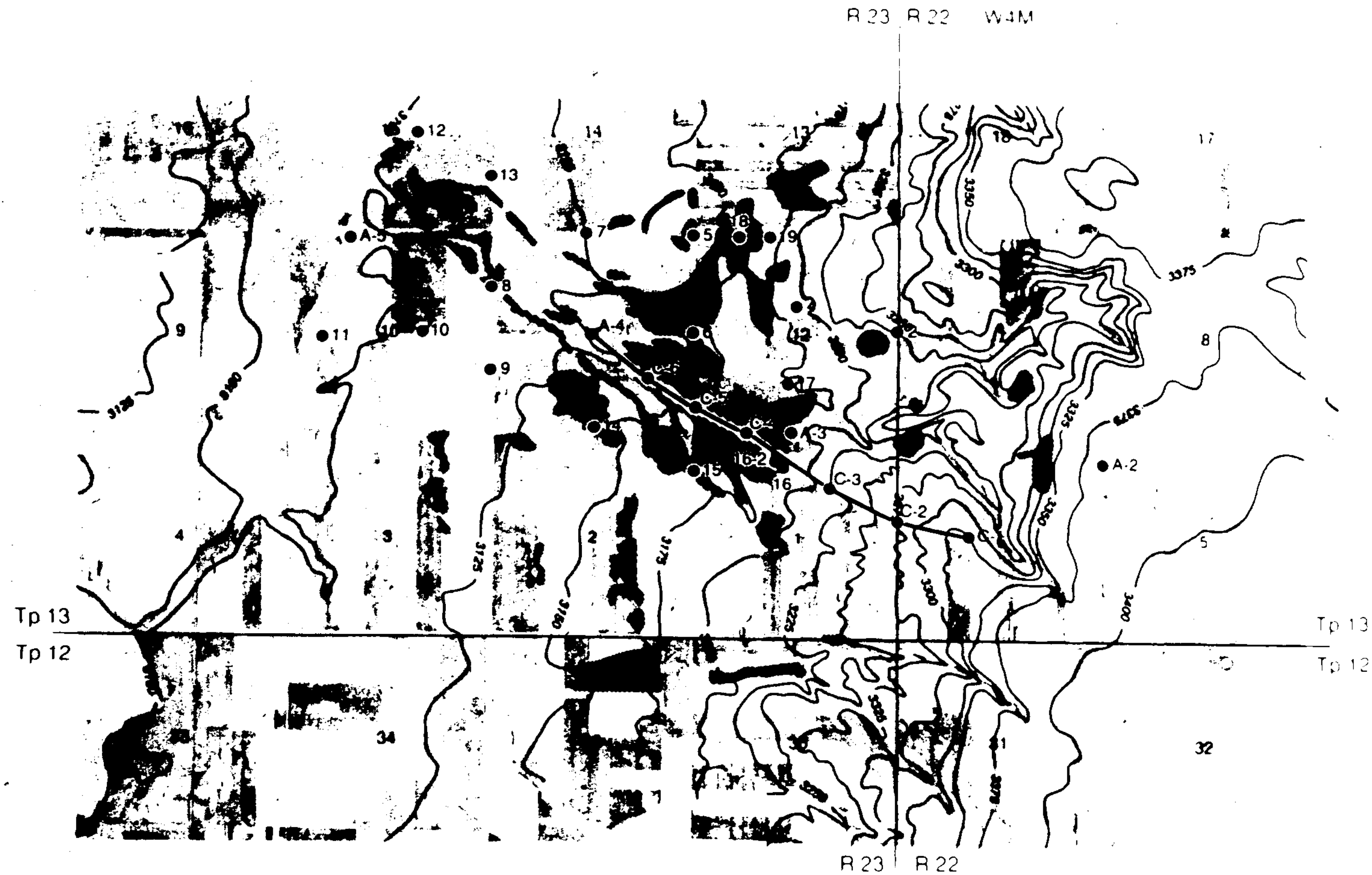

Figure 4. Areas of salinity visible on air photographs of area of local investigation.

west of the northern half of the ridge.

The intensity of surface expression of soil salinization varies greatly with location and time, even within the various landscape settings. The most severe salinization occurs at the base of Blackspring Ridge near the intersection of Sections 1, 2, 11, and 12 of 13-24 W4 Mer (Figure 4). Salinity is manifested by large areas of severe salt crusting on the surface, areas of salt-tolerant vegetation [including _Salicornia rubra_ (samphire), _Hordeum jubatum_ (wild barley), and _Kochia scoparia_ (kochia)], and areas that support only poor, or no, crop production (Plates 1 and 2). Trafficability in the more severely affected areas is so poor that in some years cultivation is not attempted. EM38 readings indicate salinity ranges from 12 to 19 dS/m in the upper 1.2 m.

A reasonably long history with respect to salinity and land management is available for 11-13-23 W4 (Mr. Roy McLeod, personal communication). The section came into the McLeod family in 1917 with about 80 ha broken. From 1934 to 1950 the remainder of the section was gradually brought into production. Mr. McLeod feels that prior to 1934 only minor salinity existed at the east border of the section, but that the white salt-crusted area at the southeast corner was present. In about 1953, after the entire section was broken, salinization intensified, with spreading from the east and southeast to the point where presently more than half of the section is affected to some degree. Remedial measures that have been attempted on Section 11 include surface drainage by ditching, and cropping of severely affected areas with alfalfa and crested wheat grass.

From about the centre of Section 11 to the Peacock Slough (in NW and SW of 10-13-23 W4) salinity exists, but is not intense enough to show strong surface expression. Salt crusting is moderate to light and appears only intermittently in the vicinity of the Peacock Slough. The problem is reflected mainly by uneven crop growth. EM38 traverses, however, show that salinity ranging from 5 to 9.5 dS/m exists in the upper 1.2 m.

A second area of salinity similar in size and intensity to that in and near Section 11-13-23 W4 exists about 3 km to the south. North of Section 11, areas of salinity along the base of Blackspring Ridge are generally much smaller in areal extent (S19-13-22 W4; S5 and 16 of 14-22 W4). These are also considered to have existed prior to cultivation.

Salinity developed in dunal areas is typified by occurrences in Sections 36-23-13 W4 and 31-13-22 W4 (Plate 3). Dunes and depressed areas between dunes trend at about 45° azimuth and salinity occurs in much of the depressed areas. It is estimated that at least 15 percent of the surface area of these two sections is affected. Mr. John McFarland (personal communication) reports that prior to breaking and cultivation of Section 36 no salinity existed. In fact, areas that are now saline produced the best crops immediately after breaking, but started to become saline about four to five years later.

Salinity distribution with depth as shown by saturation paste extract results is given in Appendix 2 and 3. Results are in good agreement with field and air-photo observations in that areas with strong surface expression also show salinity at depth.

In severely affected areas (Sites A4, C4, C5, and C6) salt content is high to depths of 15 m or more. Salinity generally decreases with depth but reversals are not uncommon. The main constituents are sodium and sulfate with magnesium and calcium being secondary. Electrical conductivity is generally above 4 dS/m and reaches a maximum of 22 dS/m at the ground surface at Site C4.

Non-saline areas, represented by profiles A1, A2, B1, B2, B3, B5, and B6, generally show strongly leached conditions in the upper 2 to about 7 m and then increase only slightly in total salt content with depth. Calcium and magnesium salts are dominant in leached portions of profiles but sodium increases with depth and total salt content. Electrical conductivity ranges from less then 1 dS/m in near-surface leached zones to about 2 or 3 dS/m in deeper areas. Conspicuous increases in total salt content exist at bedrock contacts overlain by thin drift sediment at Sites A1, A2, and B2.

2.3 Geology

2.3.1 Bedrock geology

An important part of this study involved both auger and mud-rotary drilling to better define geologic conditions. Details on the drilling, sampling and logging are provided in Appendix 1. Bedrock of the area consists of continental sandstone, siltstone, claystone, and coal beds of the upper Cretaceous Horseshoe Canyon Formation. This unit overlies silty shale and sandstone beds of the marine Bearpaw Formation (Figures 5 and 6).

The geologic base for the regional investigation was taken to be a sandstone unit within the Bearpaw Formation consisting of one to two beds with a coal seam above the lower bed. The sandstone beds range in thickness from less than 1 m to about 20 m, and are generally separated

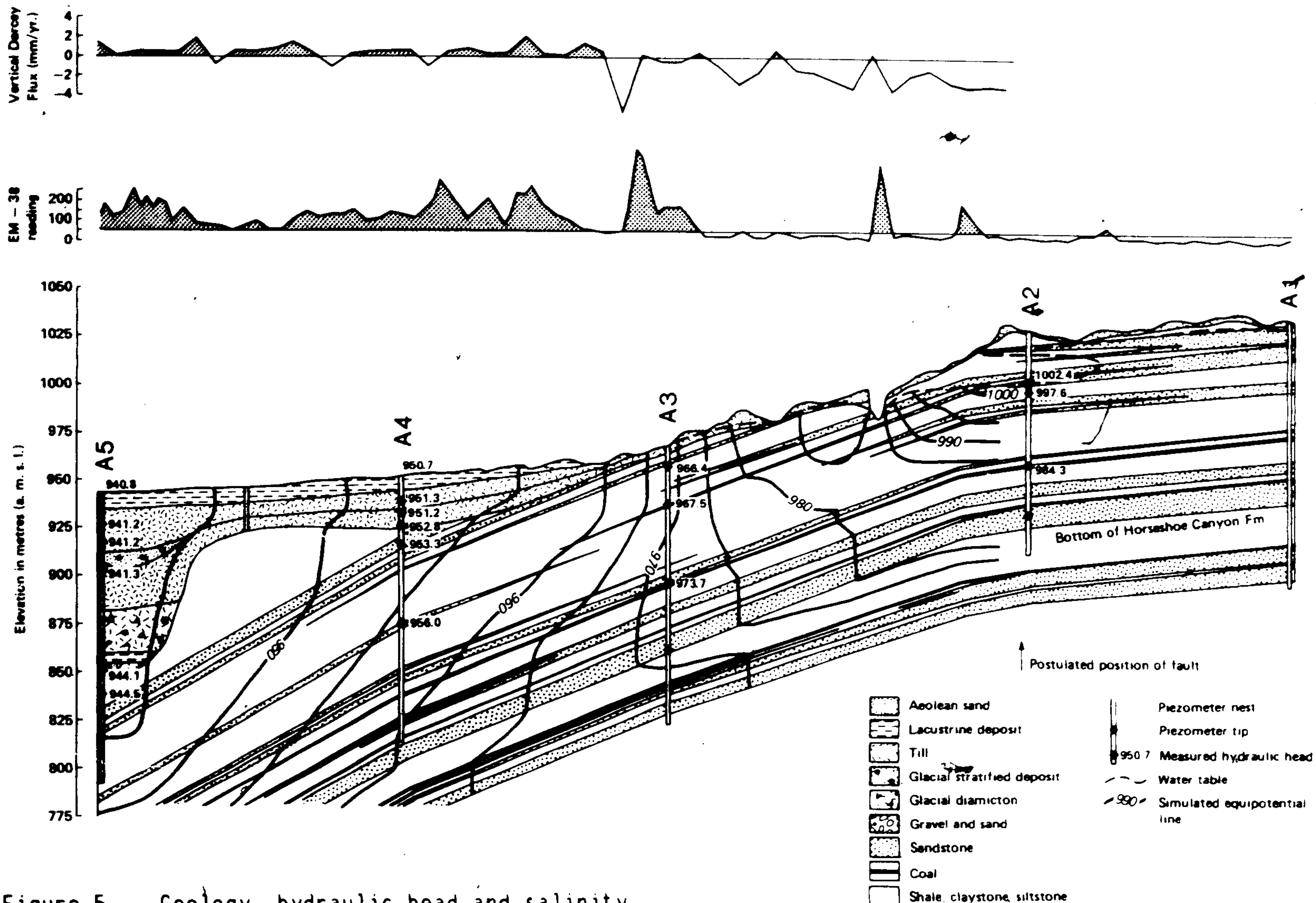

Figure 5. Geology, hydraulic head and salinity distribution along Section A.

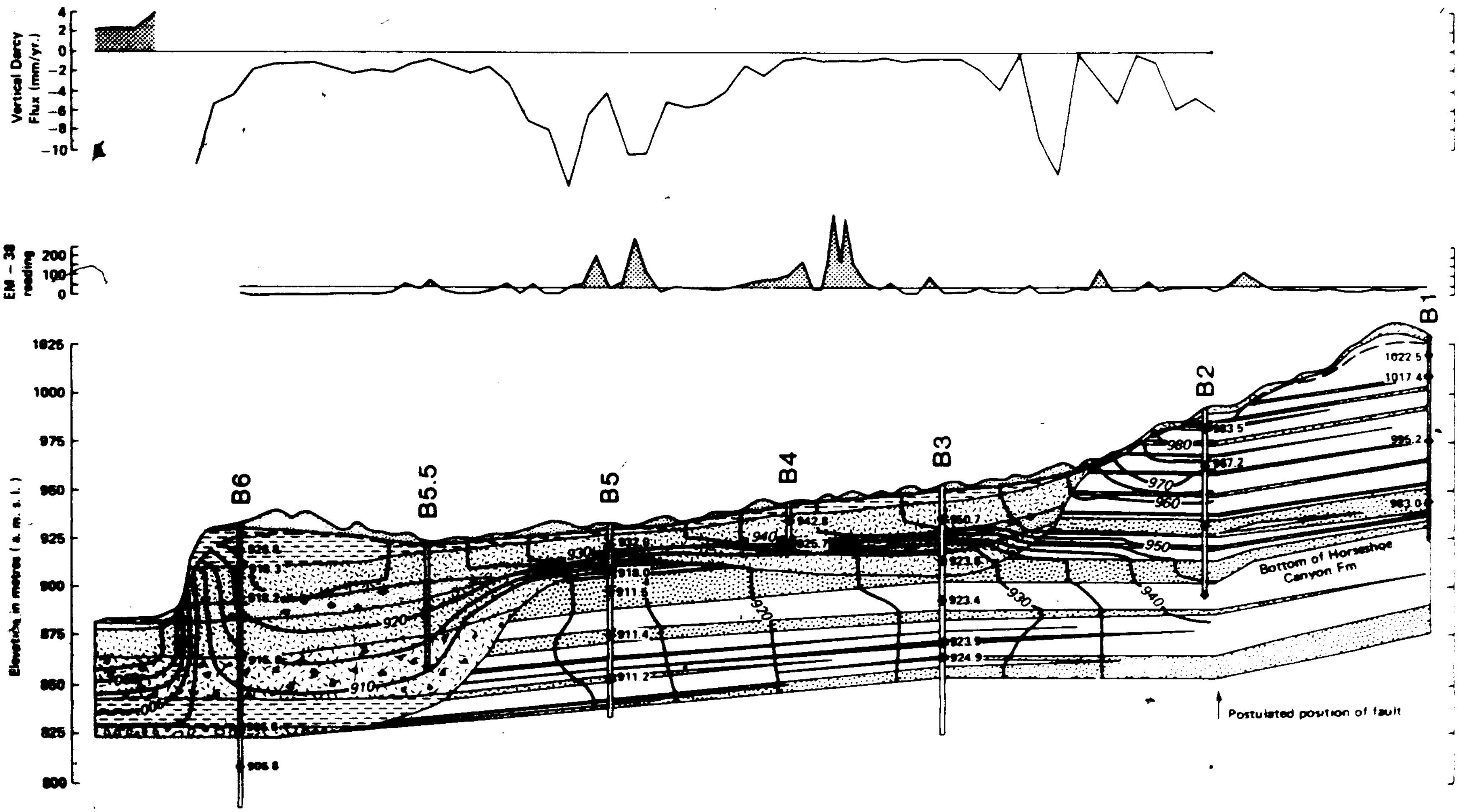

Figure 6. Geology, hydraulic head and salinity distribution along Section B.

from the basal sandstone of the overlying Horseshoe Canyon by about 20 m of silty shale. This unit is termed the Ryegrass Sandstone by Link and Childerhose (1931) and the Thelma and Oxarat Members by Lines (1963). Structure testhole and oil well geophysical log data for the area show that, except for two minor sandstone occurrences, the 190 m of Bearpaw Formation below the Ryegrass Sandstone is shale.

Only the lowermost 100 m of Horseshoe Canyon Formation were encountered during drilling. For this study this section is divided into three units. The basal unit, which is from 15 to 35 m thick, consists mainly of sandstone, but contains as much as 10 m of claystone and siltstone. This unit is overlain by a 45-m thick unit of claystone, siltstone and minor sandstone containing two to three coal seams in the lower half. Along the southern cross section another unit of increased sandstone content was encountered above the second unit; no appreciable increase in sandstone content was encountered at the equivalent stratigraphic position of the north section.

The structure contour map for the top of the Kipp Sandstone (Figure 7) shows Blackspring Ridge to be a structural high, with beds beneath and east of the ridge dipping to the north-northwest at about 8 m/km. West of the ridge, beds dip to the west at up to 55 m/km, then decline to about 20 m/km. The structure contours, along with pronounced lineations in topography and drainage that were mentioned previously, strongly suggest that faulting may account for much of the offset in the Kipp Sandstone shown in Figure 7.

In an attempt to verify the possibility of faulting, two deep seismic reflection profiles were obtained from Canadian Occidental Petroleum Ltd. Although specific data and locations of profiles are

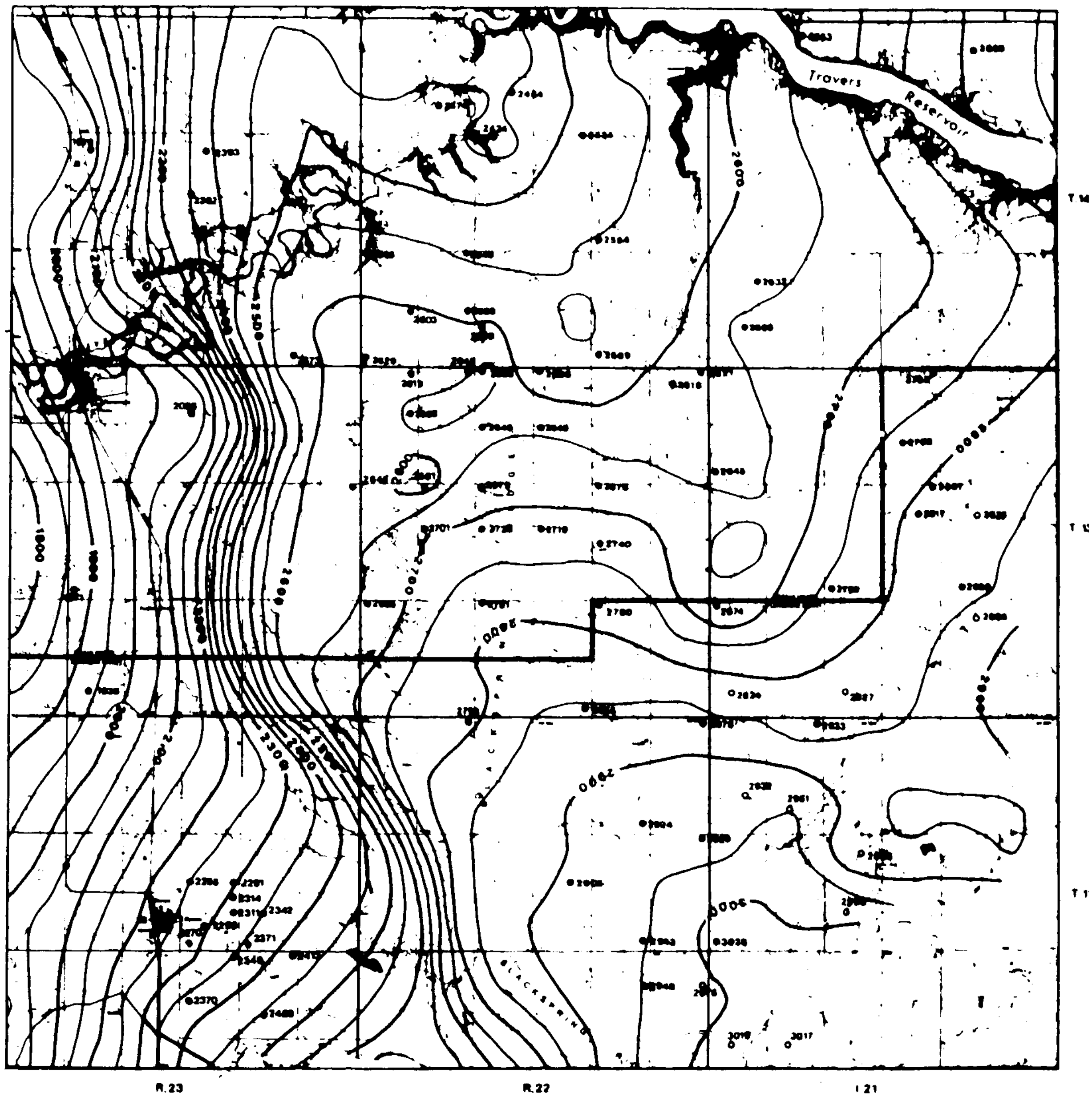

Structure Contours on Top of Kipp Sandstone

0 — 5 miles

0 — 5 kilometres

LEGEND

● 2856 Data point; elevation in feet a.m.s.l.

○ 2932 Data point, derived by adding Second Specks to Kipp isopachs to Second Specks elevation, elevation in feet a.m.s.l.

Figure 7.

confidential, some general information can be related. The profiles were independently examined by geophysicists at the University of Alberta (E.R. Kinasewich and Z. Berkes, personal communication) and both concluded that it was highly likely that a number of apparent major displacements constitute faulting. Primary evidence was taken to be a series of diffraction patterns associated with a number of the displacements.

Depths to a major reflecting horizon were determined using a travel-time versus depth plot constructed from sonic log data from an exploration borehole. Interpretation of the seismic data showed that beds immediately above the Precambrian surface at depths from 2600 to 3000 m below ground level are displaced vertically from 130 to 316 m. Both vertical displacement and resolution of reflection horizons decrease higher in the section. No data are available for the uppermost 450 m. The seismic data must thus be considered circumstantial but they do lend credence to the postulation that faulting may exist in near-surface bedrock.

Furthermore, portions of Blackspring Ridge, particularly the western, and perhaps the eastern, flanks are deformed, fractured, and faulted by glacial overriding. This type of deformation was documented by Sauer (1978) and Moell et al. (1985) for southern Saskatchewan and central Alberta. The near surface influence of glaciation has resulted in fracturing of the shallow bedrock. Evidence is provided by the following:

a) at Drill Site A2, circulation was lost in bedrock at 25 m and could only be regained with great difficulty;

b) rotary bedrock drill cuttings from most holes of the C-Line and from as deep as 25 m contained iron stains on fracture planes; and,

c) hydraulic conductivity of very fine to fine grained sandstone ranging from 10^{-6} to more than 10^{-4} m per second.

According to I. Shetsen (personal communication) the area experienced at least two glaciations, one from the northwest and the other from the northeast. It is not unreasonable to expect a dominant bedrock high such as Blackspring Ridge to undergo deformation by glacial overriding, particularly along edges exposed transverse to ice advances.

2.3.2 Surficial geology

Drift thickness ranges from 2 to 5 m on top of the ridge to about 110 m along the Little Bow River. A preglacial buried valley, the Carmangay Valley, is located at approximately the position of the Little Bow River and Travers Reservoir (Geiger, 1967). Drilling located deep preglacial gravel at the A5 Site, which is interpreted as flooring another south-to-north trending preglacial valley, probably a tributary to the Carmangay Valley.

Within the buried valleys, the basal sand and gravel is capped by a lacustrine unit as much as 10 m thick, which is in turn overlain by as much as 25 m of diamicton or glacial debris flow sediment. Overlying this sequence, and covering the entire area, are two till units. The contact between the two till units is marked in places by glacial stratified deposits ranging in composition from silt and clayey silt to sand and gravel. As much as 10 m of these stratified deposits exist above the buried valleys. At the C6 drill site about 20 m of stratified sediment exist below the upper till but lie directly on bedrock. This configuration suggests that erosion of the lower till was associated with deposition of the stratified unit. It is thus probable that the unit was deposited in a channel. The channel may be continuous from Site C6 through Sites 6WT, 5WT and to B3 and B4, but because no data are available for about 5 km between Sites 5WT and B3, this connection remains unproven. At a number of places along the western flank of the ridge as much as 3.5 m of sand lie directly on bedrock (Figures 10 and 11). This sand may be equivalent to the glacial stratified deposits or may be preglacial in age.

A glaciolacustrine unit of clay, varved silt and clay, and sand covers the upper till to an elevation of about 955 m. Glacial outwash sand overlies the lacustrine unit along the Little Bow River. A series of thin sand dunes extends from the outwash sand toward northern portions of the ridge. Although not confirmed by drilling, it is probable that alluvial fan deposits are present where coulees meet the lacustrine plain at the west ridge flank.

Both the till and the lacustrine deposits are weathered near the surface. Colours indicative of oxidation, fracturing, and iron staining were generally found to a depth of 15 m and in places to 20 m.

2.4 Hydrogeology

2.4.1 Hydraulic conductivity

Hydraulic conductivity values determined for the various hydrostratigraphic units are presented in tabulated form in Appendix 4 and graphically in Figures 8 and 9. Values presented in Figures 8 and 9 are derived from in-situ hydraulic tests that were analyzed by methods appropriate for the hydraulic settings at individual test sites

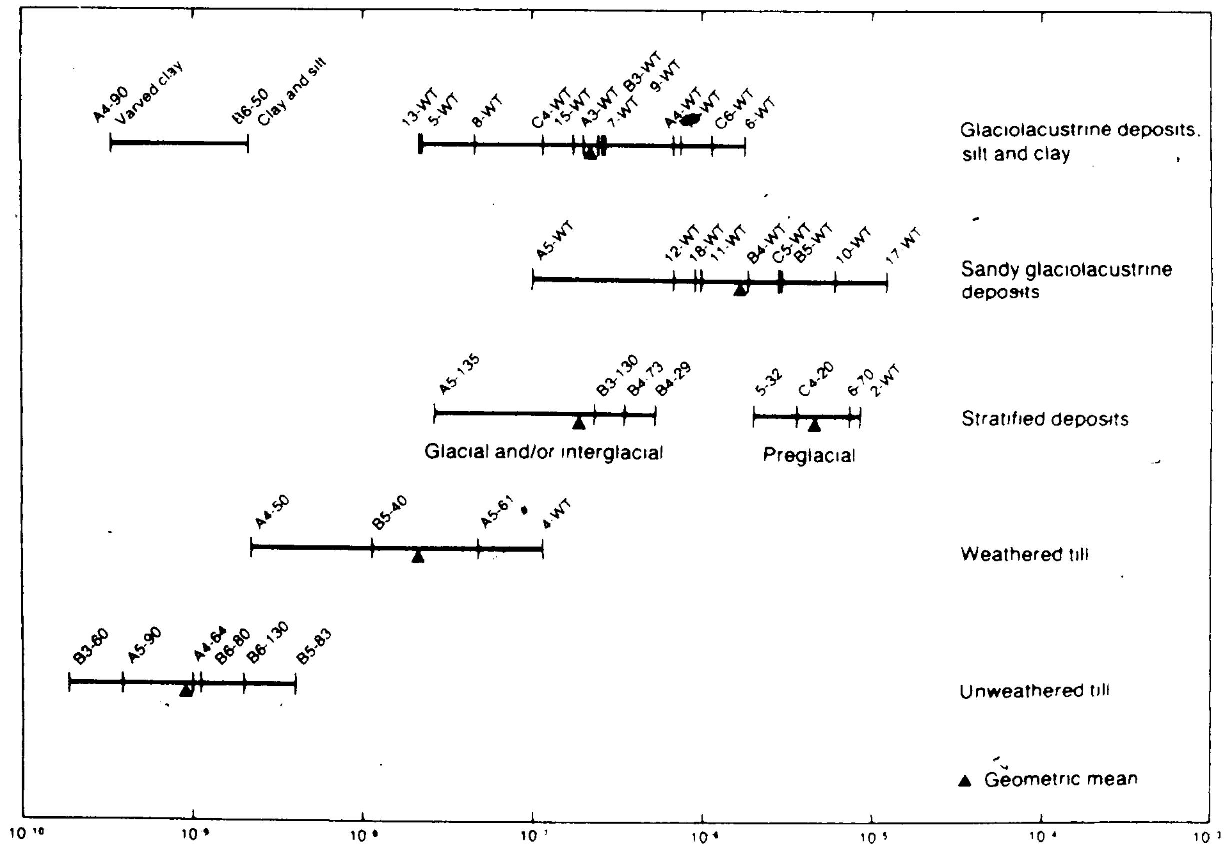

Figure 8. Horizontal hydraulic conductivity (m/sec) drift hydrostratigraphic units.

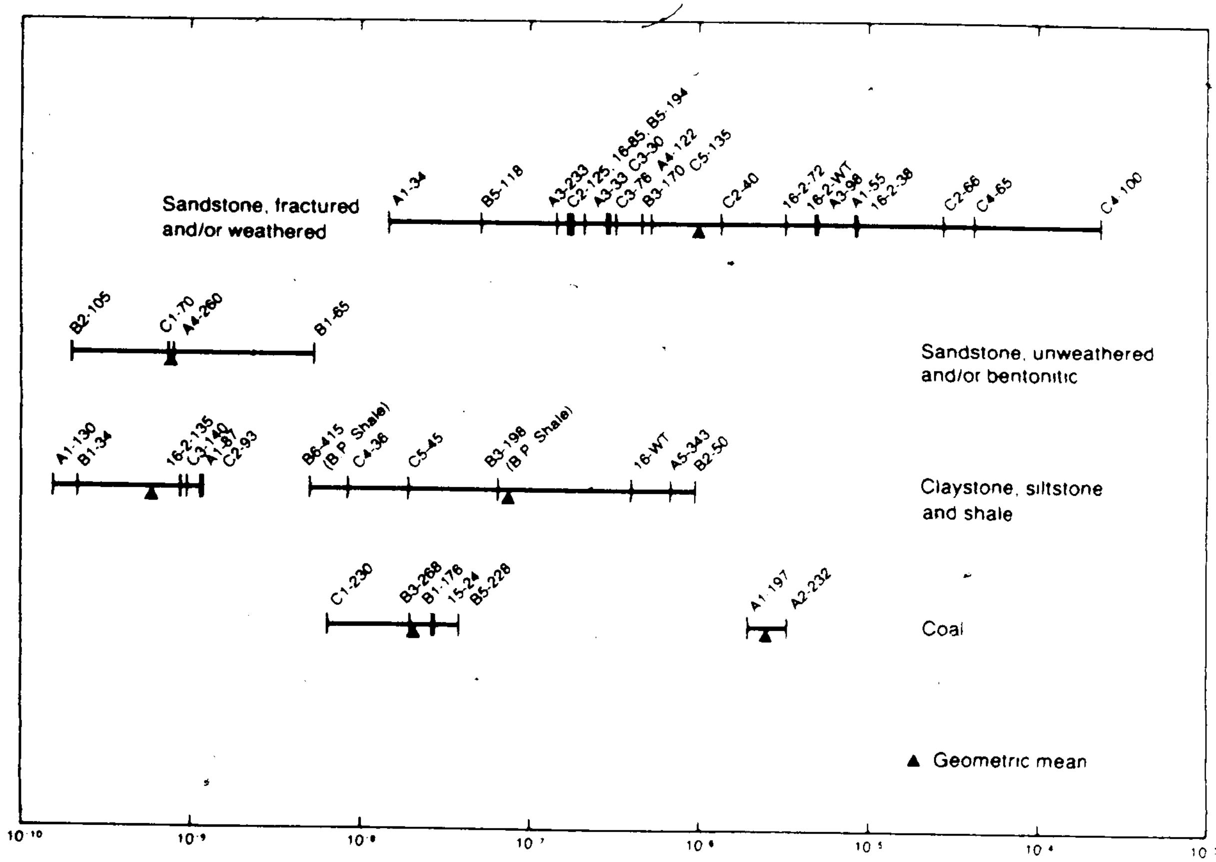

Figure 9. Horizontal hydraulic conductivity (m/sec) bedrock hydrostratigraphic units.

(Appendix 1). For purposes of calculation, digital modelling, and flux determinations, hydraulic conductivity of till was assumed to be isotropic; all other units were assumed to have vertical hydraulic conductivity one order of magnitude less than horizontal. Permeameter tests (Appendix 5) conducted on near-surface lacustrine deposits indicate that for these deposits the ratio of horizontal to vertical hydraulic conductivity is about 6.5. The latter data were not available at the time digital modelling was performed and a value of 10 was used for these solutions. Generally, ranges and geometric mean values of the various units are similar to those reported by others for southern Alberta (Hendry, 1983; Forster, 1984; Chan and Hendry, 1985).

The relatively high hydraulic conductivity values and the broad range of values (about 3.5 orders of magnitude) of glaciolacustrine deposits are probably a result of a combination of textural variation and near-surface weathering. This unit ranges texturally from clay with thin silt laminae, to clayey and silty sand. Colours indicative of oxidation and occasional fracture planes with iron stains were noted during core sample inspection. The highest hydraulic conductivity values were measured in shallow water-table wells (less than 6 m deep) and in deposits with high silt or sand content.

Hydraulic conductivities greater than 1×10^{-6} m/sec were determined from four wells (C5, C6, 6WT, and 17WT) that are located at the base of the ridge in a topographic setting that suggests alluvial deposition from coulees may be occurring. A high proportion of silt and very fine grained sand was noted in the upper 1 to 5 m of sediment from testholes C5, C6 and 6WT, and very-fine to medium grained sand to 4 m at 17WT. It could not, however, be determined if these deposits are alluvial or represent a glaciolacustrine shoreline facies; hydraulic conductivity data are grouped with those of lacustrine deposits.

Hydraulic conductivity measured in the laboratory for the lacustrine deposits is generally from one to two orders of magnitude lower than that obtained by in-situ testing of water-table wells at coinciding locations. This difference between measurements is likely caused because the larger scale field tests are influenced by thin layers of texturally coarse materials and perhaps near-surface fracturing. Because a much smaller volume of material is sampled by a core, the probability of either of these features influencing a laboratory test is much lower.

The hydraulic conductivity of bedrock units, especially sandstone units, is considerably more variable than that of drift units (Figure 9). No systematic pattern in variability could be found. The pattern of variability could however be expected, given the strong structural control and deformation produced by glacial overriding, which likely produces a strong joint and fracture control on hydraulic conductivity. In addition, the lenticular nature of continental deltaic deposits such as those of the Horseshoe Canyon Formation, can also contribute somewhat to the high degree of variability. Because of the very-fine to fine-grained texture of most sandstone beds, this contribution to variability probably only influences the lower end of the range.

Almost all of the sandstone with hydraulic conductivity greater than the mean value determined for fractured sandstone (1.0×10^{-6} m/sec) was encountered during 1986 drilling of the C-Line. Two possible explanations are:

a) completion zones during 1986 drilling were deliberately made longer to increase the probability of sampling a representative fractured rock unit volume; and,

b) bedrock of the western flank of Blackspring Ridge is more highly fractured than elsewhere.

Hydraulic conductivity values obtained for claystone and shale range from 1.6 x 10^{-10} to 9.5 x 10^{-7} m/sec. Again, this variability is caused by the extent to which fracturing has occurred. At some sites (16-2, C3, C2), fractured sandstone is observed in close proximity to apparently unfractured argillaceous units. Thus, argillaceous units as one might expect have a much smaller fracture density than the sandstone units.

2.4.2 Hydraulic head and groundwater flow distribution

2.4.2.1 Regional investigation

The regional groundwater flow distribution was investigated by matching observed values of hydraulic head derived from water-level data with hydraulic head values determined with a digital flow model developed by Schwartz and Crowe (1980), (Figures 5 and 6). This theoretical approach was used for two reasons.

First, spacing between individual piezometer nests or observation points is generally relatively large (about 1.5 km). The position of the equipotential lines thus can only be defined very crudely because of the distance between data points in the horizontal direction. Digital simulation becomes a way of using specified values of hydraulic conductivity consistently throughout the flow region to avoid investigator bias. This approach is particularly important in regions of lateral flow where slight deviations of equipotential lines around the vertical can change the interpreted direction of flow components from up to down.

Second, the trial and error method involved in matching observed and simulated head values is in itself a process that leads to additional knowledge about the flow distribution. By repeatedly changing hydraulic parameters, unit boundaries, or boundary conditions in attempting to match observed values, a significantly better understanding of hydraulic conditions of the simulated region is developed.

The model for Section A was set up using 64 and 48 nodes in the vertical and horizontal direction, respectively. The B-Line was discretized using 41 vertical and 58 horizontal nodes. In both cases, vertical node spacing was 5 m and horizontal spacing was 127 m.

The best-fit digital simulations of the hydraulic-head shown in Figures 5 and 6 are the result of a large number of trial and error runs. Various model parameters such as water-table configuration, hydraulic conductivity values, and boundary conditions were adjusted until a reasonable fit with piezometer-derived head measurements was obtained. Generally hydraulic conductivity values close to the geometric mean for the various rock units available at the time prior to C-Line drilling could be used (Table 1).

One major feature of the model was the necessity for a barrier boundary to groundwater flow situated approximately near the upper break in slope of Blackspring Ridge. The predominantly vertical gradients and measured hydraulic head values at piezometer nests A2 and B2 could not

Table 1. Horizontal hydraulic conductivity* assigned to various hydrostratigraphic units of digital models (m/sec).

A-Line	B-Line	Hydrostratigraphic Unit
3.7×10^{-7}	3.7×10^{-7}	Surface glaciolacustrine unit
	3.0×10^{-9}	. at B6
	2.0×10^{-9}	. at B6
2.0×10^{-9}	2.0×10^{-9}	Deep glaciolacustrine unit in buried valleys
1.9×10^{-8}	1.9×10^{-8}	Weathered till
1.0×10^{-10}	1.0×10^{-10}	Unweathered till
2.0×10^{-7}		Glacial stratified deposits
	1.0×10^{-6}	. at B5.5 and B6
	1.0×10^{-10}	. at B3 and B4
1.7×10^{-4}	1.7×10^{-4}	Preglacial valley gravel and sand
	1.7×10^{-4}	. as terrace joining basal unit to uppermost sandstone, B5.5 to B5
	1.0×10^{-3}	. as terrace west of B3
2.0×10^{-9}	2.0×10^{-9}	Siltstone, claystone, shale; Horseshoe Canyon
2.0×10^{-8}	5.0×10^{-9}	. fractured
4.0×10^{-7}	2.5×10^{-6}	Sandstone, basal Horseshoe Canyon and Ryegrass
5.0×10^{-9}		. Upper Horseshoe Canyon
	3.5×10^{-7}	. deep
5.0×10^{-7}	1.0×10^{-7}	Coal, Horseshoe Canyon
2.2×10^{-8}		. Bearpaw
1.0×10^{-10}	1.0×10^{-10}	Bearpaw Shale
	2.0×10^{-9}	. fractured

* For till $k_h = k_v$; for all other units $k_h = 10\ k_v$

otherwise be replicated. The barrier was simulated with the model by moving the right (eastern) vertical impermeable boundary from about the middle of Blackspring Ridge to the assumed position of the fault. The discrepancy in head values obtained in simulation trials without the barrier was 15 and 5 m for Sections A and B, respectively.

The presence of this feature is supported by field observations including the structural control implied by Figure 7, the strong bedrock lineations developed in the region, and especially the deep reflection seismic data for the area. An alternative explanation is that the lower head values are a three-dimensional effect caused by the presence of steep-sided coulees both north and west of piezometer nest A2. The much less pronounced discrepancy near B2 and high degree of fracturing in near-surface bedrock along the C-Line support the latter explanation.

It can be argued that the effect of both postulated situations on deep groundwater flow should be similar and result in less groundwater flowing toward the lacustrine plain. If a fault barrier exists, then groundwater that would normally constitute part of a deep flow system originating on top of the ridge and discharging to low portions of the plain, is diverted eastward. If the coulees are exerting a strong influence, then groundwater flow is diverted toward, and discharged in and along, coulee bottoms and sides. In either case, there would be less regional groundwater flow to the west.

A combination of three major changes to Section B was required to adequately simulate the observed distribution of hydraulic head: the measured head within the buried valley basal gravel had to be specified; a hydraulic connection between it and the sandstone units of the Horseshoe Canyon and Bearpaw Formations had to be provided along the bedrock contact; and, hydraulic conductivity of the sandstone beds had to be increased by a factor of 6. The change in hydraulic-head distribution resulting from this combination of changes was major and dramatic; it provided the only means of simulating the extremely strong downward gradient that exists in upper central portions of the section.

The required changes to Section B can be justified in view of three-dimensional effects of groundwater flow in the vicinity of the buried Carmangay Valley Aquifer at, and northeast of, the section. Fixing hydraulic head in basal gravel of the buried valley is required because groundwater flow along the line of section is not conservative. Groundwater both enters and leaves the section through this unit. Most of the groundwater flow along the section eventually exits from the unit in the third-dimension. Direct hydraulic connection between the sandstone units and the basal gravel causes lower heads in the sandstone, which in turn increases the downward, vertical gradient above the sandstone. The increase in hydraulic conductivity of the sandstone units was required to decrease the horizontal gradient within the sandstone. It is thus highly likely that the hydraulic connection provided between the sandstone units and the basal gravel by the terrace deposits extends northeast of the section and that a significant component of flow exists in that direction within the sandstone units. Although the simulation could still benefit from further adjustments, particularly in bedrock units, it is felt that it adequately represents the gross characteristics of hydraulic gradients and flow distribution within the shallow drift along portions of the section affected by soil salinity.

The potential and groundwater flow distribution along Section A are characterized by the following: predominantly recharging conditions along the west flank of the ridge; lateral and slightly upward flow in weathered units of the saline lacustrine plain; and, predominantly upward flow in unweathered drift units and bedrock underlying the lacustrine plain.

Cross section B presents a strikingly different picture with respect to potential and groundwater flow distribution. The only discharging conditions that could be simulated on the lacustrine plain are very minor and are located in the vicinity of Testhole B5.5. The hydraulic gradient within weathered drift of the lacustrine plain is primarily horizontal, within the underlying unweathered units it is strongly vertical, and almost complete drainage is provided by the basal buried valley sand and gravel, through the bedrock sandstone units. Groundwater discharge conditions exist in the Little Bow River Valley.

2.4.2.2 Local investigation

Water-level data of mid-1986 were used to derive the potential distribution along the C-Line (Figures 10 and 11). For visual ease and to allow approximate derivation of groundwater flow directions, the section is presented at a vertical exaggeration of $\sqrt{10}$ (Figure 11); flow lines should thus be approximately at right angles to equipotential lines in bedrock units. The head value of 978.8 m in coal at the base of the section at Site 16-2 is projected from Site A3. Figure 10 is included to show geologic detail that was omitted from Figure 11 because of vertical scale. In view of the extreme complexity of flow conditions that exist along the C-Line, digital simulation was not attempted.

Drilling and hydraulic testing along the C-Line revealed important

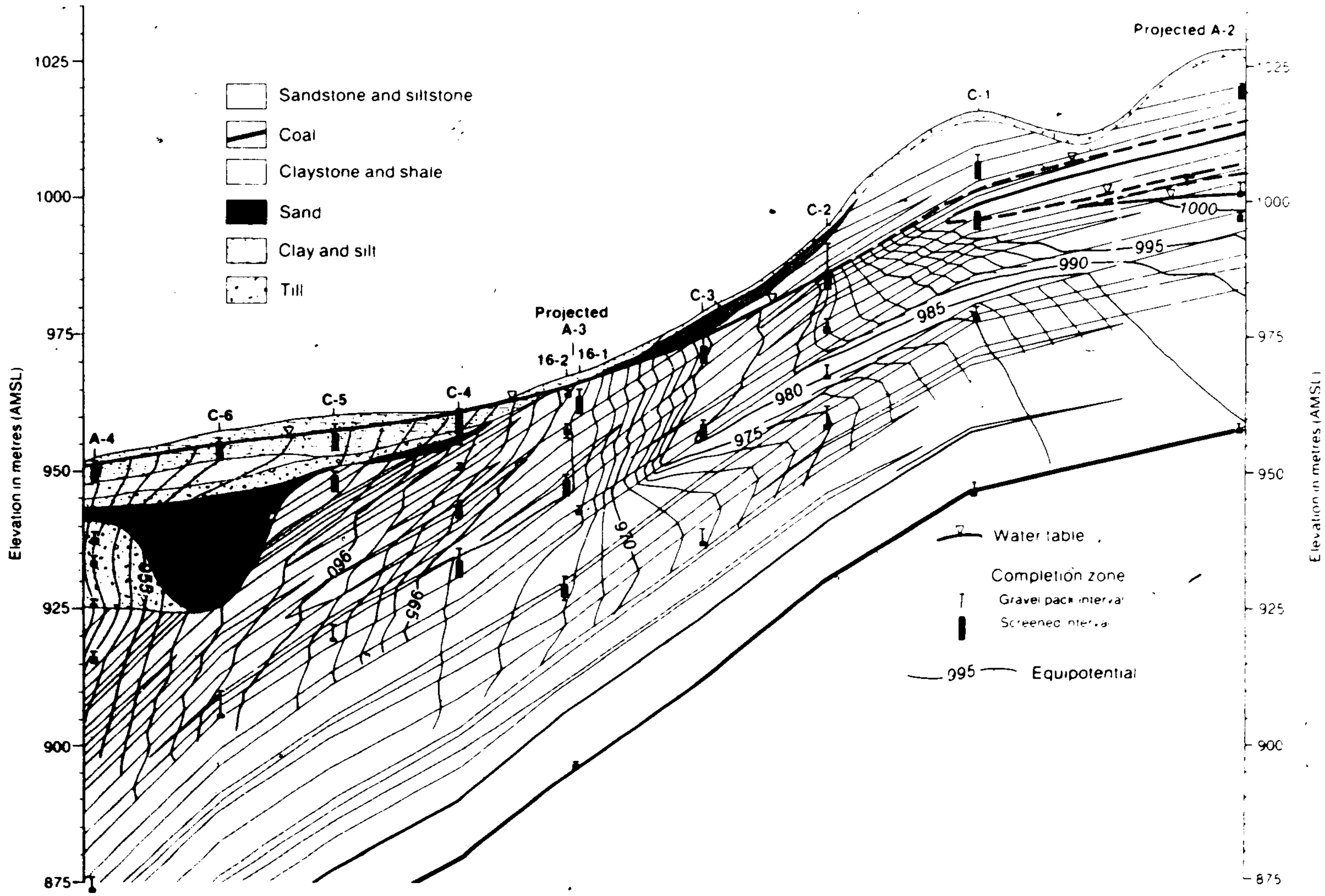

Figure 10. C-Line, geology and hydraulic head distribution.

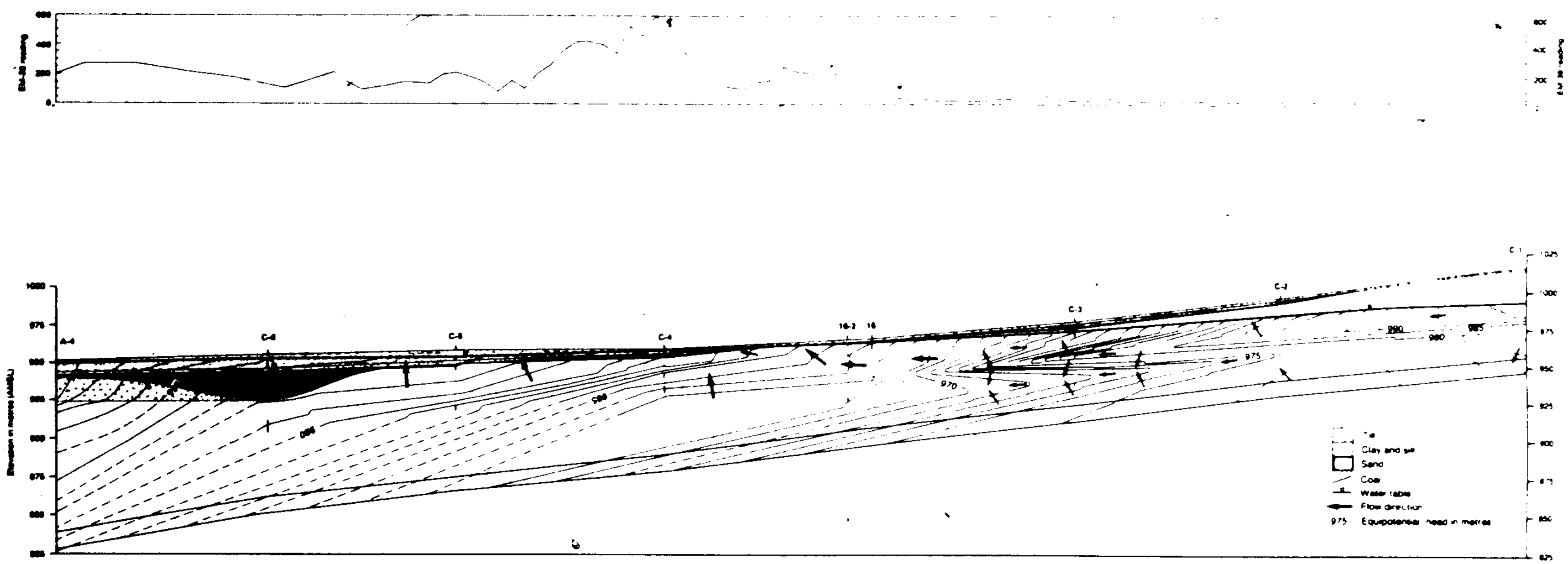

Figure 11. C-Line, hydraulic head and generalized groundwater flow distribution.

geologic information about this part of the study area. Two features, the very high degree of bedrock fracturing and the existence of a sand and gravel filled channel have already been discussed. In addition, a thin, but extensive, sand unit lies on bedrock along the lower slopes of Blackspring Ridge (Sites C2, C3, and C4).

The water table is very deep in upper portions of the section (about 21 m at C1 and 10 m at C2) and reflects lateral drainage (out of the section) toward sandstone outcrops in the coulee located about one-half kilometre to the north. Perched conditions within sandstone beds above the water table are probable.

The potential distribution is characterized by large changes in hydraulic gradients and gradient directions. In particular, a claystone unit (located from about 24 to 30 m at Site C2) partitions groundwater flow above and below the unit. Above the unit, groundwater flows preferentially in fractured sandstone beds. Upward directed components exist downslope from about midway between Sites C1 and C2. Groundwater flows downward through the claystone unit and into underlying sandstone beds from Site C1 to just upslope from Site 16. From this point on down the section, all flow is upward.

The potential configuration near Site 16 is also unique in other respects. The lateral gradient within a thin sandstone bed above the claystone unit becomes very steep between Sites C3 and 16, indicating that a discontinuity in hydraulic conductivity (either textural or structural in origin) must exist. Between Sites 16 and C4, the lateral hydraulic gradient in the same sandstone changes again to become much lower. Limited water-level data indicate that the low-gradient zone also extends below the sandstone unit.

The low-gradient region below the sandstone may result from one or more of the following conditions:

1) the region could be highly fractured and permeable and thus require a lower gradient to transmit water;
2) the hydraulic-conductivity discontinuity mentioned above dissipates gradients upstream from the discontinuity; or,
3) it could represent a stagnant point at a junction of flow systems.

A significant change in hydraulic gradient also exists above the thin sandstone bed mentioned above from about Site 16-2, upslope and midway to Site C3. The difference here is that the steep cross-formational gradient normally associated with claystone units of low hydraulic conductivity is absent, and groundwater flow has a high lateral component even in claystone units. This distribution may be caused by localized fracturing in this region, which has also affected the claystone units.

The high hydraulic conductivity measured in claystone and shale at Site 16WT ($k_h = 4 \times 10^{-7}$ m/sec) and extreme brecciation and iron staining noted in auger and rotary drill cuttings support this interpretation. Fracturing thus probably provides a good vertical hydraulic connection between the thin sandstone bed at about 25 m and the water table in this region.

Downslope from Site C4 the hydraulic gradient and groundwater flow continue to be strongly upward, particularly above the stratified channel deposits in the vicinity of Site C6.

A final observation with respect to groundwater flow along the C-Line is worth mentioning. A three-dimensional effect should be evident in the hydraulic head distribution downslope from approximately the location of Site C4. Upslope from Site C4, the section is oriented approximately normal to the topographic slope. Flow out of the section is directed toward the previously mentioned coulee. Between C4 and C5, however, the line is located at the base of a roughly bowl-shaped depression formed by several coulees. Flow from the sides of the depression should be directed toward the C-Line and thus intensify groundwater discharge in this region.

2.4.3 Water level fluctuations and responses

Hydrographs for the various piezometers and water-table wells are given in Appendix 6 along with rainfall data. Selected plots are presented in this section to illustrate specific characteristics. Symbols used to represent free-flowing and frozen conditions on hydrographs are plotted at the elevation of the top of the respective piezometer. Gaps in hydrographs represent cleaning, sampling, and hydraulic-testing intervals.

In general, water-level fluctuations are greatest in shallow wells and piezometers and can usually be correlated to precipitation events. Piezometers typically respond with reduced amplitude and increased time delays with increased depth. While the demarcation line between high and low amplitudes of fluctuation is obviously subjective, it is considered here that fluctuations of about 0.2 m or more result from host-rock conditions with respect to hydraulic conductivity that allow hydraulic head perturbations to be transmitted rapidly. Such fluctuations typically occur in water-table wells, in piezometers completed in weathered drift sediment less than 18 m deep, and in regions of bedrock with evidence of fracturing as described in previous sections.

The last bedrock zone correlates especially well with a zone of high TDS and $SO_4^=$ content (Figures 13 and 14) extending to about 30 m below the water table and the bedrock surface. In this region water level fluctuations from about 0.2 to 1 m occurred in 1986 (see hydrographs C2-40, C3-30, 16-2-38, C4-36, C4-65, C4-100, C5-45, C5-135 and C6-170; Appendix 6). Water-level fluctuations of this type probably correlate with zones of relatively active groundwater flow.

Water level fluctuations in several other deep wells in bedrock exhibit trends that may support previous geologic interpretations. Specifically, water levels in some piezometers situated in bedrock units of Section B that were postulated to be in hydraulic connection with basal gravel of the buried Carmangay Valley via terrace sand and gravel deposits, [Piezometers B3-268 and B5 (83, 118, 194 and 228)] exhibit water-level behavior similar to that in the piezometer completed in buried valley deposits (B6-355). The trend for 1984 to 1986 is, in all cases, a drop of about 1 m.

Similarly, the water level in piezometer A1-197 shows a decline of about 1 m while that of A2-232 stays essentially the same. Both are completed in the same coal seam and hydraulic conductivity is similar at both sites. It is possible that the difference in behavior is due to their location with respect to the fault postulated to exist near Site A2. In other words, they are located on different sides of the postulated hydraulic barrier. East of the barrier, the coal seam may be draining toward its subcrop, whereas west of the barrier, it is not in hydraulic connection with the subcrop.

2.4.4 Depth to water table

There is a considerable range in the depth to the water table. Although rigorous proof is not available, relative water levels, iron-stained fractures to 23 m at Site C1, loss of circulation at 25 m at Site A2, and shapes of slug test response curves indicate that a discontinuous series of perched water tables exist along about the upper half of the western ridge flank. A very steep vertical hydraulic gradient (>1.0), mirabilite and gypsum occurrences at 14 m, and an oxidized till zone at 23 m at Site B5 indicate that perched conditions may also exist in drift sediment for a considerable distance from the Little Bow River.

In general, the depth to the water table on top of Blackspring Ridge ranges from 5 to 6 m. Discontinuous unsaturated zones may occur to a depth of 25 m along the western upper edge of the ridge and for a distance of more than 3 km from the Little Bow River. On the lacustrine plain the depth ranges from less than 1 to about 3 m.

Values of the shallowest depth to the water table measured in 1986 in the area of detailed investigation are contoured in Figure 12. Shallowest water-table occurrences are in saline areas along the base of Blackspring Ridge and in the vicinity of the temporary Peacock Slough (Site A5). Depths greater than 3 m at Sites C5 and 11 result from minor surface elevation increases in areas of sandy surface deposits.

2.4.5 Hydrochemistry

The major-ion chemistry of samples from piezometer nests of the C-Line are given in Figures 13 to 19. Tabulation of hydrochemical analyses from the A, B, and C-Lines, is given in Appendix 7, and Piper

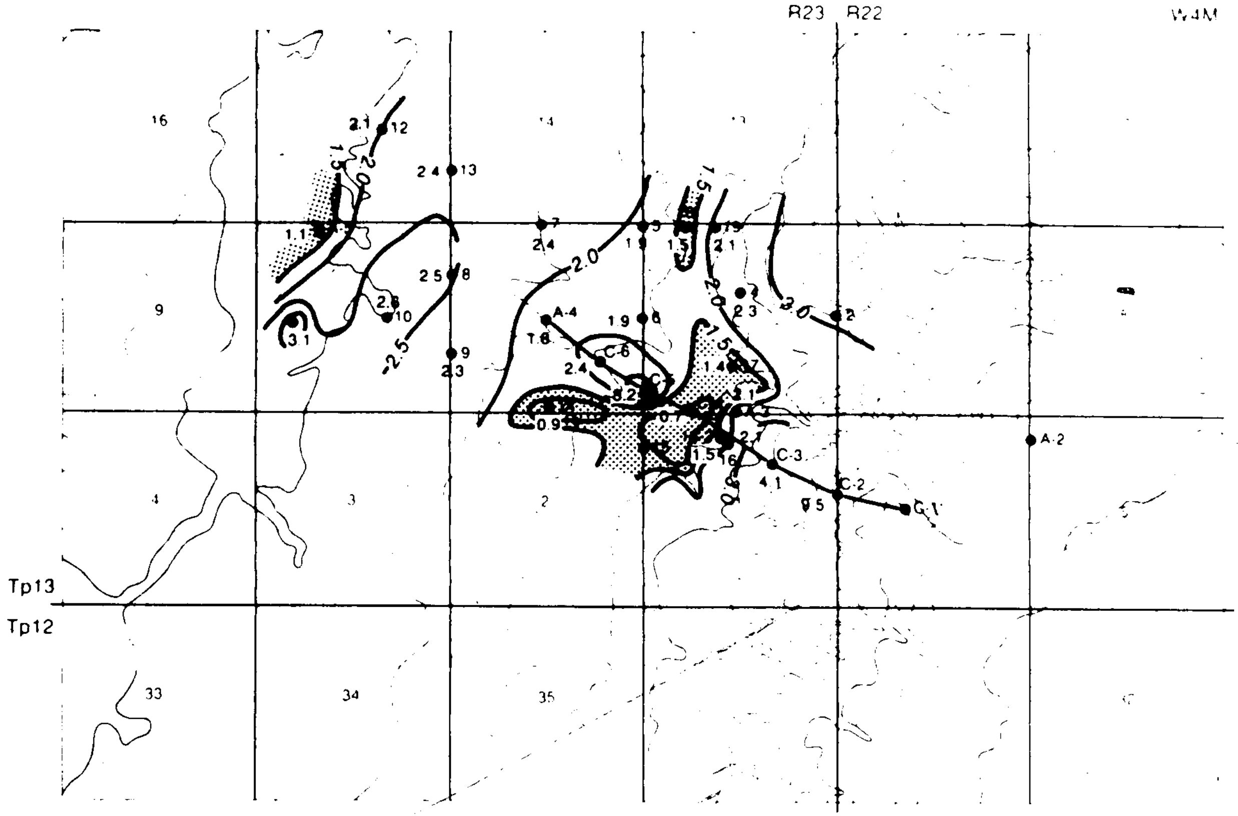

Figure 12. Shallowest depth to water table (1986).

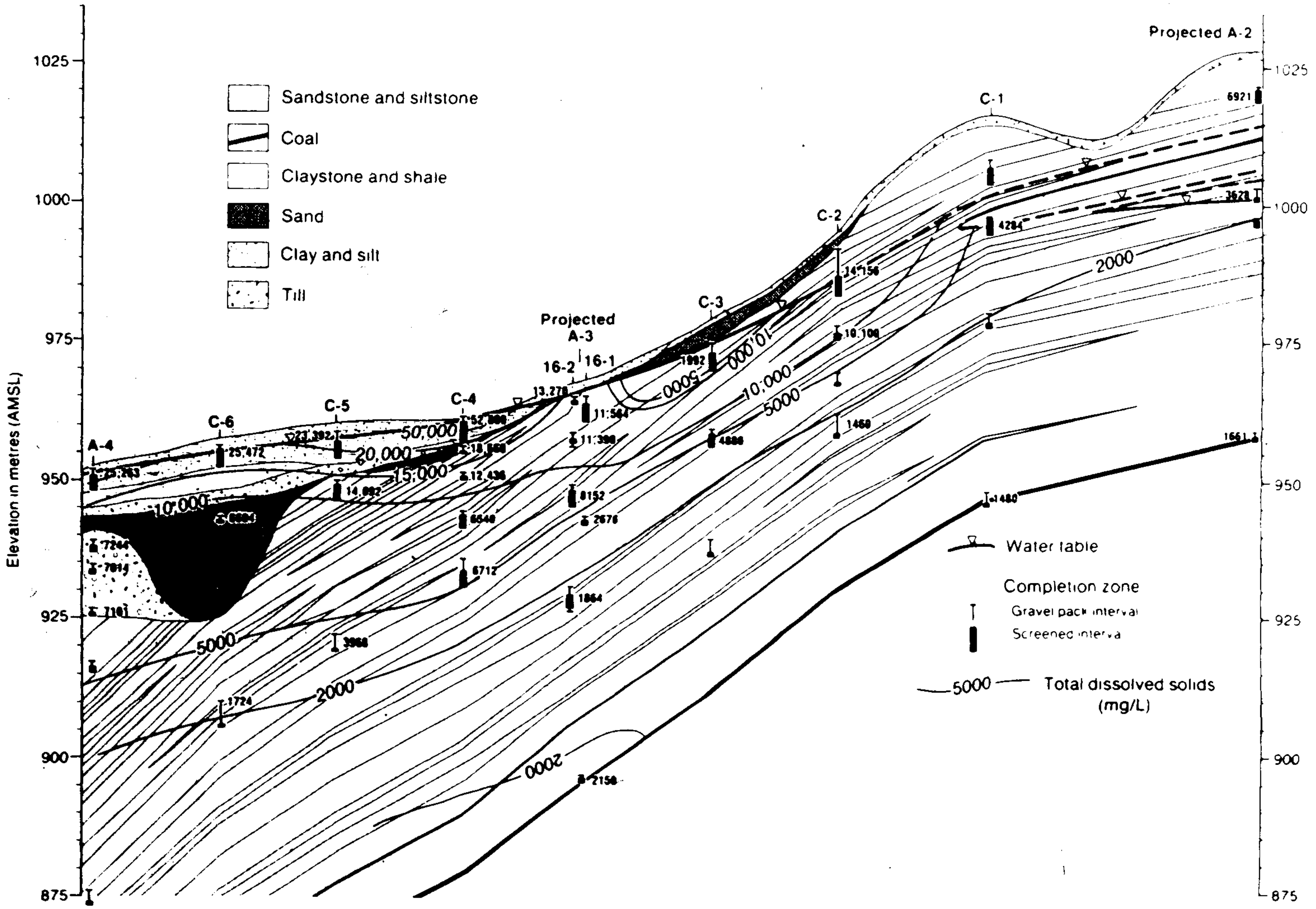

Figure 13. C-Line hydrochemistry: total dissolved solids distribution.

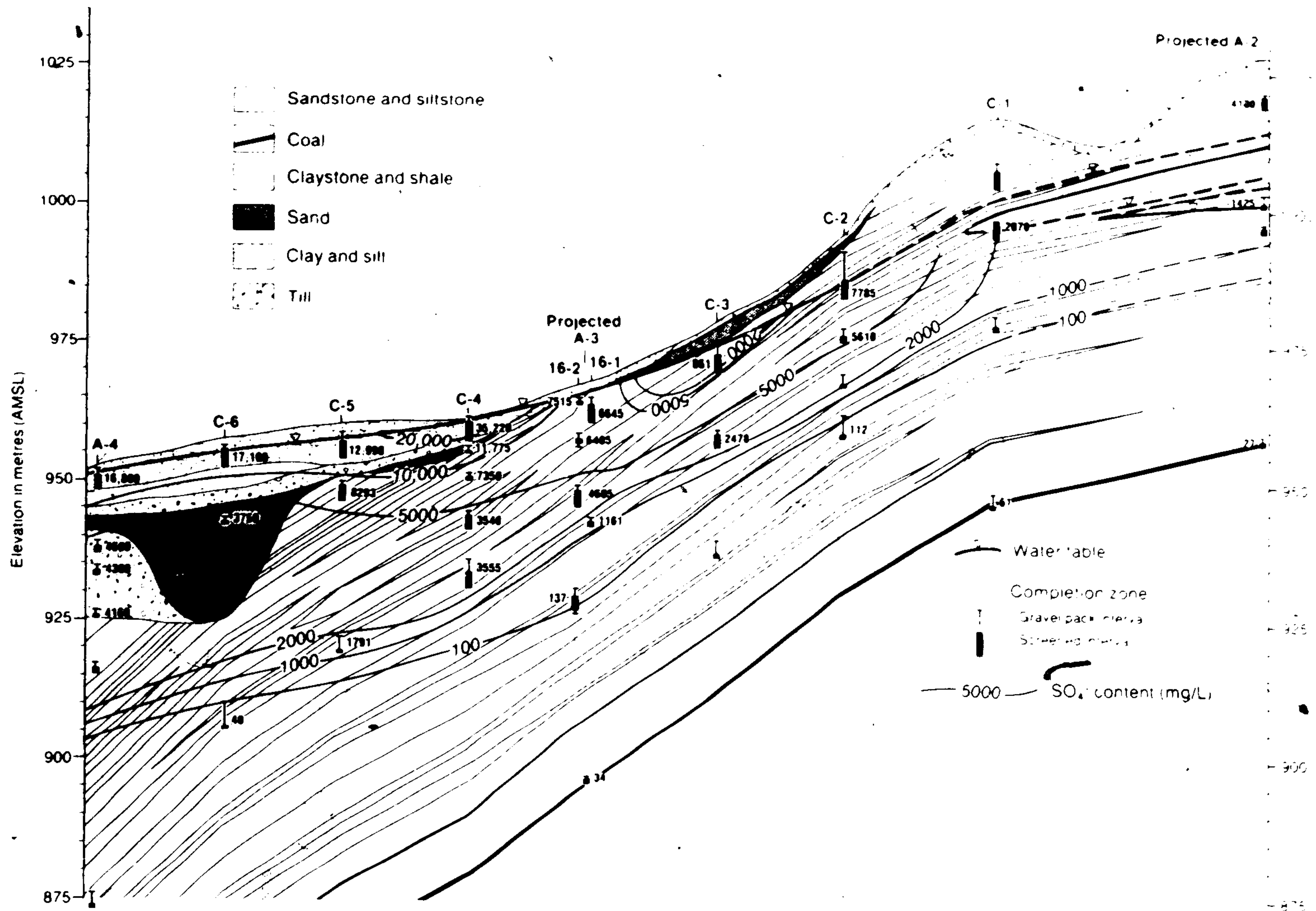

Figure 14. C-Line hydrochemistry: sulfate-ion distribution.

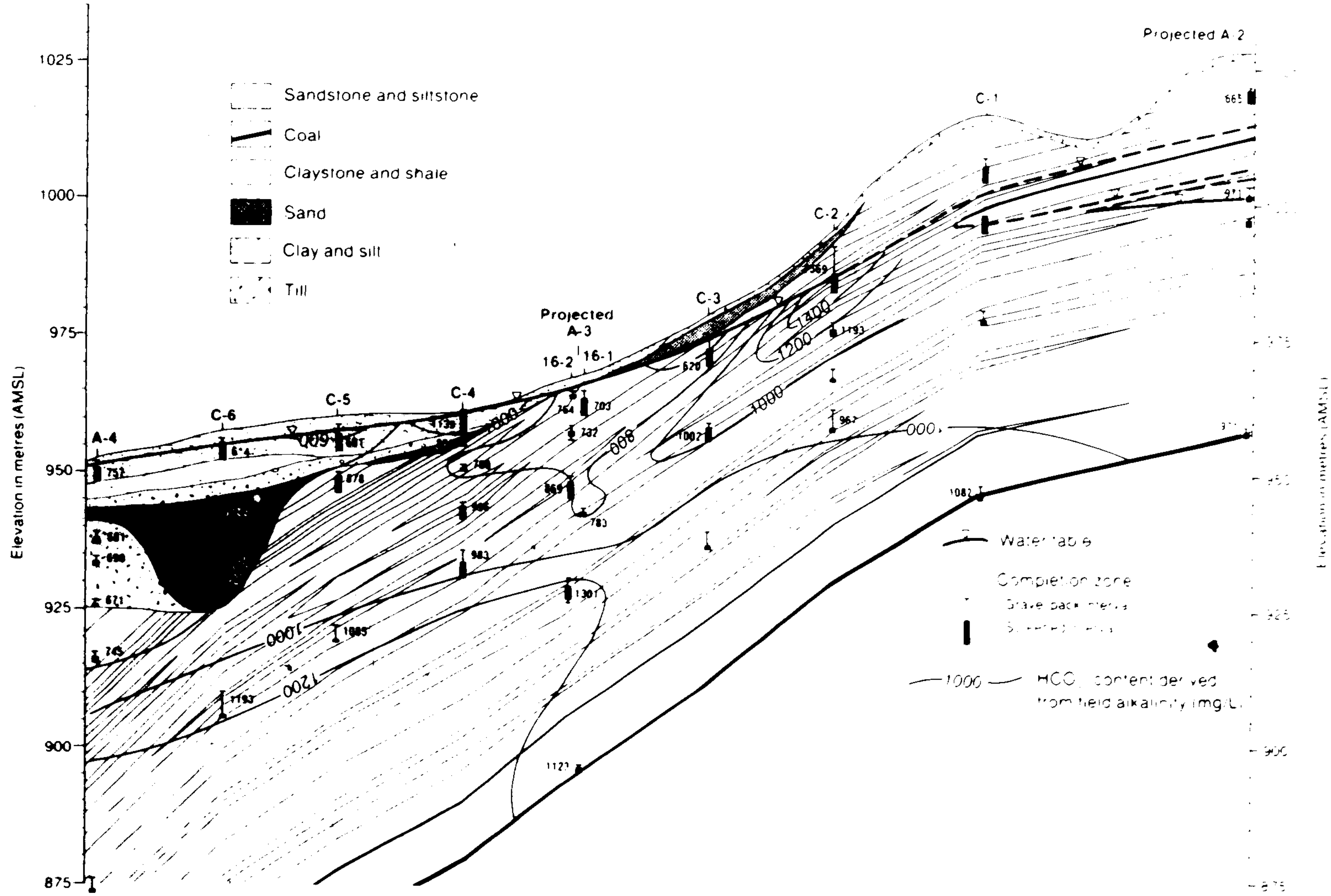

Figure 15. C-Line hydrochemistry: bicarbonate-ion distribution.

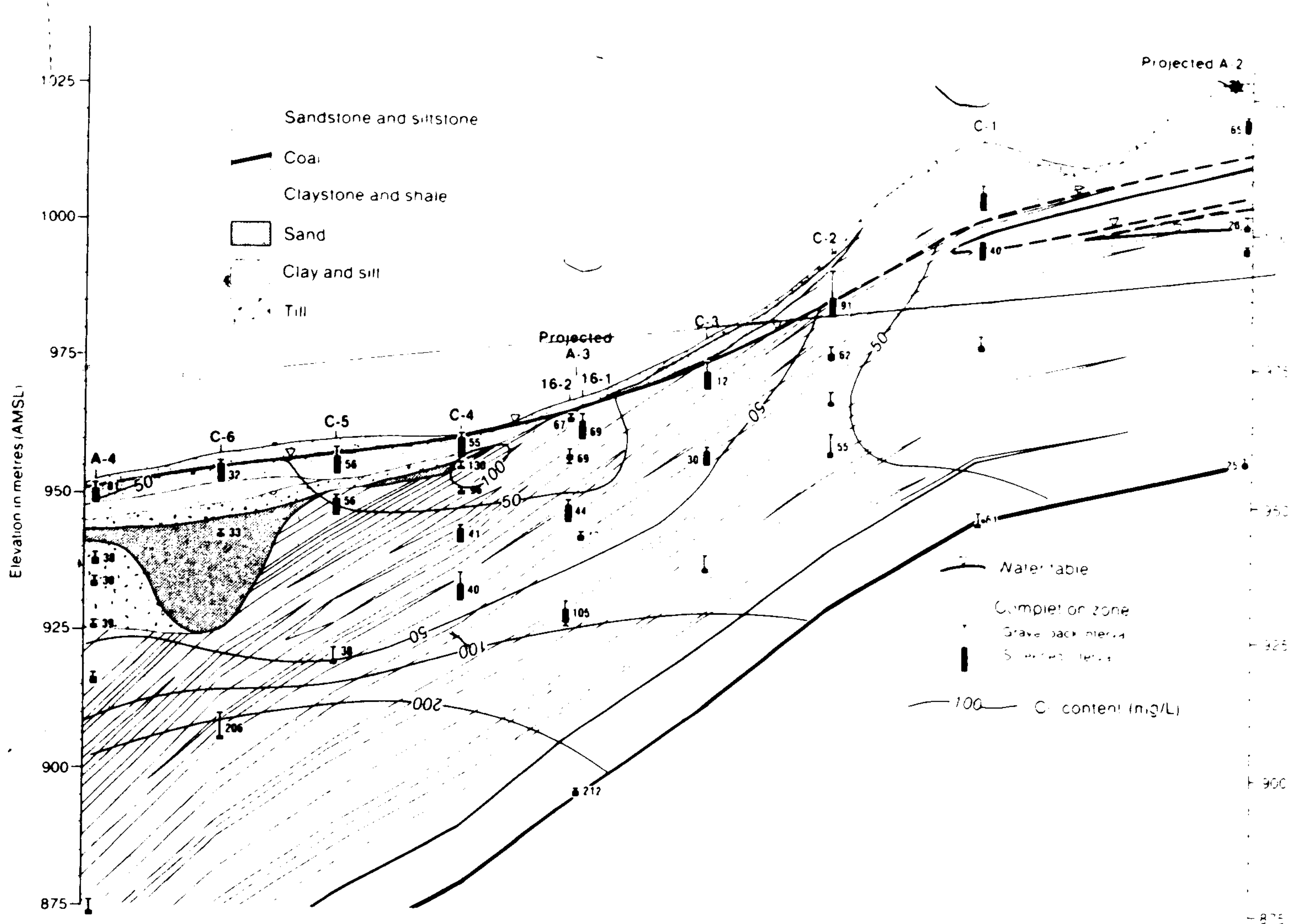

Figure 16. C-Line hydrochemistry: chloride-ion distribution.

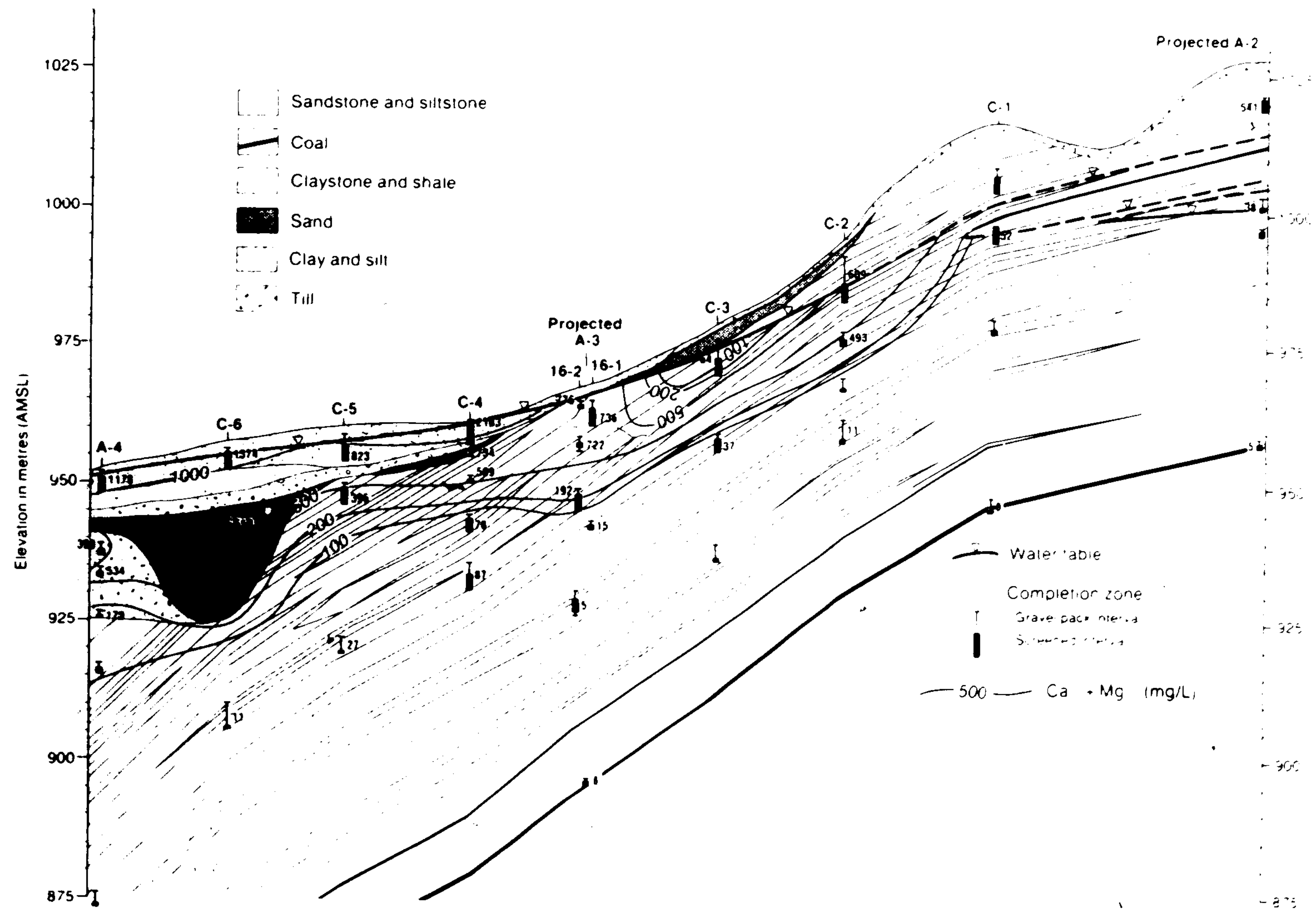

Figure 17. C-Line hydrochemistry: calcium plus magnesium-ion distribution.

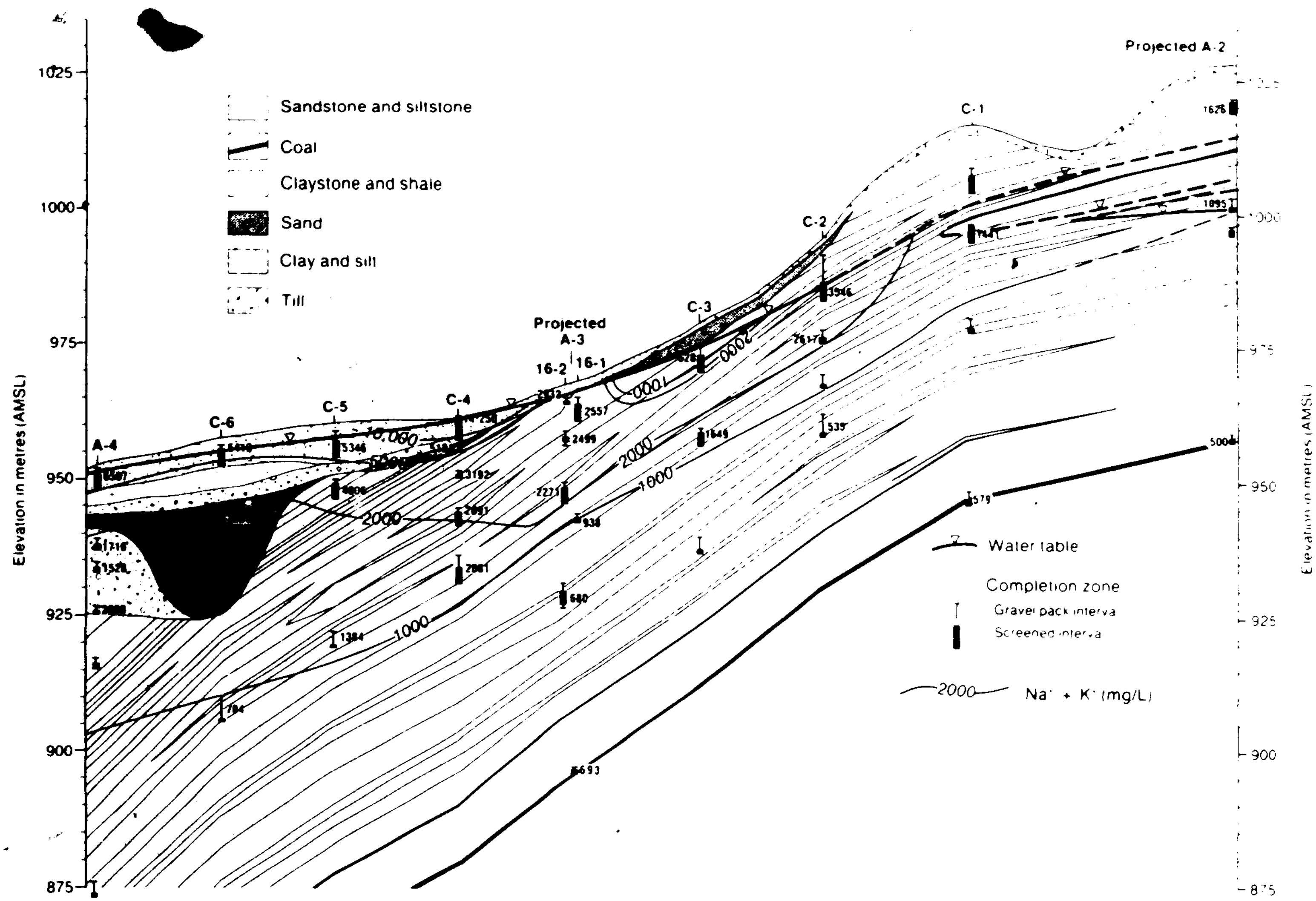

Figure 18. C-Line hydrochemistry: sodium plus potassium-ion distribution.

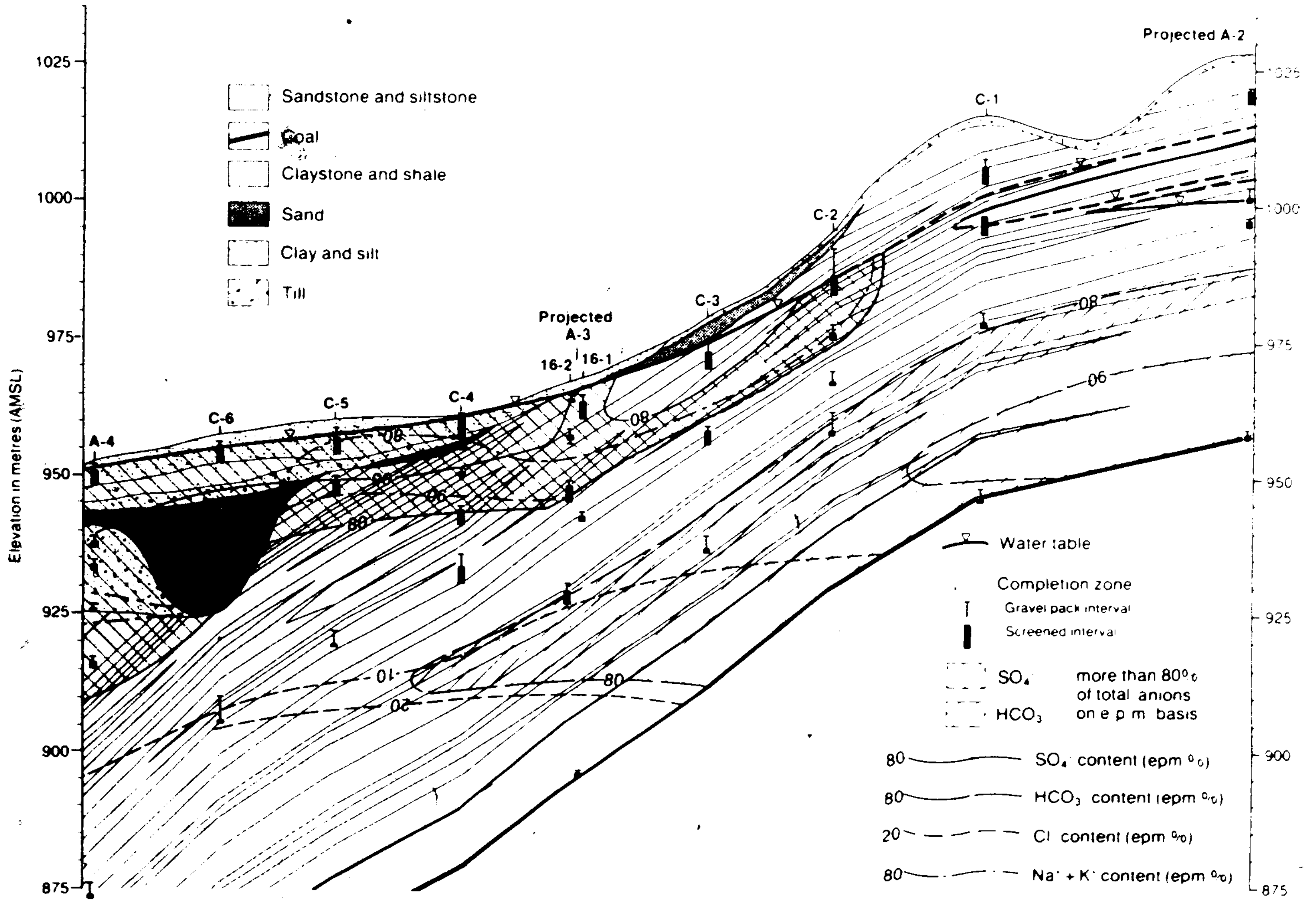

Figure 19. C-Line hydrochemistry: hydrochemical facies.

trilinear diagrams of hydrochemistry from individual piezometer nests are given in Appendix 8.

The most striking feature with respect to hydrochemistry along the C-Line is the very strong zonation of total dissolved solids (TDS) and sulfate ion ($SO_4^=$) distribution within areas extending about 30 m below the water table and the bedrock surface. The dominant cation in this region is Na^+, but Ca^{++} and Mg^{++} exist in significant amounts (up to about 35 percent of cations) in upper portions, particularly at Site C3 and in stratified channel and drift sediment at C6 and A4. TDS and $SO_4^=$ content of groundwater of this zone are generally above 6000 mg/L and 3000 mg/L, respectively, and increase toward the water table to values exceeding 20 000 and 10 000 mg/L, respectively.

Below the upper zone, $SO_4^=$ and TDS content decrease rapidly to values of less than 100 and 2000 mg/L, respectively, and groundwater tends toward a $NaHCO_3$ type of composition. This is in turn underlain by a zone of increased TDS content and water tending toward a $NaHCO_3$/Cl type of composition.

The distribution of dissolved constituents is such that the following conclusions appear valid.

1. The majority of the dissolved salts within the groundwater flow region are generated and transported within the shallow region less than 30 m below the water table. The generation of sulfate occurs over very short distances of vertical travel as evidenced by contents of 2200 and 4300 mg/L in water from Well A1-WT and Piezometer B1-34, respectively.
2. Anaeorobic reduction of sulfate appears to be occurring in the intermediate and lower zones as evidenced by severe decreases in

$SO_4^{=}$ content and general increases of HCO_3^- content with increased depth, along the same flow path.

3. The substantial Ca^{++} and Mg^{++} content of groundwater in the upper bedrock zone may be additional evidence that groundwater flow is predominantly fracture oriented. Fracture-dominated flow should result in a restricted degree of contact with clay particles and thus inhibit cation exchange processes which would otherwise be occurring.

4. There exist two distortions in hydrochemical patterns that are significant in terms of recharge to the water table. The first is situated at the C2 Site and constitutes a plume of water with very high TDS and $SO_4^{=}$ content which is being added to the system at the water table. The interpretation is that perched water-table conditions exist in sandstone beds stratigraphically and topographically above the water table in this region and that water and dissolved salts are added to the saturated zone by flow from these sandstone beds. The second is a plume of water with low TDS and $SO_4^{=}$ content being added in the vicinity of Site C3. In this area, however, a sandstone bed comes into contact with a shallow drift sand layer and relatively fresh water is added to the system.

2.4.6 Environmental isotopes

2.4.6.1 Tritium

Results of tritium analyses are tabulated in Appendix 9. Those for water extracted from cores are shown as depth profiles for selected sites in Figure 20. Depth profiles are presented both for areas

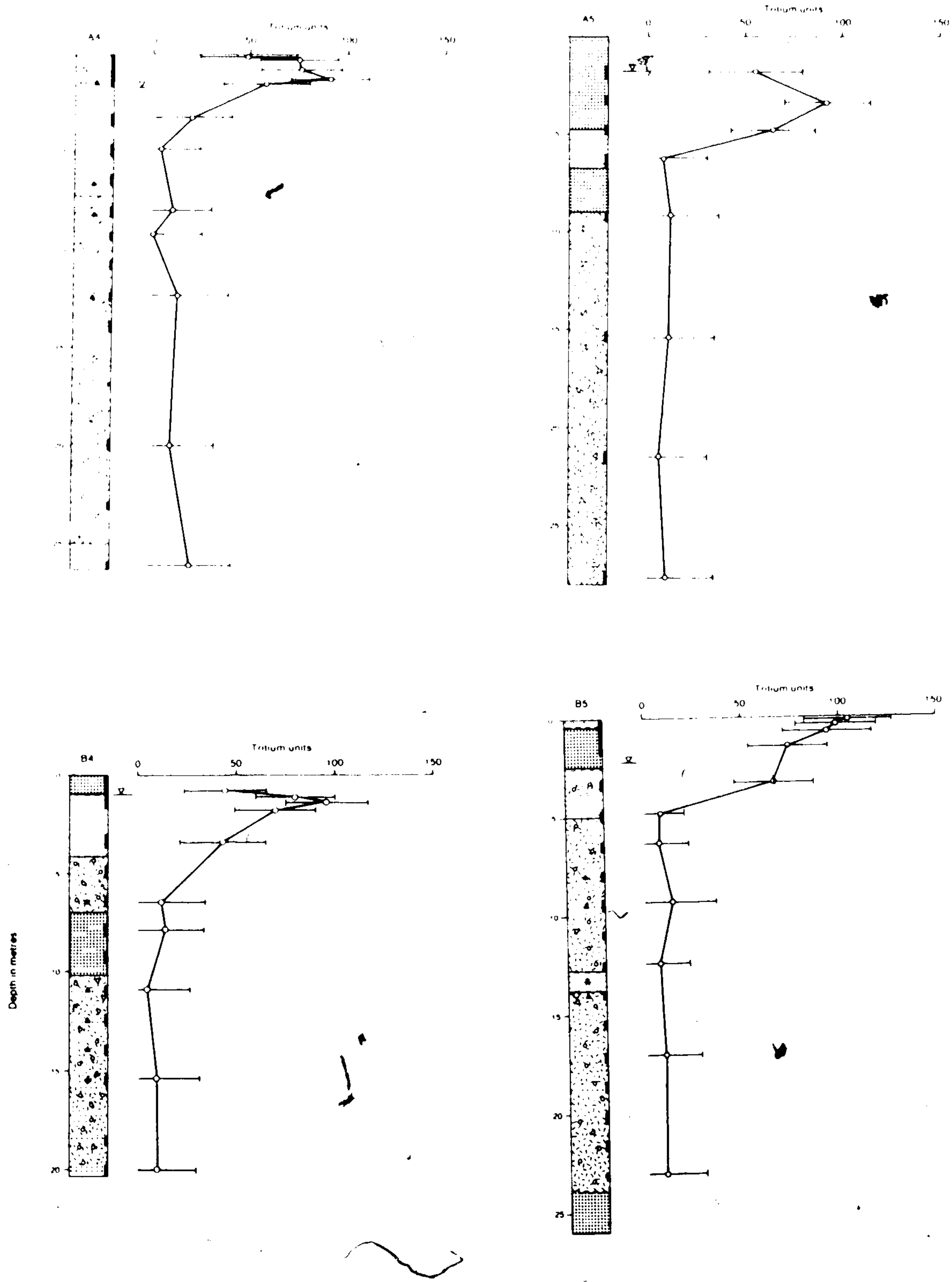

Figure 20a. Tritium content of core-water extracts from Sites A4, A5, B4, and B5.

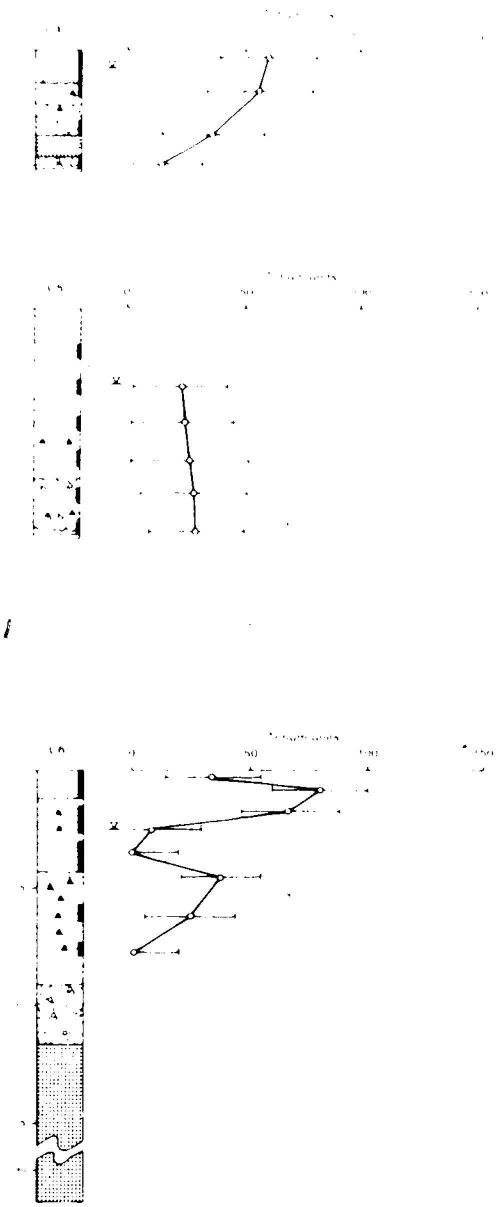

Figure 20b. Tritium content of core-water extracts from Sites C4, C5, and C6

characterized by downward hydraulic gradients (Sites B4 and B5), and by upward gradients (Sites A4, A5, C4, C5, and C6) in near-surface sediment. The profiles show that tritium levels well above detection limits are present to depths of generally 5 m, or about 3 m below the water table.

The peak in activity occurs near, or above, the water table at values of about 90 to 110 tritium units. Activities as high as 130 and 240 tritium units were measured in core-water samples from Sites 10 and 13, respectively. Because the peak values are substantially higher than those determined for 1984 to 1986 Alberta precipitation water and Blackspring Ridge area surface and snow water, they may represent water emplaced after 1952 and mixing of this with more recent water. The close association of the peaks with the position of the water table also suggests that some degree of evaporative enrichment is occurring above the water table.

Zones of high tritium content are not confined to areas of downward hydraulic gradients but appear to occur everywhere in the upper 2 to 3 m of the saturated zone. Recharge to the water table by infiltration of precipitation and snowmelt water is thus occurring both in areas of groundwater recharge and groundwater discharge. This concept is corroborated by the relationship between recharge events and water-table fluctuations (see discussion in 3.4.1).

2.4.6.2 Stable isotopes

Stable isotope values determined for the various waters of the region are plotted as $\delta^{18}O$ versus δD diagrams (Figure 21), and along the C-Line (Figure 22) to show variations within the groundwater flow

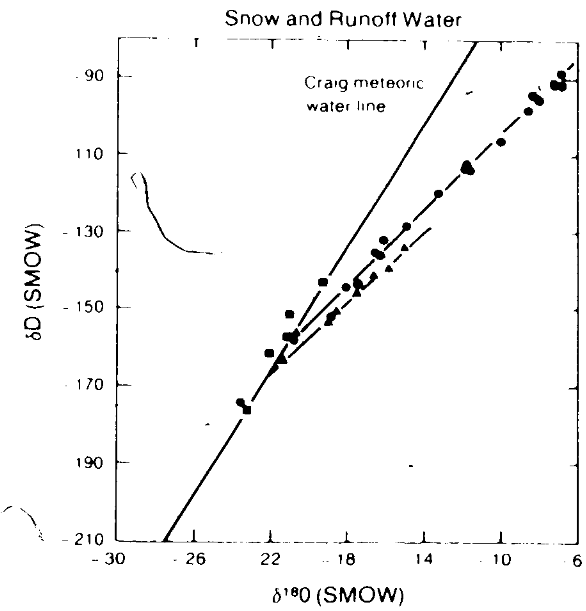

Figure 21a δD vs $\delta^{18}O$ for snow and runoff water

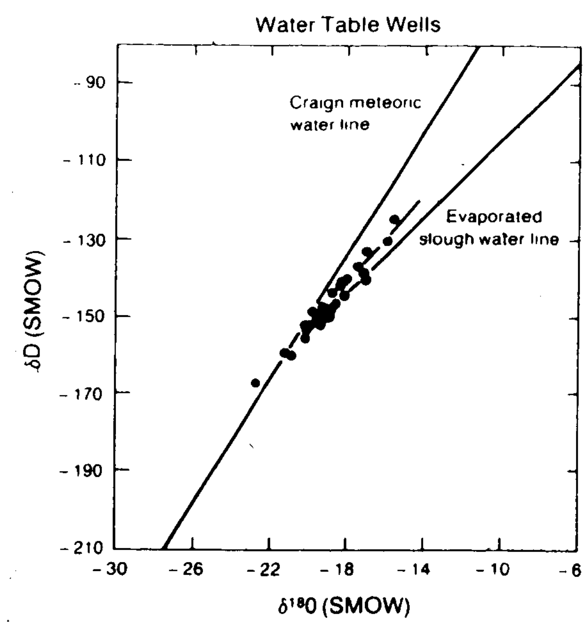

Figure 21b. δD vs $\delta^{18}O$ for water table well water

$\delta D = 5.78\,\delta^{18}O - 37.37 \quad r^2 = 0.94$

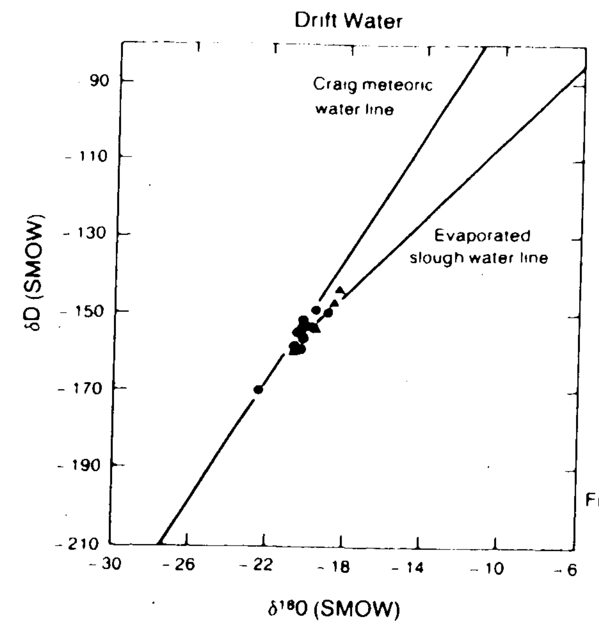

Figure 21c. δD vs δ¹⁸O for drift water

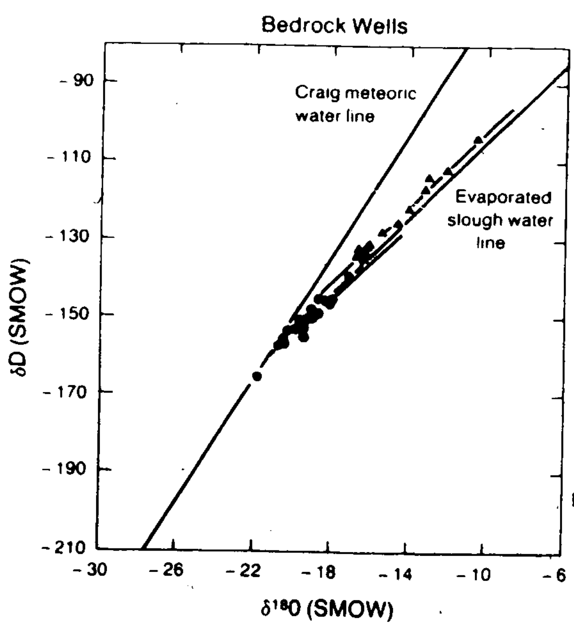

Figure 21d. δD vs δ¹⁸O for bedrock-well water.

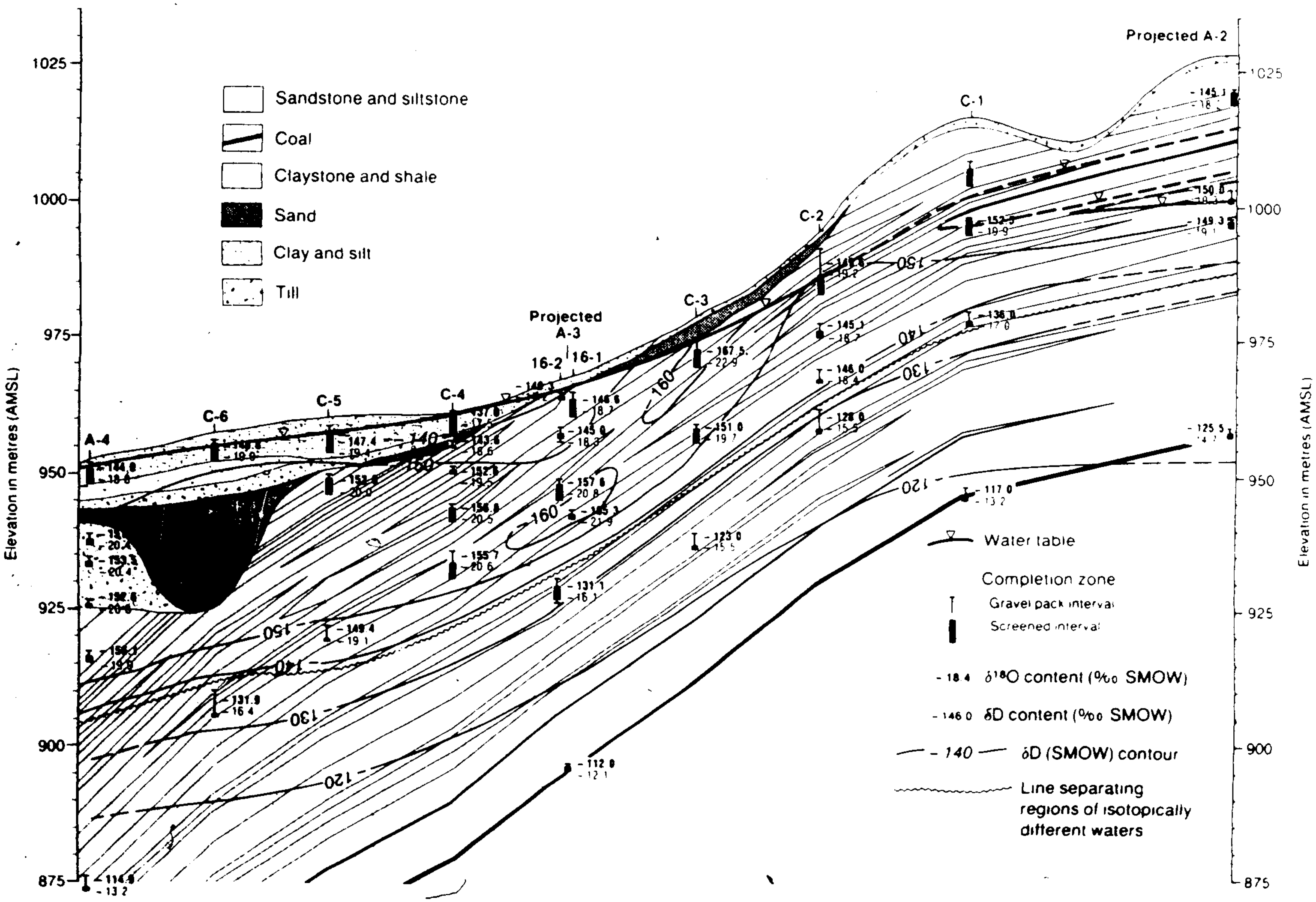

Figure 22. $\delta^{18}O$ vs. δD (SMOW) distribution along the C-Line.

domain. Individual determinations are given in Appendix 10.

Snow samples were collected from December 1983 to February 1986. Snow samples were taken if it was felt that no significant melting had occurred. These are thus felt to generally represent snow in a fresh condition. Surface water was sampled from the Peacock Slough (1985 and 1986), from a small temporary slough in SW 5-22-13 W4 (1985), and from a small dugout located about 100 m south of Site A1 (1985). Water was sampled biweekly from the time of the spring snowmelt event to dryness. Groundwater was sampled from piezometers and water-table wells in July of 1986.

Deuterium versus ^{18}O data were grouped with respect to water type. Linear regression equations characterizing these data are given in Table 2.

Table 2. Deuterium and ^{18}O relationships.

Water type	Equation	n	r^2
Spring snowmelt/runoff water Peacock and upland sloughs	*$\delta D = 4.95\ \delta\ ^{18}O - 54.80$	18	0.99
Dugout water	*$\delta D = 4.65\ \delta\ ^{18}O - 64.16$	6	0.99
Water-table water	$\delta D = 5.78\ \delta\ ^{18}O - 37.37$	34	0.94
Shallow bedrock water	$\delta D = 4.76\ \delta\ ^{18}O - 58.59$	20	0.91
Deep bedrock water	$\delta D = 4.93\ \delta\ ^{18}O - 51.75$	13	0.99

* Two values that plot along the Craig meteoric water line are omitted from the regression analysis.

The line through samples from the two sloughs is considered to represent an evaporation line for the area. There is a slight, but distinct, difference between the intercepts, of these and the evaporation line for samples from the dugout, with the meteoric water line. The dugout probably contained a larger proportion of snow that fell during colder winter months than did the snowmelt waters that accumulated in the two sloughs.

Water-table and drift water plots on or between the evaporated-water line and the Craig meteoric water line. Sources for this water are thus consistent with precipitation, evaporated precipitation, and mixtures of the two, all having occurred under climatic conditions similar to the present.

Bedrock water plots along two slightly, but distinctly, different lines (Figure 21d). The stable isotopic composition of shallow bedrock water is very close to present-day evaporated and nonevaporated water; intercepts with the meteoric water line are essentially identical. Deeper bedrock water appears to have recharged under slightly warmer climatic conditions. The intercept of the deep bedrock water line with the meteoric water line is displaced upward, consistent with precipitation under warmer conditions. This is thus considered to be considerably older water than shallow bedrock and drift water.

2.5 Surface Water Hydrology

As the study proceeded, it became increasingly apparent that surface water, and in particular snowmelt water, plays an important role in recharge to the water table. A qualitative examination was carried out to define the essential framework of the local setting.

About 25 km^2 of surface area contributes drainage to the Peacock Slough directly from the east (Figure 23), but the total area is likely at least twice as large considering contributions from the south and west. The basin is poorly defined due to the gradual slope between the base of Blackspring Ridge and the Peacock Slough.

To get a general feeling for runoff volumes and disposition of water on the landscape during the spring melt, a survey was conducted on March 4, 1986 with a small fixed-wing aircraft. Photographs, with drill and piezometer-nest sites for location reference, are given in Plate 4. The survey followed a late February snowstorm and much of the water appearing in Plate 4 is the result of snowmelt from this storm.

Winter temperature, chinook and other wind conditions in the region are such that usually snow remains on the landscape for relatively short periods of time only. It is felt that much of the snow sublimates, and melting during winter months is common. Severe winds generally redistribute the snow such that it accumulates in significant volumes only in natural or man-made depressions. Road ditches, especially those along north-south road allowances, commonly still contain snow and sometimes ice, up to the time of the spring snow melt. The largest and most persistent snow accumulations occur, however, in coulees, and in particular at the head of the coulee located in Section 7 of 13-22 W4.

During the time of spring thaw, snowmelt from the coulees, from ditches, and from late snowstorms, flows down the coulees and onto the lacustrine plain. A significant aspect of the surface drainage is that the natural, or pre-agricultural, drainage pattern has been severely disrupted. Surface water is now artificially routed along road-allowance and in-field ditches. Ditches along road allowances are

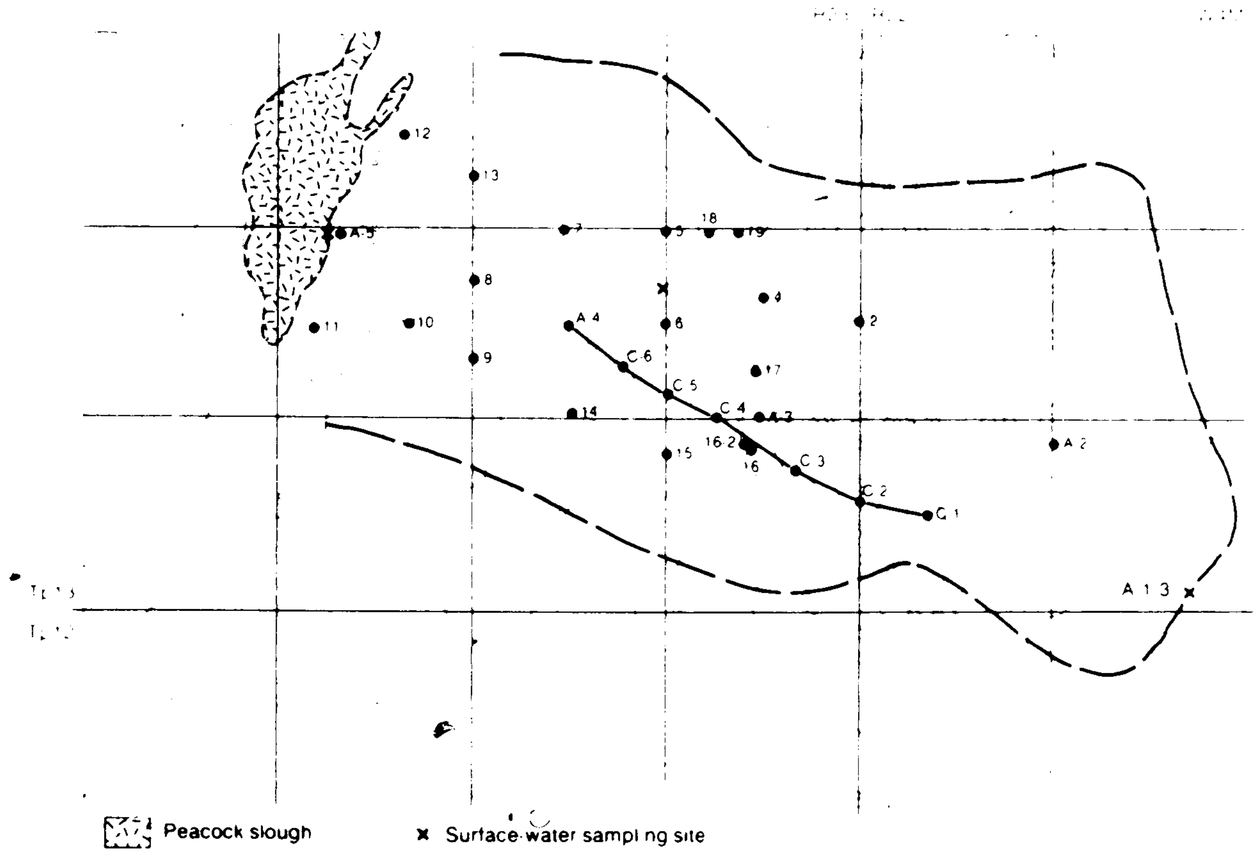

Figure 23. Drainage area for the Peacock Slough.

aligned in regular compass directions and not with topographic slope, with the result that runoff water cannot, in general, follow the shortest (or pre-agricultural) route to low areas in the landscape. Both residence time of surface water on the landscape and total surface area exposed to infiltration are now increased.

The large amount of runoff water on the landscape during the spring thaw in the three years of observation was always surprising. The culvert shown in Plate 5 was estimated to discharge at about 55 L/sec and, during the years of investigation, discharged for as much as two weeks. Similar rates of surface flows were observed to discharge onto the areas of interdunal salinity of Section 35-13-23 W4. None of this water, however, left Section 35 and 36 as surface runoff.

During the time of runoff, road ditches are commonly full and overflow onto fields, where minor drainage depressions and tillage furrows continue to distribute the surface water. When observing this phenomenon, both on the ground and from the air (see Plate 4), the impression is that the recharge to the water table that is caused by the spring thaw is only in part closed-depression oriented. A major portion of this recharge is more accurately described as a "flood irrigation" event.

3. EVALUATION OF THE ORIGIN OF SALINITY

3.1 General

Profiles of saturation extract results (Appendix 3) and EM38 traverses (Figures 5, 6, and 11), show that in the Blackspring Ridge area there exist regions of salt leaching, and regions of salt accumulation. Leached profiles occur in upland areas with a deep water table and in areas where the near-surface hydraulic gradient is strongly downward (Sites A1, A2, B1, B5, B6). This leached zone may be thick (7 and 10 m at Sites B5 and B6, respectively) or thin (2.5 m) and confined to thin drift sediment (as at Sites A1 and A2).

For example, at Sites A1 and A2 the presence of essentially unleached bedrock sediment near the surface indicates that although leaching of sulfate salts in shallow drift zones may have gone almost to completion, the process is still active in near-surface bedrock. Leached drift profiles to about 3 m at Sites C1, C2, and C3 indicate that the thin sandy drift sediment overlying bedrock of much of the west flank of Blackspring Ridge is not now a major contributor of salt to the groundwater system. Thicker drift sediment (7 m at Site 17) and sediment that does not have appreciable sand content (Sites 4 and 18) may however still be significant contributors.

The one agent common to the process of leaching, transport, redistribution, and eventual accumulation of salts is water. Trahsport of salts to their eventual location of accumulation may occur along several pathways and may involve:

1. groundwater of deep, regional flow systems originating from the top of Blackspring Ridge and discharging in low-lying portions of the

lacustrine plain,

2. groundwater of flow systems of shallow and intermediate depths and contained within fractured bedrock units to depths of about 30 m, and weathered drift units to depths of about 15 to 20 m, and

3. precipitation or surface runoff water that reaches the water table by infiltration from above.

Data from the Blackspring Ridge area indicate that accumulations of salt result from a complex interplay of all the above pathways, but that the relative importance of sources differs from place to place.

To differentiate regions of local, intermediate, and regional groundwater flow so that their relative importance with respect to groundwater and salt contributions to various areas could be determined, a quantitative flow net was constructed for the A-Line. The flow net used the digitally determined potential distribution and is given in simplified form in Figure 24.

Luthin (1957) and Harr (1962) showed that anisotropic flow regions can be represented by equivalent isotropic regions by suitably expanding or contracting spatial coordinates, and that the equivalent hydraulic conductivity of the transformed region k_e, is $\sqrt{k_h k_v}$. For a medium in which $k_h = 10k_v$ the transformation requires an expansion of $\sqrt{10}$ in the vertical direction, after which an isotropic flow net can be drawn.

Harr (1962) discussed methodology of constructing such flow nets. The method involves drawing curvilinear squares in one unit of homogeneous hydraulic conductivity using equipotential lines at a consistent interval as two sides of the squares; the other two sides are then flow lines or stream lines bounding flow channels of constant discharge rate. In other homogeneous units with hydraulic conductivity

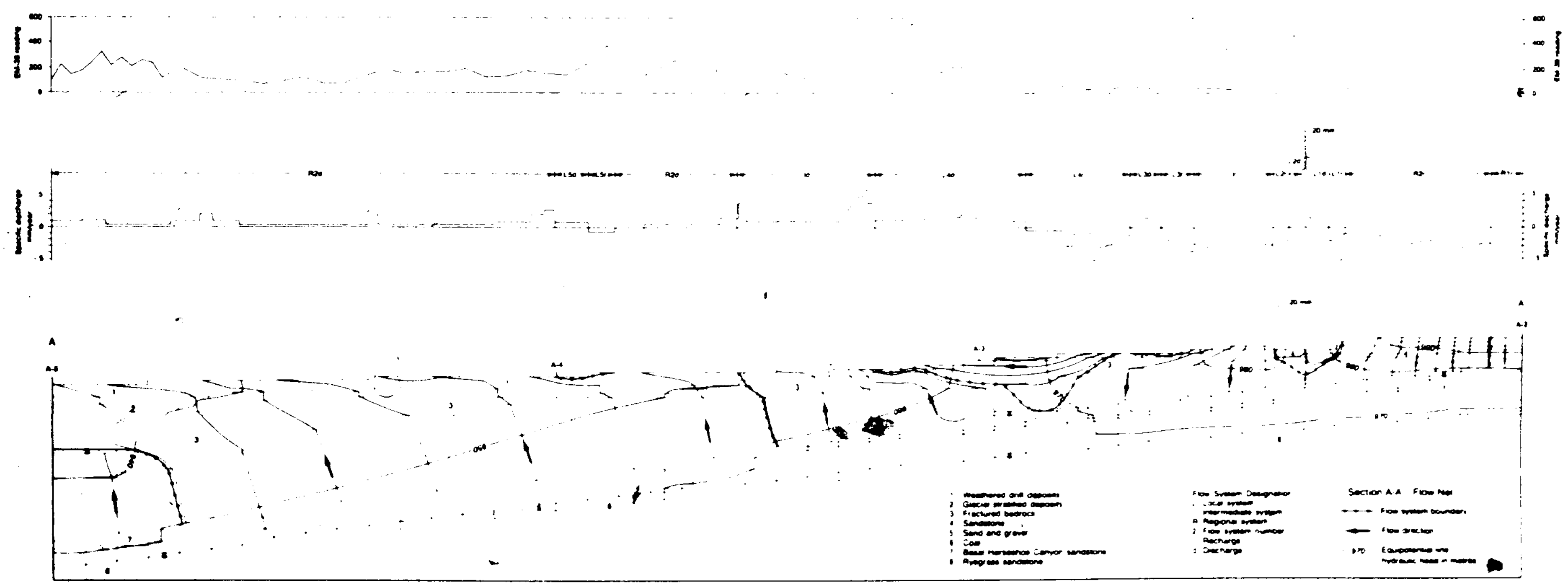

Figure 24. Flownet for transformed Section A.

different from the unit of curvilinear squares, curvilinear rectangles with a length to width ratio of k_x/k_{sq} (where k_x = hydraulic conductivity of the new unit and k_{sq} is that of the unit of curvilinear squares) are drawn. Once the flow lines have been determined the flow region can be subdivided into flow systems as defined by Toth (1962) and the disposition of all water within the flow region is known.

Freeze (1969) showed that the discharge in each flow channel derived in this manner, can be calculated by Darcy's Law as:

$$Q = k \cdot \frac{\Delta\phi}{\Delta s} \cdot \Delta m \cdot w$$

where

Q = discharge through a segment of the flow net,

k = hydraulic conductivity,

$\Delta\phi$ = drop in hydraulic head between equipotential surfaces,

Δs = length of flow path in the segment of the flow net,

Δm = width of the segment of the flow net perpendicular to the direction of flow, and

w = thickness of the flow system perpendicular to the plane of the diagram.

Since $\Delta s = \Delta m$ for any square portion of the flow net, and if a unit thickness of flow system is considered, this reduces to: $Q = k\Delta\phi$.

Figure 24 is a transformed section in which flow lines form curvilinear squares with equipotential lines spaced at 5-m head intervals in the siltstone, claystone, and shale unit of the Horseshoe Canyon Formation; every second such line is shown. The equivalent hydraulic conductivity for this unit is $[(2.0 \times 10^{-9})(2.0 \times 10^{-10})]^{1/2}$, or 6.3×10^{-10} m/sec; $\Delta\phi$ is 5 m. The discharge per flow tube is then 3.2×10^{-9} m^3/sec or 0.1 m^3/year for a cross-section width of 1 m

Dividing this rate by the length of cross section over which each flow tube recharges and discharges yields the annual recharge and discharge rates along the line of section and is also given in Figure 24.

Analysis of the flow net in Figure 24 gives the following results. The region can be divided into five local, one intermediate, and two regional flow systems. Local systems have adjacent areas of recharge and discharge; those of the intermediate and regional system are separated by one or more other systems. Total discharge of each system is given in Table 3.

Table 3. Groundwater discharge rates simulated for Section A.

Flow system		No. of Flow Channels		Discharge per year, (m^3)
(a) Regional	R1	3.9	17.9	0.4
	R2	14.0		1.4
(b) Intermediate	I	8.7	8.7	0.9
(c) Local	L1	≃2.0	19.1	0.2
	L2	≃5.0		0.5
	L3	≃4.0		0.4
	L4	7.4		0.7
	L5	≃1.0		0.1
Total		46.0		4.6

Groundwater discharging at the base of the ridge (at and below piezometer nest A3) originates from about the lower half of the ridge flank whereas that discharging under the lacustrine plain originates from about the upper half. Almost all of the flow within intermediate and regional systems is transmitted through the basal Horseshoe Canyon and Upper Bearpaw sandstone units and about 20 percent of the regional flow leaves the section via the buried valley gravel aquifer. A number of local systems are developed in response to local changes in water-table configuration, the most notable being associated with the coulee and with the lower ridge flank near piezometer nest A3.

3.2 Regional Groundwater Flow

The regional configuration of groundwater flow is strongly influenced by two major sets of geologic units of high hydraulic conductivity. First, two major bedrock valleys, the Carmangay and Peacock Valleys, act as line sinks. Deep groundwater flow is diverted toward, and transmitted along these units. The influence of the bedrock valleys is transmitted for great distances through the second set of major units - the basal sandstone of the Horseshoe Canyon Formation and the Ryegrass Sandstone within upper portions of the Bearpaw Formation. Hydraulic continuity between the two sets of units is provided by direct contact, or by terrace deposits along the flanks of the buried valley.

The overall result is that downward and lateral hydraulic gradients exist in bedrock and drift units of the lacustrine plain for distances of 5 km or more from the Little Bow River. The strength of the hydraulic influence decreases with distance from the Carmangay Valley for two reasons. Firstly, the gradients are simply dissipated over distance, and secondly, bedrock units dip more steeply south of the B-Line. The influence of the direct hydraulic connection between sediment of the bedrock valley, basal units of the Horseshoe Canyon Formation, and the Ryegrass Sandstone thus ceases to exist at some point between the A and B Lines and gradients under the lacustrine plain become directed upward. Where all regional groundwater flow (to the depth of the Ryegrass Sandstone) along the B-Line is diverted to the Carmangay Valley aquifer, only about 20 percent is diverted to the Peacock Valley aquifer of the A-Line.

Regional groundwater flow does, therefore, discharge to the lacustrine plain in southern portions of the study area. The rates of regional discharge were determined by flow net construction along the A-Line and by calculation of the vertical Darcy flux between 5 and 10 m below the water table (that is, across the second, cell below the water table) during digital simulations for both the A and B-Lines. Values in mm/year are given above each section in Figures 5 and 6 for comparison with salinity, as determined from EM38 readings, and with the regional distribution of hydraulic head.

The comparison gives mixed results. Along the B-Line all deep, regional groundwater flow is eventually directed toward the basal gravel of the Carmangay Valley; most water flows laterally within the basal gravel but from 2 to 4 mm/year discharges to the water table along the bottom of the Little Bow River valley. Soil salinity is not evident in the Little Bow River valley however, indicating that salts reaching the water table from below must be removed by some mechanism. The most likely mechanism is drainage toward the Little Bow River through coarse and permeable alluvium deposited by the river. It is clear however that regional groundwater flow cannot contribute to salinity in the vicinity of the B-Line.

Along the A-Line, diffuse salinity on the lacustrine plain does correlate with regional groundwater discharge. Calculations of the vertical Darcy flux however, indicate that only about the equivalent of 1 to 2 mm of precipitation discharges to the lacustrine plain annually from the regional flow system R2d (Figure 24). Such a discharge rate should not in itself cause the water table to be as close to the surface as it is under the plain (1 to 3 m).

The low discharge rate of the regional system (System R2, Figure 24) results, at least in part, from a combination of topographic and geologic factors. Firstly, the size of the recharge area is smaller than the discharge area by a factor of more than 4. Secondly, all discharge from the regional system originates from the basal Horseshoe Canyon and Ryegrass sandstone units which dip away from the surface in the direction of flow. The net effect is that regional groundwater discharge is diffused over a large area rather than focused to a small area. The same volume of water that recharges over a distance of 1 km discharges over a distance of 4 km.

An important consideration with respect to regional groundwater discharge is that the composition of salts in the soil profile should reflect the chemistry of the source water. Two aspects of deep groundwater composition are important. Firstly, deep groundwater contains very small quantities of $SO_4^=$ because it has evolved through the stage of sulfate reduction (for example, 11, 15, and 110 mg/L from piezometer A5-343, B3-268, and B5-265, respectively). Secondly, deep groundwater, and especially that from the Ryegrass Sandstone, contains large concentrations of Cl^- in solution (for example, 380, 3850, and 4382 mg/L from piezometers A5-343, B3-268, B5-265, respectively).

If the primary source of salts on the lacustrine plain were deep groundwater, the dominant anion associated with the salts should be chloride. Saturation extracts from Sites A4 and A5 clearly show that this is not the case. In both cases, $SO_4^=$ is the dominant anion and Cl^-

content is negligible in comparison.

Thus, the main load of dissolved mass must be assimilated as water from the regional system passes through the near-surface weathered zone. Water samples from piezometers A5-90 and A5-61 are still substantially undersaturated with respect to gypsum (log SI -0.373 and -0.160, respectively) and dissolution of gypsum by upward moving regional groundwater can be occurring.

Results of the digital simulation show that about 1 mm of groundwater discharges annually at the Peacock Slough (Figure 24). Water from piezometer A5-61 contain 3159 mg/L of TDS. The total salt flux to the water table is then (1×10^{-3} m/year) (3.2 kg/m^3) or 3.2×10^{-3} kg/m^2/ year. A salt flux of this magnitude should only be significant if very long time periods for discharge (2000 to 5000 years) are considered. The regional groundwater discharge is thus not directly responsible for high water tables and is not contributing significant volumes of salt.

3.3 Groundwater Flow in Shallow Fractured Bedrock and Weathered Drift Sediment

The most severe area of soil salinity in the study area is located in the vicinity of Sites A3, 16, and C4, and the general correlation of specific discharge determined from the flow net construction to saline soil occurrences is positive. The intensity of salinity as determined by EM38 traverses and from soil extract analysis, however, bears little or no relation to simulated intensity of groundwater discharge.

This discrepancy is explained by the fact that the flow net is of regional scale and vital data, which became available only during the later local investigation, could not be incorporated. In particular, a higher degree of bedrock fracturing with associated hydraulic conductivity values as much as two orders of magnitude higher than previously measured exists in near surface portions of flow systems I and L4. This indicates that the total discharge of these systems may as much as 100 times higher than indicated in Figure 24 and Table 3. Also, a previously unknown sand and gravel filled channel with high hydraulic heads exists upslope from Site A4 and should have a major modifying affect on groundwater flow in that region. The digital simulation of hydraulic conductivity, hydraulic head, and groundwater flow distribution, which was based on regional data, is clearly not a true representation of the field situation. The general recharge -discharge distribution and the very low amounts of groundwater flow within regional systems discharging to lower portions of the lacustrine plain, however, appear to constitute valid conclusions.

In view of the above, discussions of salinity and hydrogeology in this region are based largely on data obtained during the later, more detailed, investigation, especially along the C-Line. These data provide four lines of evidence that groundwater from local, relatively shallow (to about 30 m) flow systems is responsible for the severe salinity in the area.

Correlation between groundwater discharge and areas of high salinity along the C-Line is firstly very good (Figure 11). A vertical and upward groundwater contribution exists everywhere where salinity exists, and the correlation is strongest where units of high hydraulic conductivity are near the ground surface. The condition of groundwater discharge to a deep water table that exists upslope from Site 16 is not anomalous to the correlation when lateral drainage to coulees is considered.

Secondly, a series of geologic circumstances are responsible for significantly higher hydraulic conductivity and greater groundwater flux in this area. Bedrock along the west flank of Blackspring Ridge is highly fractured due to glaciotectonic activity. The fracturing imparts high hydraulic conductivity primarily to sandstone and siltstone units, but locally also to intervening units of claystone and shale, to a depth of about 30 m below the bedrock surface. Drift overlying the fractured bedrock is generally thin (less than 5 m) on the ridge flank and contains a higher proportion of permeable sediment than elsewhere. A sand unit (up to 3.5 m thick), lies on bedrock in a number of places. Till is generally very thin (1 to 3 m) and is weathered and fractured. Glaciolacustrine sediment is sandier than elsewhere, perhaps as a result of shoreline development near upper boundaries of the unit, or the unit may be overlain by alluvial fan sediment. Where the drift thickness does increase near the base of Blackspring Ridge, a thick deposit of interglacial sand and in places gravel, lies between the upper till and bedrock (Sites 5WT, 6WT, and C6).

Thirdly, the distribution of groundwater chemical constituents given in Figures 13 to 19 show that the region within about 30 m of the bedrock surface contains the dominant dissolved salt load. The majority of the dissolved salts are generated and transported within this zone. Flow is probably active enough to maintain water at an oxidation state such that significant sulfate reduction does not occur, and fracture dominated flow may be implied by high calcium and magnesium contents.

Fourthly, the zone is characterized by stable isotopic compositions of present-day water. Water from deeper regions has a distinctly different composition that suggests emplacement under different and warmer climatic conditions. The latter condition suggests very long residence times (in the order of thousands of years) for deep groundwater and implies that this water cannot be contributing directly and significantly to discharge at the surface.

3.3.1 Relative contribution from drift and bedrock groundwater sources

In view of the complex hydraulic head distribution along the C-Line, flow-net construction and quantification of groundwater flux was not attempted. It is concluded however, that the major salinity near Sites A3, 16, and C4 is caused by discharge of groundwater and salts primarily from bedrock units less than 30 m deep, but the possibility of a significant contribution from flow through shallow drift sediment exists. The following analysis will evaluate if the discharging groundwater is primarily of drift or shallow bedrock origin.

The major-ion composition of groundwater results from a variety of complex processes and interactions. In general terms these may be broken down as follows:

1. A natural evolution of groundwater with respect to major-ion composition that is in part a function of the host-rock assemblage interacting with groundwater along its travel path,
2. Mixing of groundwaters that have evolved to different stages of major-ion composition to form water of some new, intermediate composition, and finally,
3. A change in composition at the water table as water becomes more mineralized as a result of evaporative concentration, and minerals

of low solubility precipitate.

The pattern of evolution of water that has undergone these processes is shown on the Piper trilinear diagram of Figure 25. Water from Sites A1 and B5 was chosen to show these patterns. Both sites are in areas of strong downward gradients and in hydraulic settings that preclude significant mixing. The B5 Site includes water that initially evolved through contact with drift sediment; A1-Site water has had only minimal drift contact.

In the Blackspring Ridge area the major-ion composition of groundwater evolves as follows:

1) from Ca + Mg/SO_4 to Na + K/SO_4

2) from Na + K/SO_4 to $NaHCO_3$, and

3) from $NaHCO_3$ to NaCl.

The dominant processes thought to be responsible for the first two changes are exchange of Ca^{++} and Mg^{++} for Na^{+} as clay minerals are encountered, and anaeorobic reduction of sulfate. Sodium chloride water is found in relatively deep regions. Except for water from Site B6, the change from Ca + Mg/SO_4 to Na + K/SO_4 occurs with a bicarbonate content of about 20 percent on an equivalents per million (e.p.m.) basis. Throughout the entire evolutionary sequence Ca^{++} and Mg^{++} exist on an approximately equal e.p.m. basis.

Mixing of water that has evolved through various compositional stages can occur at junctions of flow systems or where more than one aquifer carries groundwater to the same region. On the Piper trilinear presentation, water composition that results from mixing, will plot along straight lines joining individual component compositions.

Changes in major-ion composition that are caused by evaporation

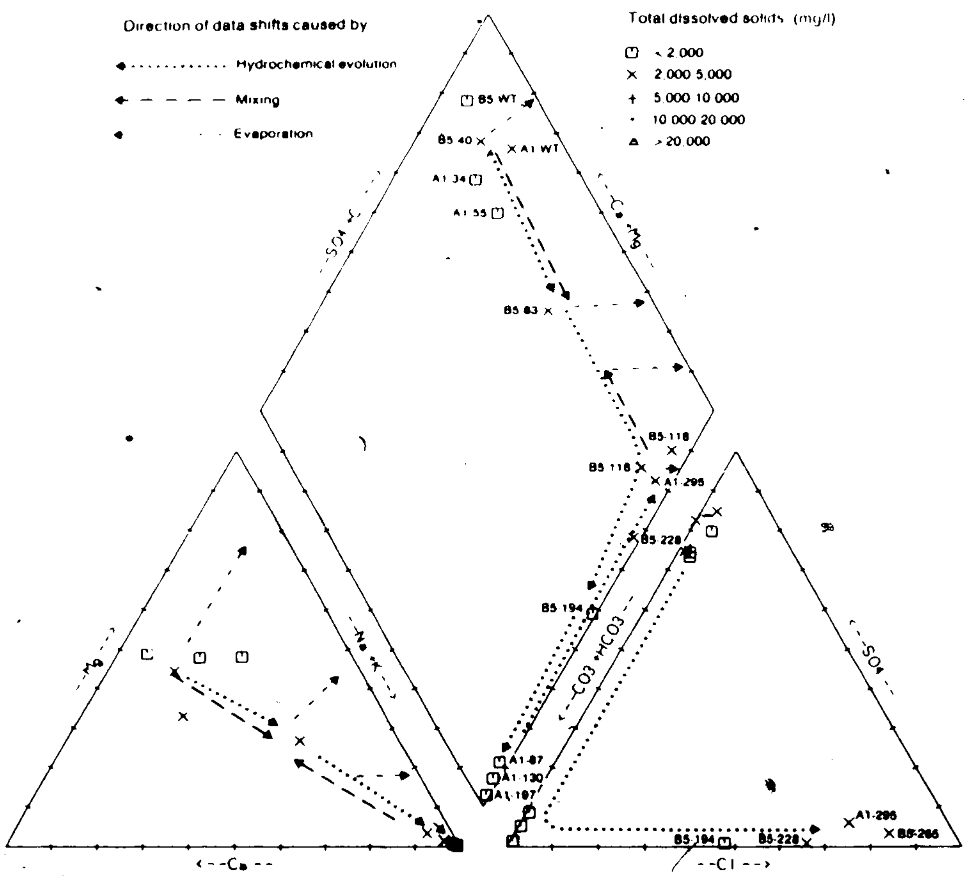

Figure 25. Effect of chemical evolution, mixing and evaporation on piper-plot presentation.

result from differences in solubility of various mineral phases. As water becomes increasingly mineralized by evaporative concentration, the less soluble minerals will precipitate first, eventually resulting in a brine enriched in components of very highly soluble minerals.

Nowhere in the Blackspring Ridge region does near-surface groundwater have appreciable Cl^- content. In terms of possible precipitation reactions, it is only the carbonate and sulfate minerals that require consideration. Solubilities for various common minerals are given by Freeze and Cherry (1979); those for carbonate and sulfate minerals are shown in Table 4.

Table 4. Solubility of carbonate and sulfate minerals (in mg/L, 25°C, pH7)

Mineral		Solubility (mg/L)	
Dolomite	$CaMg(CO_3)_2$	90*	480+
Calcite	$CaCO_3$	100*	500+
Gypsum	$CaSO_4 \cdot 2H_2O$	2100	
Epsomite	$MgSO_4 \cdot 7H_2O$	267 000	
Mirabilite	$Na_2SO_4 \cdot 10H_2O$	280 000	

* Partial pressure of $CO_2 = 10^{-3}$ bar
\+ Partial pressure of $CO_2 = 10^{-1}$ bar

Evaporative concentration will result in precipitation of dolomite, calcite and gypsum before epsomite and mirabilite, leaving the water depleted in Ca^{++}, and HCO_3^- + $CO_3^=$, and enriched in Na^+, Mg^{++}, and $SO_4^=$. Water that has undergone evaporative concentration will therefore plot at characteristic departure from water that has undergone only natural evolution and mixing. This departure will be in the direction of increased Mg^{++}, Na^{+}, and $SO_4^{=}$ content and is also shown graphically in Figure 25.

Computer simulation was used to verify possible compositional changes resulting from mixing and evaporation. Water from well B5-40 was chosen to represent a typical shallow drift water at an early stage of chemical evolution. Water from well C4-65 was chosen to represent shallow bedrock water that has undergone cation exchange and evolved to a Na + K/SO_4 composition. Chemical analysis results for these two waters were then combined on an equal molar basis to form a composite water representing a mixed source. The geochemical model PHREEQE (Parkhurst et al., 1980) was used to simulate evaporation of this combined water to approximately the TDS content of water from the water-table well at Site C4. Simulated evaporation to 0.1 of the original volume was required to approximately match the TDS of the evaporated composite water with that of water from Well C4-WT. The model was run with the constraints of P_{CO_2} at 10^{-1} bar, and with the same slight supersaturation with respect to calcite and dolomite that was exhibited by the composition of water from C4-WT. The evaporation simulation was then performed separately for water with the same composition as from Wells B5-40 and C4-65.

Results of the simulations are given in Table 5 and Figure 26. Water with the specified mixed composition evaporates to approximately the chemical composition of near-surface groundwater at Site C4. The mixing is required, as evaporation of water from either of the individual sources alone could not produce compositions that resemble that of water from C4-WT. Results do not prove that a drift water

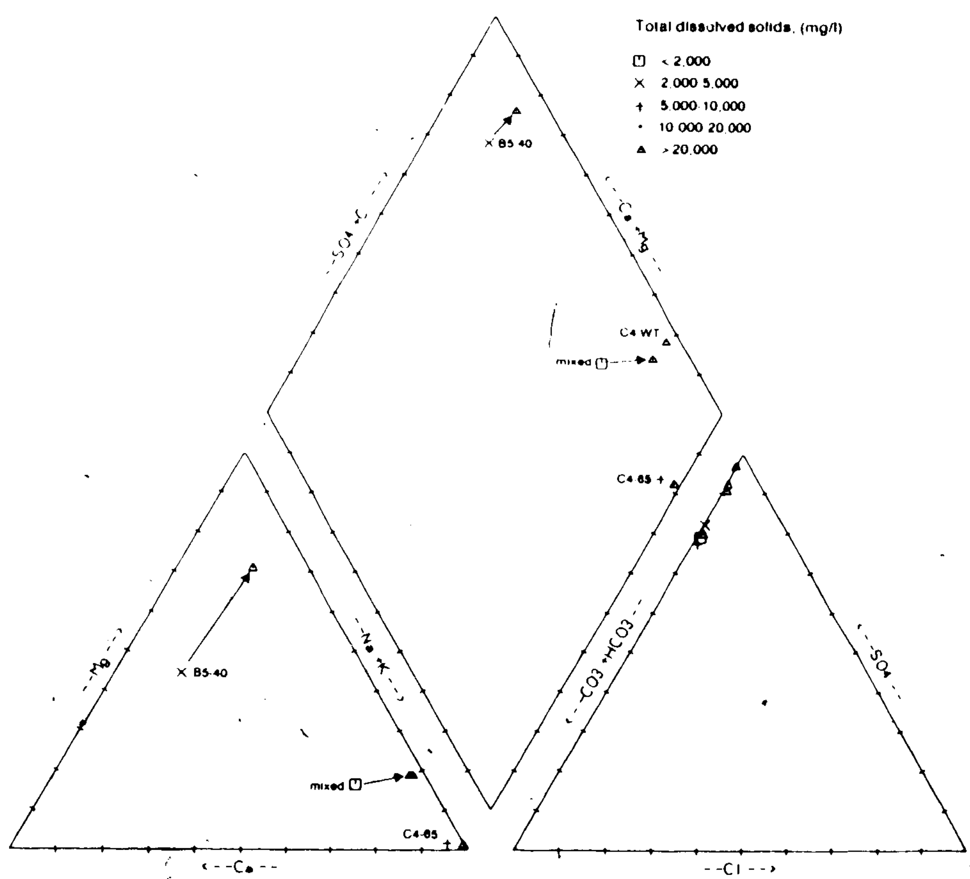

Figure 26. Piper-plot shifts caused by evaporation.

source is required because very shallow bedrock water (for example water from A1-34) is chemically similar to drift water. They do imply however, that water discharged at Site A4 should have a mixed source and are conclusive in showing that water from sandstone at depths of 20 m (C4-65) and 30 m (C4-100) cannot be the sole source.

Table 5. Groundwater evaporation simulation results.

	Drift Water B5-40 (mg/L)		Bedrock Water C4-65 (mg/L)		Composite Water (equal molar basis) (mg/L)		Water Table at C4-WT (mg/L)
	obs.	evap.	obs.	evap.	calc.	evap.	obs.
Ca^{++}	408	1102	67	40	238	423	418
Mg^{++}	266	3713	20	137	143	1414	1765
Na^{+}	160	1606	2075	20997	1118	11234	14240
K^{+}	13	125	6	62	9	94	10
HCO_3^{-}	569	2153	1260	10911	915	3382	1530
$SO_4^{=}$	2100	21074	3540	35650	2820	28350	35220
Cl^{-}	7	70	40	413	24	236	55

Two apparent discrepancies in the simulation results are the much higher concentration of K^{+} and Cl^{-} content predicted by the model. The discrepancy in K^{+} concentration exists because the simulation does not account for fixation to abundant clays in the near-surface sediment which occurs in the natural system. Chloride, however, is considered to behave in a conservative manner and the relatively low amounts in water from C4-WT can not be adequately accounted for. A mechanism involving evaporation to precipitation of mirabilite but not NaCl, later transport of chlorides in solution, and later dissolution of salts previously precipitated in the soil profile, could be involved. The discrepancy in Cl^- concentration should, however, have little bearing on the primary conclusion that a mixed source is required, because no difference in Cl^- concentration of shallow drift, shallow bedrock, and water-table water exists in the vicinity of the C-Line.

Piper plots for samples from water-table wells, are given in Figures 27 and 28. Those for samples from piezometers completed in drift and bedrock sediment are given in Appendix 8. In keeping with the lines of reasoning developed earlier in this section, there exists an entire spectrum of possibilities for groundwater sources to the water table.

In the vicinity of the C-Line the composition of water at the water table ranges from Ca + Mg/SO_4 to Na + K/SO_4, indicating source water that has undergone cation exchange to various degrees. High degrees of evaporation are indicated in a number of cases. Water samples from water-table wells located in the area of severe salinity, however, (C4, C5, C6, A3, A4) are furthest along the evolutionary path and thus appear most likely to be made up in part of bedrock water from the shallow high-sulfate zone. The mixing model postulated earlier allows the possibility that the greater the relative $Na^+ + K^+$ content, the greater the possibility for a contribution from that zone. Strong upward hydraulic gradients and high hydraulic conductivity in underlying bedrock units support this interpretation.

Figure 29 shows the areal distribution of $Na^+ + K^+$ content of water-table water as percent of total cations on an e.p.m. basis. High $Na^+ + K^+$ content correlates well with areas of high salinity and those

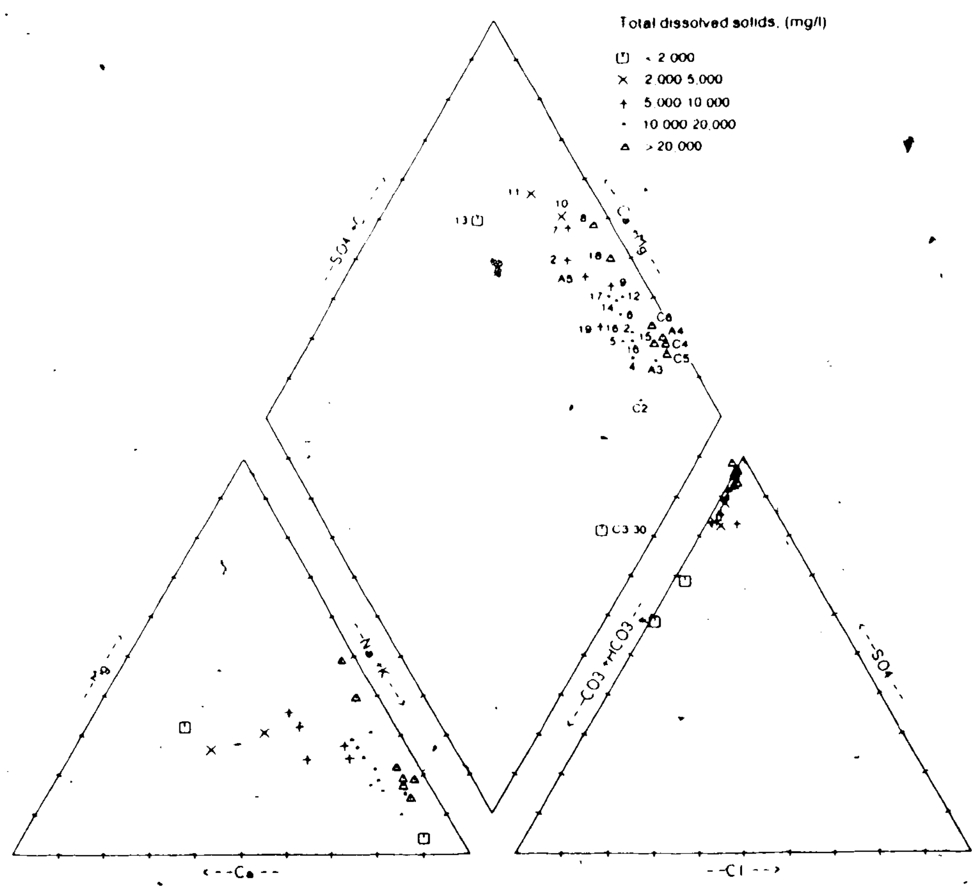

Figure 27. Hydrochemistry, C-Line and vicinity water-table well water.

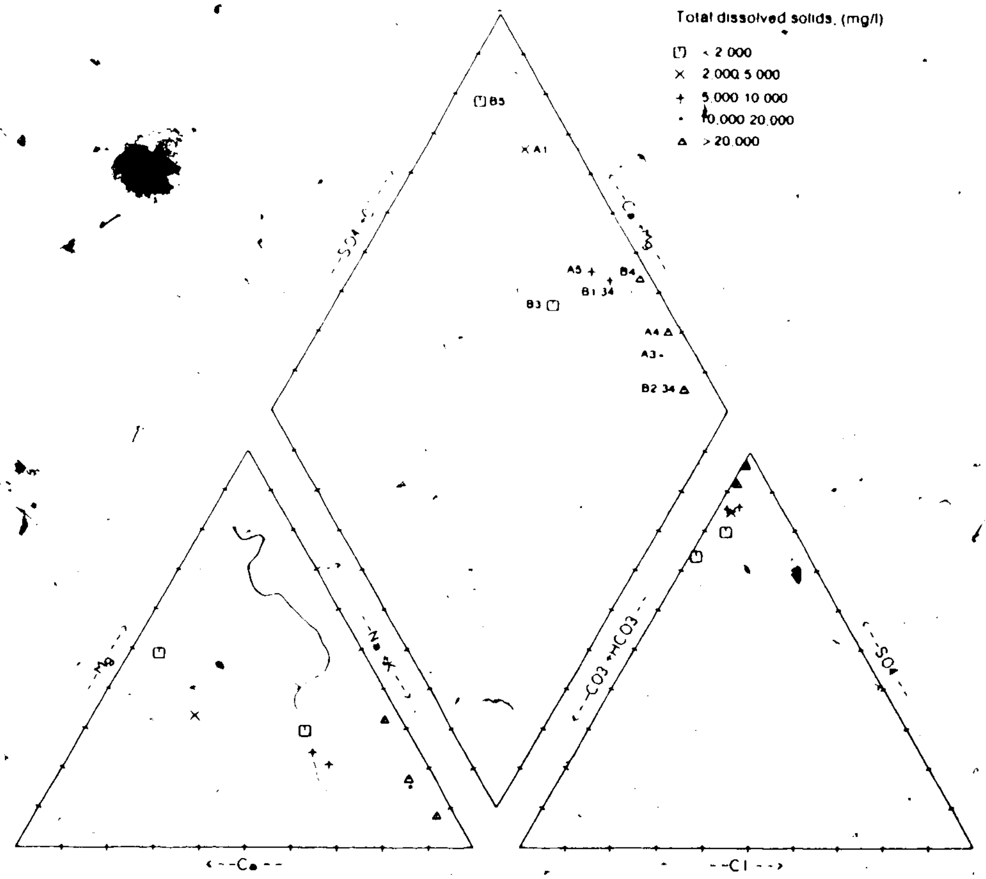

Figure 28. Hydrochemistry of water-table well water, A and B-Lines.

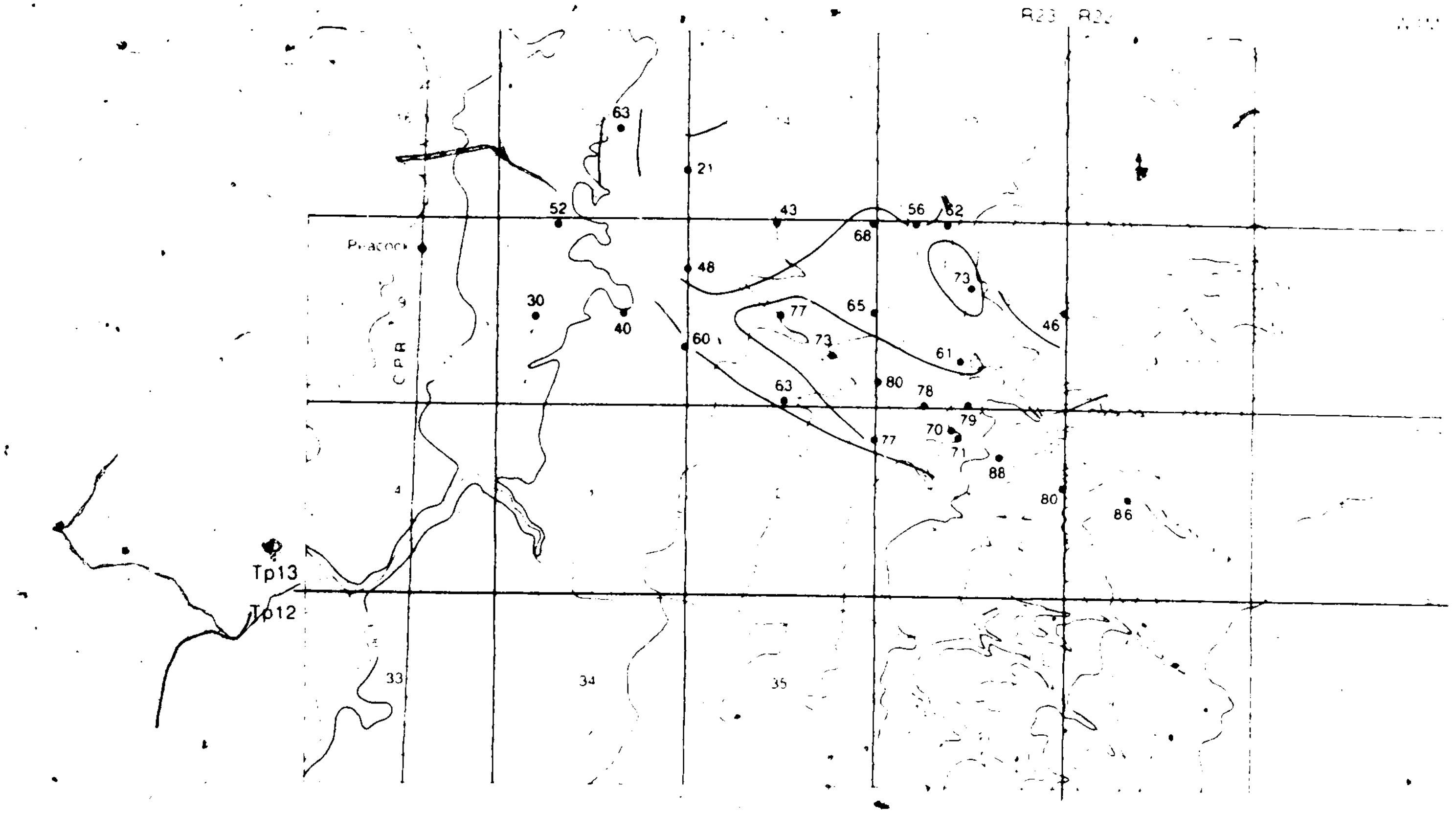

Figure 29. Distribution of $Na^+ + K^+$ content of water-table water, C-Line and vicinity (%$Na^+ + K^+$ of total cations on an e.p.m. basis).

enclosed by the 60-percent contour are interpreted to constitute regions influenced by either groundwater influxes of relatively distant origin, or as having significant input from bedrock sources.

The combination of hydrogeologic and hydrochemical data suggests that groundwater from various sources and at various stages of chemical evolution is responsible for soil salinity in the regions of the A and C-Lines. The hydraulic head and groundwater flow distribution of the region (Figure 11) imply that bedrock water is discharged to the water table in regions topographically below the approximate elevation of Site C2. Strong upward hydraulic gradients and high $Na^+ + K^+$ content between Sites 16 and C5 suggests that this is the region of maximum bedrock groundwater contribution. Occurrences of permeable sand on the bedrock surface of lower slopes of Blackspring Ridge (Sites C2, C3, C4 and 2) provide the means to transport locally recharged shallow drift groundwater to topographically lower areas, mixing with discharging bedrock water along the way. Both of these sources feed channel sand and gravel in the vicinity of Sites C6, 6 and 5, which in turn also contributes groundwater to the surface. Groundwater discharged in this manner moves laterally and downslope in silt and sand-rich clay deposits of the lacustrine shoreline or alluvial fan facies and continues to discharge in the region between Sites C4 and 8.

Along the B-Line the hydrogeologic setting is such that fewer opportunities exist for salinity to develop. This situation is reflected by the much smaller size and more scattered distribution of saline areas than those along the A and C-Lines. This, and the regional scale of the B-Line, make site-specific interpretation questionable. Several significant relationships do, however, exist. Water from B2-36 is highly mineralized and of a Na + K/SO_4 type of composition. This, the very thin drift, and numerous thin sandstone and coal subcrops (Figure 6) are good evidence that salinity in the vicinity of Site B2 results from shallow-bedrock groundwater discharging as small seeps from these units.

Water-table water at Sites B3 and B4 also exhibits the effects of cation exchange. Both sites are located in areas where aeolean sand overlies lacustrine clay and silt, and where hydraulic gradients are lateral and downward. Discharge of groundwater from below is thus precluded at these sites. Compositionally the water from Sites B3 and B4 is similar, differing only in that at B4 the water shows a much higher degree of evaporation. Both, however, appear to be influenced by groundwater of bedrock origin.

The saturation extract profile for Site B4 (Appendix 3) shows that the maximum salt load is within the sand unit at a depth of about 7 to 10 m in the upper weathered till. The Ca^{++}/Mg^{++} ratio implies that water within the zone evaporated prior to being emplaced. Deuterium and $\delta^{18}O$ values (-151.7 and -19.35 per mille, respectively) however, indicate that the water is only very slightly evaporated. Thus, salts within the sand unit were at some time deposited above the water table by evaporation concentration and then re-entered the saturated zone by downward flushing by precipitation or runoff water.

The nearest upslope occurrence of sites at which groundwater discharge and evaporative concentration occurs is a series of northeast trending saline seeps located along the base of Blackspring Ridge in NW of 30, E 1/2 of 31, and SW of 31-13-22 W4. The seeps are small, have an intense and permanent appearance, and are considered to result from groundwater discharged from shallow bedrock sources in a manner similar to that at the C4 Site.

It is concluded that salts deposited at these seeps re-enter the subsurface by downward flushing, move downslope within the intertill sand unit and along upper portions of the lacustrine unit, and cause salinization in interdunal areas where the sand cover is thinnest. Mixing of this water with locally recharged precipitation and surface water results in the chemical composition being skewed in the direction of higher Ca^{++} + Mg^{++} content. This mechanism satisfies both the evaporated nature of salt composition and the unevaporated nature of the water.

3.3.2 Mixing of drift and bedrock water

A significant aspect of the hydrochemical distribution shown in Figures 13 to 19 is a dramatic increase in TDS content within 15 to 20 m below the water table in the region downslope from Site 16-1. Sulfate, sodium plus potassium, and calcium plus magnesium contents all show a marked increase, and the increase is in the general direction of groundwater flow as indicated in Figure 12. An increase of this magnitude could be attributed to evaporative concentration at the water table but should not manifest itself at depths of 15 to 20 m unless other mechanisms of salt solution, mixing, or transport are operative.

The following mechanisms are proposed as possible causes for the phenomenon:

1. gypsum dissolution by upward moving groundwater in the region of increased TDS content, particularly in drift units, and
2. continuous mixing of upward moving bedrock water with shallow,

laterally moving drift water. The latter water contains salts that were previously formed by evaporation near and above the water table, and later dissolved again in recharge from runoff and precipitation.

To examine these possible mechanisms, the following analyses were performed.

1. Results of chemical analyse of water from piezometers and water-table wells of the C-Line were processed using WATEQF (Plummer et al., 1976). A portion of the model output includes indices for saturation with respect to various mineral phases and mole ratios for various ions such as the Ca^{++}/Mg^{++} ratio. Results for saturation with respect to gypsum and Ca^{++}/Mg^{++} ratios are tabulated in Appendix 7 and are given for the C-Line in Figure 30.
2. The degree of evaporation of piezometer and water-table well water was examined by $\delta^{18}O$ and δD relationships.

The first mechanism, that of gypsum dissolution as upward moving groundwater passes through drift sediment, appears unlikely to be responsible for the noted increases for two reasons. Firstly, the distribution of saturation indices with respect to gypsum, which are given in Figure 30, indicate that within the region in question water is supersaturated with respect to gypsum. Gypsum precipitation rather than dissolution should therefore be occurring in this zone. This observation is corroborated by abundant occurrences of gypsum crystals noted during drilling in drift sediment.

The interpretation based on results of the saturation indices is, however, not conclusive. The WATEQF model, that was used to calculate saturation indices, used extended Debye-Hückel equations to calculate

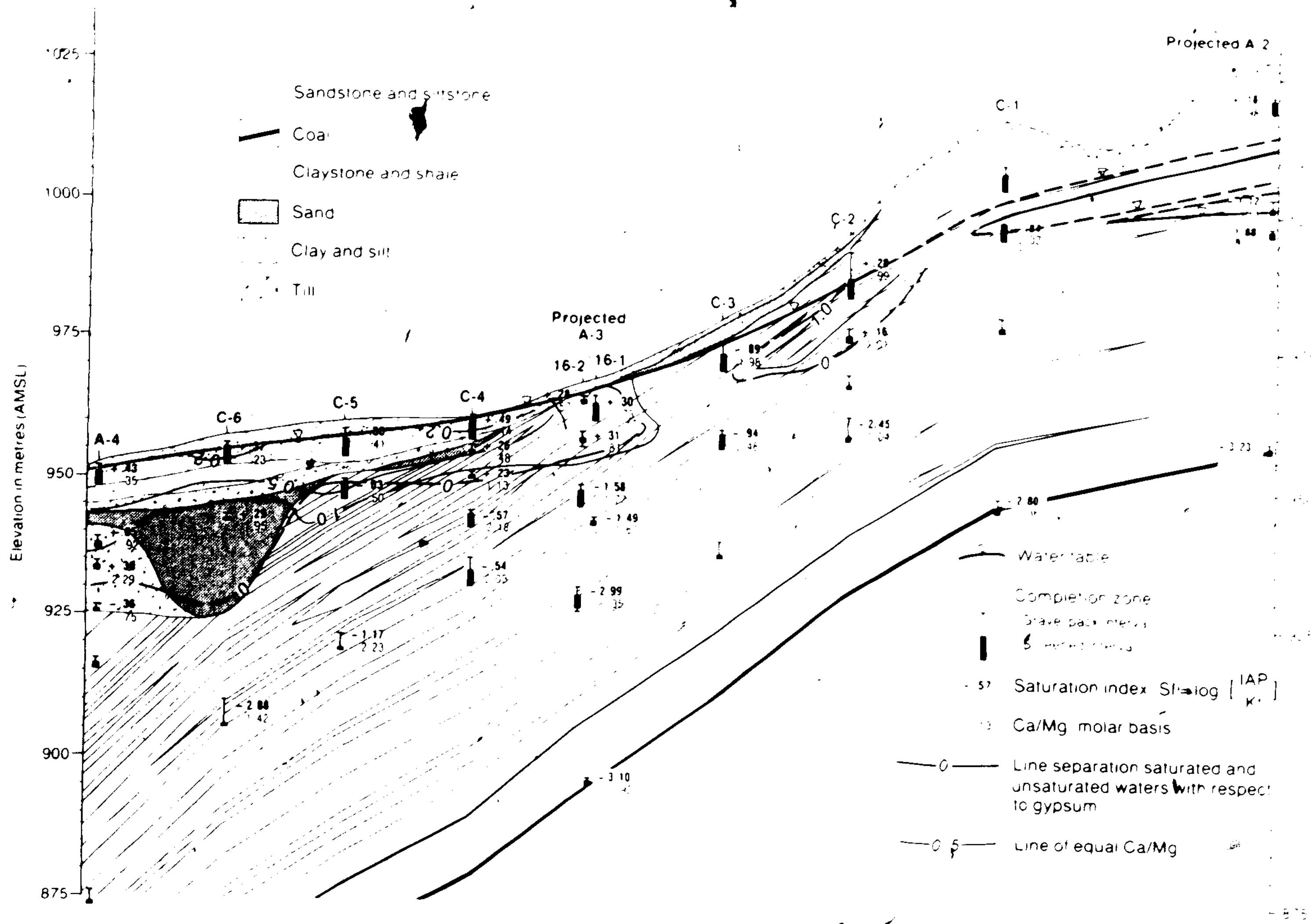

Figure 30. C-Line groundwater saturation with respect to gypsum and Ca^{++}/Mg^{++} ratios.

activity coefficients. These equations are inaccurate for solutions of high ionic strength (>0.5) (Harvie and Weare, 1980; Crowe and Longstaffe, 1987). Ionic strength of water samples from the zone that is indicated to be supersaturated with respect to gypsum by the WATEQF simulations is between 0.1 and 0.45, and 0.9 in water from Well C4-WT. Ionic strength is therefore in the range for which unreliable results are possible. Refinements to geochemical models, that use Pitzer's equations to accurately determine activity coefficients for solutions of high ionic strength, have recently been introduced (Crowe and Longstaffe, 1987) but were not commercially available at the time the simulations were performed.

Secondly, the increase in TDS and $SO_4^{=}$ concentration along the general direction of groundwater flow, and toward the water table does not occur only as water passes through drift units. At sites 16-2 and C4, the same pattern occurs in bedrock sediment before the water has contacted drift (for example, $SO_4^{=}$ concentrations of 4605, 6405, 3540, and 7350 mg/L in water from piezometers 16-2-72, 16-2-38, C4-65, and C4-36, respectively). The increase in TDS and $SO_4^{=}$ concentration is thus not limited to areas where groundwater moves through drift sediment.

The strong decrease in the Ca^{++}/Mg^{++} ratio that accompanies the increase in TDS can be accounted for by the much lower solubility of the calcium mineral gypsum as compared to the magnesium mineral epsomite. With the continued precipitation of gypsum, groundwater becomes enriched in Mg^{++} relative to Ca^{++}. The Ca^{++}/Mg^{++} ratios are thus considered further evidence that gypsum is precipitating and that solution of gypsum is not responsible for increases in the total dissolved solids content and $SO_4^=$ concentration.

The concept of mixing of upward moving bedrock water with laterally moving drift water requires what appears to be a paradoxical situation of laterally and downward moving water in areas of strong upward hydraulic gradients. The paradox can however be resolved if the magnitude and geometry of heterogeneity in hydraulic conductivity that exists in the region is considered.

Drift units between Sites 16 and C5 along Section C form a wedge that thickens in the downslope direction and contains a layer of highly permeable sand at its base (Figure 10). This wedge overlies bedrock comprising layers of highly fractured and permeable sandstone alternating with less permeable layers of claystone and shale. Bedrock strata dip in the direction of topographic slope, but at a substantially greater degree than topographic slope. One highly fractured sandstone bed intercepts a shallow water table at Site 16-2 in a region of intense soil salinization. Horizontal hydraulic conductivity of the relevant geologic strata is summarized in Table 6. The geometric mean of highly permeable units exceeds that of poorly permeable units by about three orders of magnitude.

A fundamental concept of groundwater flow is that as flow occurs across boundaries of units of different hydraulic conductivity the direction of flow is refracted (Harr, 1962; Freeze and Cherry, 1979). The amount of refraction is governed by the tangent law

$$\frac{k_1}{k_2} = \frac{\tan \theta_1}{\tan \theta_2}$$

where k_1 and k_2 are hydraulic conductivity of, and θ_1 and θ_2 are angles between a perpendicular to the boundary between, respective units as

Table 6. Horizontal hydraulic conductivity near sites 16 and C5

Site	Material	k_h (m/sec)	Geometric Mean
C4-20	Sand	3.6×10^{-6}	High k units
16-2-WT	Sandstone	4.8×10^{-6}	2.7×10^{-5}
16-2-38	Sandstone	8.5×10^{-6}	(4.1×10^{-5} if
C4-65	Sandstone	4.1×10^{-5}	ignore C4-100)
C4-100	Sandstone	2.3×10^{-3}	
16-1-WT	Claystone	4.1×10^{-7}	Low k units
C4-36	Claystone	8.3×10^{-9}	4.2×10^{-8}
C5-45	Claystone	1.9×10^{-8}	

shown in Figure 31.

Figure 31 and the presentation of the concept by Freeze and Cherry (1979) are for the special case of a horizontal boundary for which solution of the tangent law cannot yield flow lines directed below horizontal. Application to the more general case of dipping strata, as exists along the C-Line, gives the result that groundwater flow becomes increasingly oriented parallel to the permeability boundary in units of high conductivity, and transverse to the boundary in units of low conductivity.

To illustrate this point a highly simplified but representative geometry describing conditions between Sites 16-2 and A5 is given in Figure 32. Unit 1 represents poorly permeable units such as claystone or shale; Unit 2 represents highly transmissive units such as sand, fractured sandstone, or other fractured bedrock material. The dip is slightly exaggerated for the purpose of illustration.

Figure 31. The tangent law for refraction of groundwater flow lines.

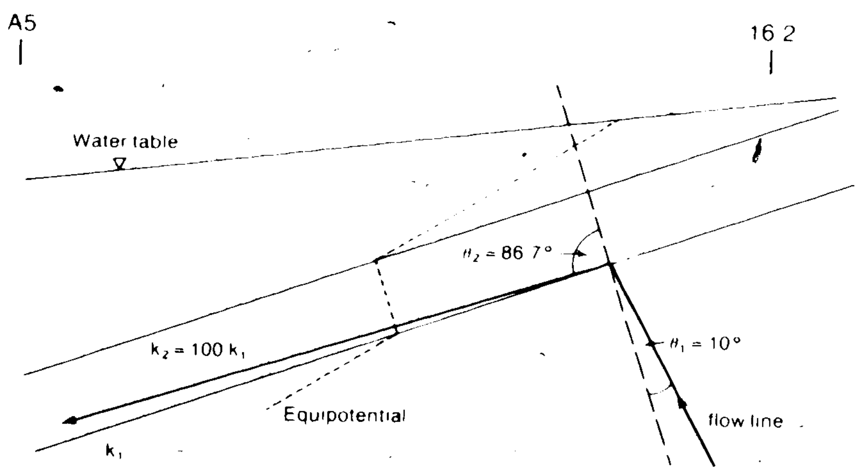

Figure 32. Approximation of flow-line refraction in area of upward gradients along the C-Section.

Solving the tangent law for θ_2 gives $\theta_2 = \tan^{-1} [k_2/k_1 (\tan \theta_1)]$. Figure 32 shows results for a hydraulic conductivity contrast of 100 and θ_1 of 10 degrees from a perpendicular to the highly conductive unit, or 10 degrees plus strata dip from vertical. Table 7 gives results for hydraulic conductivity contrasts of 100 and 1000, and for three angles of flow-line approach.

Table 7. Flow-line refraction for different initial flow-line angles and hydraulic conductivity contrasts.

k_2/k_1	θ_1 (degrees)	θ_2 (degrees)
100	1	60.2
100	10	86.8
100	30	89.0
1000	1	86.7
1000	10	89.7
1000	30	89.9

Figure 32 and Table 7 clearly show that for large permeability contrasts flow-line refraction is extreme and that flow essentially orients itself along units of high hydraulic conductivity. For contrasts of about three orders of magnitude as exist in the area of investigation, flow is generally in the direction of permeable strata within such strata. In areas of upward hydraulic gradient, addition and subtraction of water occurs below and above the units, respectively. Within highly permeable strata that dip downward in the direction of groundwater flow, flow will thus follow the dip direction and will also be oriented downward.

If the above modifications to flow direction are taken into account, it is possible for groundwater that discharges at, or comes near enough to, the water table in the region between Sites 16-2 and C4 to become concentrated by evaporation, to be subsequently diverted downward along the highly permeable sand and sandstone layers.

Continual upward discharge from these layers provides the large amounts of dissolved salts that characterize the region 15 to 20 m below the water table at Sites C4 and C5. High-TDS water that progressively discharges from the top of the highly permeable zones is progessively replaced by less mineralized water from below with the result that TDS content gradually decreases in the direction of refracted flow.

Stable isotope composition of water in the region can also be explained by this mechanism. Figure 33(a) and (b) are $\delta^{18}O$ versus δD plots for groundwater from Sites 16, 16-2, C4, and C5. Water-table water, from Sites 16-1 and 16-2 is clearly evaporated whereas deeper water (16-2-72 and 16-1-85) is not. Water at Site C4 is progressively less evaporated with depth; that from C4-65 and C4-100 is essentially unevaporated. Water from C5-WT and C5-45 is slightly less evaporated than that from Site C4.

The isotopic composition of water at the water table results from evaporation after discharge and subsequent mixing with precipitation and runoff water. The fact that some degree of evaporation is apparent in water from C4-20, C4-36, and C5-45 results from previous contact with the water table. The progressive change with depth and in the direction of refracted flow is caused by replacement of evaporated water by unevaporated water from below and mixing of the two.

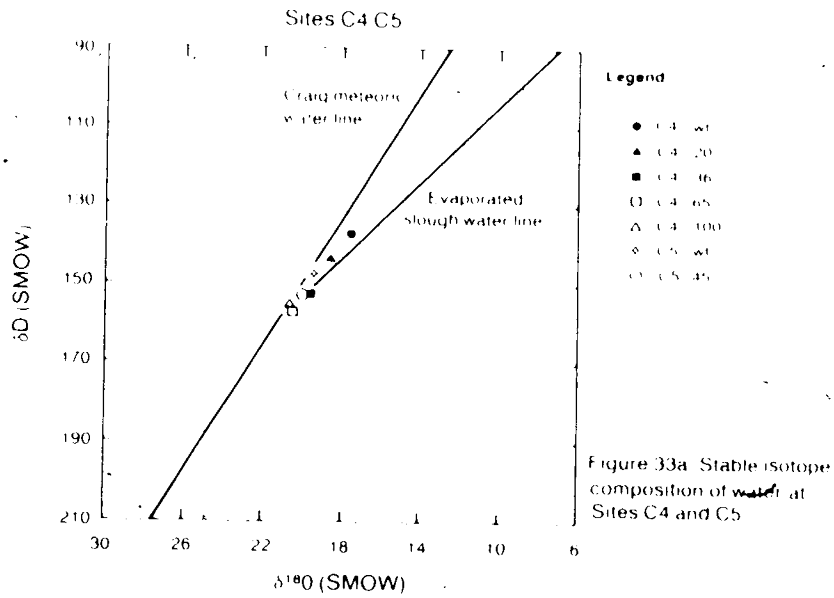

Figure 33a Stable isotope composition of water at Sites C4 and C5

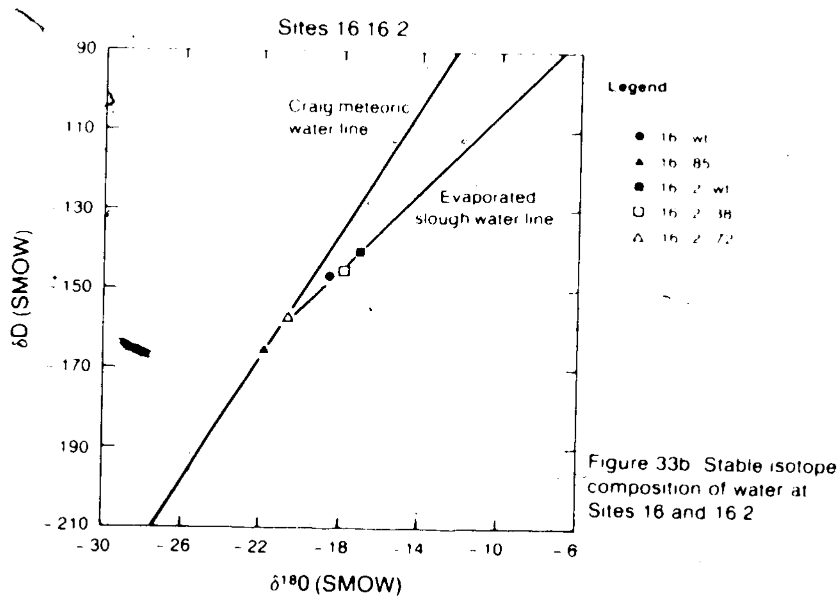

Figure 33b Stable isotope composition of water at Sites 16 and 16 2

Further evidence that the mechanism of flow refraction is operative is provided by hydrochemical patterns near Sites C2 and C3. Both sites are characterized by upward gradients and groundwater discharge to the water table (Figure 12). At Site C2 however, a plume of water with high TDS and sulfate content extends downward and along dip; from Site C3 a plume of relatively fresh water extends downslope and downdip. Both situations require that downward and laterally directed groundwater flow exist in areas of upward hydraulic gradients.

A second mechanism that appears to be operative in conjunction with flow refraction is a fluid density effect. Maathuis and Vander Kamp (1986) summarize behaviour of variable density groundwater flow in the vicinity of brine ponds in Saskatchewan and indicate that increased fluid density results in increased downward movement.

In areas of groundwater and salt discharge, high fluid densities can occur at the water table. Discharging, groundwater moving upward from the water table by capillarity, evaporates, and leaves salt in the unsaturated soil zone and at the ground surface. Because the process proceeds to evaporation, even the most highly soluble mineral phases (mirabilite and epsomite) precipitate. Water from post-growing season rainfall events, and especially spring melt runoff water, then preferentially redissolves these minerals during infiltration to the water table. The resulting chemical composition of infiltrating water will be skewed toward high Na^+, Mg^{++}, and $SO_4^=$ content.

Infiltrating water that reaches the water table in saline areas should thus be mineralized and of higher density than upward or laterally moving water below the water table. Because the solubility of mirabilite and epsomite is very high, it is not unreasonable to expect the infiltrating water to have a mineral content of about 100 000 mg/L and a density of about 1.1. The denser water would periodically create transient downward components of flow below the water table during the infiltration events. If the situation exists above a downward dipping, highly permeable unit, such as that near Sites 16 and C4, entry of highly saline water from above and subsequent down-dip movement in the zone of refracted flow is possible.

3.3.3 Rates of groundwater and salt discharge from shallow groundwater flow systems

Harr (1962) and Bear (1972) showed that a stratified medium consisting of layers with different hydraulic conductivity can be represented by an equivalent single homogenous layer. The equivalent hydraulic conductivity of the single homogenous layer in the vertical direction is then:

$$keq_v = d \Big/ \sum_{i=1}^{n} \frac{di}{ki}$$

where d is the total thickness of the layered medium, and di and ki are the thickness and hydraulic conductivity, respectively, of each individual layer.

This relationship was used at Sites C4, C6, 5, and 6, where hydraulic gradients between different drift layers were measured, to determine an approximate rate of groundwater discharge. The TDS content of the discharging water was used together with groundwater discharge rates to determine the approximate salt flux to the water table. A summary of results is provided in Table 8; calculations are given in Appendix 11.

Table 8. Calculated rates of groundwater discharge and salt flux to the water table.

k_v assigned to intervening lacustrine sediment (m/sec)	Groundwater discharge rate (m^3/m^2/year) Salt flux (kg/m^2/year) in brackets			
	C4	C6	5	6
	0.130 (2.4 kg)		0.013 (0.09 kg)	
(a) 3.2×10^{-8}		0.130 (0.86 kg)		0.468 (2.1 kg)
(b) 3.0×10^{-9}		0.026 (0.17 kg)		0.069 (0.3 kg)
(c) 3.0×10^{-10}		0.003 (0.02 kg)		0.007 (0.03 kg)

In all cases, the value of vertical hydraulic conductivity of weathered till was assumed to be 2.0×10^{-8} m/sec. Values for the uppermost (generally sandy or silty) lacustrine (or alluvial fan) deposits were based on water-table well response tests (1.7×10^{-7} and 2.6×10^{-7} at Sites C6 and 6, respectively). Where intervening clayey lacustrine sediment exists, the mean value determined for all weathered, non-sandy lacustrine deposits (3.2×10^{-8} m/sec) was used. This latter value is very close to the value of 3.7×10^{-8} m/sec established in trial and error simulations designed to fit the observed regional hydraulic head distribution. Because much lower values were measured on cores, however, the calculations were repeated using hydraulic conductivity values one and two orders of magnitude less.

The salt fluxes, as expected, are strongly dependent on the hydraulic conductivity of the intervening clayey lacustrine sediment.

The relatively low hydraulic conductivity probably is a controlling factor in determining the quantity of groundwater and salt that can be carried to the water table from underlying permeable units. More information is required on the hydraulic conductivity and lateral continuity of the lacustrine unit to enable determination of discharge rates from stratified channel deposits at Sites C6 and 6. Fluxes calculated using the hydraulic conductivity value of 3.0×10^{-9} m/sec are probably reasonable.

Because the clayey sediment is thin or absent at Sites C4 and 5W1, the calculated groundwater discharge rates and salt fluxes can be determined more exactly. It is, therefore, highly likely that the thinning, increased sand content, and eventual absence of the clayey lacustrine unit at higher elevation plays a major role in salinity development, particularly where this topology coincides with strong upward hydraulic gradients in underlying bedrock units. The major saline occurrences in the vicinity of Sites 16, A3, and C4 are developed in this type of setting.

Electrical conductivity (EC) of saturated paste extract is a commonly accepted measure of soil salinity. A value of 4 dS/m is considered high enough to adversely affect growth of most plants and at values exceeding 16 dS/m only very few salt-tolerant crops can produce satisfactory yields (Black et al., 1965). Chang et al. (1983) derived the empirical relationship: $TDS = 765.1\ EC^{1.087}$ between total dissolved solids content and electrical conductivity of saturation extracts for sulfate-rich soils of southern Alberta. This equation can be used to determine the total salt content of the soil, and with the calculated fluxes, the time required for soils to become salinized.

A saturation extract of EC = 4 dS/m contains about 3450 mg of salts per litre. Assuming the saturation paste was prepared using 0.55 g of water per gram of soil, then one gram of such soil contains 3450 mg/L x 0.55 x 10^{-3} L or about 1.9 mg of salts. This concentration equates to 0.19 percent of salt by weight. Similarly, a soil yielding an extract of EC = 16 dS/m would contain about 0.86 percent salt by weight.

These calculations are based on the total salt content of the saturation extract, which may or may not be equivalent to the total soluble salt content of the soil. Chang et al. (1983) found that comparison of total salt content of saturation extracts to extracts obtained using a 1:10 soil to water ratio yielded significant differences, with the 1:10 extracts generally being higher. They attributed the difference to the limited solubility and slow rate of dissolution of gypsum ($CaSO_4 \cdot 2H_2O$) relative to other sulfate salts. The saturation extracts should, however, give a reasonably good estimate of the total content of the more soluble sulfate salts such as epsomite ($MgSO_4 \cdot 7H_2O$) and mirabilite ($Na_2SO_4 \cdot 10H_2O$). The above calculations thus probably underestimate the total salt content.

Assuming further that salts, precipitating close to the water table, are dispersed within n cubic metres of soil (where n = depth to the water table), with 30 percent porosity, a specific gravity of 2.6, and therefore a mass of (0.7 x 0.0026 kg/cc x n x 10^6 cc/m^3) or 1820 x n kg, then the annual salt discharge can be expressed in terms of percent salt by weight of soil. Time required for salt accumulation to EC values of 4 and 16 dS/m can then be estimated. Results of these calculations are presented in Table 9.

The calculations indicate that groundwater and salt fluxes are

Table 9. Time required for salt accumulation to specified degrees of salinity.

Site	n = depth to water table (m)	Salt flux to water table ($kg/yr/m^2$)	% by weight if assume salt dispersed in n m3 of soil	Years required to salinize to	
				EC=4dS/m (0.19%)	EC=16dS/m (0.86%)
C4	1	2.4	0.13	1.5	6.6
*C6 (a)	2.3	0.86	0.02	9	40
(b)		0.17	0.004	48	215
(c)		0.02	0.0004	480	2150
5WT	2.3	0.09	0.002	90	400
*6WT (a)	2.3	2.1	0.05	4	17
(b)		0.3	0.007	28	125
(c)		0.03	0.0007	280	1250

* Calculated with k_v of clayey lacustrine unit = (a) 3.2×10^{-8} m/sec
(b) 3.0×10^{-9} m/sec
(c) 3.0×10^{-10} m/sec

sufficient to cause extreme soil salinization in very short time periods. Assuming that the hydraulic conductivity of the intervening clayey lacustrine sediment is 3×10^{-9} m/sec [case (b), Table 9], the maximum time needed for salinization to an EC of 16 dS/m is about 220 years. The same degree of salinization can result from groundwater discharge at Site C4 over a time span as short as 7 years. These calculations thus show that discharge of shallow groundwater can account for the severe soil salinity observed in the area.

3.4 Surface water and shallow unsaturated/saturated flow

3.4.1 Water table fluctuations

Because the water-table fluctuates in response to the addition or subtraction of water, the timing and nature of such fluctuations can help to identify sources of water at the water table. Water table rise can be attributed to infiltration of precipitation and runoff, and lateral or vertical inflow of water below the water table. Lowering of the water table may be caused by evaporation, evapotranspiration, and lateral or vertical outflow of water below the water table. Barring barometric effects and air entrapment during recharge events, times during which the sum of factors responsible for a water-table rise exceed that of factors responsible for water table decline, will be characterized by a rise in the water table. The water table will fall when conditions are reversed.

Typically, a major rise in the water table begins at about the end of February, about 2 to 3 weeks before the first rainfall event of the year. The rise is usually rapid, ranges from 0.4 to 1 m, and coincides with the spring snowmelt and subsequent spring precipitation events. Large quantities of water were observed on the surface during the 1984, 1985, and 1986 snowmelt events and these resulted in a large but temporary slough near Peacock (at Site A5, 11, and 12). About the beginning of May, evaporation, and later possibly evapotranspiration, cause the water table to fall until rain after the growing season again produces an increase. In late September or October, the water table begins to decline gradually until the snowmelt event of the following spring.

Response of deeper water tables is typically more subdued and lags relative to the shallower water levels. The hydrograph does not exhibit the general peaky nature that is apparent in shallow settings. In both cases, the water table rises in response to the spring snowmelt and runoff event and to spring rains, and then declines during the summer growing season. Reversals in direction caused by post growing season rainfall are, however, generally absent or very slight at deep water-table sites, but may be as large as 0.8 m at shallow sites.

Water-table hydrographs exhibit several different types of response depending on depth, the hydrogeologic setting, and the landscape. Those differences related to depth are best illustrated by comparing hydrographs of water-table wells at Sites A1 and B3 to those of others such as A5, B4 and B5 (Appendix 6). During the three years of monitoring, depth to the water table ranged from about 4.5 to 5.3 m at Site A1 and from about 3.3 to 3.8 m at Site A3. Ranges of fluctuation at Sites A5, B4 and B5 were about 1.1 to 2.4 m, 0.8 to 1.9 m, and 1.5 to 2.5 m, respectively.

Water-table fluctuations can also be grouped with respect to characteristic hydrograph shapes. Much of the following discussion is based on hydrographs of water-table wells installed early in 1986, which were not available for monitoring during the spring snowmelt events. The period of measurement related to this discussion is from May 1986 to February 1987.

The main differences in observed water-table fluctuation in this case is the response during the growing season. The first type of response is typified by that at 18WT. Other hydrographs following this pattern are at (5, 6, 12, 15, 16, 16-2, and A3) WT (Figure 34). Depth to the water table at these sites ranges from about 1.2 to 2.6 m. The decline that follows the initial rise caused by the spring thaw and spring rains begins in about mid-May, is steep, nearly linear, and equal to about 0.6 m. Response to post growing season rainfall is positive and inversely related to water-table depth.

The second response type is that shown on hydrographs of water-table wells at Sites C4, C5, and C6 (Figure 35). The water table at these sites is characterized by an increase in water-table elevation to about mid-July. The water level then stabilizes or declines slightly after this time. Rains following the post growing season result in very slight to no response. Depth to water table at these sites ranges from about 0.6 to 3.3 m. The deep water table at Site C5 is probably the result of steepening topographic gradients and the high hydraulic conductivity of the near-surface sediment.

The third type of water-table response is intermediate between the first two and is typified by water-table hydrographs (2, 4, 7, 8, 9, 10, 11, 13, 14, 17, 19, A4, and A5) WT (Figure 36). Depth to the water table at these sites ranges from 0.9 to 3.3 m. The hydrographs decline

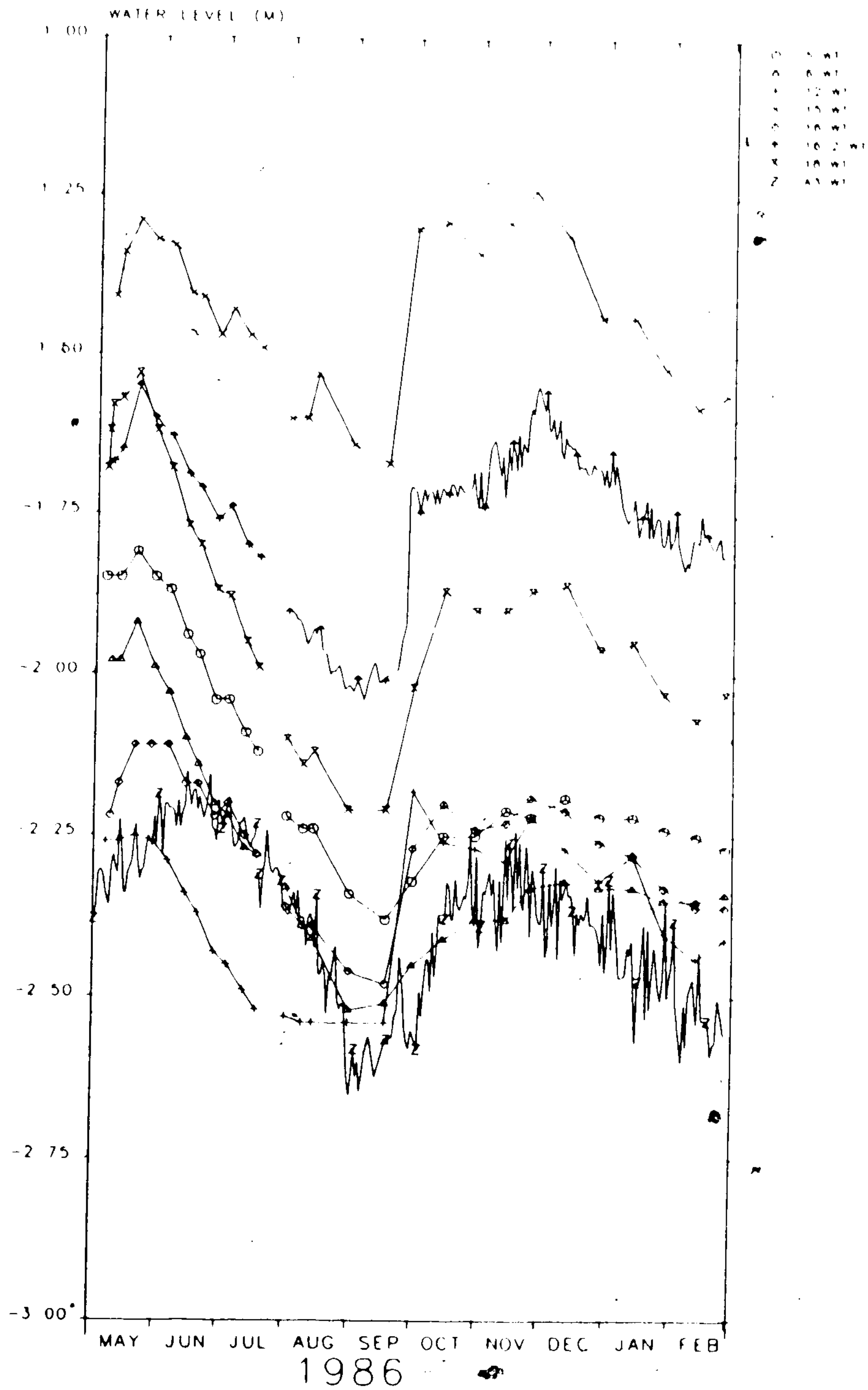

Figure 34. Type 1 water-table hydrographs.

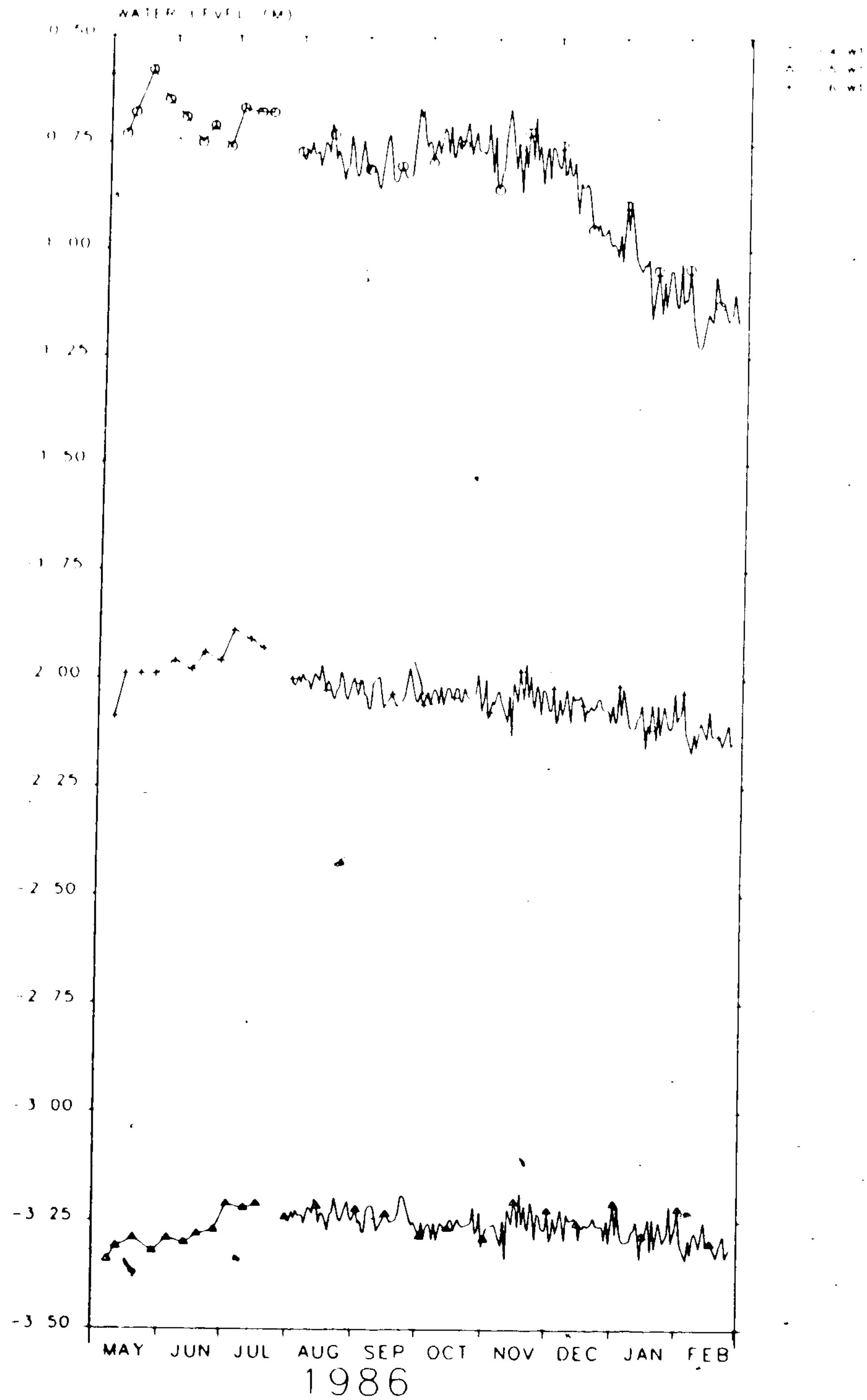

Figure 35. Type 2 water-table hydrographs.

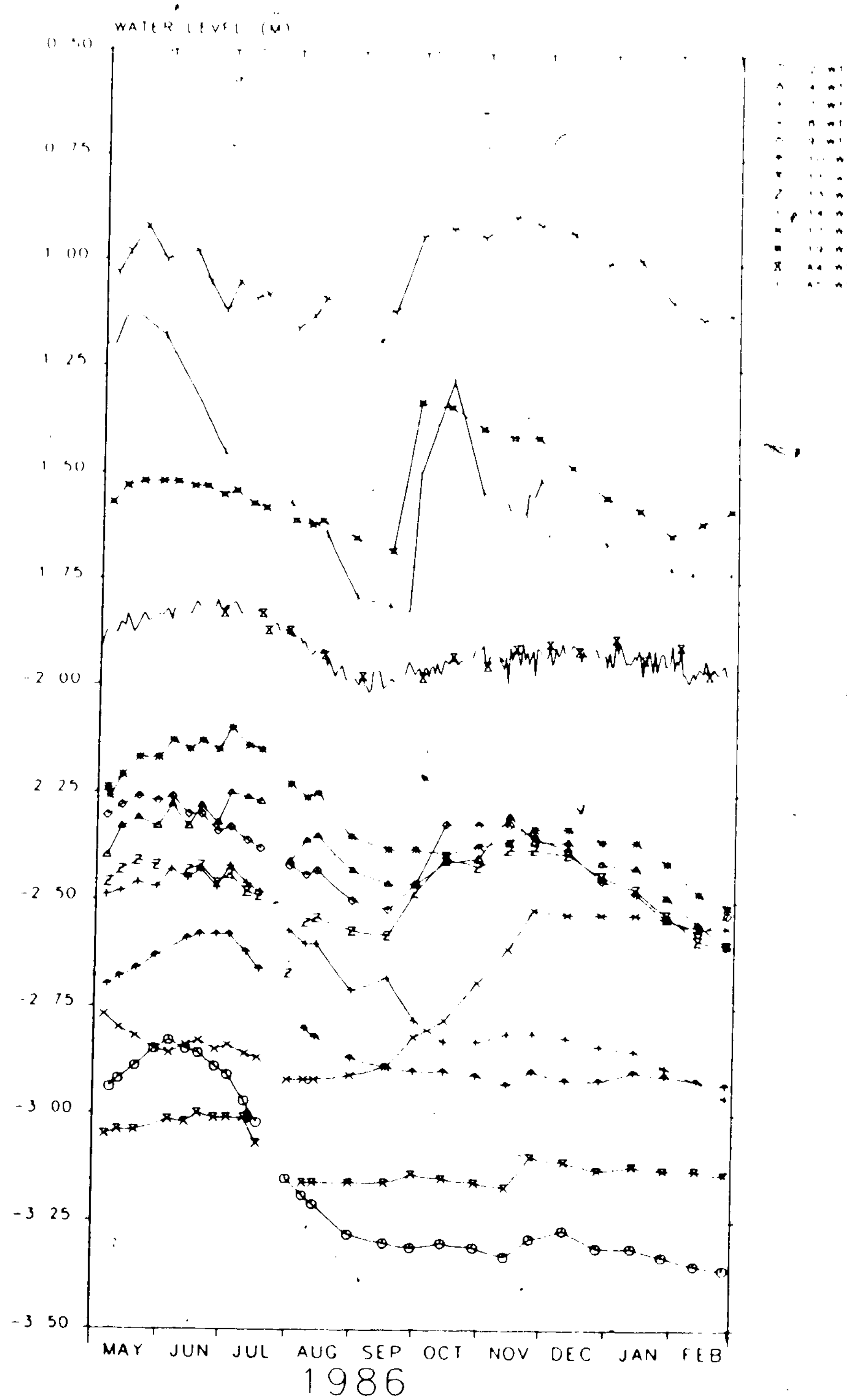

Figure 36. Type 3 water-table hydrographs.

during the growing season but the decline is less (0.1 to 0.4 m) and begins later (early June to early July) than for wells with a Type 1 response. The hydrographs typically have convex upward shapes during the decline. The water level typically responds to rains following the growing season, with the magnitude of the change being inversely related to water-table depth.

Changes in the water table can be related to water fluxes at the water table. That is, assuming the hydraulic character of the sediment to be the same, factors causing increased water-table elevation (infiltration of snowmelt and precipitation, and lateral or vertical addition of groundwater) must be greater at sites with Type 3 and especially Type 2 responses than at sites with the first type of response. Although groundwater discharge is strongly implicated at, and near, the base of Blackspring Ridge, lateral spreading of a water-table mound from the Peacock Slough should be the primary reason for continued and later addition of water to the water table in its vicinity. At sites with a relatively deep water table (2, 8, 10, and 11) WT the delayed spring response may result from restricted evaporation rates and more water being held in the unsaturated zone. However, at sites with a water table of less than about 2.5 m (less than or equal to sites with Type 1 response) addition of groundwater is implicated (4, 7, 9, 13, 14, 17 and 19) WT.

It should be noted that none of the Type 1 hydrograph configurations precludes additions of groundwater laterally or from below. The configurations simply imply that factors responsible for removal of water from the water table (evaporation and evapotranspiration) during the summer decline exert a greater influence than those responsible for addition. This situation is particularly true for Type 1 sites with a shallow water table (15WT).

The winter water-table decline that is observable on water-table hydrographs of the A and B-Line in late Fall and Winter means that a net loss of water from the water table is occurring during this time. Some of the loss may reflect lateral or downward movement of water away from the water table, particularly at B-Line Sites with downward hydraulic gradients. Because this feature exists also at sites with upward gradients, such as A4 and A5, however, it is almost certain that continued upward losses from the water table exist during winter months.

Similar declines were attributed by Schneider (1961) to upward movement of capillary moisture under the influence of thermal gradients toward the frost layer. Willis et al. (1964) showed that upward transfer of water to the frost zone can also occur in the vapor phase. Schneider (1961) attributed initial spring rises in water-table elevation to melting of the frost layer from below. It is thus probable that not all of the spring water-table rise noted in the study region can be attributed to recharge by snowmelt. Some unknown but possibly significant component of the water table rise merely represents a temperature-dependent vertical redistribution of groundwater and soil water at individual sites.

The conspicuous water-table rise that occurred in mid-January of 1986 represented such a frostmelt event. Early January was characterized by above-freezing daytime temperature and a major snowfall occurred in late February. The snow melted within days and wet and muddy conditions existed during field monitoring at the end of February. The January water-table rise thus corresponds to a temperature increase and not to infiltration of snowmelt.

The concept of infiltration to the water table in areas of upward groundwater flow, or areas of groundwater discharge, may be important from several points of view. Firstly, in the Blackspring Ridge area it is generally true (but with exceptions) that the water table is shallower in areas where groundwater discharge is indicated by strong upward gradients than elsewhere. It was shown in the preceding discussion of water-table responses that infiltration effects are more strongly apparent in areas with a shallow water table (less than 2.5 m). The combination of these features suggests that infiltration will in general cause a larger rise of the water table in groundwater discharge areas than in areas with strong downward components to flow.

Also, areas of groundwater discharge generally occupy topographically low areas and thus experience greater surface water accumulations, in response to runoff from snowmelt and high-intensity rainfall events, than upland areas. Therefore, water will be available for infiltration in larger quantities and for longer periods of time in low-lying areas than in upland areas. In addition to the net influx of groundwater that characterizes discharge areas, the increased and combined effects of infiltration of precipitation and runoff water probably play a greater role in maintaining a high water table in areas of groundwater discharge than elsewhere.

3.4.2 Tritium content of water from water-table wells

Tritium content determined for water samples from water-table wells in the area extending from the Peacock Slough to the west flank of Blackspring Ridge is shown in Figure 37. Depths of water-table wells

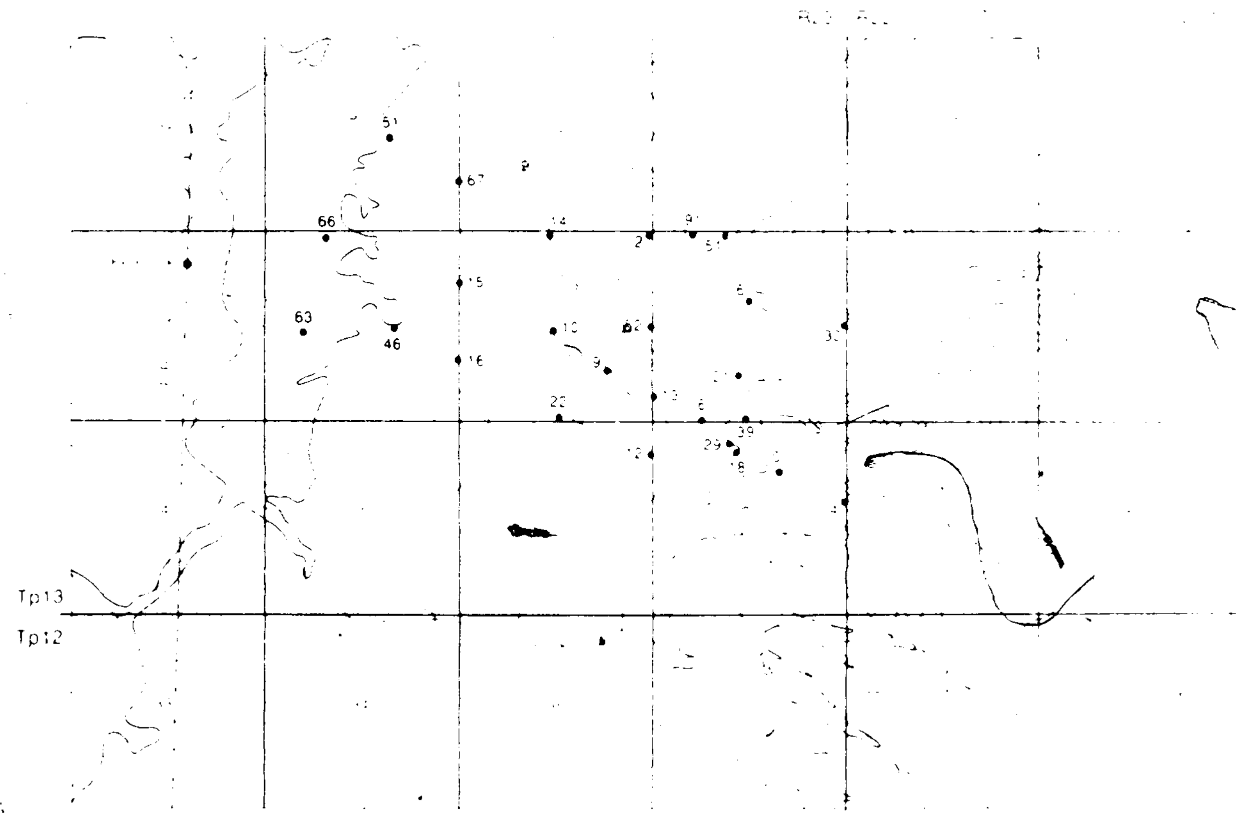

Figure 37. Tritium content of water-table well water.

represented in Figure 37 generally range from 3.5 to 6.5 m. Most were constructed to a depth of about 5.5 m, with the exception of 8WI (9.1 m), 16WI (7.6 m), C1WI (12 m), C2WI (12 m), and C3WI (9 m). With the exceptions noted, therefore, most wells are constructed to depths that are generally associated with high tritium content in pore waters. In a qualitative sense, the water sampled from water table wells should represent a composite value of tritium content that exists in the profile at each site, and should be weighted toward that of the largest contributing water source.

In this sense, and to the degree allowed by laboratory detection limits, primary sources of water to the water table can be qualitatively derived. Three groups of primary sources are identified:

1. Water in the vicinity of the Peacock Slough (Sites A5, 10, 11, 12 and 13) has tritium content ranging from 46 to 67 TU (mean = 59) or about twice the mean of present-day snowmelt and runoff water. The prime source to the water table is here considered to be the runoff accumulated in the Peacock Slough and water emplaced during time of peak activity in precipitation water (post 1952) still appears to be present.
2. Water-table water at Sites C4, C5, C6, A4, 4, 5, and 15, contains a large component of pre-1952 water which, because of upward gradients and hydrogeologic setting, is considered to be laterally and vertically contributed groundwater. Water from C3-30 and C2-40 is pre-1952 and has a distant bedrock source (see Figure 29).
3. Primary-source determination for water-table water at the remaining sites is somewhat more problematic since several scenarios are possible. Water at Sites 7, 8, and 9 is likely a combination of

recent precipitation and runoff mixed with groundwater transported laterally from Sites C6 and A4 and 5. Due to upward hydraulic gradients a deep groundwater contribution cannot be dismissed. High tritium values at Sites 6, 18, and 19 indicate that the major water source is a mixture of recent and post 1952 water. Recent precipitation and runoff, or combinations of these and groundwater, are possible for the remaining sites (2, 14, 16, 16-2, and 17).

The above qualitative analysis must, however, be tempered with the fact that many tritium determinations are well below laboratory detection limits at a confidence level of 95 percent. Group three interpretations are thus particularly suspect.

3.4.3 Surface water

The timing of water table fluctuations and tritium content of water at the water table indicate that surface water from the spring melt event is an important cause for the shallow water table on the lacustrine plain (sections 3.4.1 and 3.4.2). The following analysis examines the amount of salt that this same water can transport to low-lying areas.

Surface water was sampled periodically in 1985 from the time of the spring-melt event (March 11) to June 20. Samples were collected from a small temporary slough on top of Blackspring Ridge (A1.3), at two locations near the base of the ridge (the culvert shown on Plate 5, and runoff entering the area of interdunal salinity at the SW corner of 30-13-22 W4), and at the Peacock Slough. Chemical analyses are given in Appendix 7.

An important characteristic of the surface runoff is that it flows across areas of salinity that are caused by groundwater discharge (as described in 3.3) before it reaches its final destination. In doing so, the salts that were previously brought to the surface by groundwater discharge are redissolved and redistributed to topographically lower areas. For example, runoff water flows along the saline bottoms of coulees in Sections 6 and 7 of 13-22 W4, across the severely saline area near Sites A3, 16, and C4, and across saline areas in Section 11 and NW 12 of 13-23 W4 (Plate 4, Figure 4) before it reaches the Peacock Slough. Similarly, surface runoff that enters the areas of interdunal salinity in 25-13-23 W4 first crosses areas of saline groundwater discharge located at the base of the northern part of Blackspring Ridge.

The process of salt redistribution by surface runoff is reflected in the dissolved salt load of the surface water. Samples collected on March 11, 1985 had a TDS content of 112 mg/L on top of the ridge, 532 mg/L at the base of the ridge (culvert on Plate 4), and 492 mg/L at the Peacock Slough. Water that entered the interdunal saline area had a TDS content of 292 mg/L.

The total volume of water that forms the Peacock Slough annually can only be crudely estimated, but the following calculations are probably conservative. Assuming that the average annual area covered by water is 1 km^2, and the average depth is 0.2 m, then the total volume of water in the slough is 2×10^5 m^3 per spring-melt event. Given a TDS content of 500 mg/L, or 0.5 kg/m^3, the total salt load brought to the Peacock Slough annually is about 1×10^5 kg or 100 tonnes. On an areal basis, the average assumed depth of 0.2 m and TDS of 0.5 kg/m^3 mean that about 0.1 kg of salt per square metre of slough is available for addition to the soil.

Comparison of the above value to that of 3.2×10^{-3} kg/m^2/yr calculated as the salt flux from groundwater of regional origin (section 3.2) shows that the salt load contributed by spring runoff water is about 30 times greater than that from groundwater discharge.

Near surface salts at Site A5, which is located adjacent to the Peacock Slough, are mainly distributed in the upper 3.5 m (Appendix 3). This zone also correlates with the active recharge zone indicated by Tritium content of pore water, and with sandy lacustrine surface sediment. EC of saturation extracts from cores in the upper 3.5 m is about 5 dS/m.

Application of the conditions and concepts derived in section 3.3.3 to the salt load within the upper 3.5 m at Site A5 gives the following results. Saturation extracts with an EC of 5 dS/m should contain about 4400 mg/L of salt. One gram of soil yielding such an extract should therefore contain about 4400 mg/L x 0.5 x 10^{-3} L or about 2.2 mg of salt, which equates to about 0.22% by weight. To a depth of 3.5 m, the soil should thus contain about (3.5 m x 1820 kg/m^3 x .0022) kg/m^2 or about 14 kg salt per square metre of surface area. If the rate of accumulation by surface water inflow is 0.1 kg/m^2/year, then the existing salt load in the upper 3.5 m near the Peacock Slough required only 140 years to accumulate.

If it is assumed that climatic and runoff conditions similar to those of the present time have existed for the past 5000 years, then about 35 times the required time for salt accumulation is available. In other words, the degree of salinization at the Peacock Slough should be much higher than exists at present. This situation has three possible ramifications:

1. the calculated salt influx is grossly overestimated,
2. the Peacock Slough is not a closed system with respect to water, or
3. high salt influxes have only occurred for a very short period of time.

The first possibility is not likely the case. Discussions with local residents indicate that the average annual amount of surface runoff to the Peacock Slough is probably higher than that used in the preceeding calculations. In some years the slough receives more water than can infiltrate and evaporate and exists from one year to the next. Also, the calculations do not consider runoff from occasional high-intensity rainfall. The salt influx to the area of the Peacock Slough is thus probably underestimated.

The second condition is probable. The elevation of the water table near the Peacock Slough was about 941.1 and 940.5 m at Sites A5 and 12, respectively, in 1986. A hydraulic gradient of about 0.6 m/km or 0.0006 therefore exists at the water table and toward the north. The average hydraulic conductivity of the surface sand unit is 3.9×10^{-7} m/sec, and its thickness is about 5 m. An average linear velocity of:

$$v = [(3.9 \times 10^{-7}\ \text{m/sec})(6 \times 10^{-4})(5\ \text{m}^2)]/0.1$$

(assuming an effective porosity of 0.1) or 1.2×10^{-8} m/sec is thus possible to the north. This value equates to about 0.4 m/year. In 5000 years, the possible distance of water and salt movement away from the Peacock Slough is thus about 2000 m.

The third condition is also possible, although the argument can only be qualitative and in part speculative. Because native grasses would have existed along and on Blackspring Ridge in pre-agricultural time, the water table would have been lower. Saline areas would thus have been smaller in areal extent and the amount of salt on the ground surface at the base of the ridge would have been less. The pre-agricultural drainage pattern would also have been different. The present pattern is conducive to exposing a greater surface area to surface runoff for longer periods of time (see section 2.5). It is thus probable that more salt, that is distributed over larger areas of groundwater discharge, is now available for solution and redistribution by the surface water. The influx of salt to the Peacock Slough may thus have increased with the onset of agriculture.

The concepts developed in this section are more generally applicable than just to the area of the Peacock Slough. The latter was chosen for analysis because the slough is a well-defined area for which reasonable assumptions regarding salt and water fluxes can be made. The amount and TDS content of surface water entering the interdunal saline areas in S25 and 36 of 13-23 W4 are similar to those of the Peacock Slough. Soil salinity in the area of dunes may thus have a similar cause. Also, a large slough exists on the same lacustrine plain about 4 km SSW of the Peacock Slough. Its position with respect to hydrogeology, hydrology, and saline areas along the base of Blackspring Ridge is also similar to that of the Peacock Slough. Runoff water and its contained salt load may thus be responsible for soil salinity over large areas of the lacustrine plain.

4. SUMMARY AND CONCLUSIONS

4.1. Regional groundwater flow

Direct transport of solutes in deep, regional flow systems does not contribute significantly to the development of saline soils in the Blackspring Ridge area. The regional configuration of groundwater flow is strongly influenced by two major sets of geologic units of high hydraulic conductivity. Firstly, two major bedrock valleys, the Carmangay and Peacock Valleys, act as line sinks. Deep groundwater moves laterally toward, and eventually is transmitted along, these units. The influence of the bedrock valleys is reflected for relatively large distances in the second set of major units - the basal sandstone of the Horseshoe Canyon Formation and the Ryegrass Sandstone. Hydraulic continuity between the two sets of units is provided by either direct contact with permeable valley sediment, or by terrace deposits along buried-valley flanks. Thus, downward and lateral hydraulic gradients exist in bedrock and drift units of the lacustrine plain for distances of 5 km or more from the Little Bow River.

The strength of the hydraulic influence of the Carmangay Valley decreases with distance for two reasons. Firstly, the gradients are simply dissipated over distance, and secondly, bedrock units dip more strongly south of the B-Line. The influence of the direct hydraulic connection between bedrock valley sediment, basal units of the Horseshoe Canyon Formation and the Ryegrass Sandstone thus ceases to exist at some point between the A and B-Lines and gradients under the lacustrine plain become directed upward. Where all regional groundwater flow (to the depth of the Ryegrass Sandstone) along the B-Line ends up in the

Carmangay Valley aquifer, only about 20 percent flows to the Peacock Valley aquifer along the A-Line.

Regional groundwater flow discharges to the lacustrine plain in southern regions of the study area. Calculation of the groundwater flux shows, however, that discharge from the regional system is generally less than the equivalent of 2 mm of precipitation per year and should not in itself be a direct cause of salinity in these regions.

4.2 Local groundwater flow

Investigations in the vicinity of the C-Line lead to the conclusion that groundwater flow from local, relatively shallow (to about 30 m) systems is responsible for severe soil salinization in that region. Calculations based on combinations of hydraulic conductivity and hydraulic heads in near-surface unconsolidated sediment show that salt-fluxes in excess of 2 $kg/m^2/yr$ are possible in extreme cases. The following generalized model is proposed to explain the severe soil salinity.

Bedrock along the west flank of Blackspring Ridge is highly fractured as a result of glaciotectonic activity. The fracturing imparts high hydraulic conductivity primarily to sandstone units, but locally also to intervening units of claystone and shale, to a depth of about 30 m below the bedrock surface. The fractured-bedrock zone constitutes a region of active groundwater flow in which salts are generated and transported, and from which highly mineralized water is discharged to the surface or to other drift units in the area between Sites 16 and C6.

Where fractured bedrock units subcrop or crop out along coulees and upper portions of the west flank of Blackspring Ridge, groundwater discharge from the units is a direct cause for soil salinity. Examples of such areas are the localized saline areas in NE of 6, West half of 7, and SW of 29 of Township 13, Range 22, W4.

Several drift units of high hydraulic conductivity are also important features that help create salinity in the vicinity of the C-Line. Firstly, a preglacial sand as much as to 2 m thick exists on portions of the western flank of Blackspring Ridge and acts as a conduit to move shallow groundwater to lower portions of the ridge. Secondly, an interglacial sand and gravel unit exists in channel form at the base of the Ridge (Sites C6, 6 and 5). This unit receives water from adjacent fractured bedrock and from the preglacial sand unit. The hydraulic gradient in the channel unit is strongly upward and groundwater discharges to the surface. Thirdly, a highly permeable lacustrine or alluvial unit exists at the surface in, and topographically below, the area of major groundwater discharge and salt accumulation. This unit receives groundwater and dissolved salts from the fractured bedrock, from the preglacial sand unit, and from the channel unit. Water and salt then move laterally downslope within the unit and are redistributed to areas of the lacustrine plain that are downslope from the original points of discharge.

The conclusion that the severe salinity in the vicinity of the C-Line is caused by groundwater discharge from relatively shallow (<30 m) zones is supported by chemical and isotopic data. The shallow zone contains the dominant salt load. TDS and $SO_4^{=}$ concentration is always above 6000 and 3000 mg/L, respectively and increases to as much as 52 800 and 35 200 mg/L, respectively at the water table. Groundwater flow appears active enough to maintain an oxidation state such that sulfate reduction does not occur; fracture-dominated flow may be implied by high Ca^{++} and Mg^{++} content. Concentration of Ca^{++} and Mg^{++} relative to Na^{+} and K^{+}, in water at the water table of saline areas, implies that a mixed drift and shallow-bedrock groundwater source is required.

Water from the shallow active-flow zone has $\delta^{18}O$ and Deuterium content similar to present-day precipitation; deeper water has an isotopic composition of water emplaced during climatic conditions different from the present. This implies a very long residence time and sluggish flow in deeper zones and indicates that significant discharge from deep systems is not likely. Furthermore, deep groundwater has a much lower salt load than shallow water because the former has undergone sulfate reduction. Thus significant discharge of neither groundwater nor salt is possible from the deeper zone.

4.3 Topography and surface water hydrology

Several topographic factors are important with respect to soil salinization in the Blackspring Ridge area. Firstly, the major salinity in the area (near Site C4) exists in a topographic setting dominated by a broad, bowl-shaped depression on the flank of the ridge, which contains several coulees. The depression focuses flow of both surface water and groundwater, resulting in larger volumes of inflow than would otherwise exist. This increased groundwater discharge transports the necessary quantities of salt to the area, and abundant surface water input maintains a higher water table and facilitates salt deposition at or close to the ground surface.

Secondly, the surface drainage is such that topographically low areas will be more influenced by surface-water runoff than high areas. Low areas will experience larger volumes of runoff whose residence time on the surface will, in general, be longer, than the higher areas. A longer time thus exists for infiltration to the water table. Also, because groundwater discharge areas generally occupy low portions of the landscape, surface water contributions to the water table can, in general, not drain vertically because of an hydraulic-perch effect. The combination of these two factors results in a higher water table in affected areas than elsewhere.

Water-table hydrographs show that the depth to the water table and the magnitude of positive response to precipitation events are negatively correlated. Thus, in addition to receiving larger volumes of surface runoff and a possible groundwater contribution, the high water table in topographically low areas is also more strongly affected by recharge from precipitation. All of the above factors are combined to the greatest extent in the region of the temporary Peacock Slough. This feature constitutes a low point in the landscape, has no surface outlet, is fed by a large catchment area, and has lateral and upward directed hydraulic gradients.

In addition to causing a high water table, the surface water carries a substantial salt load to low-lying areas and is the prime cause for soil salinity on much of the lacustrine plain. The salt load is picked up as surface water from the spring-melt events flows across areas in which salt has been brought to the surface by groundwater discharge and is then redistributed to topographically lower areas. In areas where surface water accumulates, such as at the Peacock Slough, as much as 100 tonnes, or 0.1 kg/m^2/year of salt is added to the soil.

This rate is high enough to cause salinization to an EC of 5 dS/m, to a depth of 3.5 m, in as little as 140 years.

REFERENCES

Babcock, E.A. (1974): Photolineaments and regional joints: Lineament density and terrain parameters, south-central Alberta. Bull. Can. Petr. Geol., V.22, No. 2, p. 89-105.

Ballantyne, A. (1963): Recent accumulation of salts in the soils of southeastern Saskatchewan. Can. J. Soil Sci. 43, p. 52-58.

Bear, J. (1972): Dynamics of fluids in porous media. American Elsevier Publishing Company, Inc., New York, N.Y., p. 151-165.

Black, C.A., D.D. Evans, J.L. White, L.E. Ensminger, and F.E. Clark, Editors (1965): Methods of soil analysis, Part 2, Chemical and microbiological properties. American Society of Agronomy, Inc., Publisher. Madison, Wisconsin, U.S.A.

Bouwer, H. and R.C. Rice (1976): A slug test for determining hydraulic conductivity of unconfined aquifers with completely or partially penetrating wells. Water Resources Research, V. 12, No. 3, p. 423-428.

Brown, P.L. and M.R. Miller (1978): Soil and crop management practices to control saline seeps in the U.S. Northern Great Plains. Proceedings of the Subcommission on Salt-affected Soils, ISSS Congress, Edmonton.

Brown, P.L., A.D. Halvorson, F.H. Siddoway, H.F. Mayland, and R.M. Miller (1983): Saline-seep diagnosis, control, and reclamation. United States Department of Agriculture, Conservation Research Report Number 30.

Chan, G.W. and M.J. Hendry (1985): Impact of irrigation expansion on salinity adjacent to the Monarch branch canal. Alberta Agriculture, Drainage Branch.

Chang, C., T.G. Sommerfeldt, J.M. Carefoot, and G.B. Schaalje (1983): Relationships of electrical conductivity with total dissolved salts and cation concentration of sulfate-dominant soil extracts. Can. J. Soil Sci. 63, p. 79-86.

Cooper, H.H. Jr., J.D. Bredehoeft, and I.S. Papadopulus (1967): Response of a finite-diameter well to an instantaneous charge of water. Water Resources Research, V. 3, No. 1, p. 263-269.

Craig, H. (1961): Isotopic variations in natural waters. Science 133. p. 1702-1703.

Crowe, A.S. and F.J. Longstaffe (1987): Extension of geochemical modelling techniques to brines: coupling of the Pitzer equations to PHREEQE. Proceedings of the Solving Ground Water Problems with Models Conference and Exposition, V. 1, p. 110-129. Feb., 1987, Denver, Colorado.

Doering, E.J. and L.C. Benz (1972): Pumping an artesian source for water-table control. J. of the Irrigation and Drainage Division, Proc. Amer Soc. of Civil Eng., June 1972, p. 275-287.

Doering, E.J. and F.M. Sandoval (1975): Hydrology of saline seeps in the Northern Great Plains. Trans. Am. Soc. Agr. Engineers 19(5), p. 856-865.

Fontes, J. Ch. (1980): Environmental isotopes in groundwater hydrology. in Handbook of environmental isotope geochemistry. P. Fritz and J.Ch. Fontes, editors.

Forster, J.T. (1984): Soils and hydrogeologic investigations, Keho Lake reservoir enlargement project. Alberta Env., Environmental Protection Services.

Freeze, R.A. (1969): Theoretical analysis of regional groundwater flow. Canada Department of Energy, Mines and Resources, Inland Waters Branch, Scientific Series No. 3.

Freeze, R.A. and J.A. Cherry (1979): Groundwater. Prentice Hall, Inc., Englewood Cliffs, N.J.

Geiger, K.W. (1967): Bedrock topography at the Gleichen map-area, Alberta. Alberta Research Council Map 67-2A, 1:250,000.

Government and The University of Alberta (1969): Atlas of Alberta. University of Alberta Press.

Harr, M.E. (1962): Groundwater and Seepage, McGraw-Hill Book Company, Inc.

Harvie, E. and J.H. Weare (1980): The prediction of mineral solubilities in natural waters: the Na-K-Mg-Ca-Cl-SO_4-H_2O system from zero to high concentration at 25°C. Geochimica et Chosmochimica Acta, 44, p. 981-997.

Hendry, M.J. (1983): Origins of groundwater causing soil salinization in the Horsefly Lake area. Alberta Agriculture, Drainage Branch.

Hendry, M.J., J.A. Cherry, and E.I. Wallick (1986): Origin and distribution of sulfate in a fractured till in southern Alberta, Canada. Water Resources Research, Vol. 22, No. 1, p. 45-61.

Hendry, M.J. and F.W. Schwartz (1982): Hydrogeology of saline seeps. Proceedings, First Annual Western Provincial Conference, Rationalization of Water and Soil Research and Management, Soil Salinity; Lethbridge, Alberta. p. 25-40.

Henry, J.L., P.R. Bullock, T.J. Hogg, and L.D. Luba (1985): Groundwater discharge from glacial and bedrock aquifers as a soil salinization factor in Saskatchewan. Can. J. Soil Sci. 65, p. 749-768.

Hvorslev, M.J. (1951): Time lag and soil permeability in groundwater observations. U.S. Army Corps Engrs. Waterways Exp. Sta. Bulletin 36, Vicksburg, Miss.

INTERA Environmental Consultants Limited (1983a): LANDSAT dryland salinity demonstration program, Salinity summary map, Lethbridge, Alberta, N.T.S. 82H, 1:250,000.

INTERA Environmental Consultants Limited (1983b): LANDSAT dryland salinity demonstration program, Salinity summary map, Gleichen, Alberta, N.T.S. 82I, 1:250,000.

Lines, F.G. (1963): Stratigraphy of Bearpaw Formation of southern Alberta. Bull. Can. Petr. Geol., V. 11, No. 3, p. 212-227.

Link, T.A. and A.J. Childerhose (1931): Bearpaw shale and contiguous formations in the Lethbridge area, Alberta. Am. Assoc. Petr. Geol. Bull., V. 15, No. 10, p. 1227-1242.

Longley, R.W. (1968): Climatic maps for Alberta. Dept. of Geog., University of Alberta.

Maathuis, H. and G. Vander Kamp (1986): Theory of groundwater flow in the vicinity of brine ponds and salt tailings piles. Saskatchewan Research Council Technical Report No. 152, 39 pages.

Meyboom, P. (1966): Groundwater Studies in the Assiniboine River Drainage Basin, Part I: The evaluation of a flow system in south-central Saskatchewan. Geol. Surv. of Canada, Bulletin 139.

Moell, C.E., J.G. Pawlowicz, M.R. Trudell, M.M. Fenton, C.W. Langenberg, G.J. Sterenberg, and C.E. Jones (1985): Highwall Stability Project, Highvale Mine, Report on 1984 activities. Alberta Research Council unpublished report prepared for TransAlta Utilities Corporation.

Parkhurst, D.L., D.C. Thorstenson and L.N.P. Plummer (1980): PHREEQE - a computer program for geochemical calculations. United States Geological Survey. Water Resources Investigations. p. 80-96. NTIS report No. USGS/WRD/WRI-80/018.

Plummer, L.N., B.F. Jones, and A.H. Truesdell (1976): WATEQF - Fortran 4 version of WATEQ, a computer program for calculating chemical equilibrium of natural waters. USGS Water Resources Investigations 76-13.

Rhoades, J.D. and D.L. Corwin (1981): Determining soil electrical conductivity - depth relations using an inductive electromagnetic soil conductivity meter. Soil Sci. Soc. Am. J., Vol. 45, p. 255-260.

Sauer, E.K. (1979): The engineering significance of glacier ice-thrusting. Can. Geotech. Jour., V. 15, No. 4, p. 457-472.

Schneider, R. (1961): Correlation of ground water levels and air temperatures in the winter and spring in Minnesota. U.S. Geol. Surv. Water Supply Paper 1539 D.

Schwartz, F.W. and A. Crowe (1980): A deterministic probabilistic model for contaminant transport. U.S. Nuclear Reg. Comm., Wash. D.C.

Toth, J. (1962): A theoretical analysis of groundwater flow in small drainage basins. Proceedings of Hydrology Symposium No. 3 Groundwater.

Vander Pluym, H. (1978): Extent, causes and control of dryland saline seepage in the Northern Great Plains region of Northern America. Proceedings of the Subcommission on Salt affected Soils, ISSS Congress, Edmonton.

Vander Pluym, H. (1982): Salinity in western Canada. Proceedings, First Annual Western Provincial Conference, Rationalization of Water and Soil Research and Management, Soil Salinity; Lethbridge, Alberta, p. 9-23.

Wallick, E.I. (in press): Origin of the sodium sulfate/sodium carbonate deposit at Horseshoe Lake, Mestiskow, east central Alberta. Alberta Research Council Bulletin.

Willis, W.O., H.L. Parkinson, C.W. Carlson, and H.J. Haas (1964): Water table changes and soil moisture loss under frozen conditions. Soil Science, Vol. 98, No. 4.

THE QUALITY OF THIS MICROFICHE IS HEAVILY DEPENDENT UPON THE QUALITY OF THE THESIS SUBMITTED FOR MICROFILMING.

UNFORTUNATELY THE COLOURED ILLUSTRATIONS OF THIS THESIS CAN ONLY YIELD DIFFERENT TONES OF GREY.

LA QUALITE DE CETTE MICROFICHE DEPEND GRANDEMENT DE LA QUALITE DE LA THESES SOUMISE AU MICROFILMAGE.

MALHEUREUSEMENT, LES DIFFERENTES ILLUSTRATIONS EN COULEURS DE CETTE THESES NE PEUVENT DONNER QUE DES TEINTES DE GRIS.

Plate 1. Severe developmennt of soil salinity near the base of Blackspring Ridge. SW¼-12-13-23W4

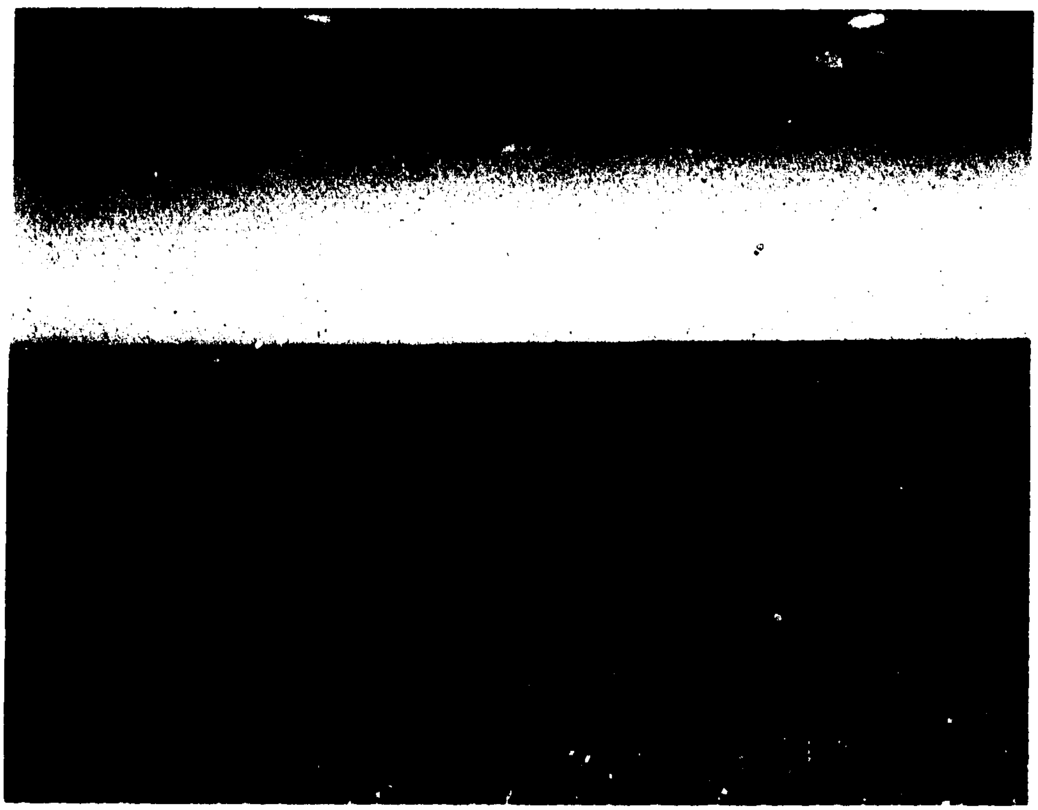

Plate 2. Poor cereal production in a salt affected area. SE¼-11-13-23W4

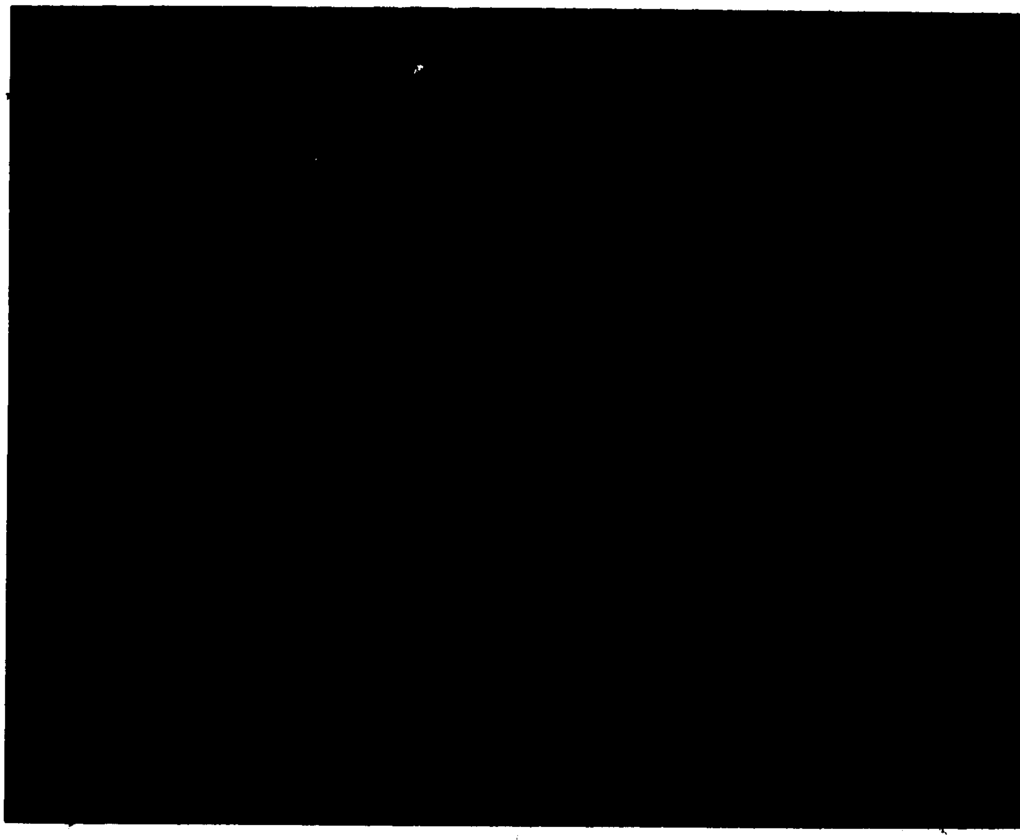

Plate 3. Salinity developed in an interdunal setting in 31-13-22W4. Distance across the photograph is 1.5 km.

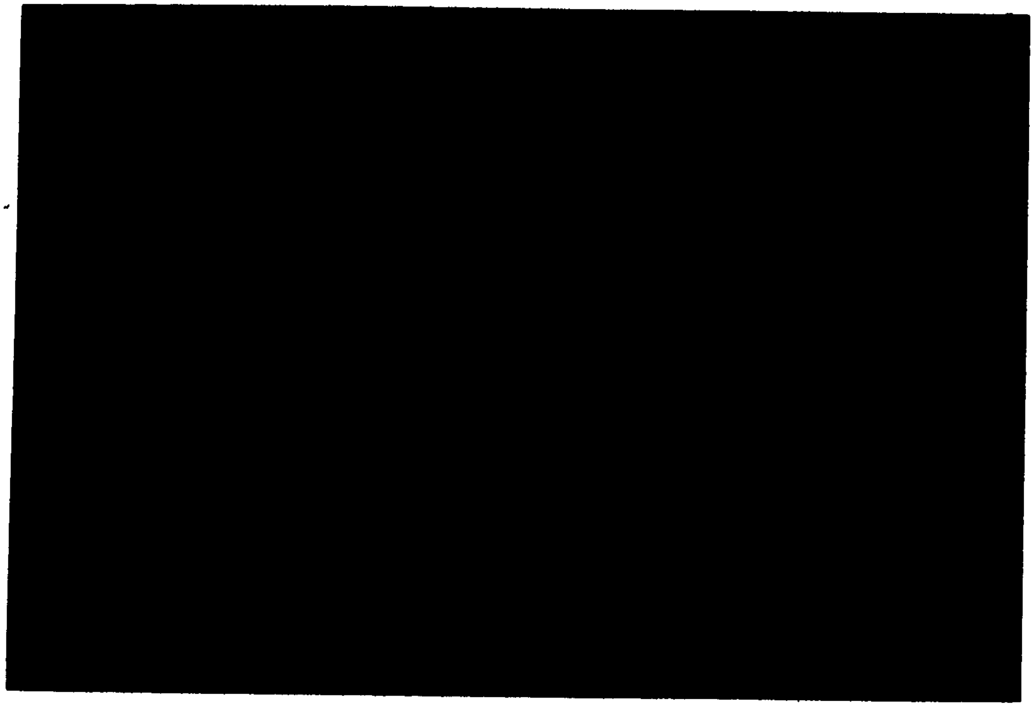

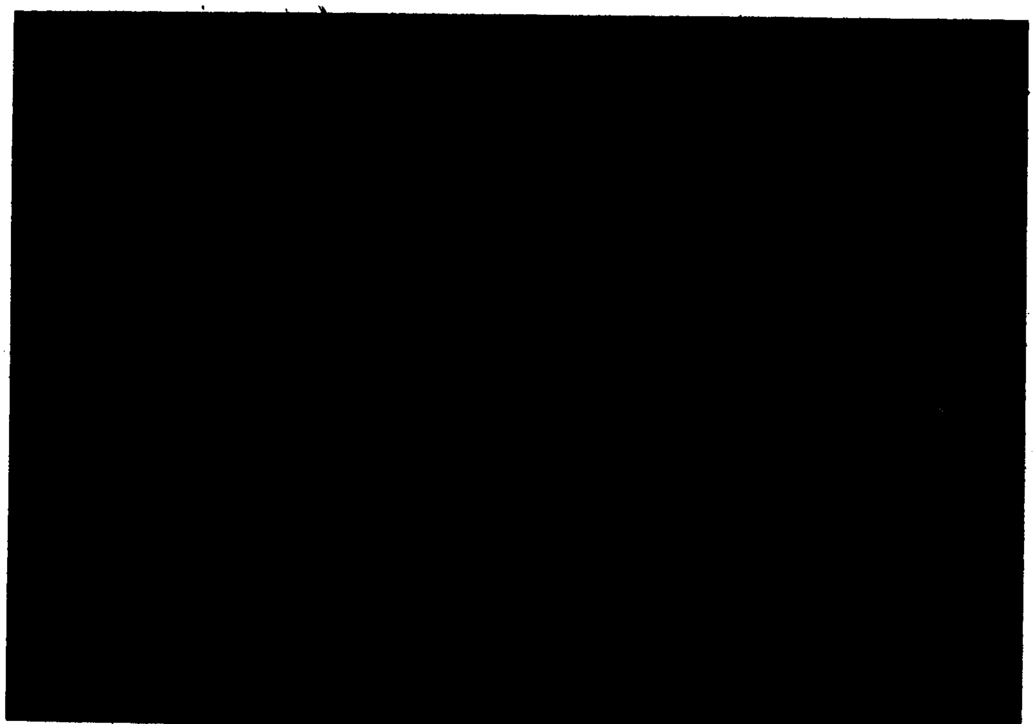

Plate 4. Spring runoff, March 4, 1986.

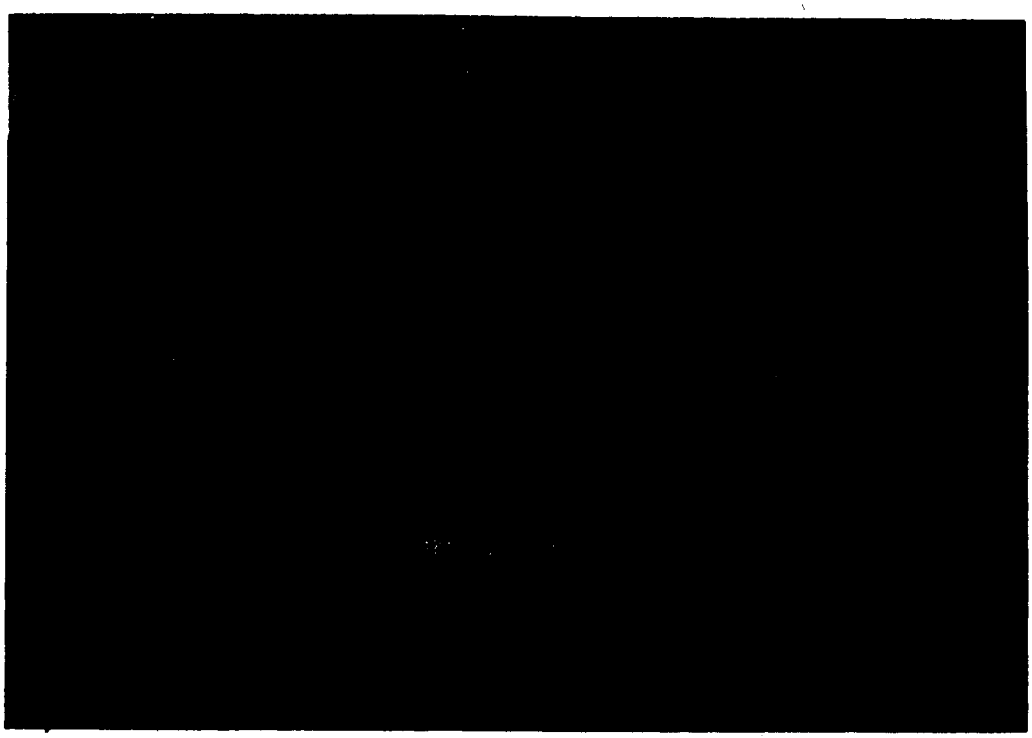

Plate 5. Spring runoff, 1985. Culvert is located about 0.2 km north of site 6 in NE¼-11-13-23W4.

APPENDIX 1

Methods of Investigation

Saline soil distribution

Areas of saline soil were determined by visual inspection of 1:10 000 scale colour air photographs (where available), 1:40 000 scale black and white air photographs, and from published 1:250 000 scale soil salinity maps (INTERA Environmental Consultants Ltd. 1983a, 1983b).

In addition to visual checks, electrical conductivity was measured at 100-m intervals along the lines of section using a Geonics EM38 ground conductivity meter. The meter was positioned with both transmitter and receiver ends in contact with the ground surface. Measurements were taken with both ends aligned normal to the ground surface (vertical position) and parallel to the ground surface (horizontal position). Rhoades and Corwin (1981) correlated conductivity values obtained in the vertical position to salinity in the root zone (0 to 120 cm). To convert field measurements to electrical conductivity requires calibration equations. The equations here are based on correlation of EM38 data with saturation extracts of 110 samples taken at coinciding locations. The resulting equations are:

(a) horizontal $\ln(EC) = 0.996 \ln(R) - 3.435$ $r^2 = 0.675$

(b) vertical $\ln(EC) = 0.940 \ln(R) - 3.085$ $r^2 = 0.682$

where EC is electrical conductivity in dS/m (deciSiemens per metre) and R is the meter reading.

Geologic Studies

Regional geological studies involved constructing maps and cross-sections. A structure contour map was constructed on an easily recognizable bentonite and sandstone horizon (top of the Kipp Sandstone) within the Bearpaw Formation, using structure testhole and oil well electric logs. This map helped to define geologic structure and to correlate bedrock stratigraphic and hydrostratigraphic units. Two deep seismic reflection profiles, provided courtesy of Canadian Occidental Petroleum Ltd., were used to evaluate whether deep-seated faulting influences the structure and continuity of geologic units.

Deep testholes were drilled using conventional mud-rotary techniques to the anticipated base of regional groundwater flow or about 150 m, whichever was less. Ten mud-rotary testholes, spaced 1.5 to 2.5 km apart, were drilled for the initial regional investigation. These ranged in depth from 97 to 150 m and were drilled along two lines of section. A further six testholes, 30 to 80 m deep and at about 0.4 km spacing, were drilled during the detailed phase of the investigation. Drill cuttings were collected at 1.5-m intervals, described in the field, and stored for further examination. Borehole geophysical surveys consisted of caliper, linear density, gamma ray, neutron-neutron, sonic, spontaneous potential, focused electric and temperature logs. Spontaneous potential and resistivity logs only were run in the latter six rotary testholes.

Shallower test-holes in drift were completed with an auger rig. A 20-cm diameter hole was augered at each regional drilling site. Depths ranged from 5.5 to 31 m and were controlled by geologic and machine constraints. Metal tube push cores were taken continuously for the first 1.8 m, at 1.5-m intervals to 15 m, and at 3-m intervals from 15 m to bottom. Deviation from this sampling plan was not unusual and was necessary due to changing borehole conditions such as quick conditions or boulders.

Core samples were sealed immediately after collection with rubber caps and electrical tape. Later they were extruded, split, and vacuum sealed in polyethylene sleeves. One split was used for visual examination for lithology, fracturing, degree of weathering, and secondary mineralization. A subset of samples was submitted to Research Council laboratories for saturation paste extract preparation and analyses.

The second set of split cores was shipped to the Alberta Environmental Centre (Vegreville) Radiocarbon and Tritium Laboratory for pore water extraction (by a toluene reflux process) and tritium analysis. Seventy-six intervals were selected for pore water extraction, based on core depth and results of the visual examination.

<u>Piezometer and Water-Table Well Construction and Testing</u>

Completion zones for piezometers were selected using geophysical logs of rotary testholes, lithologic logs of rotary and auger holes, and noted occurrences of water during auger drilling. The completion zones were chosen to represent the diverse hydrochemical and hydraulic environments in the area, and to provide hydraulic conductivity data representative of different geologic units.

Piezometers were emplaced in boreholes drilled using either hollow-stem or solid augers, or conventional mud-rotary techniques. In hollow-stem auger construction, a 20-cm hole was drilled to the bottom of the completion zone and the piezometer assembly installed through the auger. The drill pipe was retracted to expose the completion zone and a gravel pack and bentonite-pellet seal were installed. Proper placement of the gravel pack and seal was checked with a weighted tape. Next the augers were backed out of the hole, leaving cuttings on the auger flights to fill the annular space between the piezometer pipe and auger-hole wall. In holes drilled using solid augers, the piezometer assembly was installed in an open, 15-cm hole, that in most cases was dry. The gravel pack and bentonite-pellet seal were placed down the open hole. The remaining open hole was backfilled with auger cuttings.

The following procedure was used for piezometer construction in rotary-drilled holes. Depending on expected geologic conditions, holes ranging from 13 to 17 cm in diameter were drilled to the bottom of the completion zone. Natural mud was used at all sites except A2, where circulation loss occurred. The deepest piezometer at each site was installed in the previously drilled testhole after it was backfilled and sealed with bentonite pellets below the completion zone. Drilling mud was lightened by circulation with clean water and the piezometer assembly installed. Clean water was then circulated through the screen and washdown fitting until returns were clean. A gravel pack and bentonite-pellet seal were installed and depths checked with a weighted tape. A slurry consisting of about 0.3 kg of granular or powdered bentonite per litre of water was used to seal the annular space between the piezometer pipe and borehole wall.

Five-cm schedule 40 plastic pipe was used for piezometer and water-table well casing. Sixty-cm long, continuous wound plastic, 20-slot screens were used for piezometer tips during the regional investigation. Because the regional investigation indicated that fracturing of bedrock sediment is an important mechanism of hydraulic conductivity modification, most bedrock piezometers installed during the later, more detailed investigation, were completed using 3 m of 15-slot, machine slotted pipe. The intention was to sample a rock volume sufficiently large to have a high probability of encountering a representative number of fractures. Piezometers installed in the rotary drilled boreholes were equipped with a washdown valve to improve circulation while washing. Plastic centralizers, to prevent screen contact with the borehole wall and to allow an even gravel pack around the piezometer tips, were used in piezometers constructed with rotary and solid auger drilling machines.

Water-table wells were completed with 15-slot, machine slotted plastic pipe and were gravel packed from bottom to within about 1.2 m of the ground surface. The annular space above the gravel pack was sealed with bentonite pellets and drill cuttings to prevent surface water contamination.

Gravel packs used in all wells and piezometers consisted of No. 9 Sil Silica sand. All piezometers and wells were developed twice by production with compressed air or bailing. Completion details of individual wells and piezometers are given in Appendix 12.

Piezometers and water-table wells were hydraulically tested and results analyzed by methods appropriate to individual hydraulic settings. The Bouwer and Rice (1976) solution was used for unconfined settings and Hvorslev (1951) methodology for confined situations. Piezometers C4-65 and C4-100 flow freely if open to the atmosphere. These were produced by air lifting and the solution of Cooper and Jacob (1946) was used to analyze recovery data. The basal sand and gravel aquifer of the Peacock Channel was tested with a pumping well and two piezometers. Data were analyzed using the solution of Vandenberg (1976) for a leaky artesian aquifer in a parallel channel. The latter solution uses computer generated type curves for the configuration of well position and aquifer boundaries specific to the test sites.

Water Level Monitoring

Water levels were monitored, initially daily, then weekly, and biweekly beginning in late January 1984. A battery-operated Oll tape, accurate to within 0.25 cm, was used to measure depths of water levels from the top of each piezometer and water-table well. Selected water table wells and piezometers were fitted with Stevens type F, weight driven, automatic water-level recorders. Location and elevation were surveyed.

Water Sampling

Waters from piezometers and water-table wells were sampled using a Bennett Model 180-500, compressed-gas operated, peristaltic, noncontaminating pump. In cases where water levels were too low for pump use, samples were collected with a stainless steel bailer equipped with a plastic foot-valve. At least one casing volume of water was removed from each well prior to sample collection and the sample pump purged with compressed air after each sample was collected.

Samples were collected in 1-L, 250-mL, and 20-mL polyethylene bottles. One-litre and 250-mL sample bottles were soaked in deionized and demineralized water for at least one week prior to use and kept sealed until the time of sampling. A few drops of concentrated nitric acid were added to the soaking bath of the 250-mL bottles to bring the pH to less than two.

Temperature, conductivity, and dissolved oxygen were measured immediately upon sampling using a YSI Model 57 dissolved oxygen and temperature meter and a HACH Model 2510 conductivity meter. Two one-litre samples were kept on ice for transport to a mobile field laboratory.

Samples for major ion analysis were filtered into 20 ml vials, sealed, and refrigerated until delivery to either Chemex Ltd. in Calgary, or the Research Council laboratory. Unfiltered 1 L samples were collected for tritium analysis and were sealed with tape to prevent air and water transfer. Samples for ^{18}O and deuterium analysis were collected in 20-mL bottles. Deuterium and ^{18}O analyses were performed by the University of Calgary, Physics Department Isotope Laboratory. Total alkalinity and pH were determined in the field laboratory using standard titration methods. Electrodes, buffers, and samples were kept refrigerated until analysis. Total iron was determined using a filtered 25-mL sample and a spectrophotometric method.

Snow and ponded surface water from snowmelt were periodically sampled in both upland and lowland settings and analysed for ^{3}H, $\delta^{18}O$ and deuterium content.

SITE	DEPTH	SAT'N	EC	Na	K	Ca	Mg	SO4	pH	Cl	ALK
	m	kg/kg	dSm	<-----	mmol/L			--->		<--- ppm	--->
A1	1.5	.475	3.46	15.6	.3	2.8	15.0	12.0	7.9	9.6	163
	2.0	.564	3.26	6.0	.5	7.6	15.3	12.5	7.7	6.9	129
	3.5	.538	4.25	7.6	.6	12.2	20.4	17.7	7.6	28.4	139
A2	.3	.625	.86	1.2	.5	3.3	1.2	.3	6.8	26.2	385
	.8	.602	.57	.7	.1	2.4	.9	.2	7.4	5.2	358
	1.1	.607	.54	.9	.1	11.9	.1	.3	7.8	6.1	169
	1.4	.514	.68	2.1	.1	1.7	1.2	.7	8.0	5.9	188
	1.8	.484	.73	6.7	.1	.2	.7	.6	8.6	5.7	302
	3.3	.585	5.35	37.8	.1	9.4	10.1	19.2	7.8	6.1	145
A4	.3	.785	7.03	64.6	.6	10.1	7.2	23.4	7.9	44.3	248
	.8	1.220	8.67	88.9	.2	9.4	6.7	28.8	8.2	79.2	180
	1.2	.875	7.69	76.1	.1	10.3	6.1	26.3	7.8	44.4	164
	1.8	.885	6.14	58.5	.0	7.3	4.7	20.4	8.0	33.2	130
	3.0	.750	6.93	71.3	.3	5.7	5.3	22.6	8.1	35.9	165
	3.7	.840	4.82	53.0	.1	1.0	1.0	13.8	8.7	19.1	156
	4.6	1.467	9.06	97.6	.2	9.5	6.0	31.8	8.2	10.7	130
	5.1	1.270	7.89	83.9	.2	4.9	6.2	26.4	8.1	12.4	132
	6.1	.890	9.03	93.9	.2	8.9	8.1	32.0	8.1	12.7	148
	6.7	1.895	6.40	66.5	.2	4.2	5.2	21.4	8.2	10.4	137
	7.6	.720	8.39	88.9	.2	9.4	6.0	29.7	8.1	13.5	156
	8.2	.660	4.82	51.1	.1	1.3	1.8	13.8	8.3	9.8	205
	9.3	.345	6.30	74.8	.2	2.6	3.6	21.6	8.0	28.9	165
	10.8	.345	6.71	75.4	.5	5.4	5.3	23.9	8.0	29.9	192
	12.3	.550	4.53	45.2	.5	3.6	1.8	13.5	8.0	12.4	217
	13.7	.325	3.94	40.9	.4	4.2	2.4	13.1	8.0	24.3	142
	14.3	.640	3.74	35.1	.5	3.2	1.8	10.8	8.0	17.4	219
	16.8	.625	3.06	27.2	.5	3.2	1.6	8.7	7.9	9.9	193
	17.2	.615	3.31	28.7	.6	4.5	1.7	9.8	8.0	9.1	199
	20.0	.705	4.34	39.3	.9	5.0	2.5	13.3	8.0	9.3	220
	22.9	.705	5.40	42.1	.8	11.6	6.4	18.7	7.9	11.2	321
	23.3	.780	1.91	19.0	.3	1.4	.5	15.1	8.2	6.5	192
	25.9	.765	3.00	30.6	.2	1.4	.7	7.9	8.2	12.9	186
	26.3	.746	2.75	27.6	.1	1.3	.6	7.2	8.2	12.4	184
A5	1.7	.500	4.65	44.6	.5	2.7	4.1	13.9	8.2	34.0	161
	1.9	.490	4.72	43.3	.5	3.5	4.8	14.5	8.1	45.0	160
	3.1	.480	5.31	50.9	.5	3.6	5.7	16.8	8.2	62.4	159
	3.3	.435	6.24	53.5	.5	9.1	10.1	21.4	7.9	65.8	140
	4.7	.789	1.98	16.1	.2	1.6	1.7	4.7	8.2	65.0	166
	4.9	.740	1.06	9.4	.1	.7	.5	2.0	8.2	36.7	167
	6.2	.910	2.67	21.4	.4	3.1	2.1	7.3	8.0	22.0	183
	6.5	.855	2.54	18.6	.4	3.6	2.1	6.9	7.9	17.2	177
	9.3	.285	3.54	25.8	.7	8.2	4.3	11.9	7.6	31.7	282
	15.4	.425	2.48	18.8	.5	3.5	1.6	6.5	7.9	21.7	197
	21.3	.485	2.41	17.7	.6	3.6	1.9	6.4	7.9	11.2	249
	21.6	.500	1.89	14.6	.5	2.6	.7	14.7	8.0	6.5	206
	27.7	.465	2.05	14.0	.5	3.8	1.7	5.5	7.8	7.4	206

SITE	DEPTH m	SAT'N kg/kg	EC dSm	Na	K	Ca	Mg	SO4	pH	Cl	ALK
				<------	---mmol/L	----------	-------	---->		<---ppm	-->
B1	.3	.655	.60	.7	.3	2.4	.8	.4	7.2	7.6	286
	.9	.545	.45	.5	.1	1.9	.7	.3	7.8	5.5	216
	1.5	.475	.44	.7	.1	.8	1.6	.4	8.2	5.8	169
B2	.3	.590	.68	.5	.4	2.9	.7	.3	7.7	7.7	211
	.7	.485	.62	.8	.3	2.3	1.1	.3	7.8	6.6	224
	1.1	.420	.39	1.1	.1	.8	1.0	.3	8.2	5.8	167
	1.5	.455	.66	8.1	.0	.1	.2	.5	8.8	6.8	337
	3.3	.590	5.76	39.9	.6	11.1	12.9	22.3	7.6	5.6	127
B3	.3	.460	.44	.5	.6	1.8	.6	.4	7.6	7.6	207
	.9	.375	.30	.5	.2	1.3	.4	.2	8.0	5.9	162
	1.5	.380	.31	.4	.4	1.1	.4	.2	7.9	8.9	134
	3.4	.430	.90	5.5	.1	1.3	1.4	2.0	8.1	11.9	144
	4.7	.810	.88	5.4	.2	1.4	1.1	2.0	8.0	9.1	121
	4.9	.865	.75	5.0	.1	1.0	.8	1.6	8.1	7.5	107
	7.7	1.005	3.49	15.6	.5	12.0	6.2	12.8	7.7	7.8	94
	10.8	.450	3.68	18.8	.6	12.0	5.9	13.5	7.7	11.5	126
	11.0	.480	3.74	18.5	.5	12.0	6.4	13.8	7.7	9.3	103
	13.9	.455	2.27	11.2	.5	5.7	4.0	7.1	7.8	11.0	132
	18.4	.480	3.17	12.3	.9	10.7	6.5	11.4	7.7	12.0	139
	18.6	.495	2.84	10.7	.9	9.8	5.3	9.9	7.8	10.3	138
	24.6	.415	2.64	13.7	.8	7.4	3.6	8.5	7.8	10.7	144
	30.6	.450	2.50	12.9	.5	7.2	3.5	8.1	7.8	8.5	106
	30.9	.490	2.74	13.0	.6	8.3	4.0	9.0	7.8	6.5	126
B4	.1	.410	1.09	2.3	1.6	3.6	1.1	1.2	7.4	13.4	243
	.4	.425	2.66	12.0	.8	9.2	3.4	8.0	7.4	16.9	206
	.9	.345	5.55	54.8	.3	10.8	5.5	21.4	6.7	22.8	162
	1.5	.865	4.42	46.7	.2	1.5	2.3	12.7	8.0	19.7	213
	3.2	.520	5.33	50.0	.3	6.5	4.4	17.3	7.9	31.4	121
	3.5	.785	4.96	52.6	.2	1.4	3.4	15.1	8.4	19.4	156
	4.7	.740	7.42	78.0	.3	5.0	7.2	25.1	8.0	22.9	153
	5.0	.650	6.58	72.0	.2	1.8	5.6	21.1	8.2	30.6	183
	6.2	.725	5.84	62.4	.3	2.4	4.1	18.3	8.4	19.1	182
	6.5	.647	8.05	76.5	.4	10.0	12.1	29.9	7.9	20.0	114
	7.9	.345	10.14	115.0	.5	9.4	20.7	43.8	7.6	56.5	124
	9.2	.330	11.49	130.4	.7	10.1	27.0	51.1	7.7	58.7	167
	9.4	.300	12.15	137.2	.7	9.8	29.0	53.6	7.5	94.0	168
	10.8	.645	7.41	66.1	.5	9.5	12.4	27.6	7.8	30.2	150
	11.0	.670	6.27	54.8	.5	7.7	9.8	22.2	7.8	24.6	151
	12.4	.565	5.77	44.1	.5	10.4	10.2	21.3	7.6	27.7	127
	13.9	.595	5.52	41.1	.6	10.5	9.9	20.1	7.8	26.6	147
	14.1	.590	2.67	22.1	.4	2.5	2.7	7.4	7.8	35.5	135
	15.4	.505	3.27	23.2	.7	5.5	4.4	10.1	7.9	37.8	164

SITE	DEPTH m	SAT'N kg/kg	EC dSm	Na	K	Ca	Mg	SO4	pH	Cl	ALK
				<-------		mmol/L		------->		<---ppm	-->
B4	15.6	.525	3.77	27.4	.7	6.6	5.2	12.1	7.8	28.5	165
	18.4	.535	4.78	33.7	.8	10.3	6.8	16.7	7.8	41.8	143
	18.6	.395	4.16	34.0	.6	8.3	5.6	15.0	7.7	66.4	120
	20.0	.215	5.88	55.6	.8	10.8	7.3	21.8	7.8	59.3	243
	20.2	.460	4.16	34.6	.7	6.6	3.7	13.3	7.8	35.1	169
B5	.2	.482	.40	.9	.1	1.1	1.1	.5	8.1	7.6	157
	.4	.457	.43	.8	.1	1.0	1.3	.5	8.0	5.7	158
	.9	.365	.44	.8	.2	1.5	.8	.5	7.9	12.5	160
	1.5	.405	.44	.6	.2	1.8	.6	.2	7.6	7.4	179
	3.2	.595	.74	1.1	.2	2.2	1.9	1.7	7.8	17.5	105
	3.4	.779	.48	1.0	.2	1.2	1.1	.8	7.9	10.4	106
	4.7	.739	.54	1.2	.2	1.5	1.1	1.0	7.9	14.1	109
	4.9	.415	.40	1.0	.2	1.1	.8	.5	8.0	14.2	113
	6.2	.434	.72	2.1	.3	2.1	1.2	1.6	7.8	11.9	121
	6.4	.415	.53	1.1	.2	1.7	.9	1.0	7.9	4.9	100
	7.8	.480	11.68	1.8	.4	8.3	2.9	5.1	7.6	8.6	83
	8.0	.500	12.32	1.5	.5	12.5	4.7	8.8	7.7	7.0	85
	9.3	.468	12.53	2.7	.6	12.2	5.8	9.3	7.4	7.7	104
	9.5	.514	2.23	1.5	.5	10.7	5.4	8.2	7.5	6.4	93
	10.8	.533	1.25	1.7	.4	4.3	3.1	3.6	7.7	7.1	116
	11.0	.497	.89	1.4	.4	2.9	2.0	2.3	7.8	6.5	109
	12.3	.384	1.06	1.9	.4	3.9	2.7	2.9	7.7	9.0	179
	12.5	.505	1.07	1.5	.4	3.8	2.3	3.0	7.7	6.1	97
	13.9	.475	2.68	1.7	.6	13.9	6.2	10.4	7.6	8.8	100
	14.1	.505	2.21	1.7	.6	10.7	5.0	8.1	7.6	6.1	95
	15.4	.531	1.37	1.9	.5	5.2	2.9	4.0	7.7	7.3	126
	16.9	.535	1.97	5.0	.9	6.2	4.6	6.2	7.7	8.9	148
	17.1	.515	2.10	4.7	.9	7.0	5.2	6.8	7.7	6.2	81
	18.4	.505	2.32	7.8	.9	7.1	5.1	7.6	7.7	7.5	76
	18.6	.509	2.92	8.5	1.5	9.3	6.9	10.0	7.8	7.3	178
	20.0	.615	2.40	10.4	1.2	6.6	4.6	7.7	7.9	7.4	157
	20.2	.610	2.53	10.6	1.3	6.8	4.8	8.1	7.9	6.5	163
	21.5	.580	2.15	11.6	1.1	4.6	3.1	5.9	7.9	7.3	229
	21.7	.616	2.29	10.4	1.1	5.8	3.7	6.8	7.8	7.0	203
	23.0	.428	1.23	8.0	.4	2.0	1.1	3.0	8.1	7.3	135
B6	.3	.410	.35	.3	.5	1.6	.3	.1	7.8	5.6	178
	.9	.400	.34	.4	.2	1.5	.4	.1	7.9	5.5	168
	1.5	.400	.33	.4	.1	1.2	.7	.2	8.0	6.8	156
	2.0	.300	.24	.8	.2	.6	.5	.2	8.1	11.2	111
	4.8	.725	.28	.9	.2	.7	.5	.2	8.1	4.8	101
	6.3	.375	.17	.5	.1	.5	.3	.1	8.1	4.9	134
	9.3	.495	1.33	1.1	.4	5.8	2.6	4.1	7.7	4.9	89
	9.5	.470	1.13	2.0	.4	4.1	2.0	3.2	7.7	3.5	88
	10.8	.495	1.99	2.5	.4	9.0	3.9	6.9	7.6	8.6	78
	11.0	.670	1.84	2.0	.5	8.5	3.7	6.3	7.6	9.1	92
	12.3	.616	1.54	2.4	.5	6.5	2.8	4.8	7.6	6.6	114

SITE	DEPTH m	SAT'N kg/kg	EC dSm	Na	K	Ca	Mg	SO4	pH	Cl	ALK
				<-------mmol/L				---------->		<---ppm	-->
B6	12.5	.475	1.52	1.7	.5	6.6	2.8	4.8	7.6	4.4	102
	13.9	.595	1.63	2.0	.5	7.2	3.0	5.2	7.6	5.0	107
	15.4	.782	1.72	2.8	.6	7.3	3.0	5.4	7.7	5.9	127
	15.6	.898	1.51	2.3	.6	6.4	2.6	4.6	7.7	3.6	120
	18.4	.805	1.83	3.1	.7	8.0	3.3	6.1	7.7	4.3	117
	18.6	.768	1.61	3.4	.7	6.8	2.5	5.0	7.7	5.5	123
	21.5	.777	2.08	5.3	.7	8.7	3.5	7.0	7.6	7.7	121
	21.7	.747	2.42	5.4	.8	10.8	4.2	8.5	7.6	8.0	130
	24.5	.385	1.73	5.4	.7	6.3	2.5	5.1	7.8	6.4	146
	24.7	.587	1.81	6.2	.7	6.4	2.5	5.5	7.7	6.2	144
	27.6	.390	1.75	7.7	.6	5.1	2.1	5.0	7.8	7.4	142
C1	.1	.570	.63	.7	.3	2.6	.8	.3	7.2	6.1	268
	.4	.630	.53	1.1	.0	2.1	.6	.7	7.7	4.8	174
	.9	.430	.48	1.4	.0	1.4	.6	.6	7.9	6.4	137
	1.2	.565	.68	2.5	.1	.8	1.6	.7	8.1	6.1	125
C2	.1	.610	.92	.9	1.0	3.1	1.1	.5	7.3	11.5	216
	1.1	.626	.52	.9	.5	1.8	.6	.5	6.8	7.1	202
	1.5	.520	.60	.7	.2	2.1	.9	.5	7.4	6.4	207
	2.1	.485	.68	1.4	.2	2.1	1.2	1.0	7.8	6.0	133
	2.6	.560	.69	.7	.0	1.1	2.3	1.6	8.1	3.8	117
C3	.5	.540	.60	.7	.2	2.4	.8	.4	7.3	5.3	259
	1.2	.380	.70	2.5	.2	1.3	1.5	1.1	8.1	7.5	155
C4	.1	.810	22.20	313.5	2.1	10.2	24.3	90.2	8.2	55.0	300
	.6	.863	18.82	244.8	.4	9.6	23.1	75.9	8.3	105.0	223
	1.5	1.783	14.74	187.8	.2	9.4	5.9	54.3	8.6	17.2	183
	2.1	1.775	12.31	146.5	.1	8.8	6.8	44.8	8.3	17.7	170
	3.0	1.020	10.99	126.7	.1	9.4	4.1	38.3	8.1	27.3	150
	4.6	.505	6.22	73.9	.1	1.4	.9	18.7	8.6	39.0	230
C5	2.4	.825	5.03	59.8	.1	1.0	2.3	16.1	8.6	19.5	191
	3.5	.820	8.39	85.7	.2	10.0	7.1	29.9	8.1	18.8	155
	4.6	1.205	3.13	41.6	.0	.7	.9	10.9	8.7	13.4	139
	5.2	1.443	3.47	36.3	.0	.5	.7	9.2	8.7	13.9	183
	6.1	1.286	10.06	117.6	.2	8.9	1.6	34.3	8.4	9.1	164
	6.7	1.860	7.71	77.6	.1	9.8	4.4	26.9	7.7	10.4	124
	7.6	.775	7.07	80.2	.1	1.4	2.2	21.5	8.5	13.1	175
	8.2	.565	10.13	118.9	.1	5.4	5.4	35.2	8.0	14.9	159
	9.1	.805	5.45	61.7	.1	.5	.3	15.3	8.9	21.5	230
	9.6	.775	7.65	89.8	.2	1.0	2.7	23.7	8.3	16.4	220

SITE	DEPTH m	SAT'N kg/kg	EC dSm	Na	K	Ca	Mg	S04	pH	Cl	ALK
				<-----	---mmol/L	----------	--->			<---ppm	-->
C6	.1	.600	1.23	3.5	1.0	3.2	1.8	1.3	7.1	5.1	233
	.6	.400	4.44	23.7	.6	11.6	9.8	16.0	7.8	14.7	141
	1.2	.505	4.52	50.9	.3	.5	.9	11.9	9.5	16.9	372
	1.5	.675	4.26	51.1	.1	.6	1.6	13.0	8.6	13.4	218
	2.1	1.360	7.51	78.9	.1	6.6	6.2	26.4	7.0	10.5	134
	2.7	.750	7.85	82.8	.2	5.3	7.7	27.1	8.1	13.8	164
	3.0	1.095	7.97	89.8	.1	5.7	5.0	27.5	8.4	12.4	191
	3.7	.765	9.47	100.4	.1	8.8	10.2	35.0	8.2	14.3	144
	4.3	.835	3.69	42.6	.1	.7	1.5	11.4	8.4	10.1	127
	5.8	.690	8.28	95.4	.1	2.6	6.0	28.1	8.3	19.3	171
	6.4	1.110	9.53	100.7	.2	9.8	10.4	35.4	8.0	17.4	155
	7.3	1.030	5.82	77.8	.1	.3	.6	17.7	9.3	15.1	560
	7.9	1.745	6.48	64.5	.2	6.1	10.0	22.4	7.9	12.1	230

APPENDIX 3

Saturation Paste Extract Profiles

Legend

Clay	Claystone
Silt	Shale
Sand	Siltstone
Till	Sandstone

Bedrock contact

Mirabilite occurrence

Gypsum occurrence

Saturation extract results

Ca^{++} (m mol/L)

Mg^{++} (m mol/L)

Na^{+} (m mol/L)

$SO_4^{=}$ (m mol/L)

Electrical conductivity (dS/m)

Cl (ppm)

Appendix 3 Saturation Paste Extract Profiles

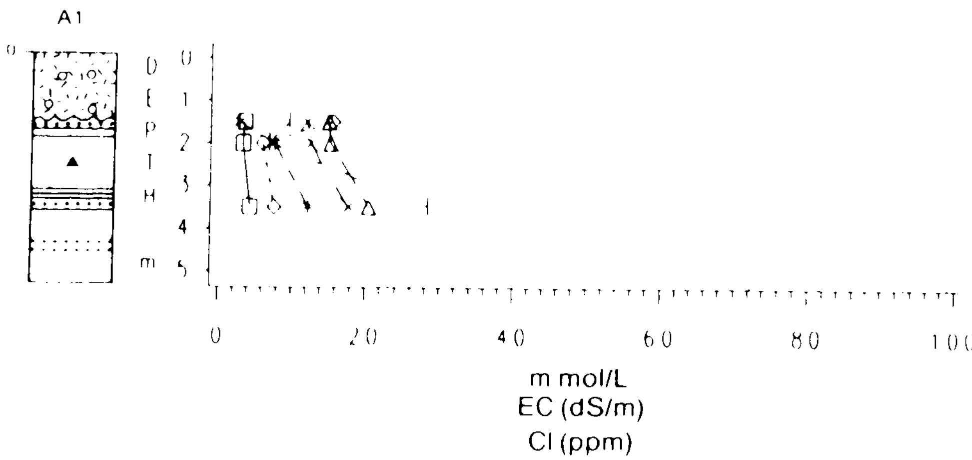
A1
D E P T H
m
0
1
2
3
4
5
0
20
40
60
80
100
m mol/L
EC (dS/m)
Cl (ppm)

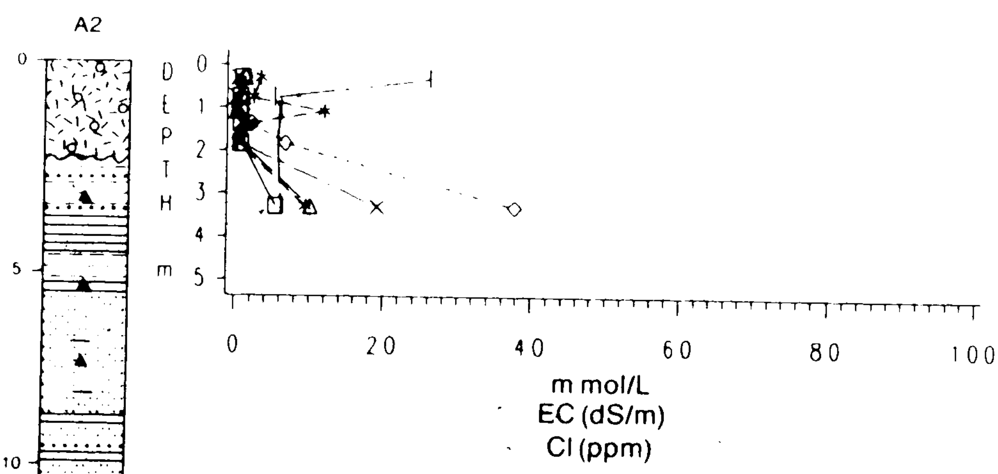
A2
0
5
10
D E P T H
m
0
1
2
3
4
5
0
20
40
60
80
100
m mol/L
EC (dS/m)
Cl (ppm)

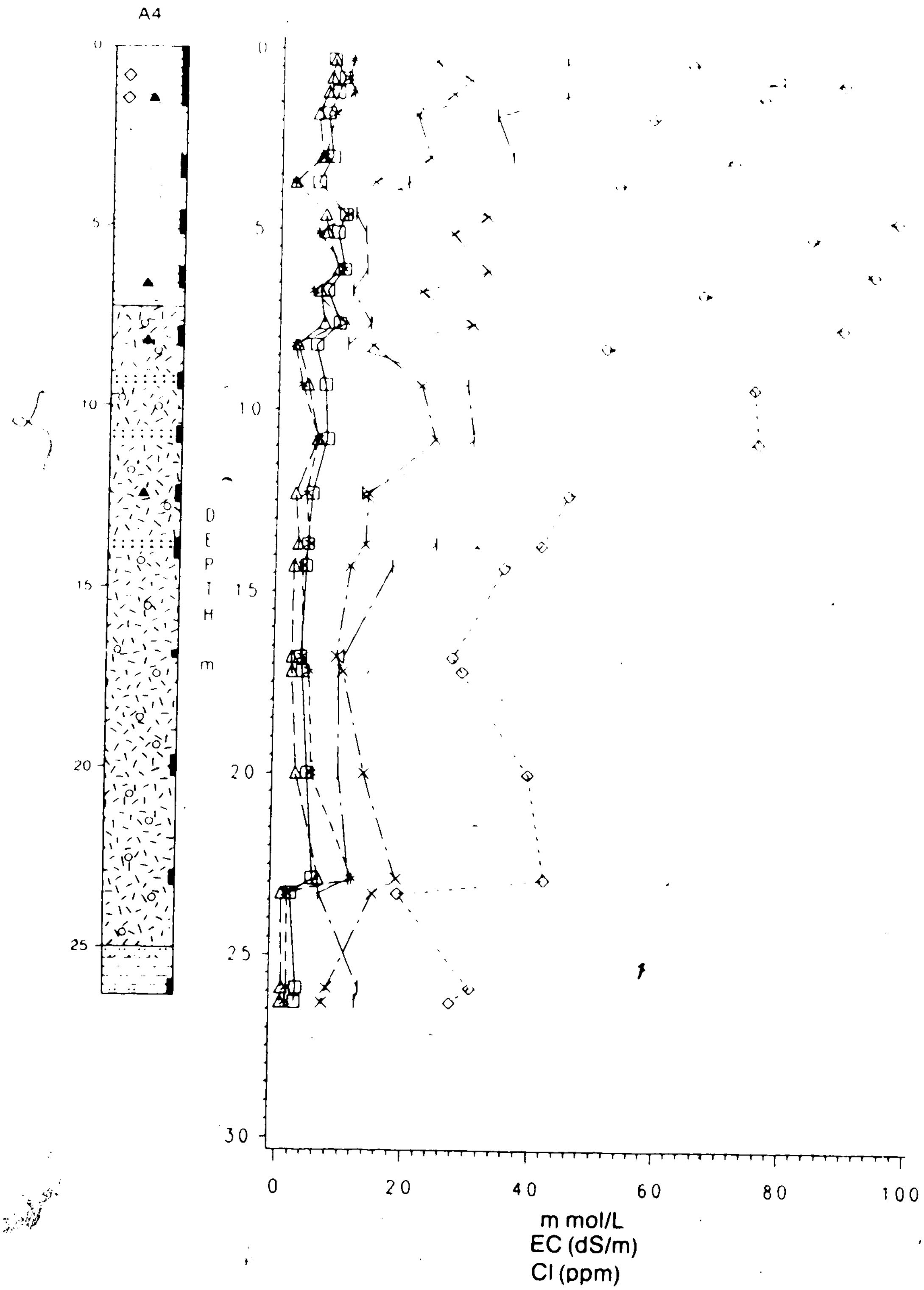
A4
DEPTH m
0
5
10
15
20
25
30
0
20
40
60
80
100
m mol/L
EC (dS/m)
Cl (ppm)

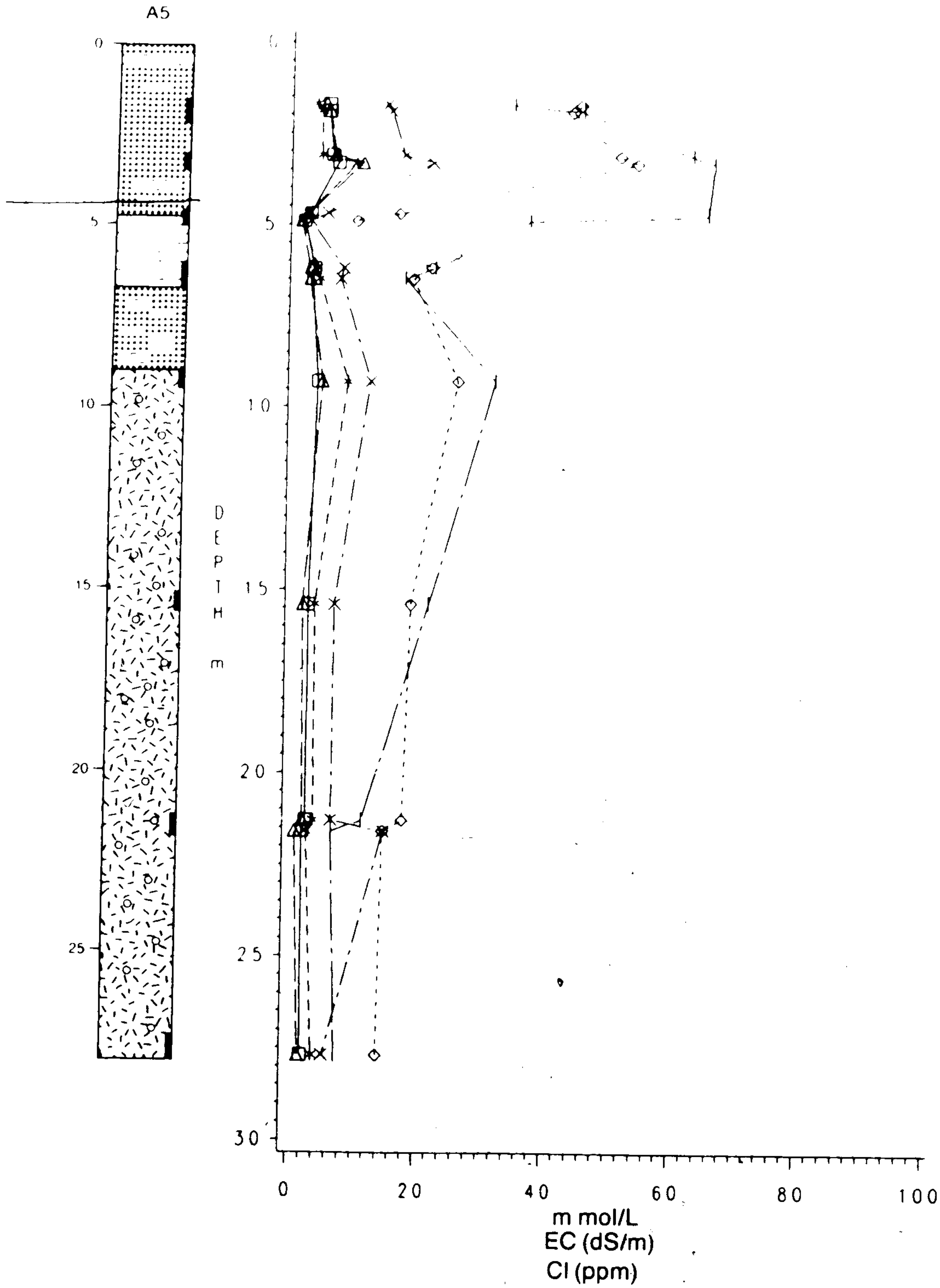
A5
0
5
10
15
20
25
D E P T H m
30
0
20
40
60
80
100
m mol/L
EC (dS/m)
Cl (ppm)

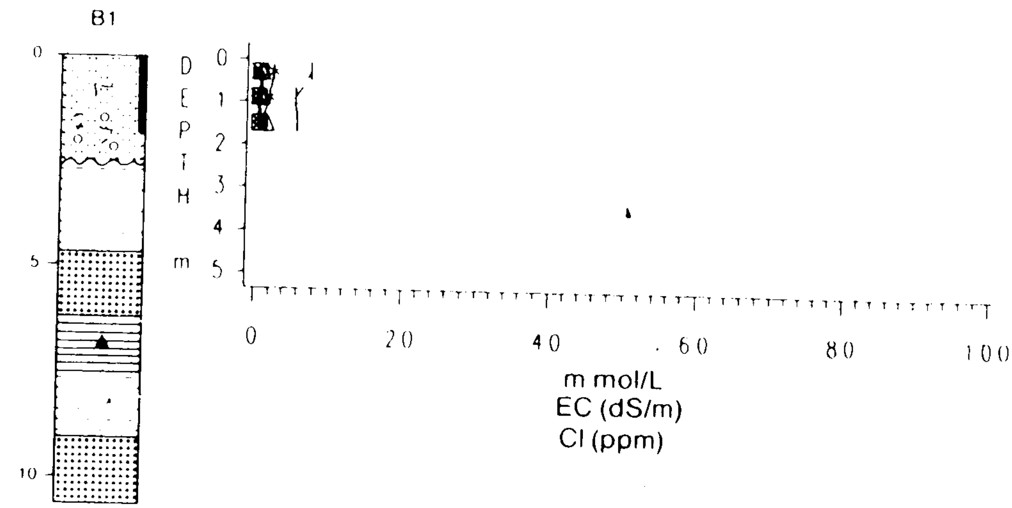
B1
D E P T H m
m mol/L
EC (dS/m)
Cl (ppm)

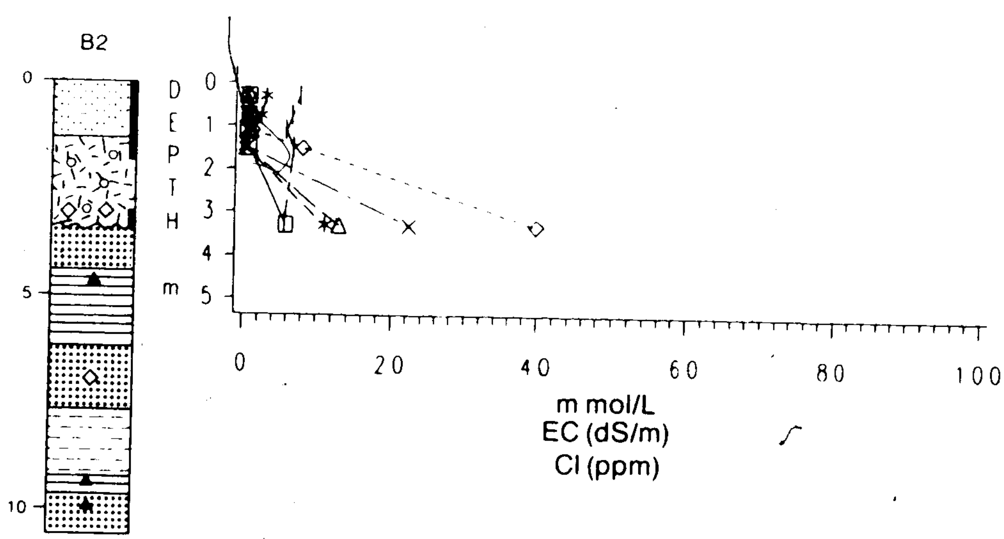
B2
D E P T H m
m mol/L
EC (dS/m)
Cl (ppm)

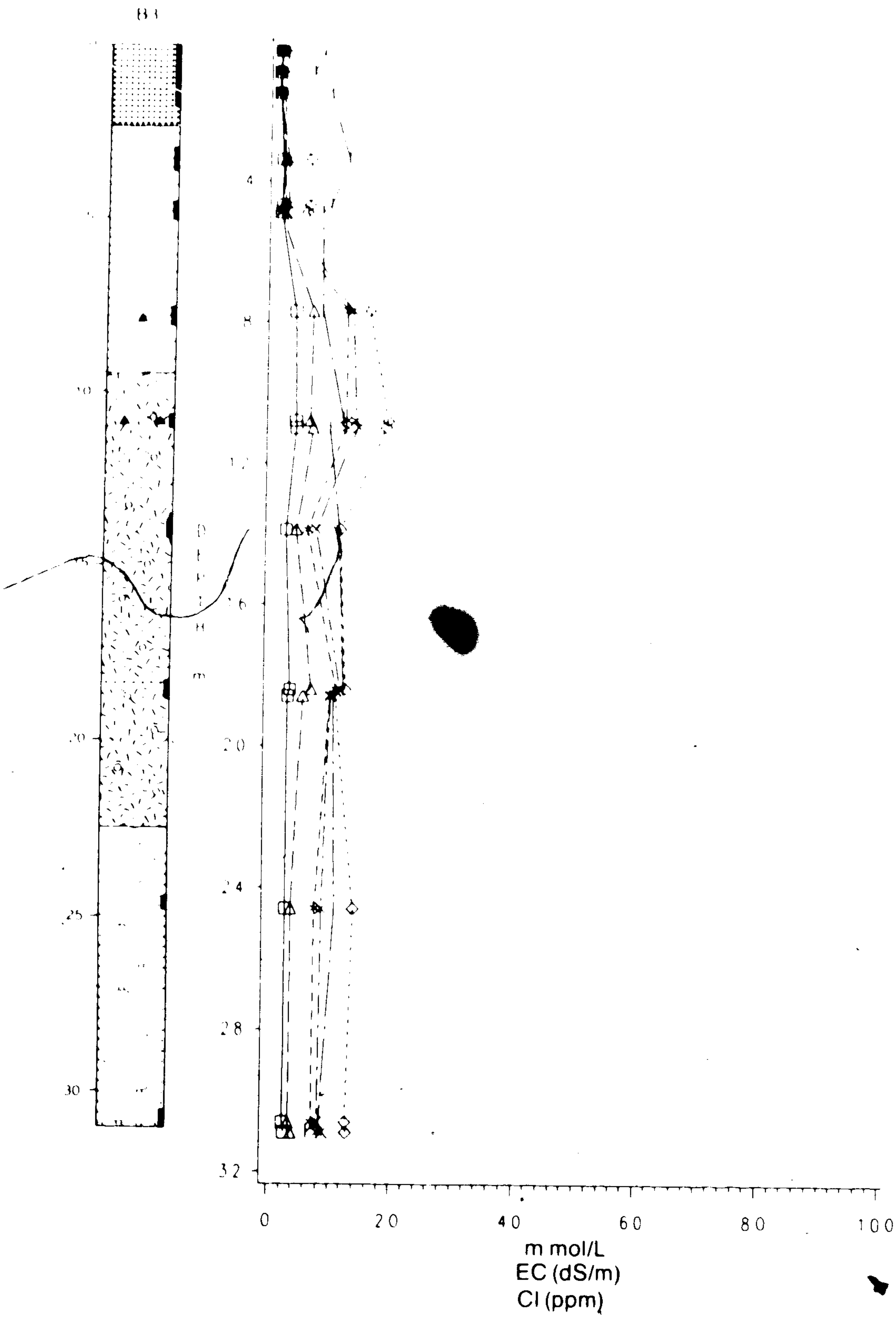

B3
0
20
40
60
80
100
m mol/L
EC (dS/m)
Cl (ppm)

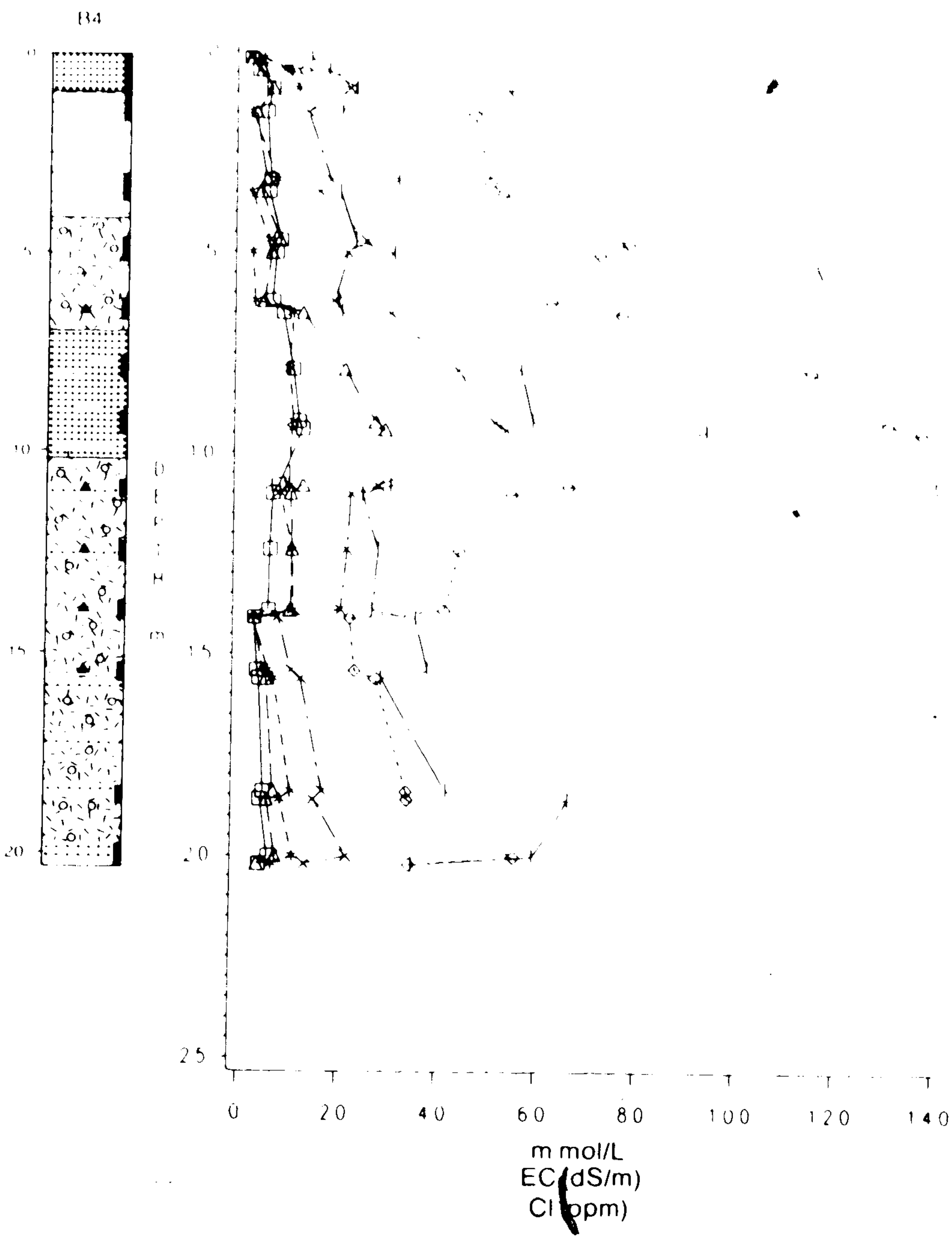
B4
DEPTH
m
0
5
10
15
20
25
0
20
40
60
80
100
120
140
m mol/L
EC (dS/m)
Cl (ppm)

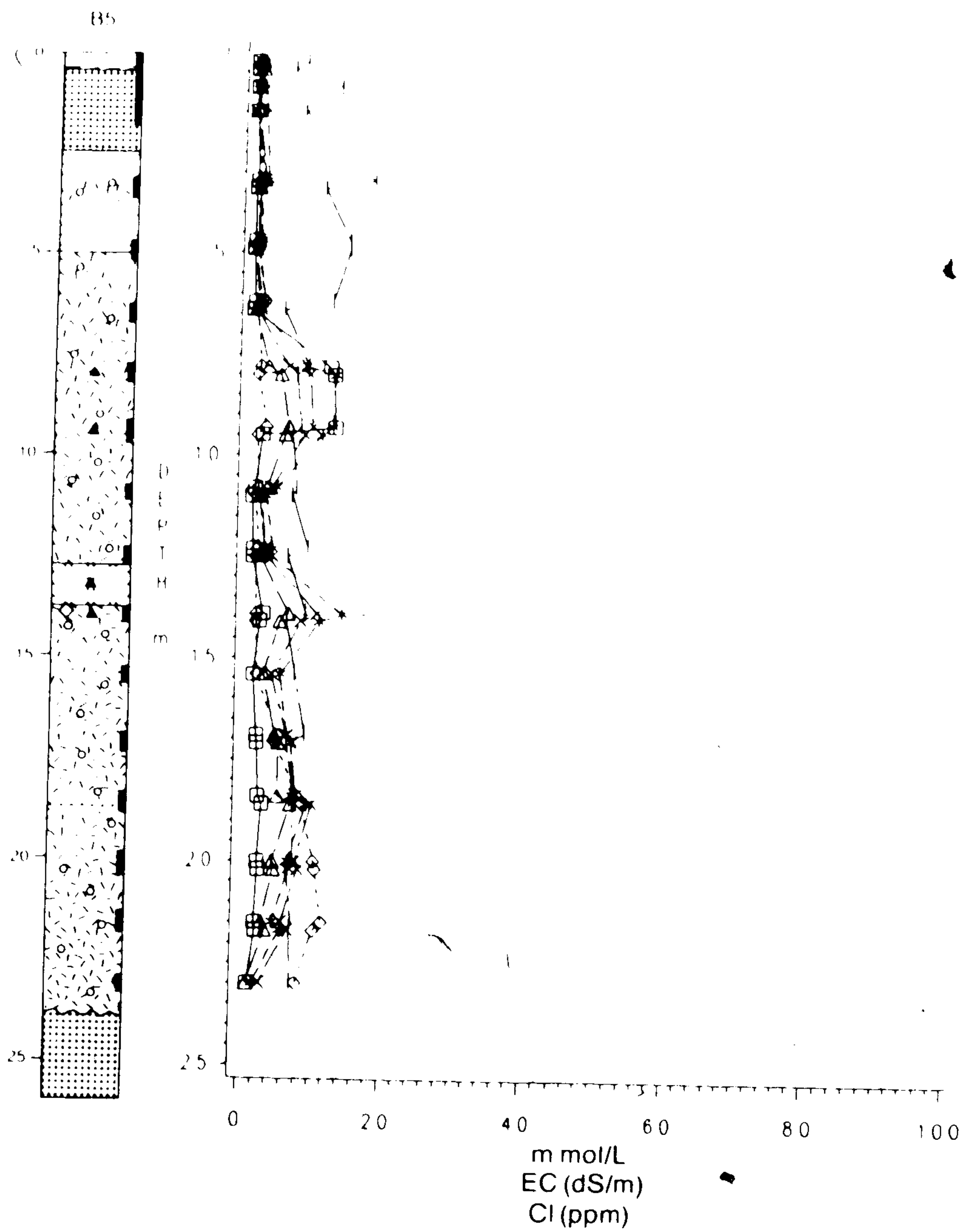
B5
DEPTH
m
0
5
10
15
20
25
0
20
40
60
80
100
m mol/L
EC (dS/m)
Cl (ppm)

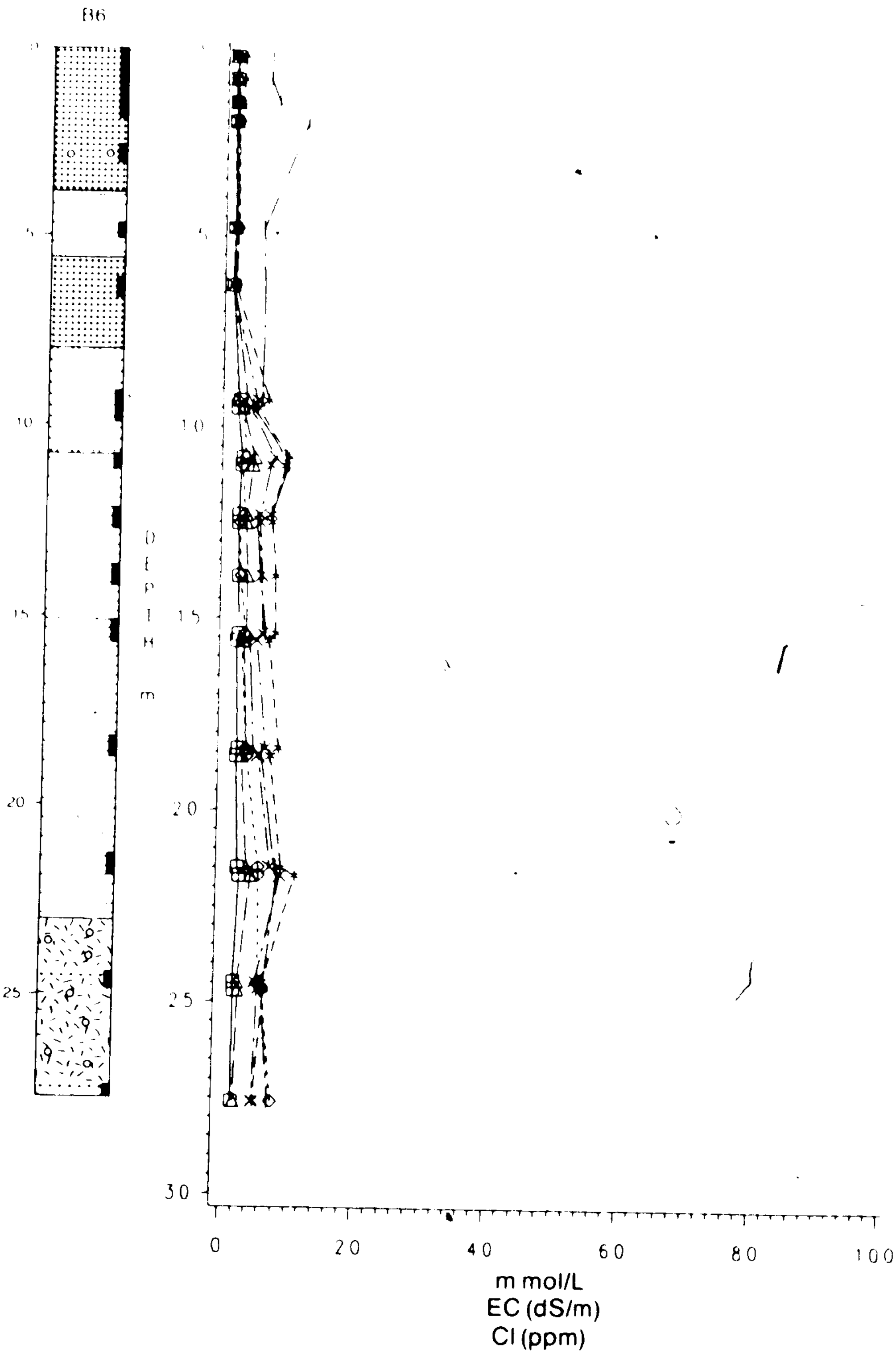

B6
DEPTH m
0
20
40
60
80
100
m mol/L
EC (dS/m)
Cl (ppm)

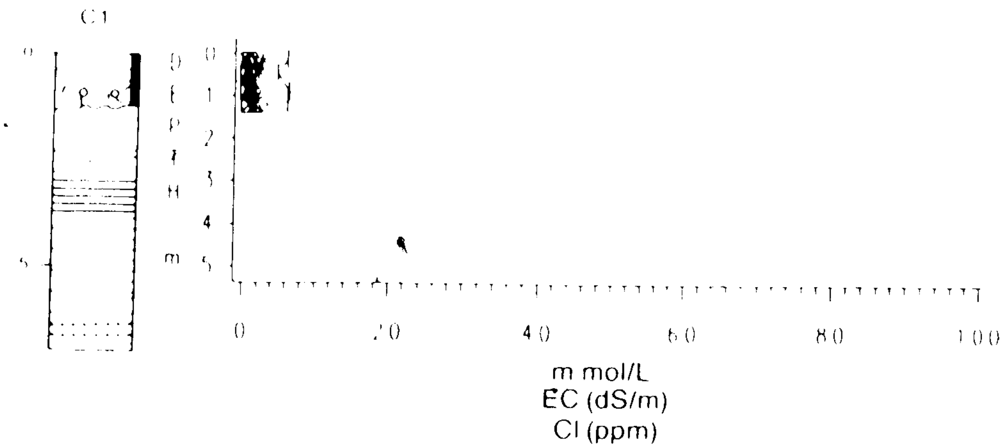
C1
DEPTH
m
0 20 40 60 80 100
m mol/L
EC (dS/m)
Cl (ppm)

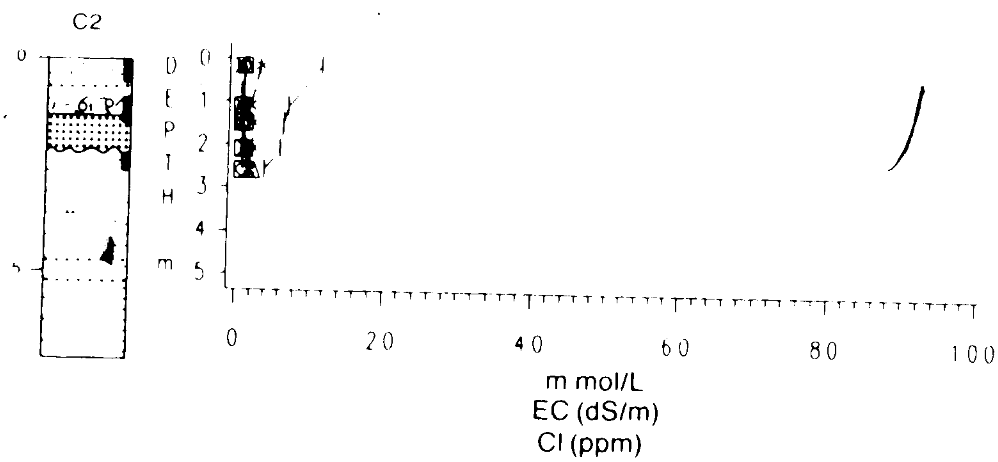
C2
DEPTH
m
0 20 40 60 80 100
m mol/L
EC (dS/m)
Cl (ppm)

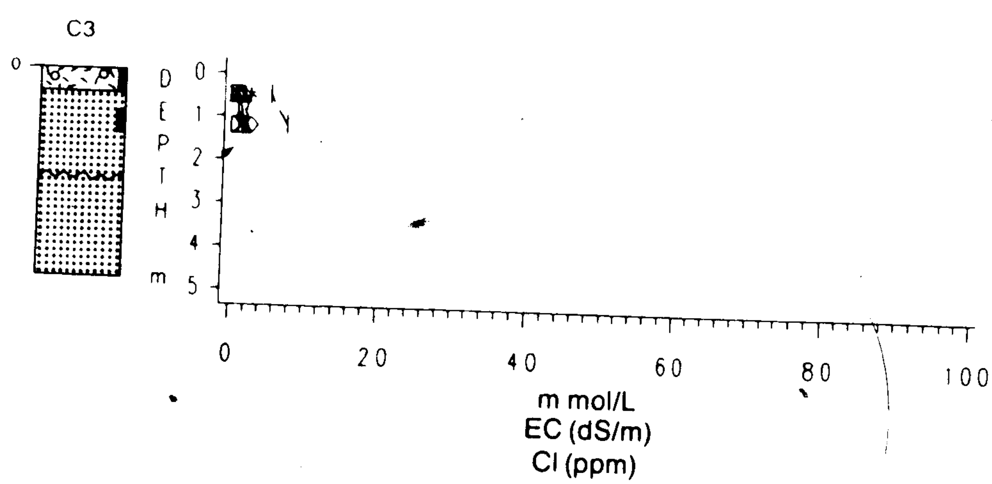
C3
DEPTH
m
0 20 40 60 80 100
m mol/L
EC (dS/m)
Cl (ppm)

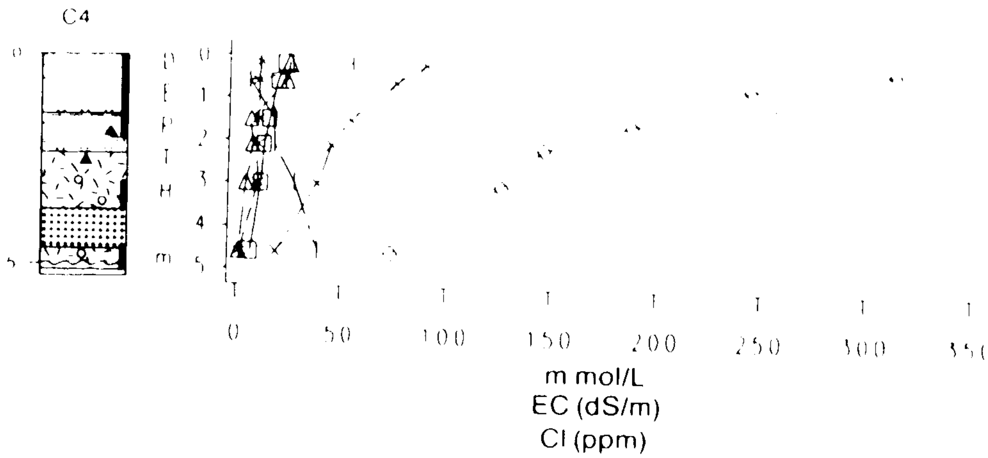
C4
D
E
P
T
H
m
0
1
2
3
4
5
0
50
100
150
200
250
300
350
m mol/L
EC (dS/m)
Cl (ppm)

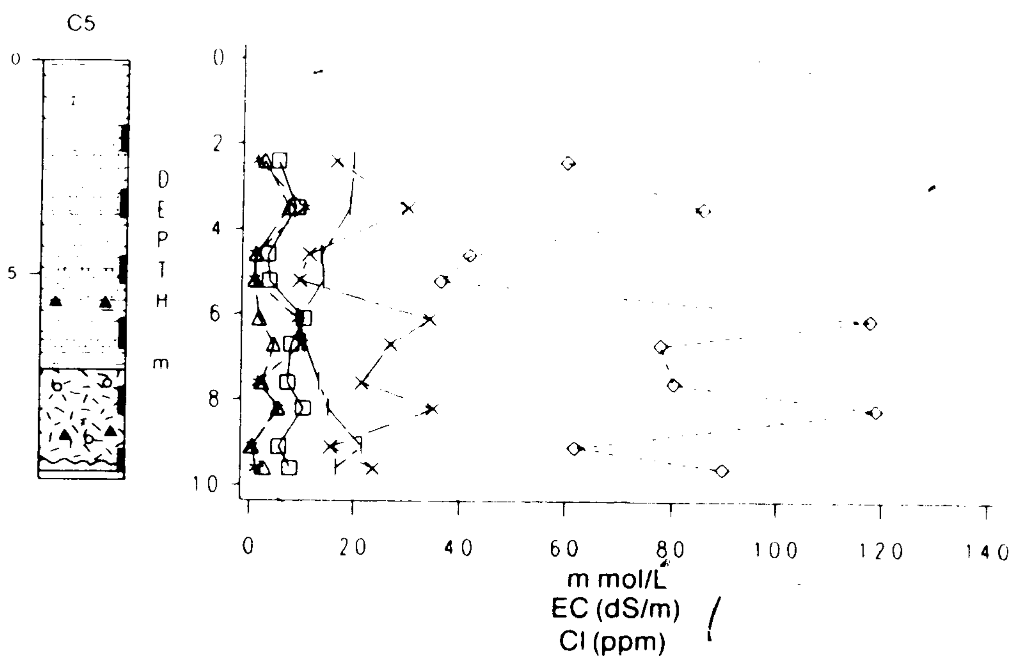
C5
0
5
D
E
P
T
H
m
0
2
4
6
8
10
0
20
40
60
80
100
120
140
m mol/L
EC (dS/m)
Cl (ppm)

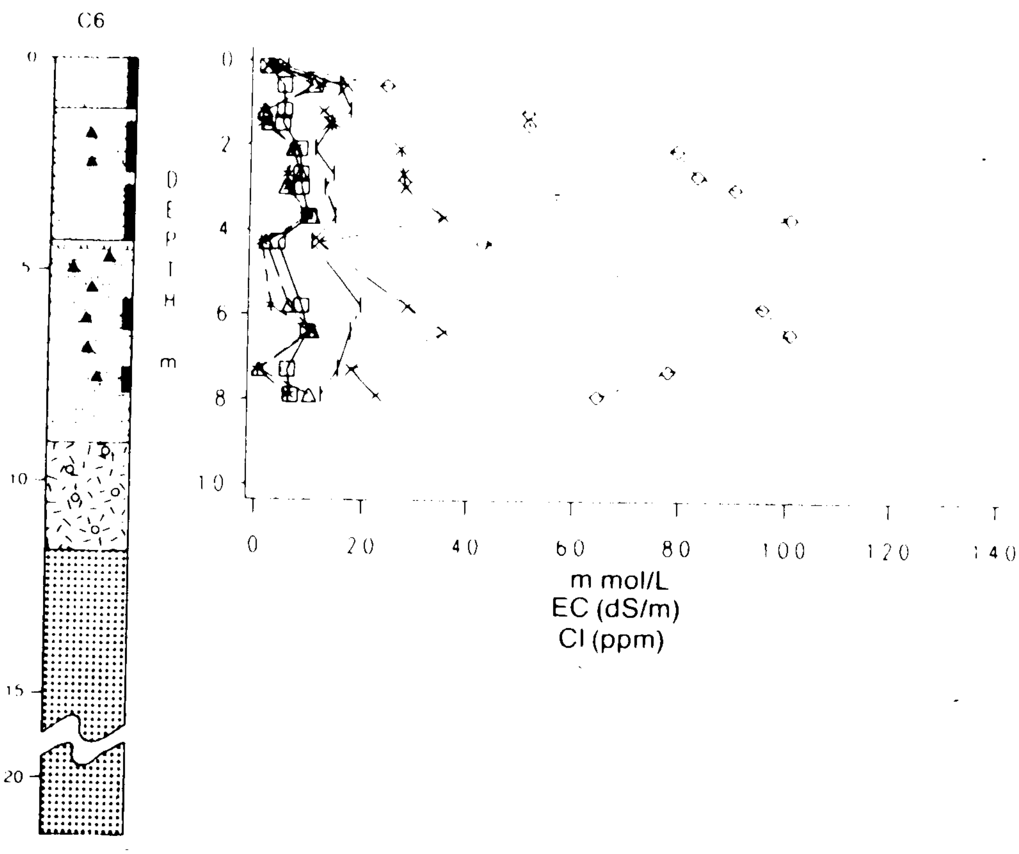
C6
DEPTH
m
m mol/L
EC (dS/m)
Cl (ppm)

APPENDIX 4

Hydraulic Conductivity Tabulation

Lithostratigraphic Unit	Piezometer or Well No.	Hydraulic Conductivity (m/sec) k_h	k_v	m	Solution Used	Statistical Group	Comments
Sandstones							
(a) Upper St. Mary River	A1-34	1.4×10^{-8}	1.4×10^{-9}	10	H	1	
	A1-55	8.4×10^{-6}	8.4×10^{-7}	10	H	1	
	A3-33	2.1×10^{-7}	2.1×10^{-8}	10	H	1	
	A3-98	5.0×10^{-6}	5.0×10^{-7}	10	H	1	
	A3-233	1.4×10^{-7}	1.4×10^{-8}	10	H	1	
	A4-122	3.2×10^{-7}	3.2×10^{-8}	10	H	1	
	A4-260	8.0×10^{-10}	8.0×10^{-11}	10	H	2	
	B1-65	5.2×10^{-9}	5.2×10^{-10}	10	H	2	Poor curve fit
	B2-105	1.1×10^{-10}	1.1×10^{-11}	10	H	2	Long-term recovery, very poor fit
	C1-70	7.4×10^{-10}	7.4×10^{-11}	10	B	2	Suspect undeveloped piezometer
	C2-40	1.3×10^{-6}	1.3×10^{-7}	10	B	1	
	C2-66	2.8×10^{-5}	2.8×10^{-6}	10	H	1	
	C2-125	1.7×10^{-7}	1.7×10^{-8}	10	H	1	
	C3-30	2.8×10^{-7}	2.8×10^{-8}	10	B	1	
	C3-76	2.9×10^{-7}	2.9×10^{-8}	10	H	1	
	16-85	1.7×10^{-7}	1.7×10^{-8}	10	H	1	
	16-2-WT	4.8×10^{-6}	4.8×10^{-7}	10	B	1	
	16-2-38	8.5×10^{-6}	8.5×10^{-7}	10	H	1	
	16-2-72	3.1×10^{-6}	3.1×10^{-7}	10	H	1	
	C4-65	4.1×10^{-5}	4.1×10^{-6}	10	C	1	Recovery after Production with air
	C4-100	2.3×10^{-4}	2.3×10^{-5}	10	C	1	Recovery after production with air
	C5-135	5.2×10^{-7}	5.2×10^{-8}	10	H	1	
(b) Basal St. Mary River	B3-170	4.6×10^{-7}	4.6×10^{-8}	10	H	1	
	B5-118	5.1×10^{-8}	5.1×10^{-9}	10	H	1	
(c) Transitional St. Mary River/B.P.	B5-194	1.7×10^{-7}	1.7×10^{-8}	10	H	1	
Statistics: Group 1 Weathered and/or Fractured Sandstone		21	21	n			
		-6.00	-7.00	$\overline{\log x}$			
		1.0×10^{-6}	1.0×10^{-7}	$\bar{x}$			
		1.06	1.06	s log x			
Statistics: Group 2 Unweathered and/or Bentonitic Sandstones		4	4	n			
		-9.12	-10.12	$\overline{\log x}$			
		7.6×10^{-10}	7.6×10^{-11}	$\bar{x}$			
		0.68	0.68	s log x			

Lithostratigraphic Unit	Piezometer or Well No.	Hydraulic Conductivity (m/sec) k_h	Hydraulic Conductivity (m/sec) k_v	m	Solution Used	Statistical Group	Comments
Claystone, Siltstone and Shale							
(a) St. Mary River	A1-87	1.1×10^{-9}	1.1×10^{-10}	10	H	1	
	A1-130	1.6×10^{-10}	1.6×10^{-11}	10	H	1	
	A5-343	6.7×10^{-7}	6.7×10^{-8}	10	H	2	Below buried valley
	B1-34	2.1×10^{-10}	2.1×10^{-11}	10	H	1	
	B2-50	9.5×10^{-7}	9.5×10^{-8}	10	H	2	Fractured
	C2-93	1.1×10^{-9}	1.1×10^{-10}	10	H	1	
	C3-140	9.5×10^{-10}	9.5×10^{-11}	10	H	1	
	16-WT	4.0×10^{-7}	4.0×10^{-8}	10	B	2	Fractured
	16-2-135	8.6×10^{-10}	8.6×10^{-11}	10	H	1	
	C4-36	8.3×10^{-9}	8.3×10^{-10}	10	H	2	Fractured
	C5-45	1.9×10^{-8}	1.9×10^{-9}	10	H	2	Fractured
Shale Fractured							
(b) Bearpaw	B3-198	6.4×10^{-8}	6.4×10^{-9}	10	H	2	Hvorslev poor fit
	B6-415	5.0×10^{-9}	5.0×10^{-10}	10	H	2	
Statistics: Group 1		6	6	n			
St. Mary River, Claystone,		-9.25	-10.25	$\overline{\log x}$			
Siltstone and Shale		5.7×10^{-10}	5.7×10^{-11}	$\bar{x}$			
		0.38	0.38	$s_{\log x}$			
Statistics: Group 2		7	7	n			
Fractured Claystone,		-7.13	-8.13	$\overline{\log x}$			
Siltstone and Shale		7.5×10^{-8}	7.5×10^{-9}	$\bar{x}$			
		0.94	0.94	$s_{\log x}$			

Lithostratigraphic Unit	Piezometer or Well No.	Hydraulic Conductivity (m/sec) k_h	k_v	m	Solution Used	Statistical Group	Comments
Coal							
(a) St. Mary River	A1-197	1.9×10^{-6}	1.9×10^{-7}	10	H	1	
	A2-232	3.3×10^{-6}	3.3×10^{-7}	10	H	1	
	B1-176	2.6×10^{-8}	2.6×10^{-9}	10	H	2	
	15-24	2.6×10^{-8}	2.6×10^{-9}	10	H	2	
	C1-230	6.4×10^{-9}	6.4×10^{-10}	10	H	2	
(b) Bearpaw	B3-268	1.9×10^{-8}	1.9×10^{-9}	10	H	2	
	B5-228	3.8×10^{-8}	3.8×10^{-9}	10	H	2	
Statistics: Group 1 Fractured Coal		2	2	n			
		-5.60	-6.60	$\overline{\log x}$			
		2.5×10^{-6}	2.5×10^{-7}	$\bar{x}$			
		0.17	0.17	$s \log x$			
Statistics: Group 2 Unfractured or Poorly Fractured Coal		5	5	n			
		-7.70	-8.70	$\overline{\log x}$			
		2.0×10^{-8}	2.0×10^{-9}	$\bar{x}$			
		0.30	0.30	$s \log x$			

Lithostratigraphic Unit	Piezometer or Well No.	Hydraulic Conductivity (m/sec) k_h	k_v	m	Solution Used	Statistical Group	Comments
Glaciolacustrine Deposits							
(a) Varved Clay	A4-90	3.2×10^{-10}	4.9×10^{-11}	6.5	H		Long-term recovery
(b) Clay and Silt	B6-50	2.1×10^{-9}	3.3×10^{-10}	6.5	H		
(c) Weathered Silt and Clayey Silt	A3-WT	2.0×10^{-7}	3.1×10^{-8}	6.5	B	1	Lithology uncertain
	A4-WT	6.8×10^{-7}	1.1×10^{-7}	6.5	B	1	
	B3-WT	2.4×10^{-7}	3.6×10^{-8}	6.5	B	1	
	5-WT	2.2×10^{-8}	3.4×10^{-9}	6.5	B	1	
	6-WT	1.7×10^{-6}	2.6×10^{-7}	6.5	B	1	
	7-WT	2.6×10^{-7}	4.0×10^{-8}	6.5	B	1	
	8-WT	4.5×10^{-8}	7.0×10^{-9}	6.5	B	1	
	9-WT	2.6×10^{-7}	4.0×10^{-8}	6.5	B	1	
	13-WT	2.1×10^{-8}	3.2×10^{-9}	6.5	B	1	
	14-WT	7.4×10^{-7}	1.1×10^{-7}	6.5	B	1	
	15-WT	1.7×10^{-7}	2.5×10^{-8}	6.5	B	1	
	C4-WT	1.1×10^{-7}	1.7×10^{-8}	6.5	B	1	
	C6-WT	1.1×10^{-6}	1.7×10^{-7}	6.5	B	1	
(d) Sand; Silty and Clayey Sand; Weathered	A5-WT	1.0×10^{-7}	1.6×10^{-8}	6.5	B	2	
	B4-WT	1.8×10^{-6}	2.8×10^{-7}	6.5	B	2	
	B5-WT	3.0×10^{-6}	2.8×10^{-7}	6.5	B	2	
	10-WT	6.0×10^{-6}	9.3×10^{-7}	6.5	B	2	
	11-WT	9.9×10^{-7}	1.5×10^{-7}	6.5	B	2	
	12-WT	6.7×10^{-7}	1.0×10^{-7}	6.5	B	2	
	17-WT	1.2×10^{-5}	1.8×10^{-6}	6.5	B	2	
	18-WT	9.0×10^{-7}	1.4×10^{-7}	6.5	B	2	
	C5-WT	2.7×10^{-6}	4.1×10^{-7}	6.5	B	2	
Statistics: Group 1 Weathered Silt and Clayey Silt		13	13	n			
		-6.69	-7.50	$\overline{\log x}$			
		2.1×10^{-7}	3.2×10^{-8}	$\bar{x}$			
		0.61	0.61	$s_{\log x}$			
Statistics: Group 2 Sand; Silty and Clayey Sand; Weathered		9	9	n			
		-5.80	-6.61	$\overline{\log x}$			
		1.6×10^{-6}	2.4×10^{-7}	$\bar{x}$			
		0.60	0.60	$s_{\log x}$			
Statistics: Group 1 and 2 combined:		22	22	n			
		-6.33	-7.14	$\overline{\log x}$			
		4.7×10^{-7}	7.3×10^{-8}	$\bar{x}$			
		0.74	0.74	$s_{\log x}$			

Lithostratigraphic Unit	Piezometer or Well No.	Hydraulic Conductivity (m/sec) k_h	k_v	m	Solution Used	Statistical Group	Comments
Stratified Deposits							
(a) Glacial and/or Interglacial	A5-135	2.6×10^{-8}	4.0×10^{-9}	6.5	H	1	
	B3-130	2.2×10^{-7}	3.4×10^{-8}	6.5	H	1	
	B4-29	5.1×10^{-7}	7.9×10^{-8}	6.5	H	1	
	B4-73	3.4×10^{-7}	5.2×10^{-8}	6.5	H	1	
(b) Preglacial, Lying on Bedrock	2-WT	8.4×10^{-8}	1.3×10^{-8}	6.5	B	2	
	5-32	2.0×10^{-8}	3.1×10^{-7}	6.5	B	2	
	6-70	7.3×10^{-8}	1.1×10^{-8}	6.5	H	2	
	C4-20	3.6×10^{-8}	5.5×10^{-7}	6.5	H	2	
Statistics: Group 1 — n		4	4				
log $\bar{x}$		-6.75	-7.56				
$\bar{x}$		1.8×10^{-7}	2.7×10^{-8}				
s log x		0.58	0.58				
Statistics: Group 2 — n		4	4				
log $\bar{x}$		-5.34	-6.15				
$\bar{x}$		4.6×10^{-8}	7.0×10^{-7}				
s log x		0.29	0.29				
Statistics: Group 1 and 2 Combined — n		8	8				
log $\bar{x}$		-6.04	-6.86				
$\bar{x}$		9.0×10^{-7}	1.4×10^{-7}				
s log x		0.86	0.86				
Preglacial Sand and Gravel; Buried Valley Floor Deposits	A5-302	1.7×10^{-4}		1	V		$S = 3.0 \times 10^{-5}$; Kv underlying shale 1.6 X 10-8
	B6-355	1.7×10^{-7}		1	H		

Lithostratigraphic Unit	Piezometer or Well No.	Hydraulic Conductivity (m/sec) k_h	k_v	m	Solution Used	Statistical Group	Comments
Till							
(a) Upper Till, Weathered	A4-50	2.2×10^{-9}		1	H	1	
	A5-61	4.6×10^{-8}		1	H	1	
	B5-40	1.1×10^{-8}		1	H	1	
	4-WT	1.1×10^{-7}		1	B	1	
(b) Upper Till, Non-weathered	A5-90	3.8×10^{-10}		1	H	2	Long-term recovery
	[illegible]	1.8×10^{-10}		1	H	2	Long-term recovery
	B6-80	1.1×10^{-9}		1	H	2	
	B6-130	2.0×10^{-9}		1	H	2	Long-term recoveery
(c) Lower Till, Non-weathered	A4-64	1.0×10^{-9}		1	H	2	
	B5-83	4.0×10^{-9}		1	H	2	Hvorslev poor fit
Statistics: Group 1		4		n			
Weathered Till		-5.73		$\overline{\log x}$			
		1.9×10^{-8}		$\bar{x}$			
		0.74		s log x			
Statistics: Group 2		6		n			
Non-weathered Till		-9.04		$\overline{\log x}$			
		9.1×10^{-10}		$\bar{x}$			
		0.49		s log x			

* Solutions used:

B: Bouwer and Rice
C: Cooper and Jacob
H: Hvorslev
V: Vanden Berg

$m = k_h/k_v$

APPENDIX 5

Hydraulic Conductivity Determinations from Laboratory Permeameter Tests

Testhole No.	Sample depth (m)	Hydraulic Conductivity (m/sec) k_h	k_v	k_h/k_v
C5	1.5 2.0	3.2×10^{9}	no test	
	3.0 3.7	1.8×10^{7}	3.5×10^{9}	51.4*
	4.6 5.2	4.0×10^{10}	3.4×10^{11}	11.8
	6.1 6.7	1.0×10^{9}	1.2×10^{10}	8.3
12WI	1.5 2.1	4.3×10^{8}	8.6×10^{9}	5.0
	3.0 3.7	6.5×10^{9}	1.3×10^{9}	5.0
	4.6 5.2	1.6×10^{9}	4.2×10^{10}	3.8
	6.1 6.7	no test	2.6×10^{10}	
13WI	1.5 2.1	3.4×10^{9}	4.1×10^{10}	8.3
	3.0 3.7	2.2×10^{9}	3.4×10^{10}	6.5
	4.6 5.2	1.2×10^{9}	3.4×10^{10}	3.5
Statistics	n	10	10	n = 8
	log x	8.40	9.31	x 6.5
	x	4.0×10^{9}	4.9×10^{10}	s 2.8
	s log x	0.80	0.69	

* omitted from mean k_h/k_v calculation

k_v determined on 60.0 cm diam. by 2.67 cm disk

k_h determined on 7.2 cm diam by 2.7 cm thick disk taken from immediately adjacent to k_v sample.

APPENDIX 6

Rainfall and Hydrographs

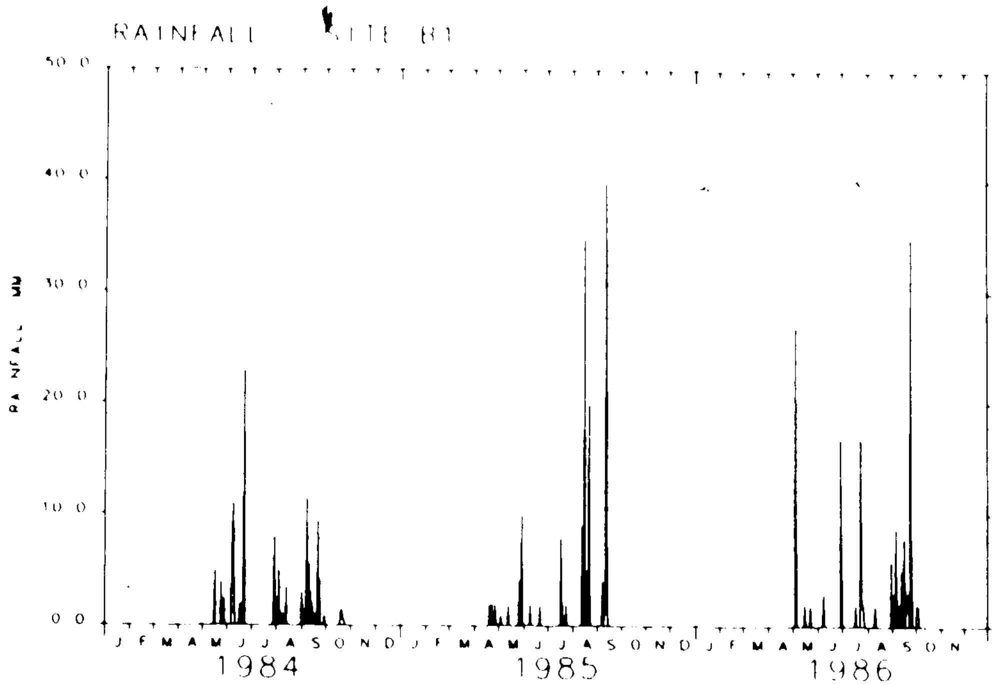
RAINFALL SITE B1
50.0
40.0
30.0
20.0
10.0
0.0
RAINFALL MM
J F M A M J J A S O N D J F M A M J J A S O N D J F M A M J J A S O N
1984
1985
1986

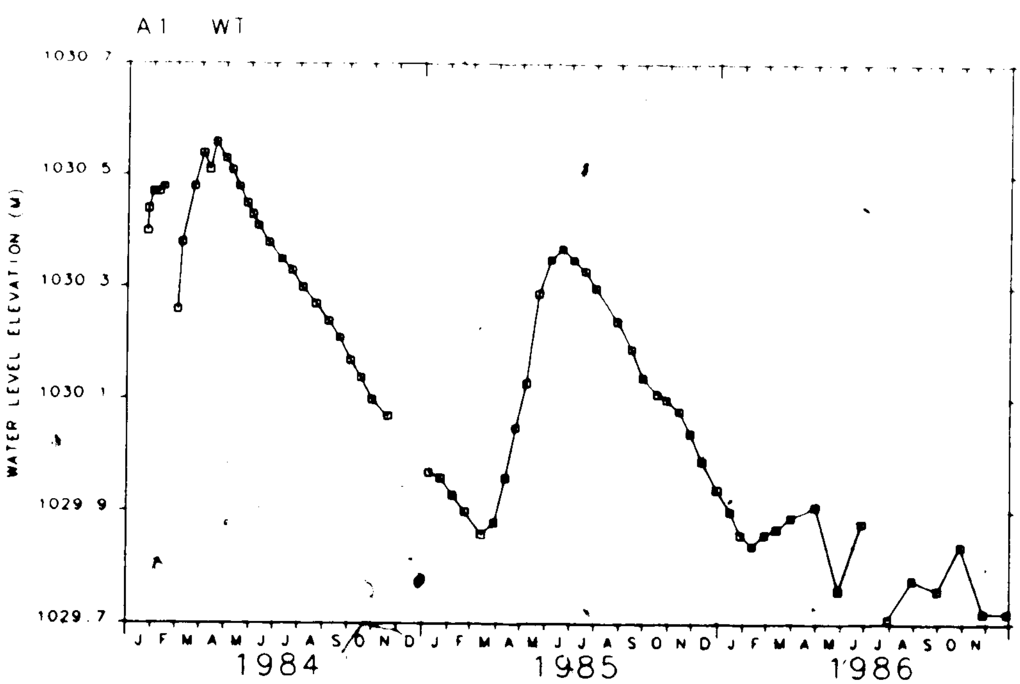
A1 WT
1030.7
1030.5
1030.3
1030.1
1029.9
1029.7
WATER LEVEL ELEVATION (M)
J F M A M J J A S O N D J F M A M J J A S O N D J F M A M J J A S O N
1984
1985
1986

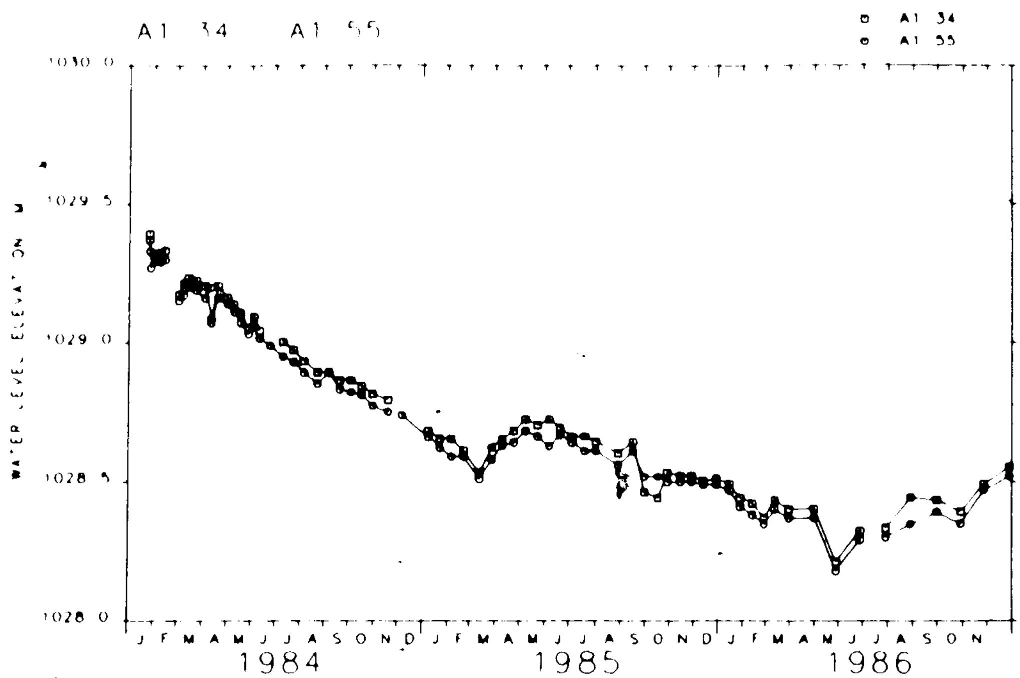
A1 34 A1 55
A1 34
A1 55
WATER LEVEL ELEVATION M
1030.0
1029.5
1029.0
1028.5
1028.0
J F M A M J J A S O N D J F M A M J J A S O N D J F M A M J J A S O N
1984
1985
1986

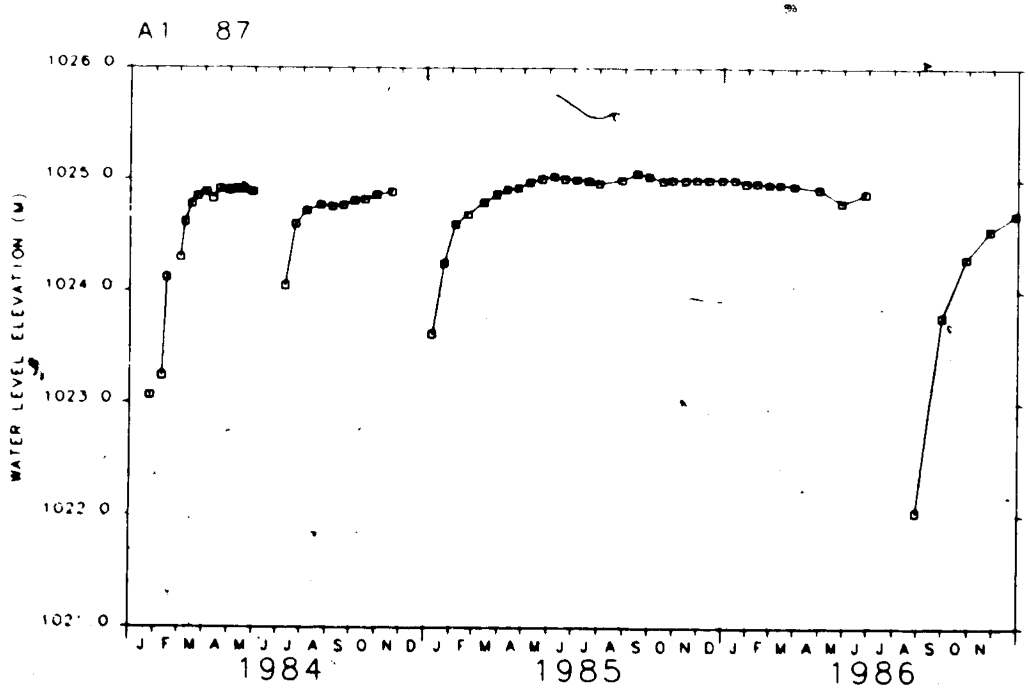
A1 87
WATER LEVEL ELEVATION (M)
1026.0
1025.0
1024.0
1023.0
1022.0
J F M A M J J A S O N D J F M A M J J A S O N D J F M A M J J A S O N
1984
1985
1986

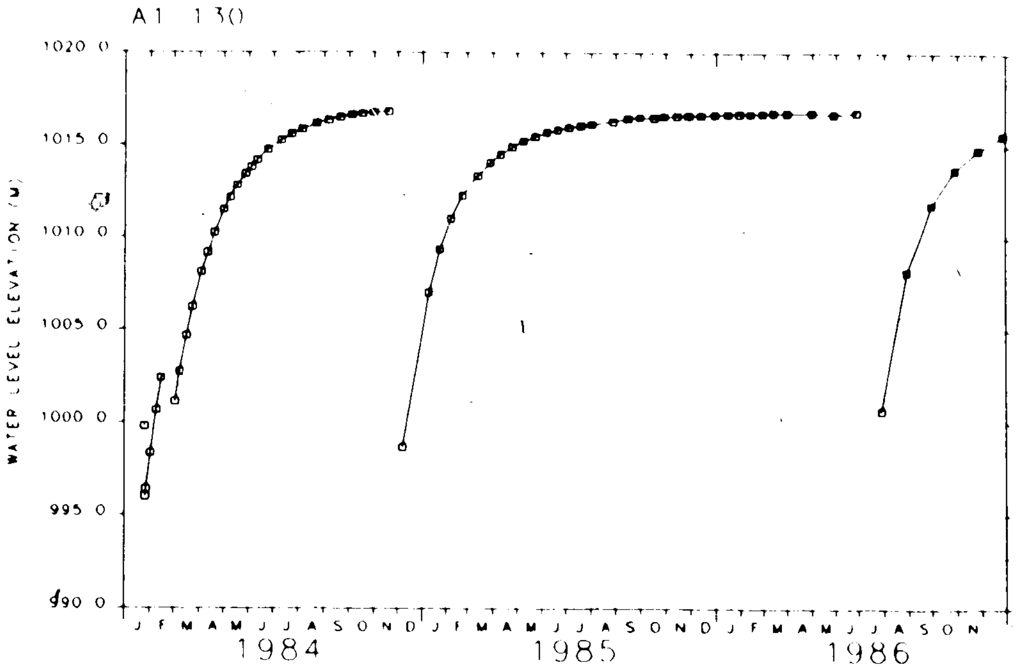
A1 130
WATER LEVEL ELEVATION (M)
1020.0
1015.0
1010.0
1005.0
1000.0
995.0
990.0
J F M A M J J A S O N D J F M A M J J A S O N D J F M A M J J A S O N
1984
1985
1986

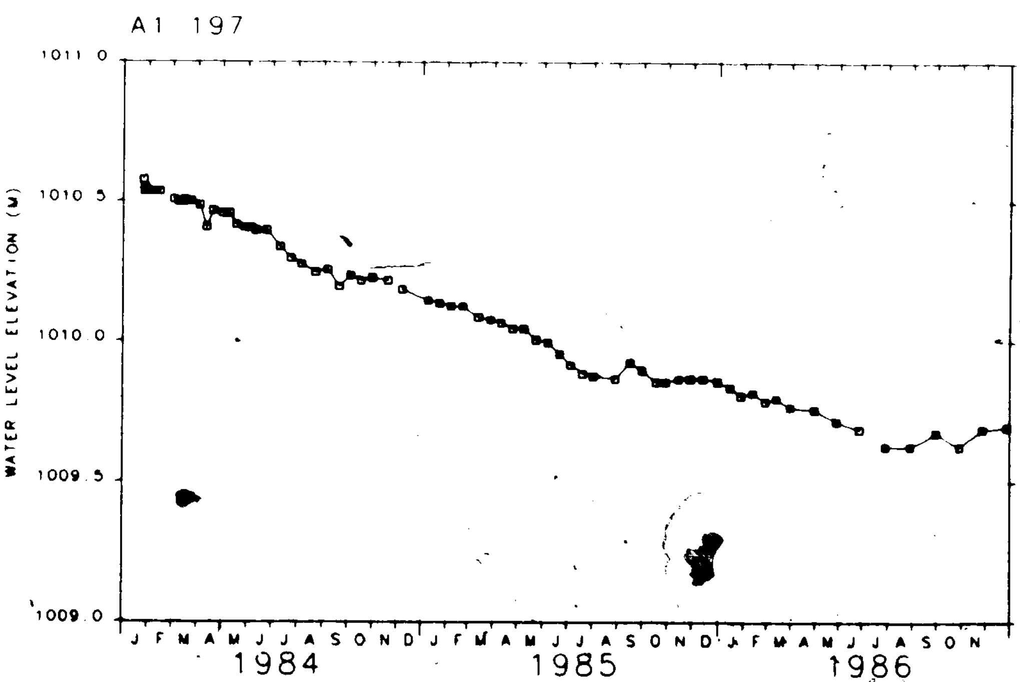
A1 197
WATER LEVEL ELEVATION (M)
1011.0
1010.5
1010.0
1009.5
1009.0
J F M A M J J A S O N D J F M A M J J A S O N D J F M A M J J A S O N
1984
1985
1986

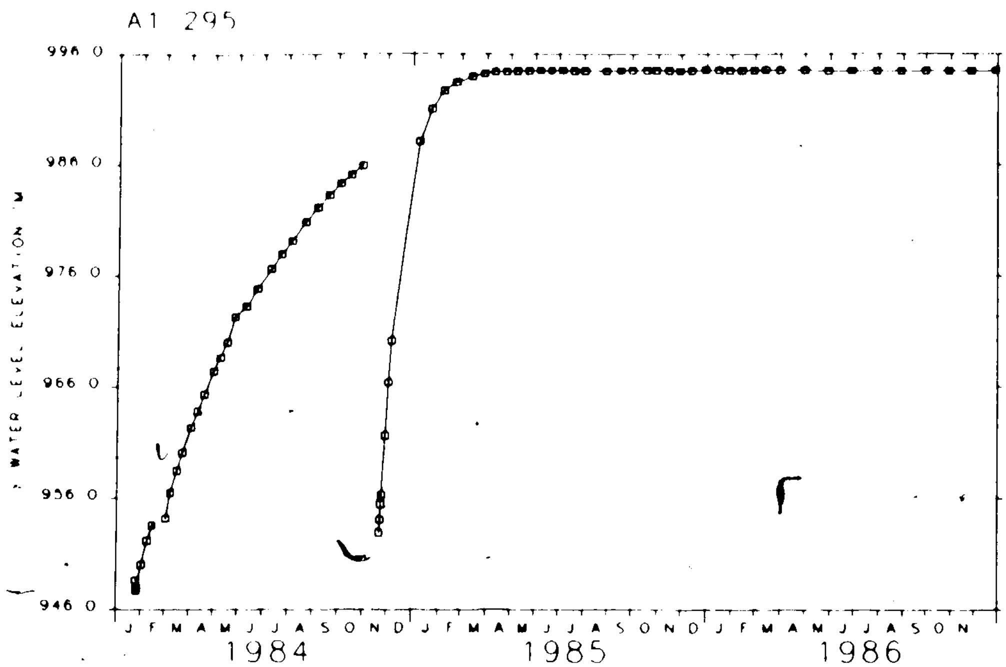
A1 295
996.0
986.0
976.0
966.0
956.0
946.0
WATER LEVEL ELEVATION (M)
J F M A M J J A S O N D J F M A M J J A S O N D J F M A M J J A S O N
1984
1985
1986

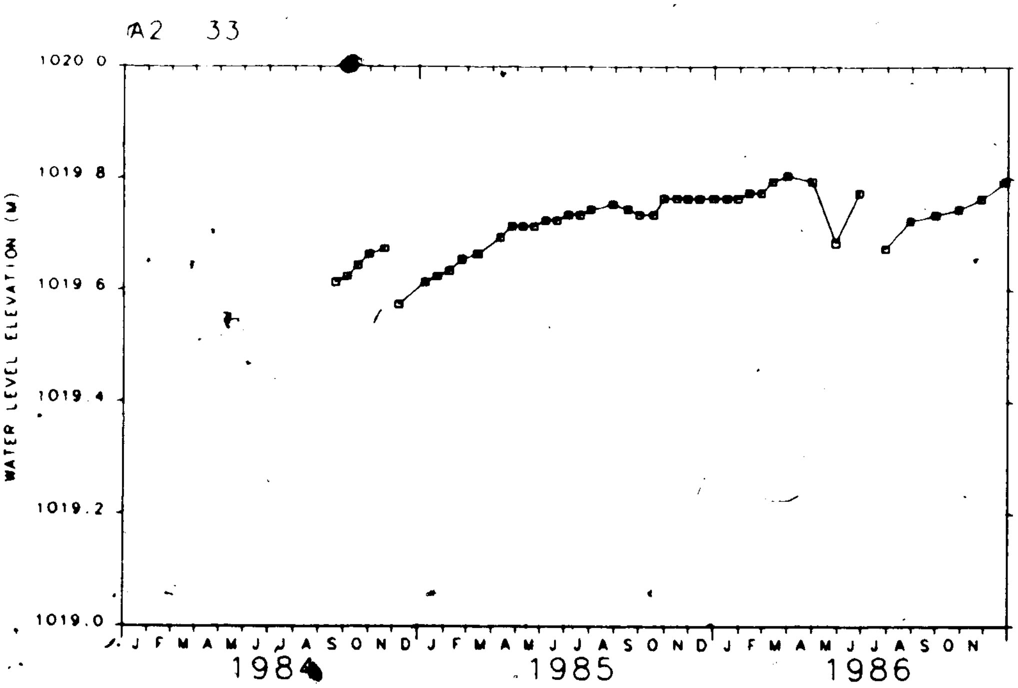
A2 33
1020.0
1019.8
1019.6
1019.4
1019.2
1019.0
WATER LEVEL ELEVATION (M)
J F M A M J J A S O N D J F M A M J J A S O N D J F M A M J J A S O N
1984
1985
1986

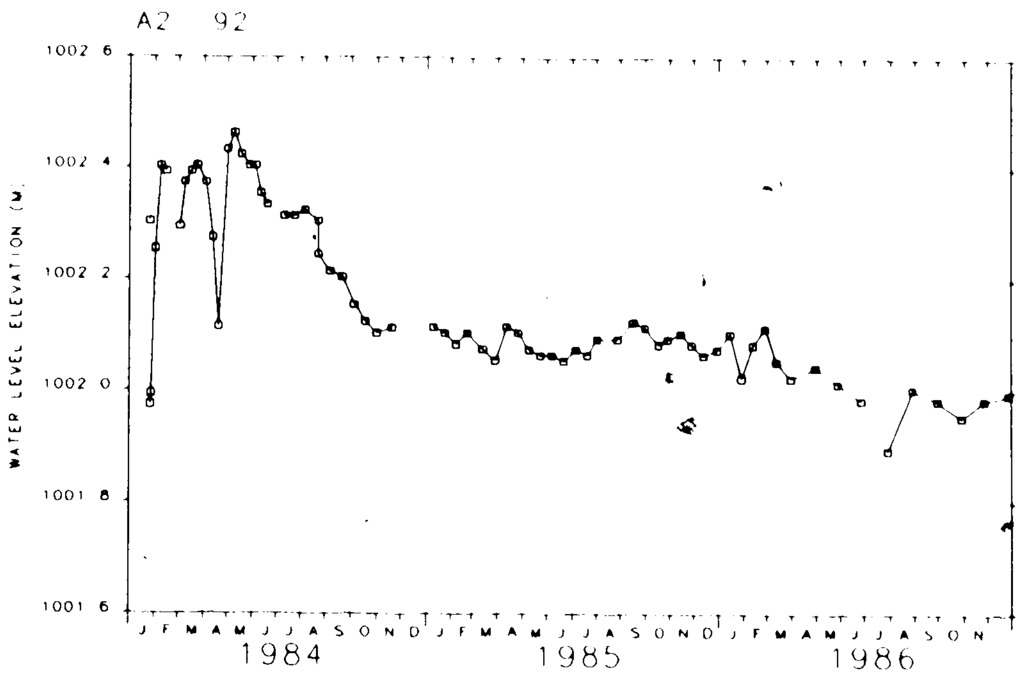
A2 92
1002.6
1002.4
1002.2
1002.0
1001.8
1001.6
WATER LEVEL ELEVATION (M)
J F M A M J J A S O N D J F M A M J J A S O N D J F M A M J J A S O N
1984
1985
1986

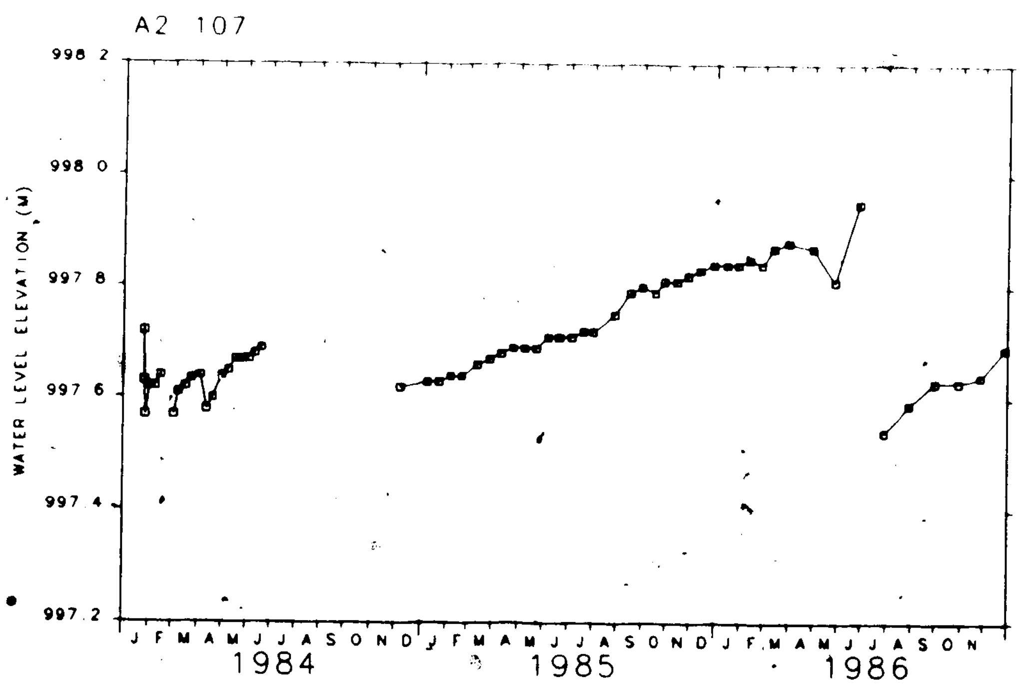
A2 107
998.2
998.0
997.8
997.6
997.4
997.2
WATER LEVEL ELEVATION (M)
J F M A M J J A S O N D J F M A M J J A S O N D J F M A M J J A S O N
1984
1985
1986

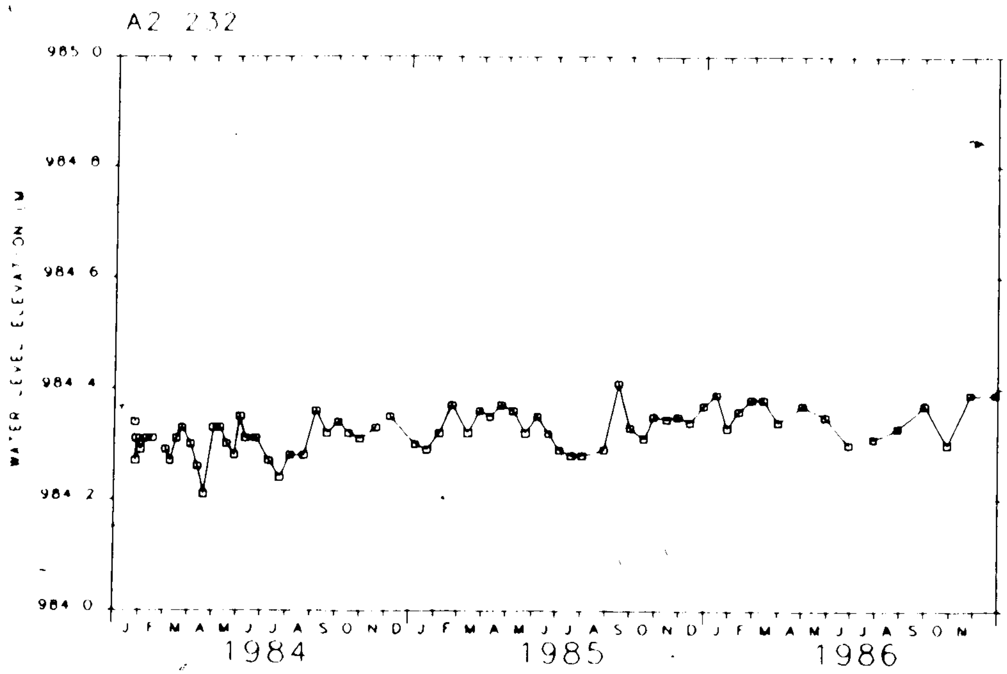
A2 232
985.0
984.8
984.6
984.4
984.2
984.0
WATER LEVEL ELEVATION (M)
J F M A M J J A S O N D J F M A M J J A S O N D J F M A M J J A S O N
1984
1985
1986

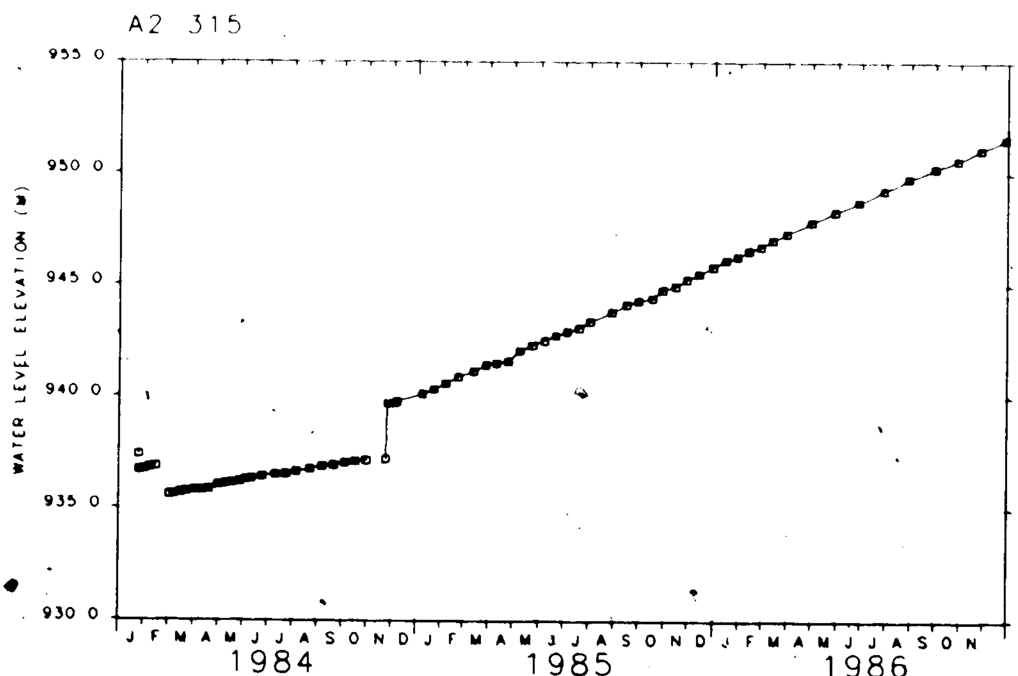
A2 315
955.0
950.0
945.0
940.0
935.0
930.0
WATER LEVEL ELEVATION (M)
J F M A M J J A S O N D J F M A M J J A S O N D J F M A M J J A S O N
1984
1985
1986

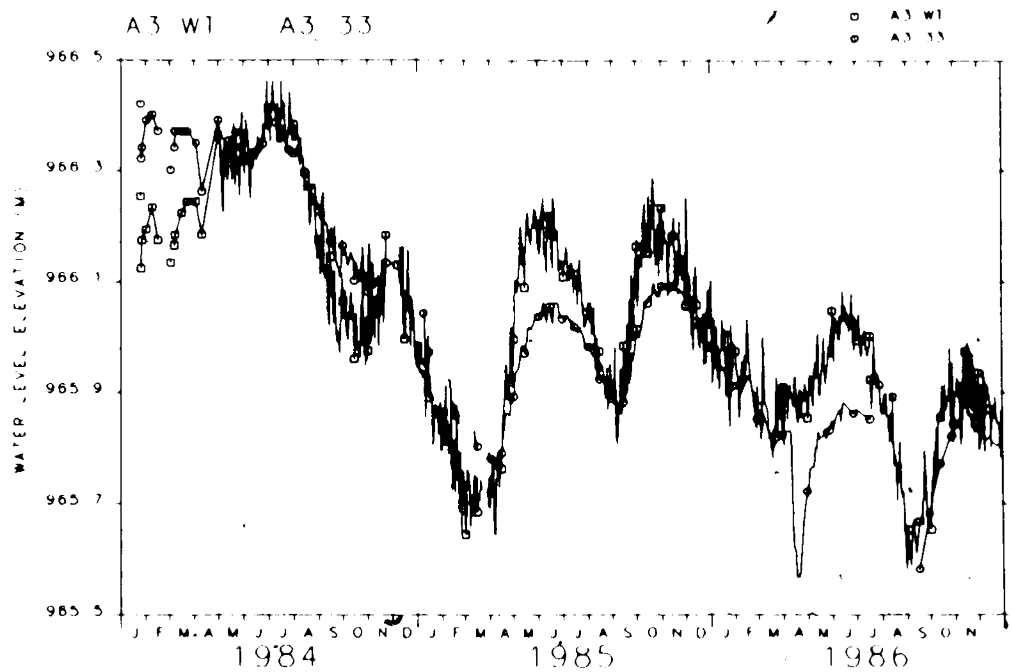
A3 W1 A3 33
A3 W1
A3 33
WATER LEVEL ELEVATION (M)
966.5
966.3
966.1
965.9
965.7
965.5
J F M A M J J A S O N D J F M A M J J A S O N D J F M A M J J A S O N
1984
1985
1986

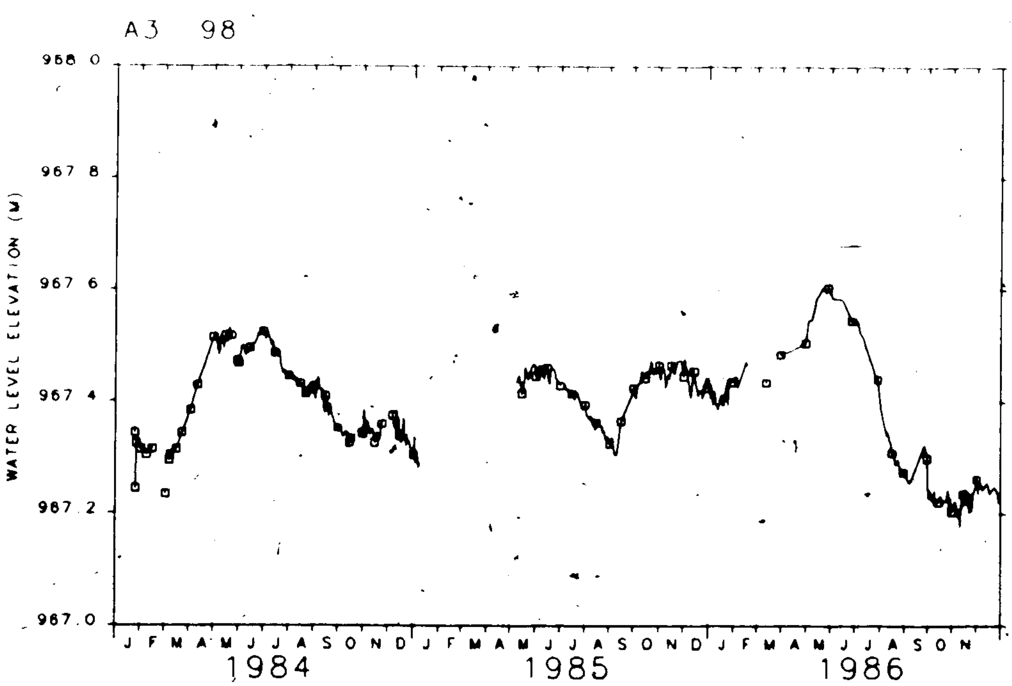
A3 98
WATER LEVEL ELEVATION (M)
968.0
967.8
967.6
967.4
967.2
967.0
J F M A M J J A S O N D J F M A M J J A S O N D J F M A M J J A S O N
1984
1985
1986

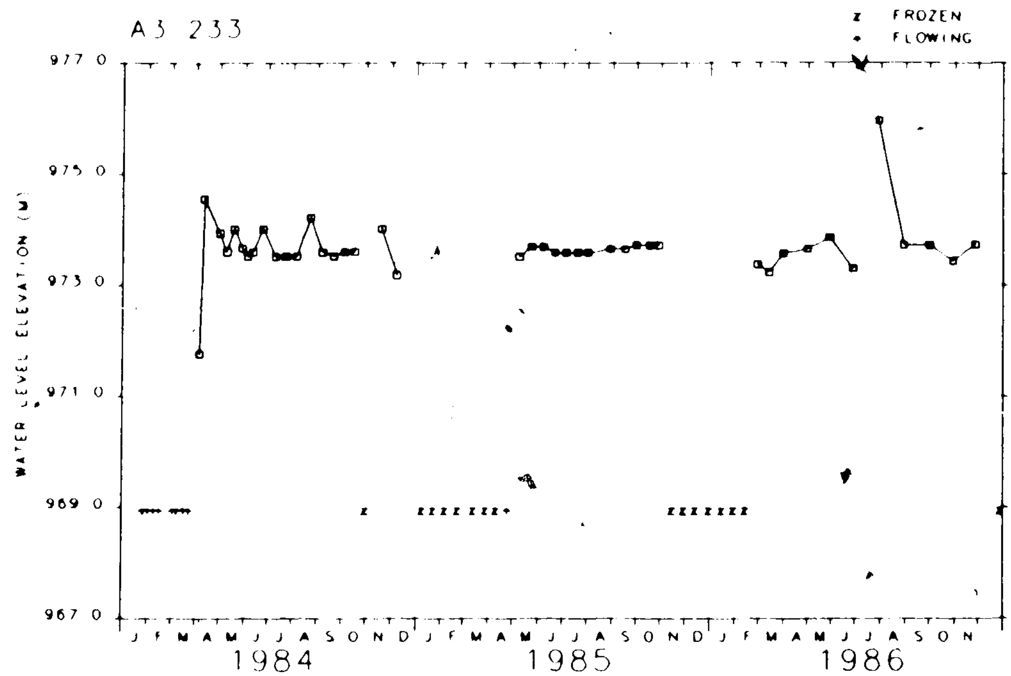
A3 233
z FROZEN
+ FLOWING
977.0
975.0
973.0
971.0
969.0
967.0
WATER LEVEL ELEVATION (M)
J F M A M J J A S O N D J F M A M J J A S O N D J F M A M J J A S O N
1984
1985
1986

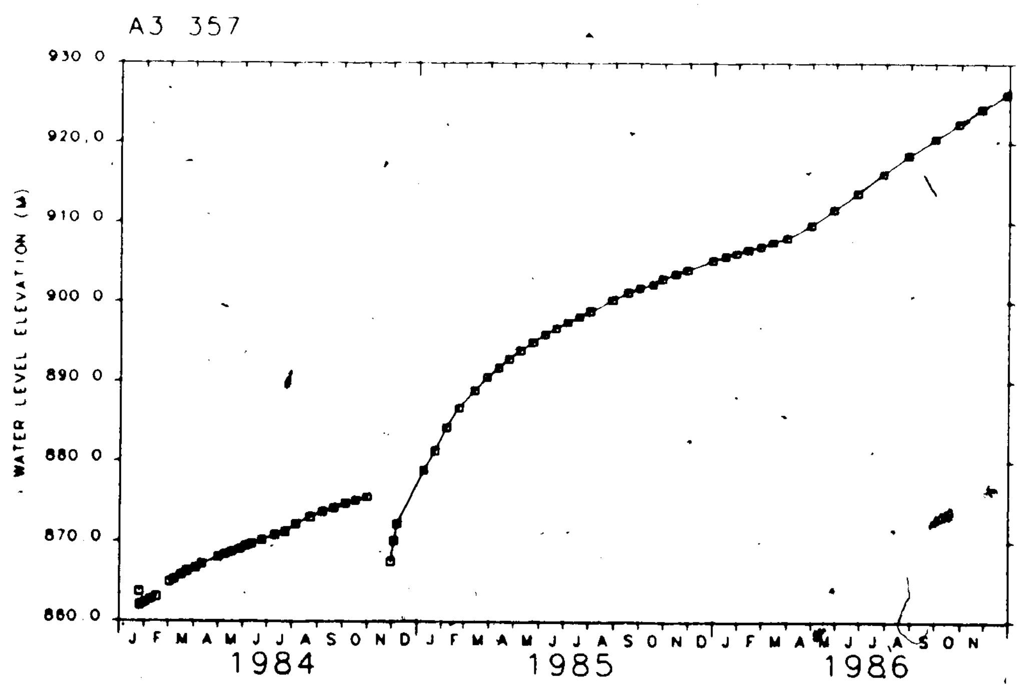
A3 357
930.0
920.0
910.0
900.0
890.0
880.0
870.0
860.0
WATER LEVEL ELEVATION (M)
J F M A M J J A S O N D J F M A M J J A S O N D J F M A M J J A S O N
1984
1985
1986

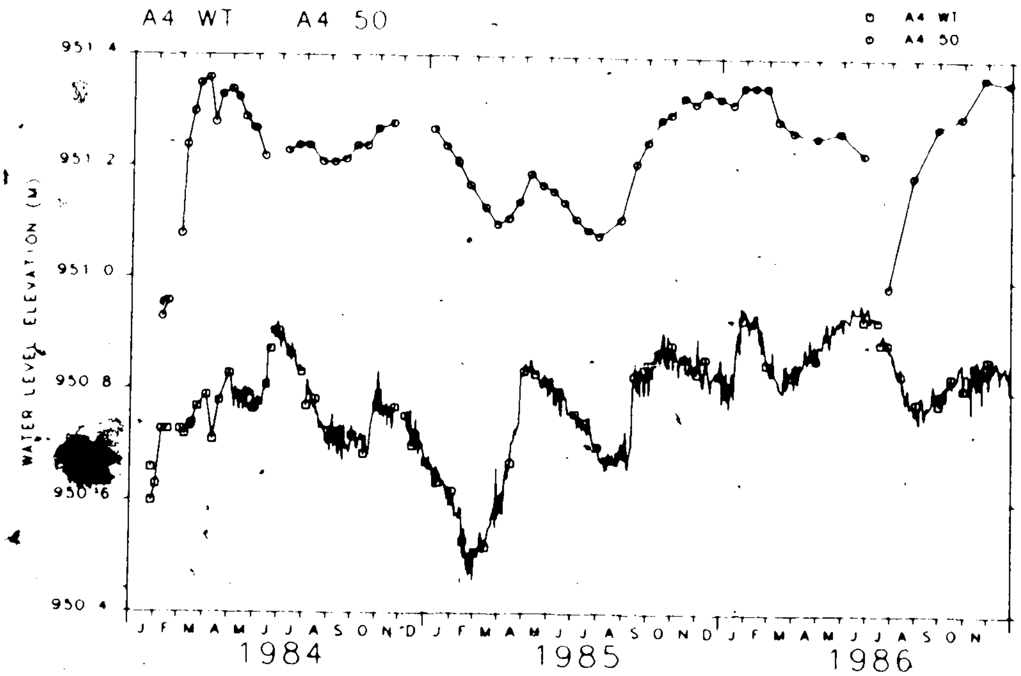
A4 WT A4 50
A4 WT
A4 50
951.4
951.2
951.0
950.8
950.6
950.4
WATER LEVEL ELEVATION (M)
J F M A M J J A S O N D J F M A M J J A S O N D J F M A M J J A S O N
1984
1985
1986

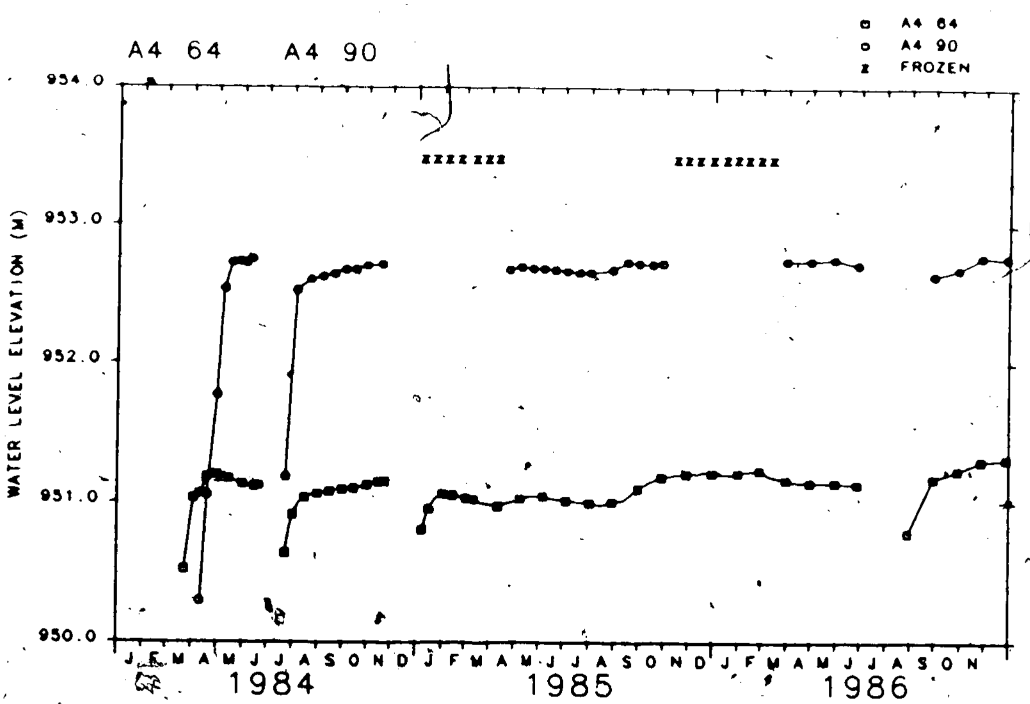
A4 64 A4 90
A4 64
A4 90
FROZEN
954.0
953.0
952.0
951.0
950.0
WATER LEVEL ELEVATION (M)
J F M A M J J A S O N D J F M A M J J A S O N D J F M A M J J A S O N
1984
1985
1986

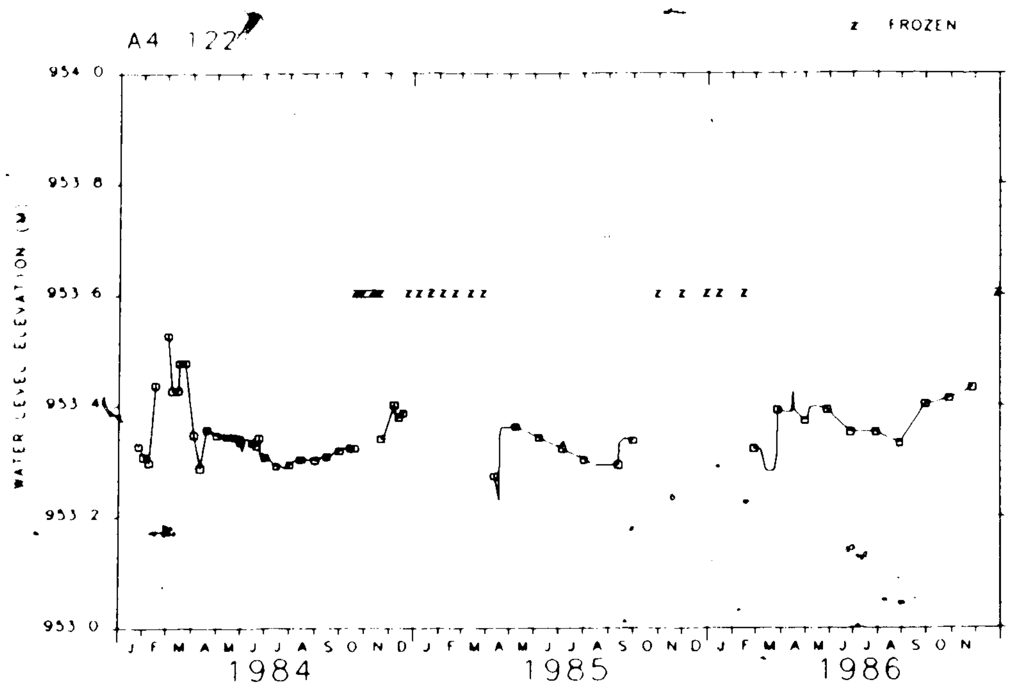
A4 122
z FROZEN
954.0
953.8
953.6
953.4
953.2
953.0
WATER LEVEL ELEVATION (M)
J F M A M J J A S O N D J F M A M J J A S O N D J F M A M J J A S O N
1984
1985
1986

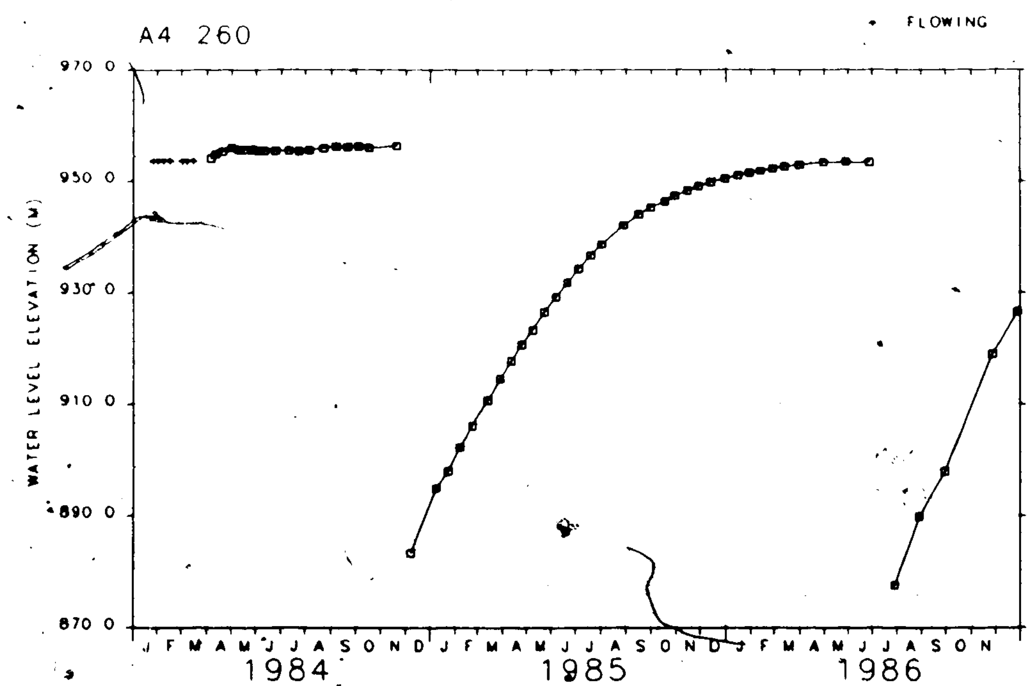
A4 260
FLOWING
970.0
950.0
930.0
910.0
890.0
870.0
WATER LEVEL ELEVATION (M)
J F M A M J J A S O N D J F M A M J J A S O N D J F M A M J J A S O N
1984
1985
1986

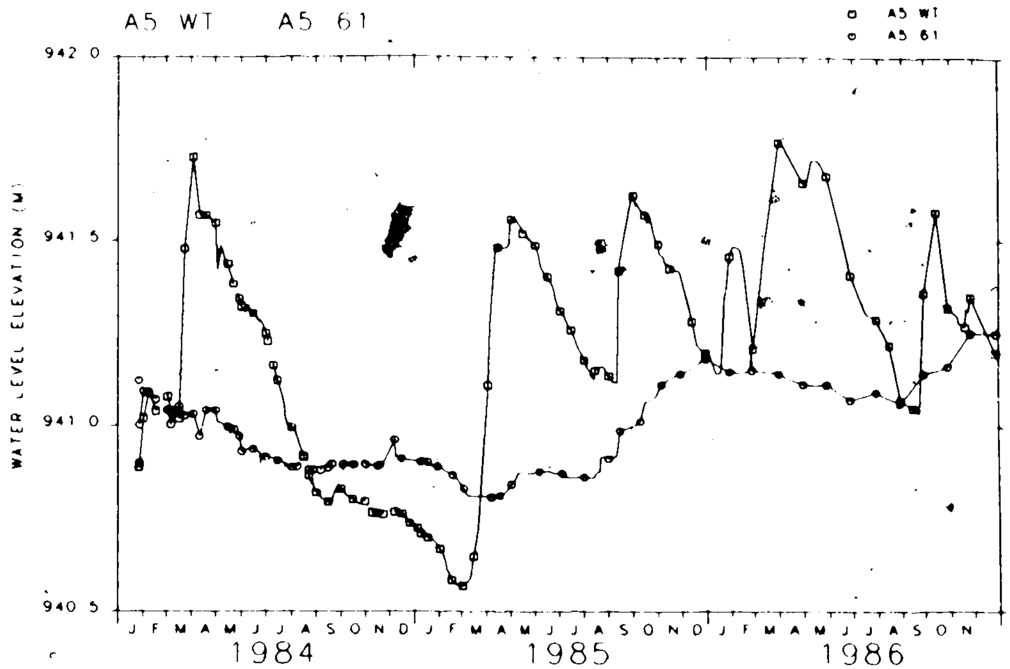
A5 WT A5 61
A5 WT
A5 61
942.0
941.5
941.0
940.5
WATER LEVEL ELEVATION (M)
J F M A M J J A S O N D J F M A M J J A S O N D J F M A M J J A S O N
1984
1985
1986

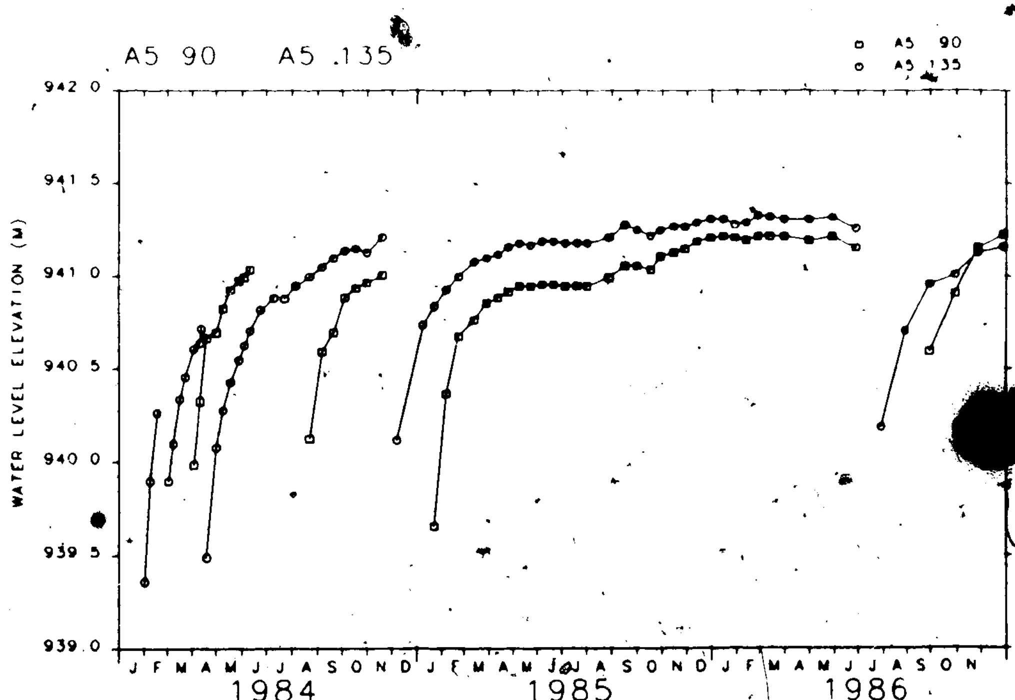
A5 90 A5 135
A5 90
A5 135
942.0
941.5
941.0
940.5
940.0
939.5
939.0
WATER LEVEL ELEVATION (M)
J F M A M J J A S O N D J F M A M J J A S O N D J F M A M J J A S O N
1984
1985
1986

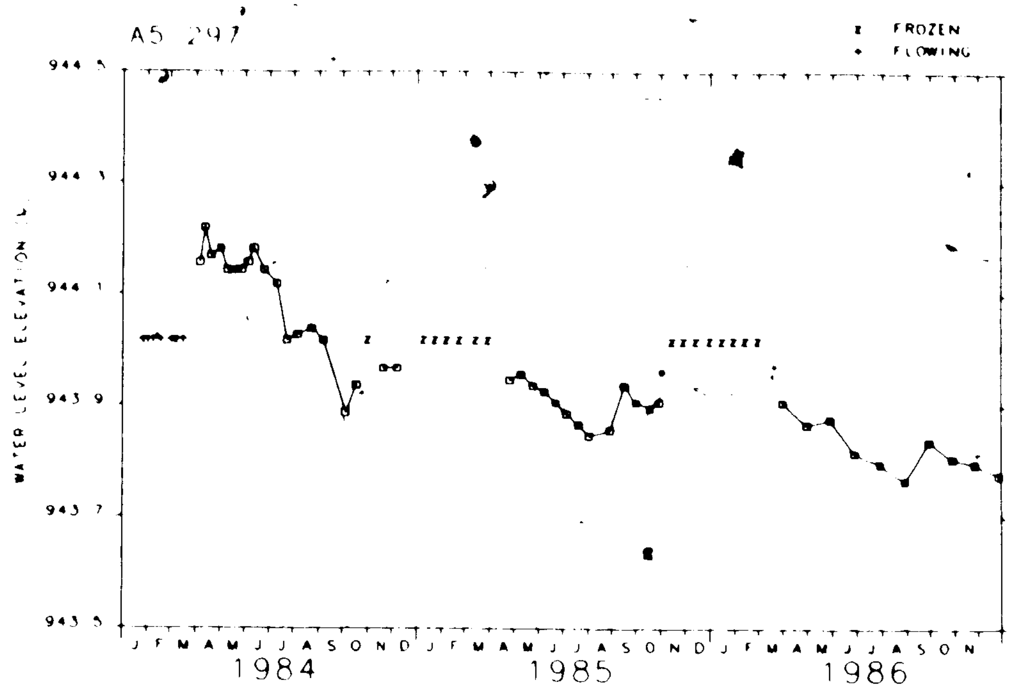
A5 297
FROZEN
FLOWING
944.5
944.3
944.1
943.9
943.7
943.5
WATER LEVEL ELEVATION (M)
J F M A M J J A S O N D J F M A M J J A S O N D J F M A M J J A S O N
1984
1985
1986

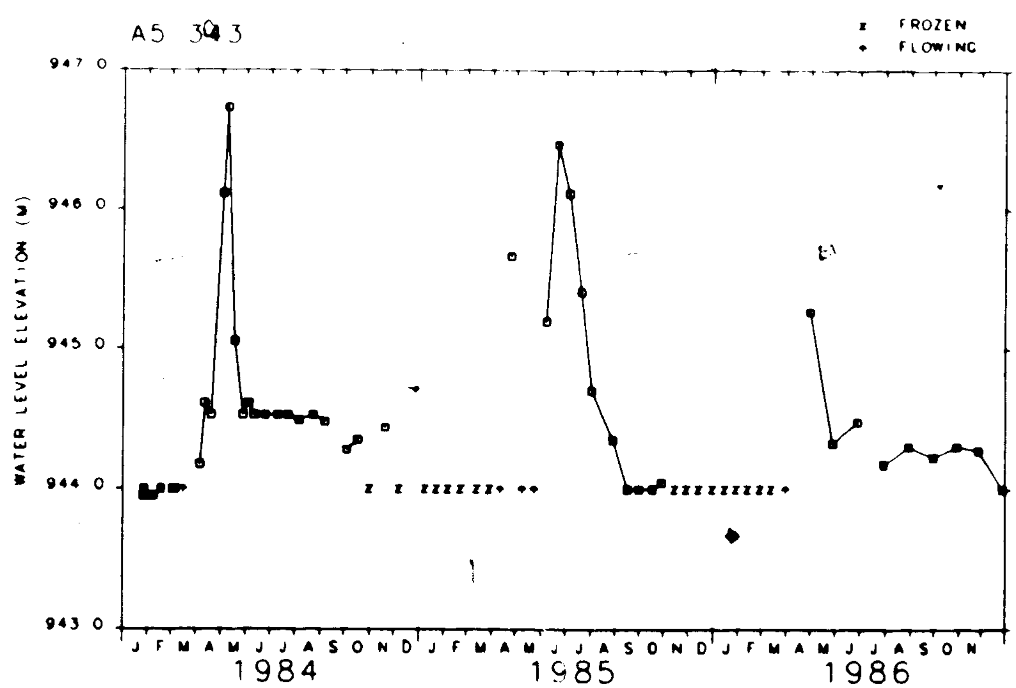
A5 343
FROZEN
FLOWING
947.0
946.0
945.0
944.0
943.0
WATER LEVEL ELEVATION (M)
J F M A M J J A S O N D J F M A M J J A S O N D J F M A M J J A S O N
1984
1985
1986

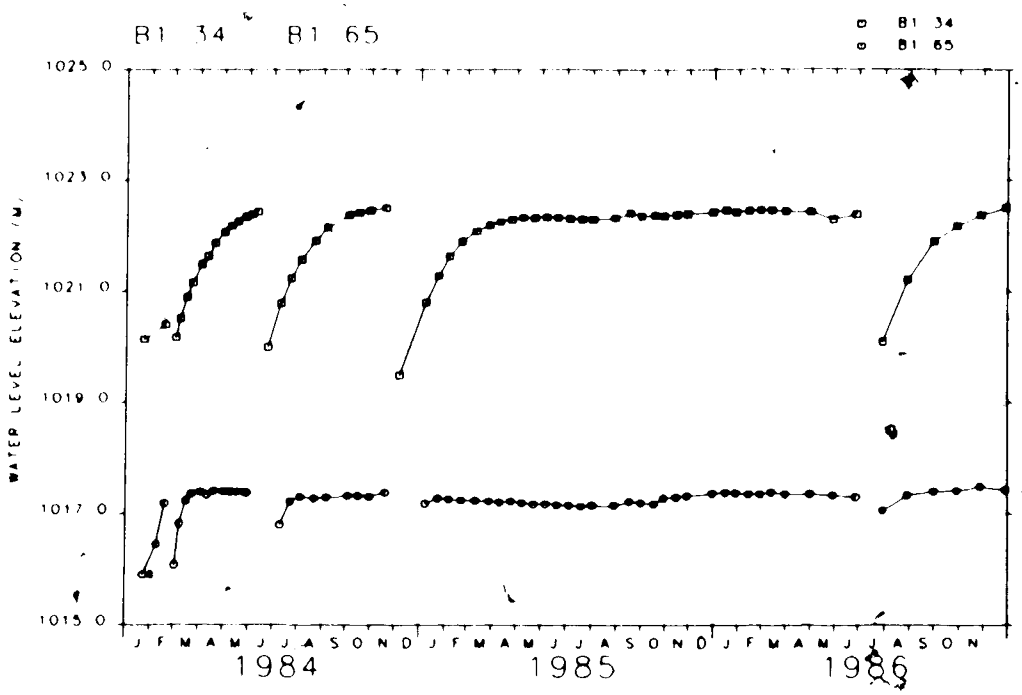
B1 34 B1 65
B1 34
B1 65
1025.0
1023.0
1021.0
1019.0
1017.0
1015.0
WATER LEVEL ELEVATION (M)
J F M A M J J A S O N D J F M A M J J A S O N D J F M A M J J A S O N
1984
1985
1986

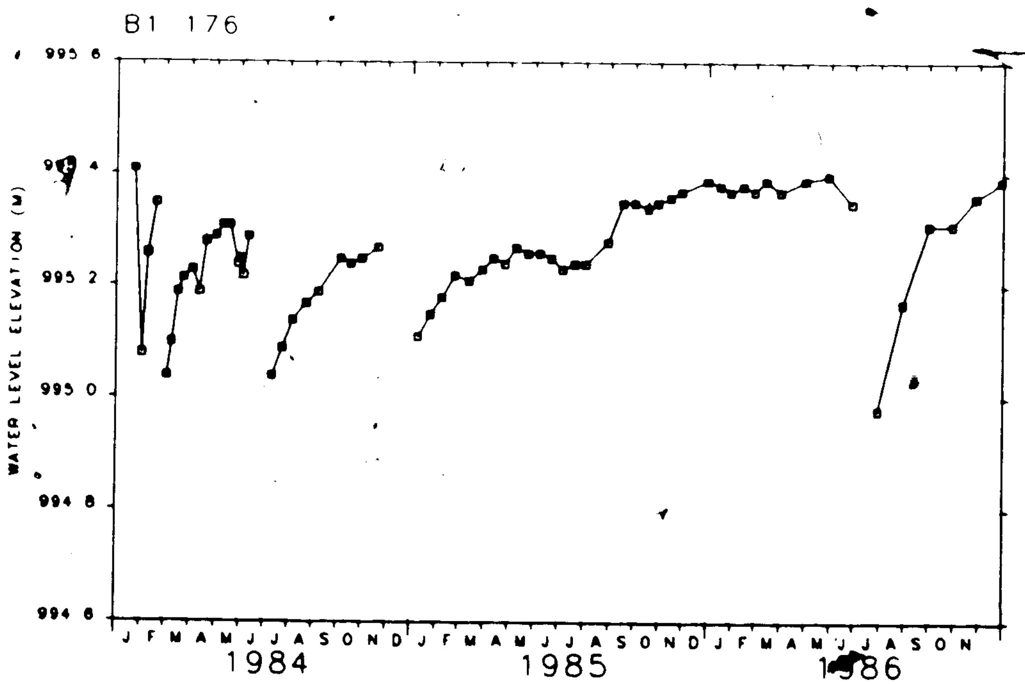
B1 176
995.6
995.4
995.2
995.0
994.8
994.6
WATER LEVEL ELEVATION (M)
J F M A M J J A S O N D J F M A M J J A S O N D J F M A M J J A S O N
1984
1985
1986

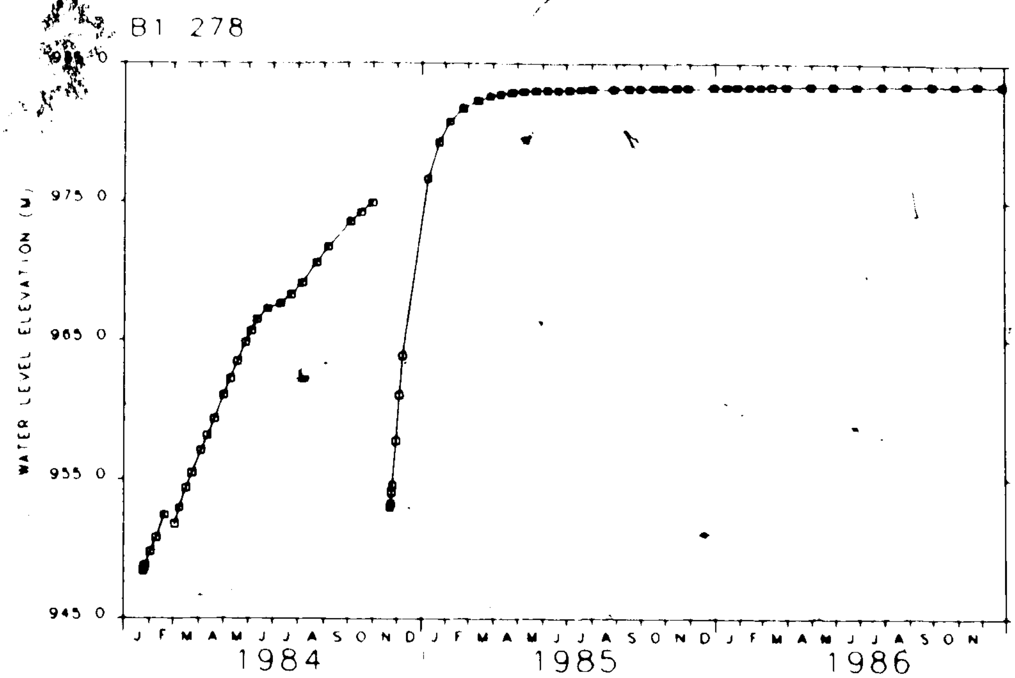
B1 278
WATER LEVEL ELEVATION (M)
975.0
965.0
955.0
945.0
J F M A M J J A S O N D J F M A M J J A S O N D J F M A M J J A S O N
1984
1985
1986

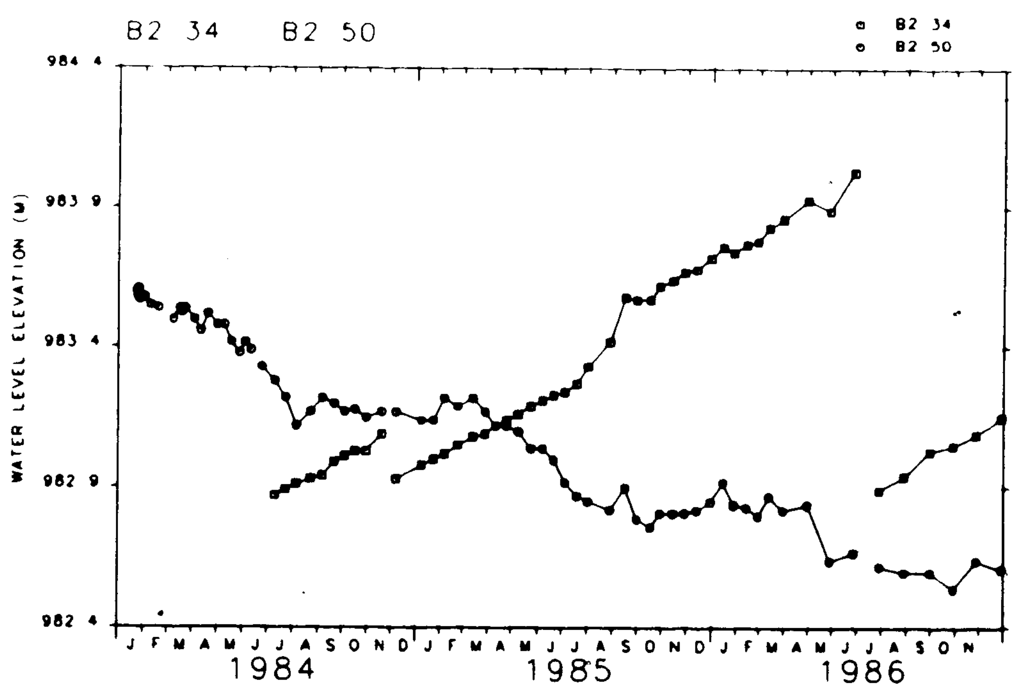
B2 34 B2 50
B2 34
B2 50
WATER LEVEL ELEVATION (M)
984.4
983.9
983.4
982.9
982.4
J F M A M J J A S O N D J F M A M J J A S O N D J F M A M J J A S O N
1984
1985
1986

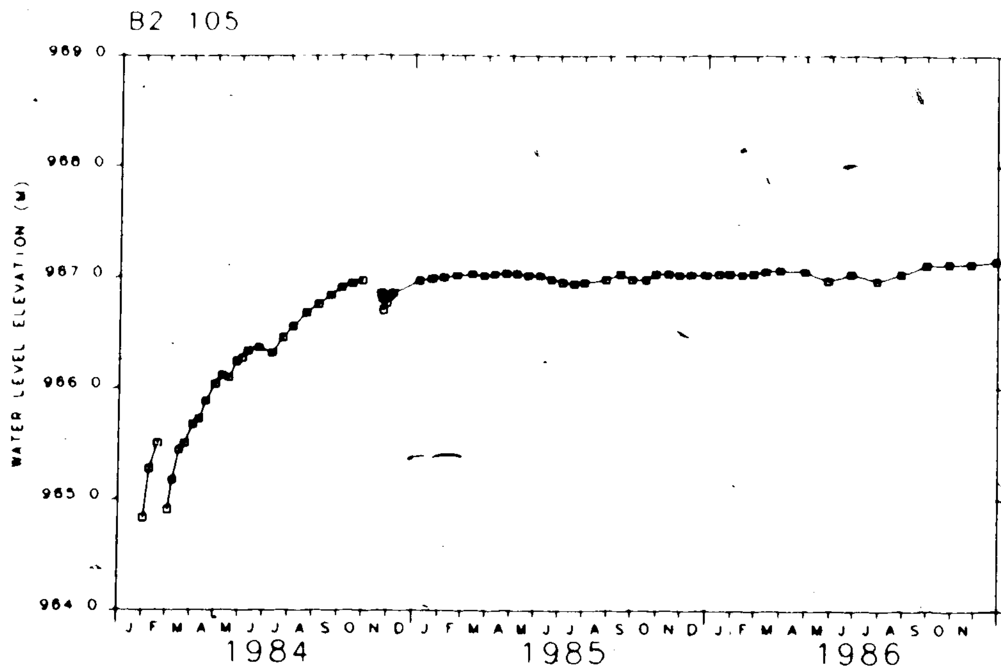
B2 105
969.0
968.0
967.0
966.0
965.0
964.0
WATER LEVEL ELEVATION (M)
J F M A M J J A S O N D J F M A M J J A S O N D J F M A M J J A S O N
1984
1985
1986

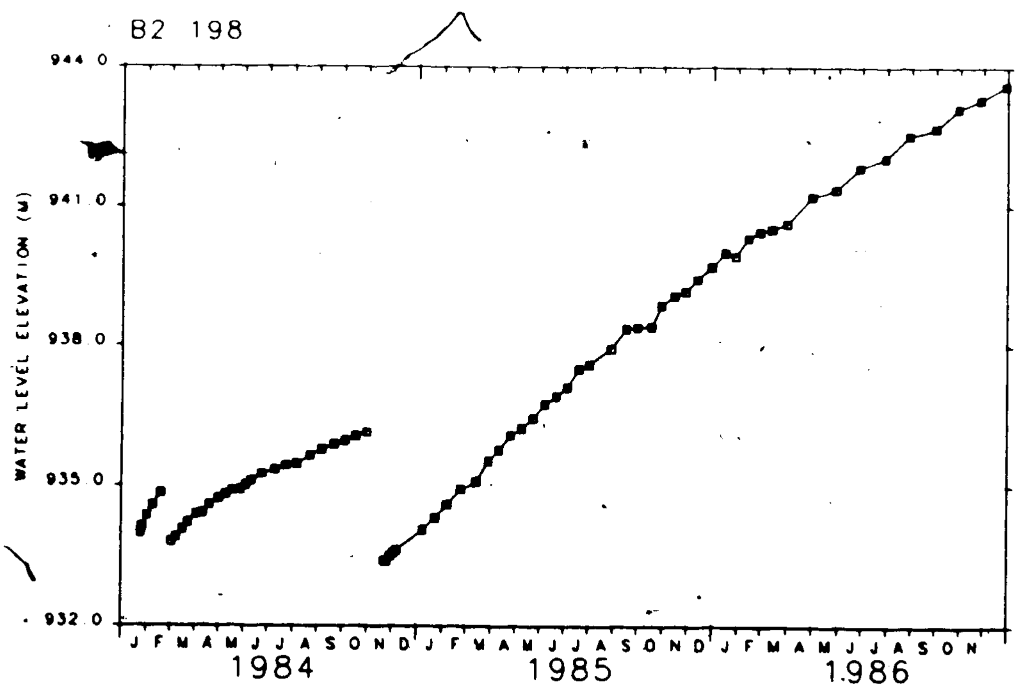
B2 198
944.0
941.0
938.0
935.0
932.0
WATER LEVEL ELEVATION (M)
J F M A M J J A S O N D J F M A M J J A S O N D J F M A M J J A S O N
1984
1985
1986

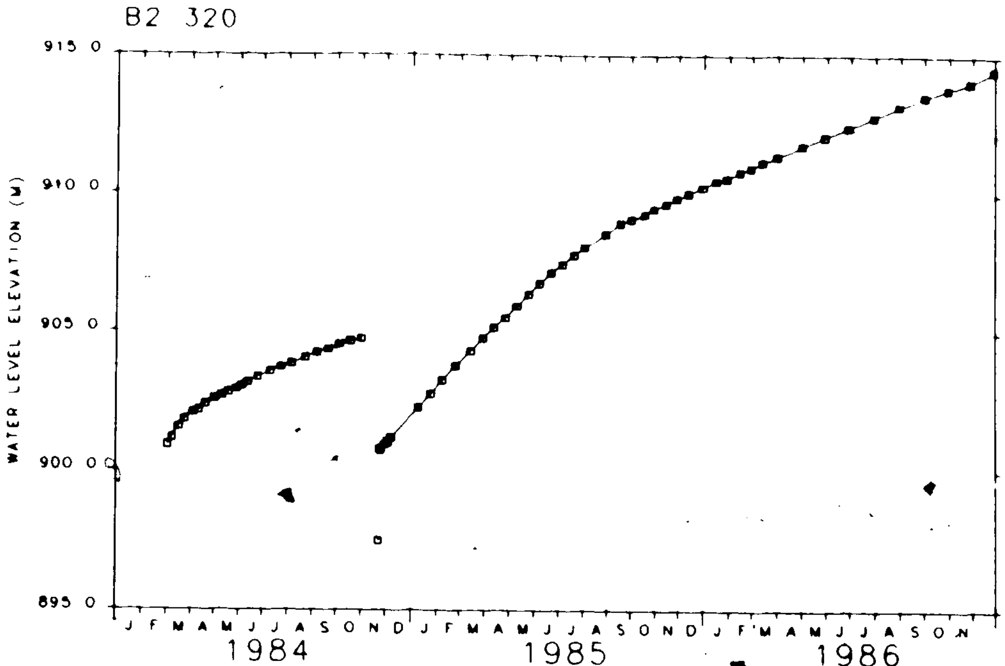
B2 320
915.0
910.0
905.0
900.0
895.0
WATER LEVEL ELEVATION (M)
J F M A M J J A S O N D J F M A M J J A S O N D J F M A M J J A S O N
1984
1985
1986

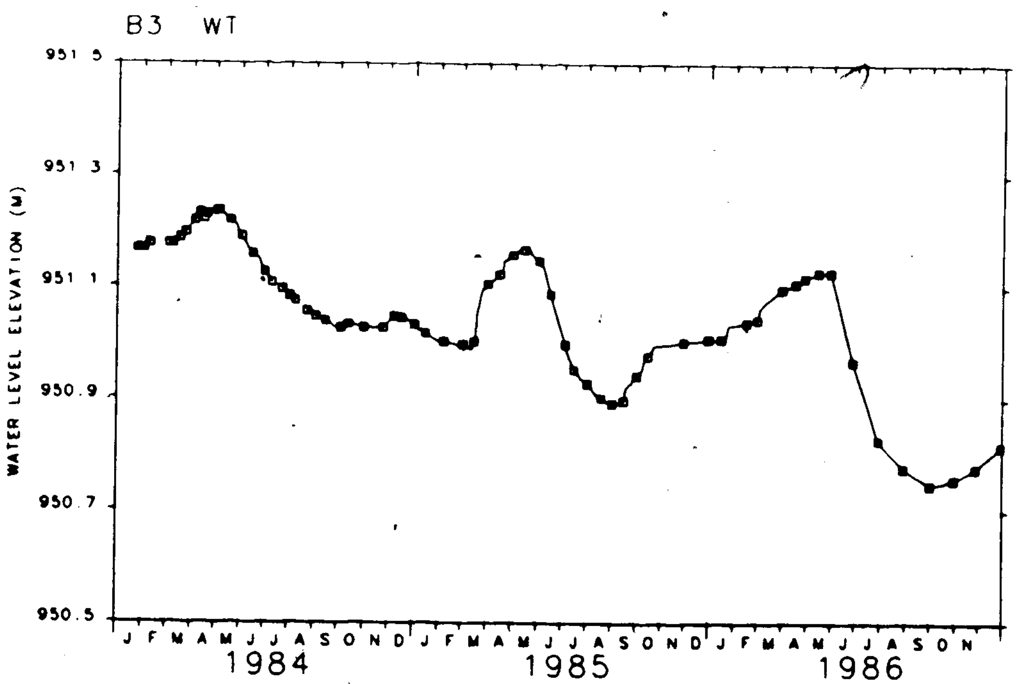
B3 WT
951.5
951.3
951.1
950.9
950.7
950.5
WATER LEVEL ELEVATION (M)
J F M A M J J A S O N D J F M A M J J A S O N D J F M A M J J A S O N
1984
1985
1986

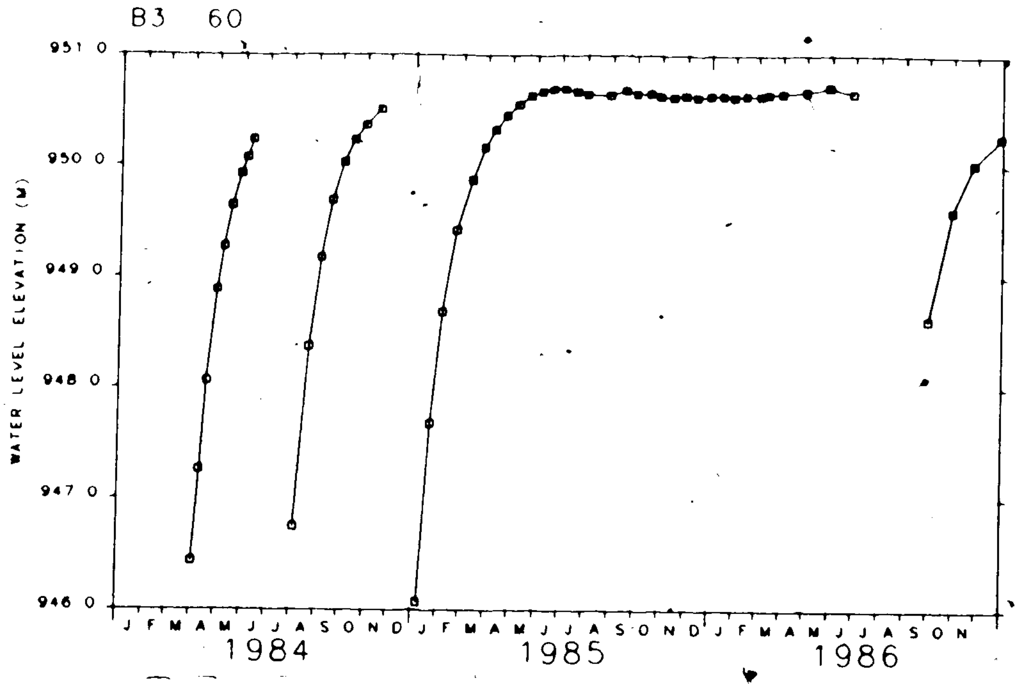
B3 60
951.0
950.0
949.0
948.0
947.0
946.0
WATER LEVEL ELEVATION (M)
J F M A M J J A S O N D J F M A M J J A S O N D J F M A M J J A S O N
1984
1985
1986

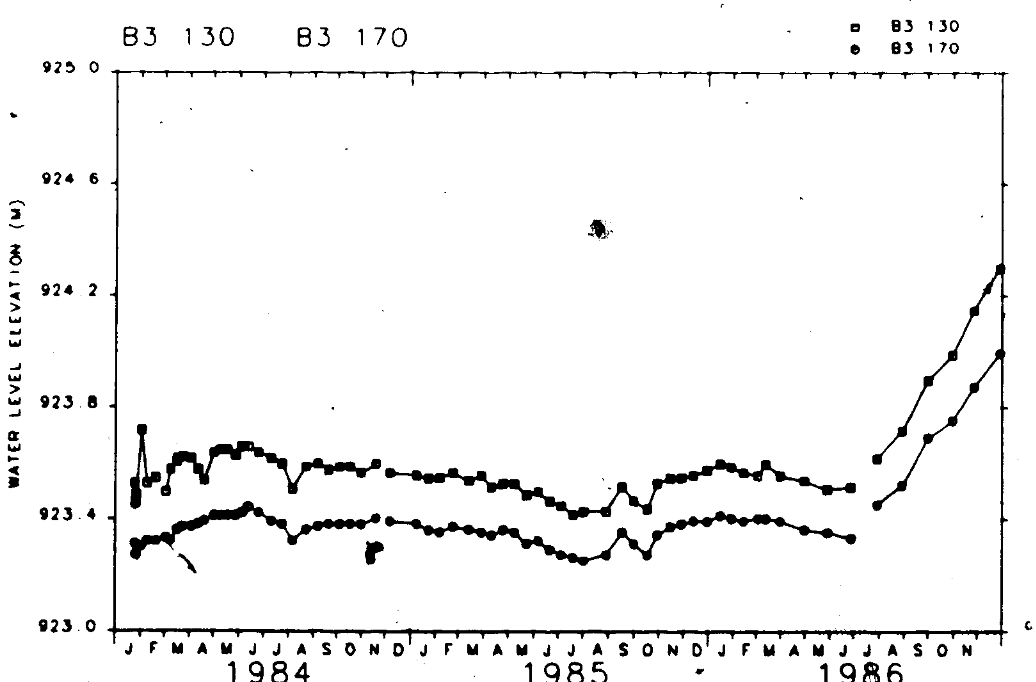
B3 130 B3 170
B3 130
B3 170
925.0
924.6
924.2
923.8
923.4
923.0
WATER LEVEL ELEVATION (M)
J F M A M J J A S O N D J F M A M J J A S O N D J F M A M J J A S O N
1984
1985
1986

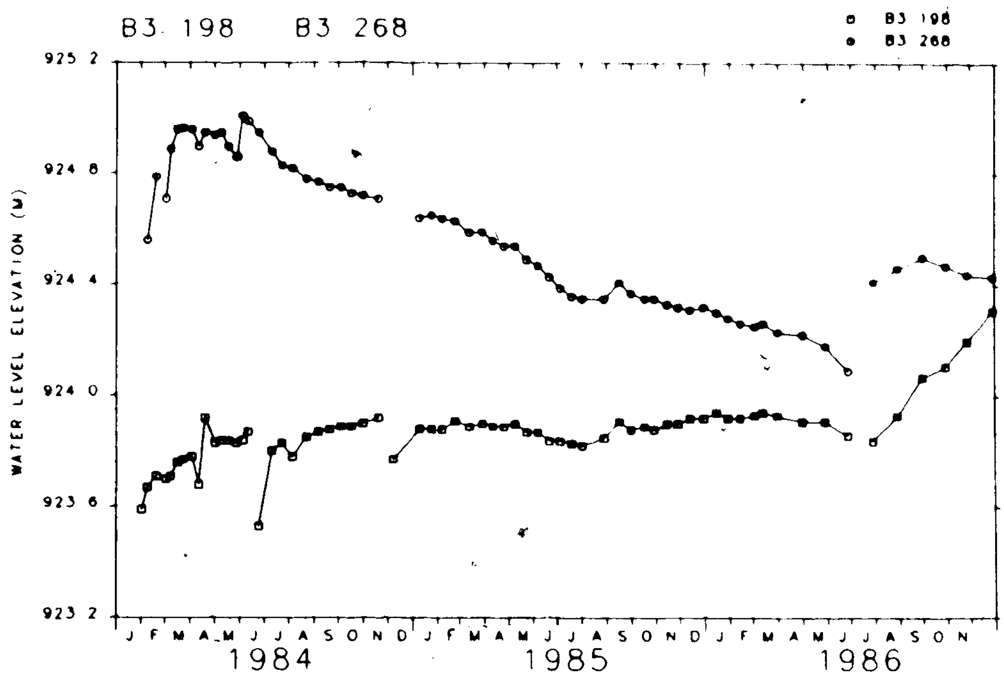
B3 198 B3 268
B3 198
B3 268
925.2
924.8
924.4
924.0
923.6
923.2
WATER LEVEL ELEVATION (M)
J F M A M J J A S O N D J F M A M J J A S O N D J F M A M J J A S O N
1984
1985
1986

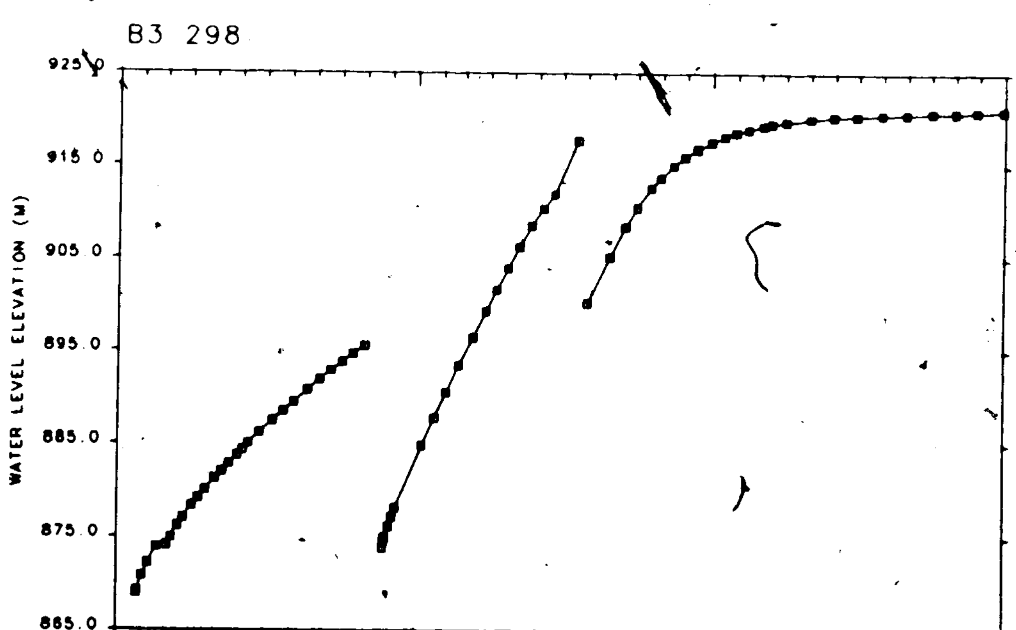
B3 298
925.0
915.0
905.0
895.0
885.0
875.0
865.0
WATER LEVEL ELEVATION (M)
J F M A M J J A S O N D J F M A M J J A S O N D J F M A M J J A S O N
1984
1985
1986

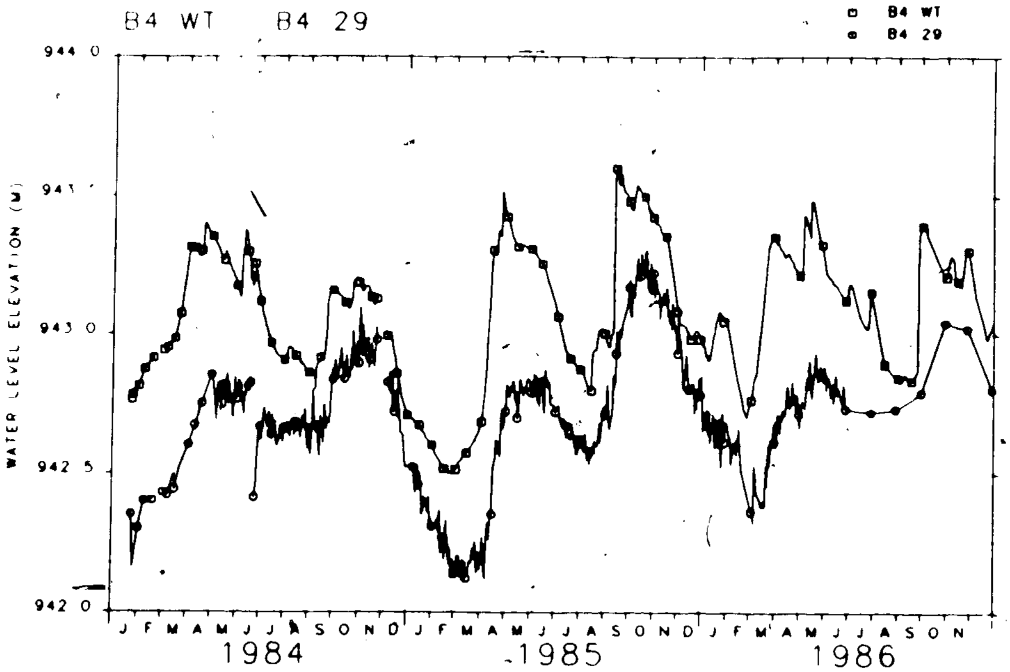
B4 WT B4 29
B4 WT
B4 29
944.0
943.0
942.5
942.0
WATER LEVEL ELEVATION (M)
J F M A M J J A S O N D J F M A M J J A S O N D J F M A M J J A S O N
1984
1985
1986

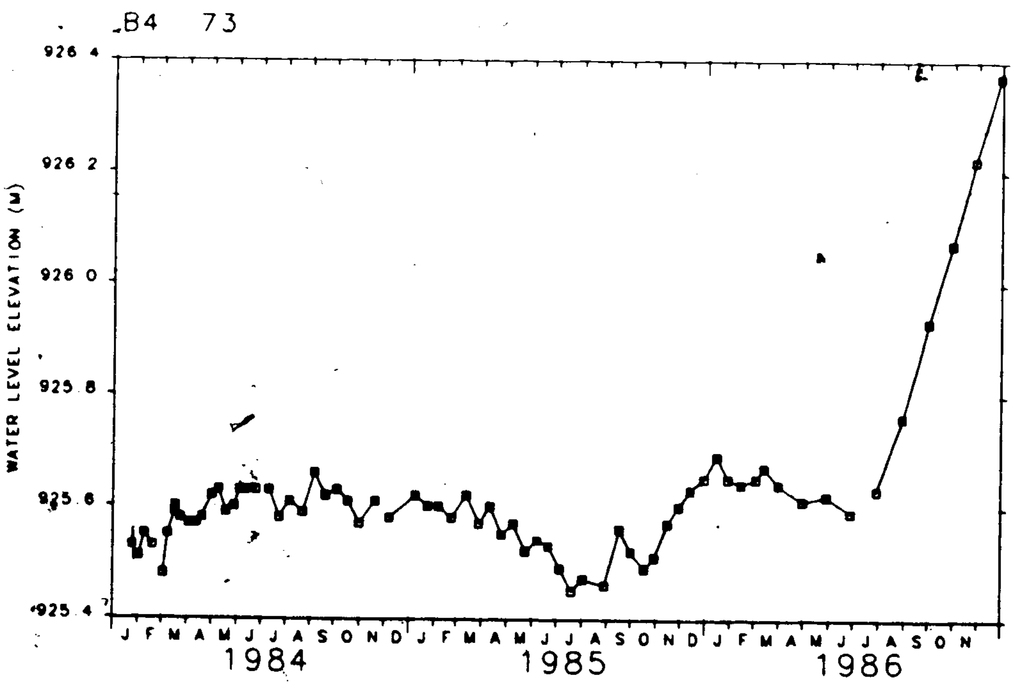
B4 73
926.4
926.2
926.0
925.8
925.6
925.4
WATER LEVEL ELEVATION (M)
J F M A M J J A S O N D J F M A M J J A S O N D J F M A M J J A S O N
1984
1985
1986

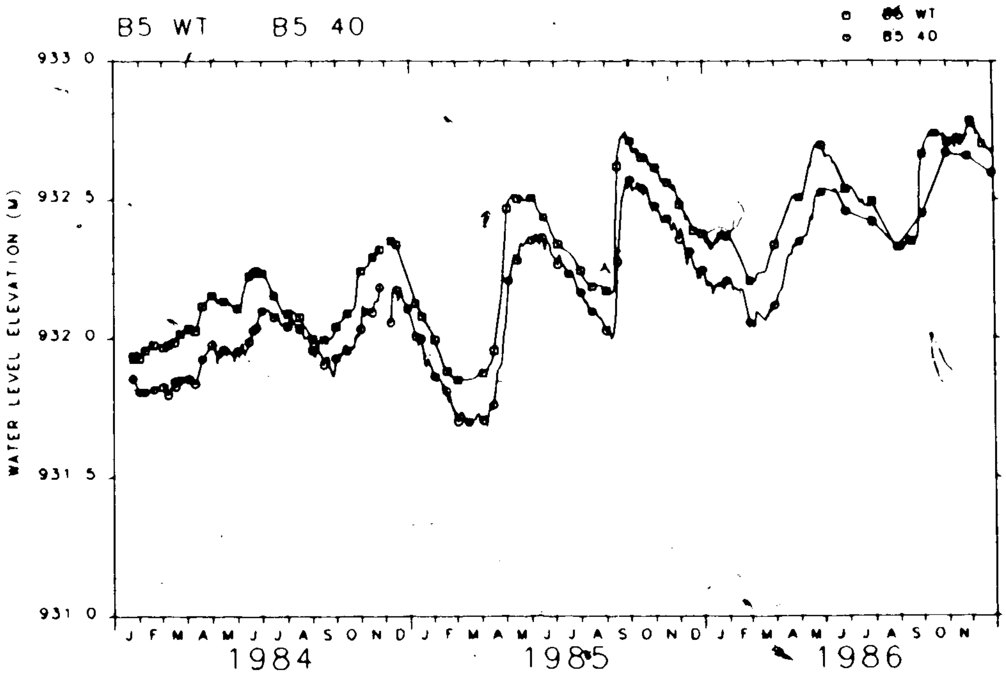
B5 WT B5 40
B5 WT
B5 40
933.0
932.5
932.0
931.5
931.0
WATER LEVEL ELEVATION (M)
J F M A M J J A S O N D J F M A M J J A S O N D J F M A M J J A S O N
1984
1985
1986

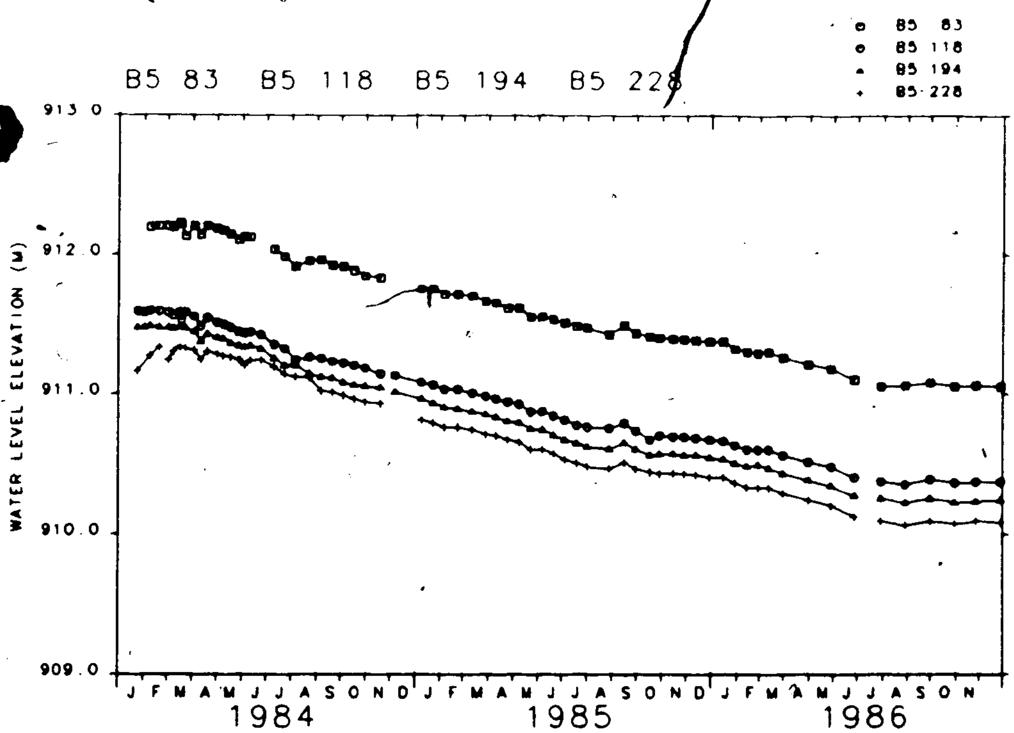
B5 83 B5 118 B5 194 B5 228
B5 83
B5 118
B5 194
B5 228
913.0
912.0
911.0
910.0
909.0
WATER LEVEL ELEVATION (M)
J F M A M J J A S O N D J F M A M J J A S O N D J F M A M J J A S O N
1984
1985
1986

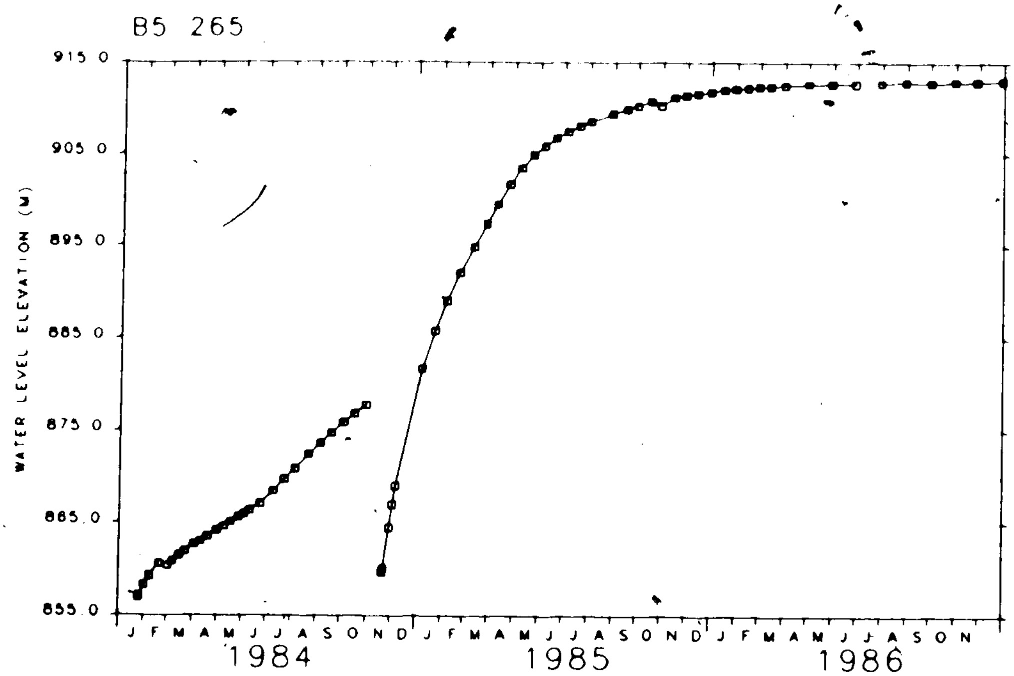
B5 265
915.0
905.0
895.0
885.0
875.0
865.0
855.0
WATER LEVEL ELEVATION (M)
J F M A M J J A S O N D J F M A M J J A S O N D J F M A M J J A S O N
1984
1985
1986

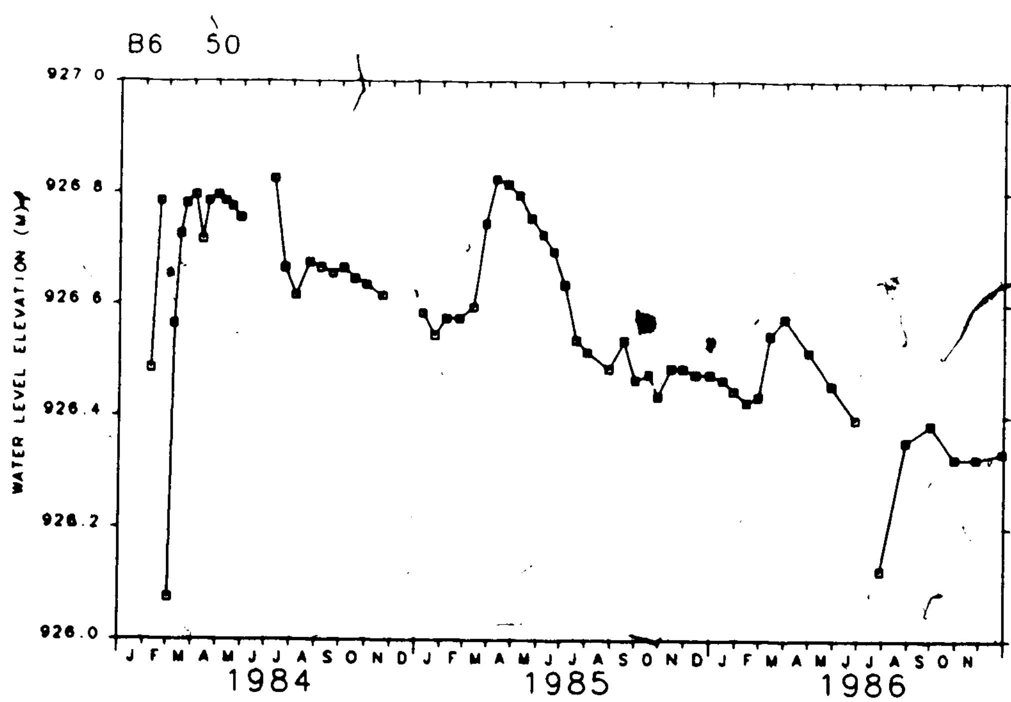
B6 50
927.0
926.8
926.6
926.4
926.2
926.0
WATER LEVEL ELEVATION (M)
J F M A M J J A S O N D J F M A M J J A S O N D J F M A M J J A S O N
1984
1985
1986

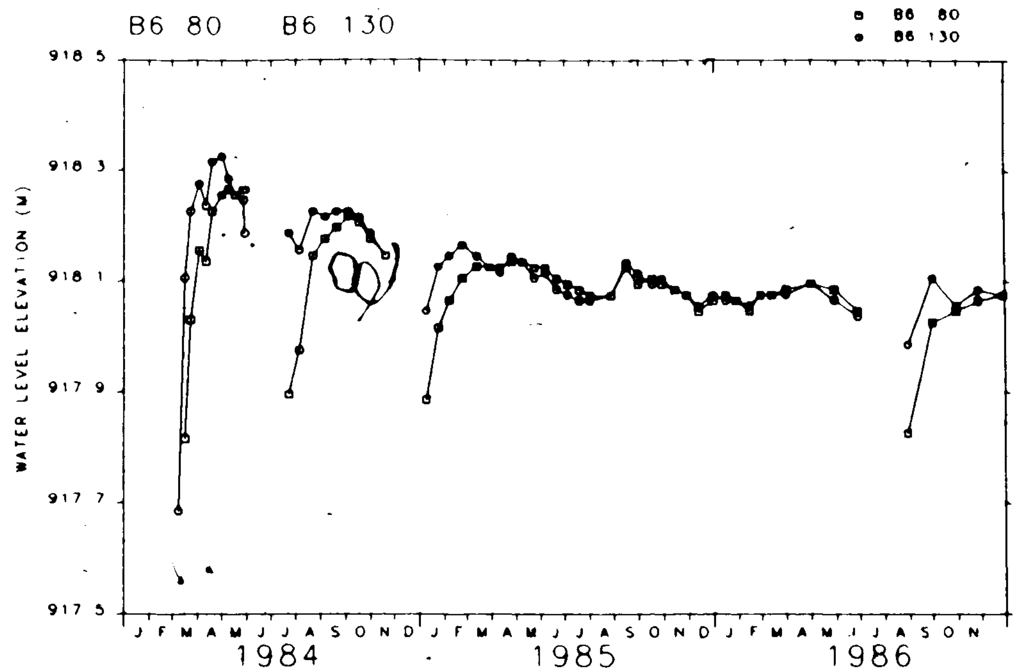
B6 80 B6 130
B6 80
B6 130
918.5
918.3
918.1
917.9
917.7
917.5
WATER LEVEL ELEVATION (M)
J F M A M J J A S O N D J F M A M J J A S O N D J F M A M J J A S O N
1984
1985
1986

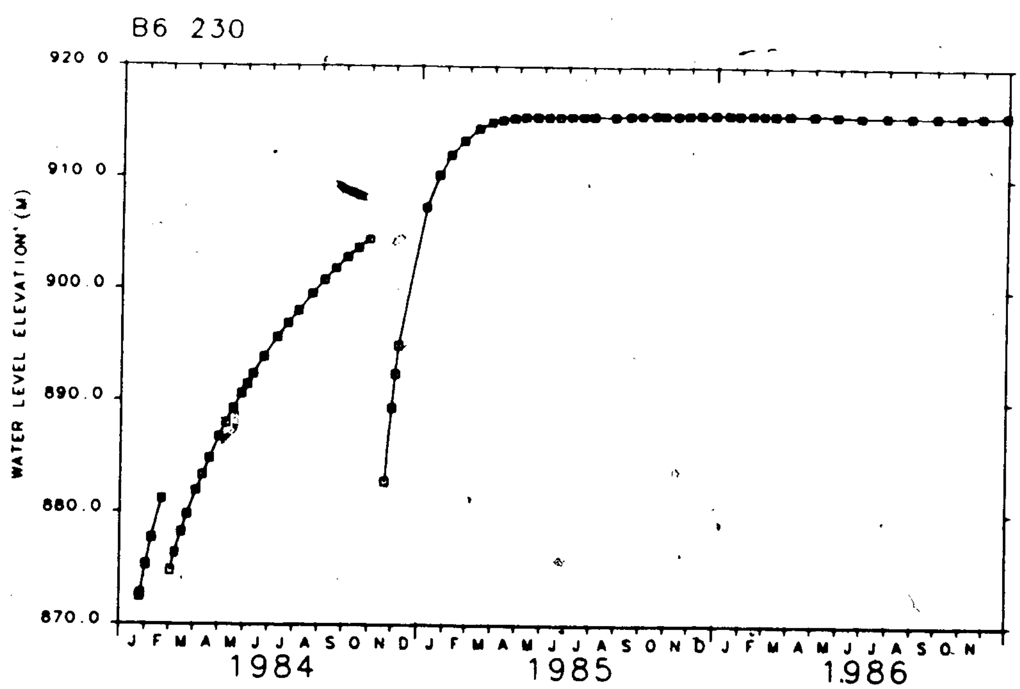
B6 230
920.0
910.0
900.0
890.0
880.0
870.0
WATER LEVEL ELEVATION (M)
J F M A M J J A S O N D J F M A M J J A S O N D J F M A M J J A S O N
1984
1985
1986

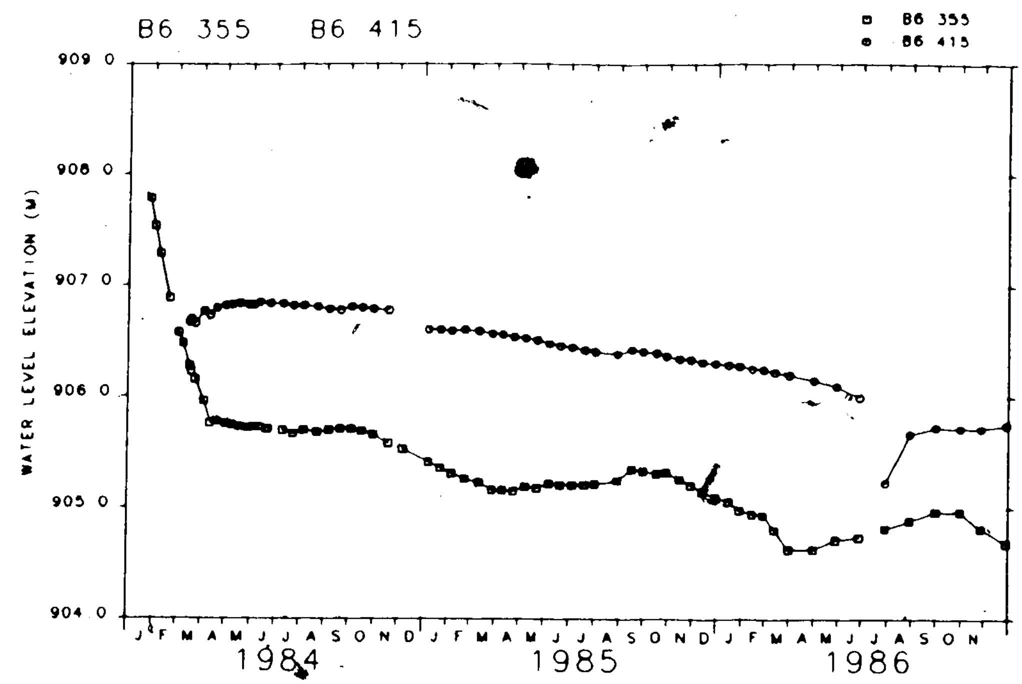
B6 355 B6 415
B6 355
B6 415
909.0
908.0
907.0
906.0
905.0
904.0
WATER LEVEL ELEVATION (M)
J F M A M J J A S O N D J F M A M J J A S O N D J F M A M J J A S O N
1984
1985
1986

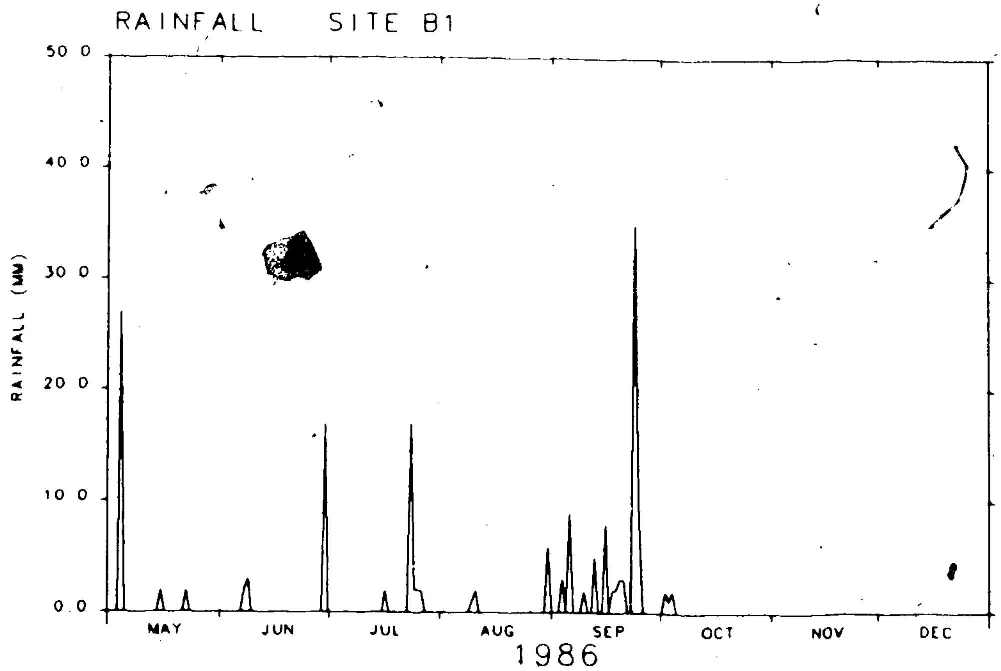
RAINFALL SITE B1
50.0
40.0
30.0
20.0
10.0
0.0
RAINFALL (MM)
MAY
JUN
JUL
AUG
SEP
OCT
NOV
DEC
1986

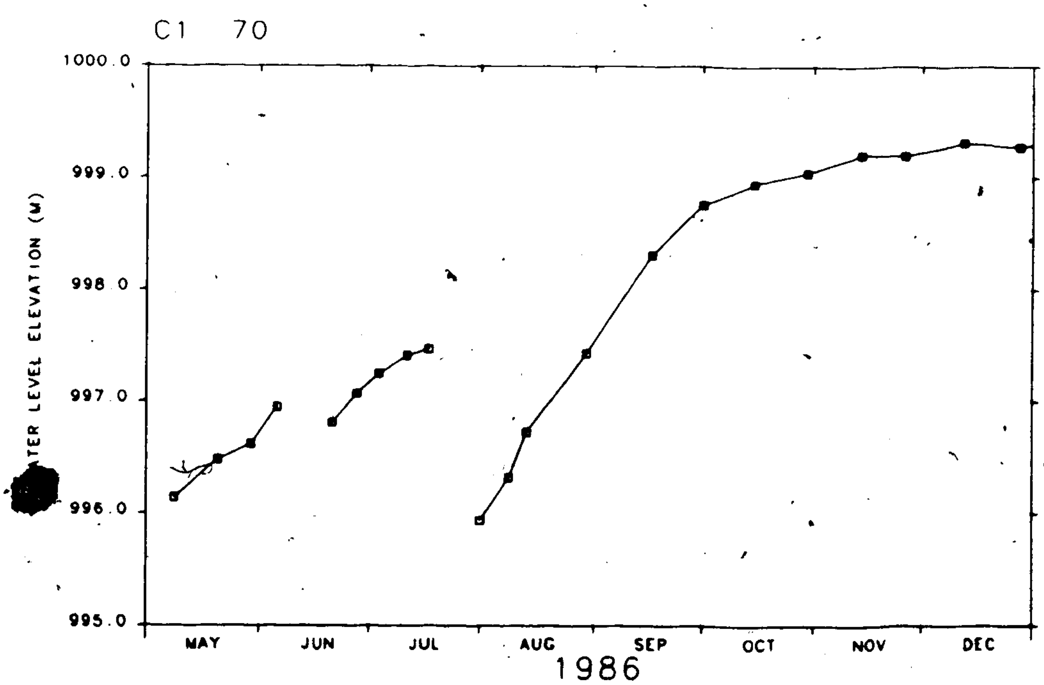
C1 70
1000.0
999.0
998.0
997.0
996.0
995.0
TER LEVEL ELEVATION (M)
MAY
JUN
JUL
AUG
SEP
OCT
NOV
DEC
1986

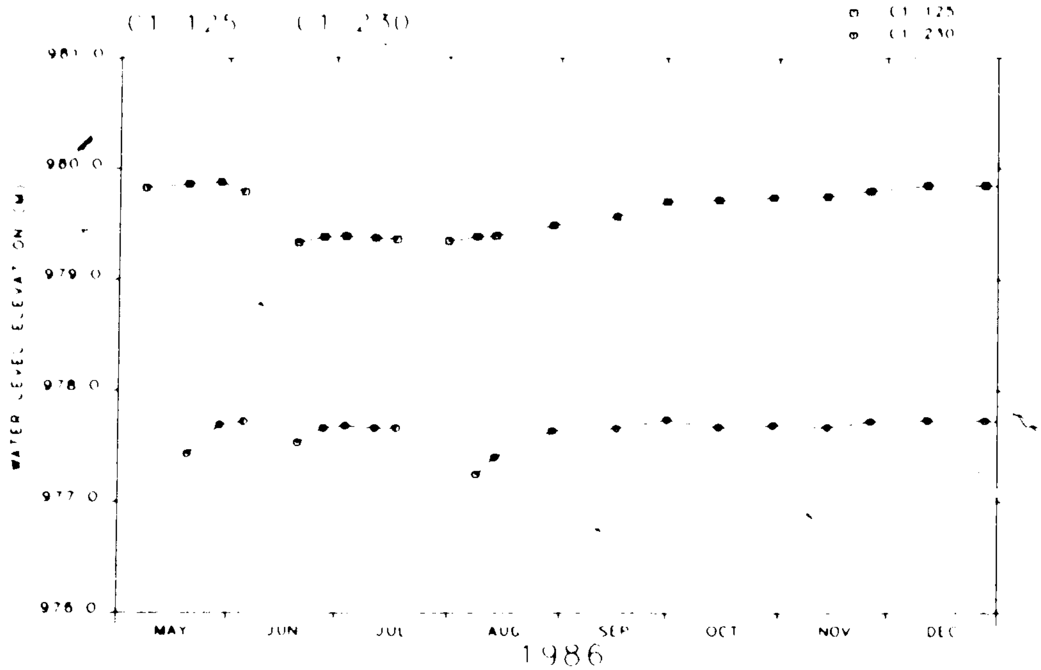
C1 125 C1 230
C1 125
C1 230
980.0
979.0
978.0
977.0
976.0
WATER LEVEL ELEVATION (M)
MAY
JUN
JUL
AUG
SEP
OCT
NOV
DEC
1986

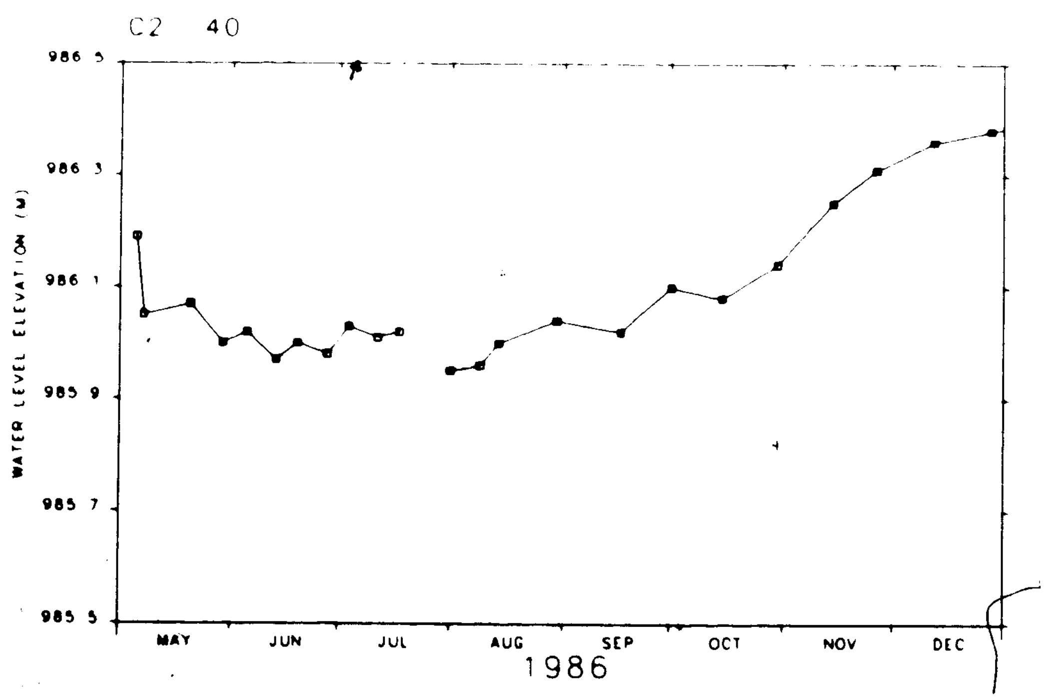
C2 40
986.5
986.3
986.1
985.9
985.7
985.5
WATER LEVEL ELEVATION (M)
MAY
JUN
JUL
AUG
SEP
OCT
NOV
DEC
1986

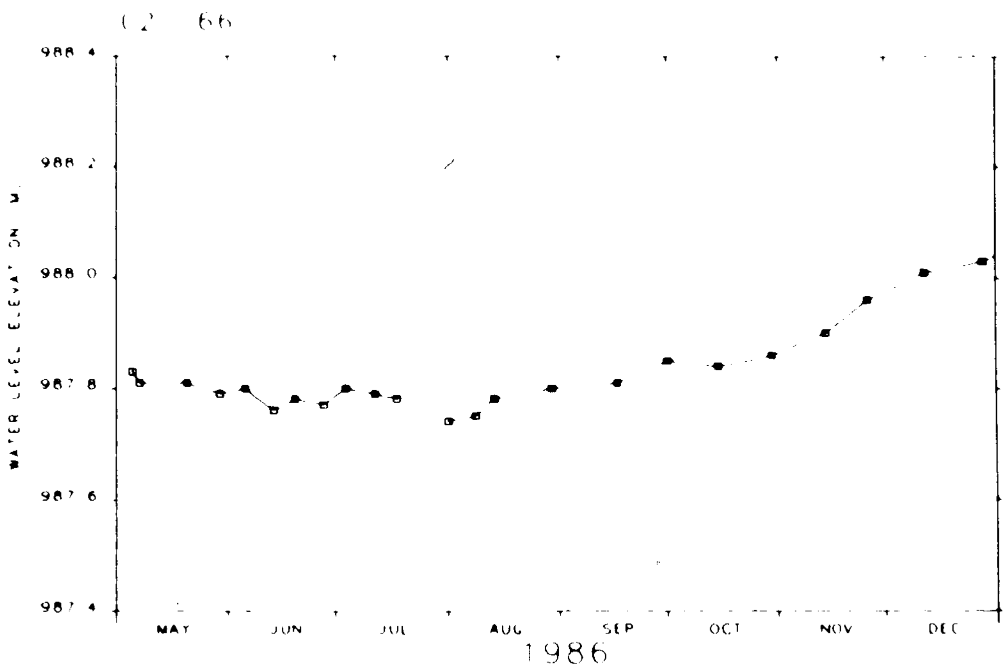
C2 66
988.4
988.2
988.0
987.8
987.6
987.4
WATER LEVEL ELEVATION (M)
MAY
JUN
JUL
AUG
SEP
OCT
NOV
DEC
1986

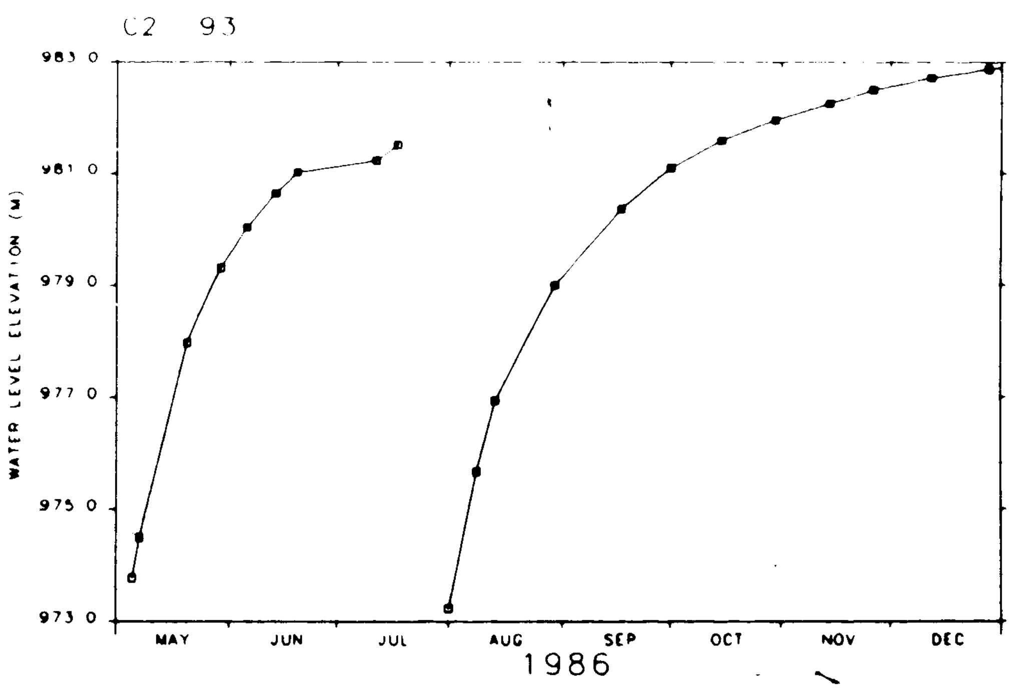
C2 93
983.0
981.0
979.0
977.0
975.0
973.0
WATER LEVEL ELEVATION (M)
MAY
JUN
JUL
AUG
SEP
OCT
NOV
DEC
1986

C2 125

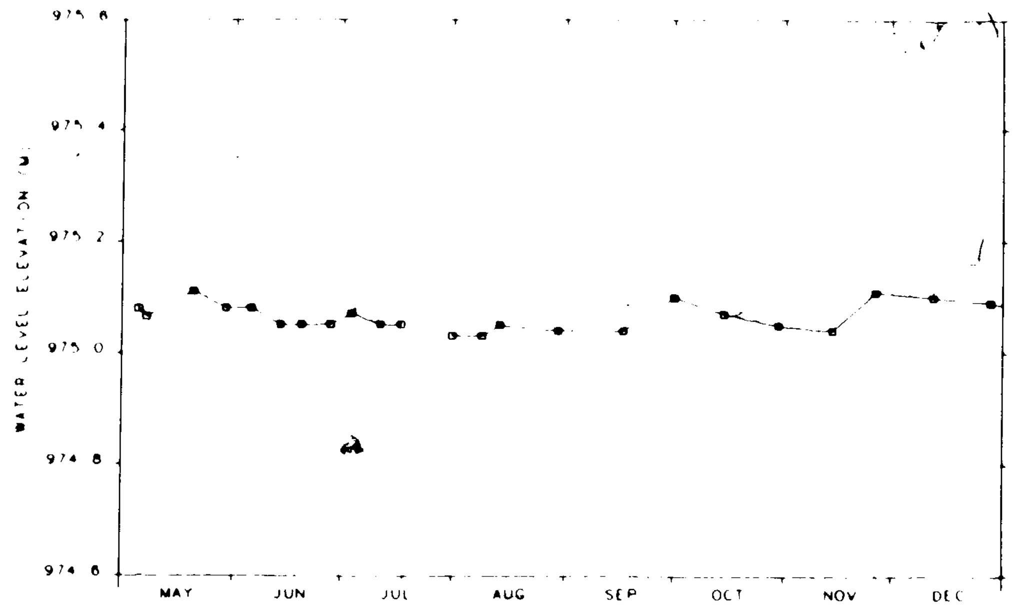

1986

C3 30

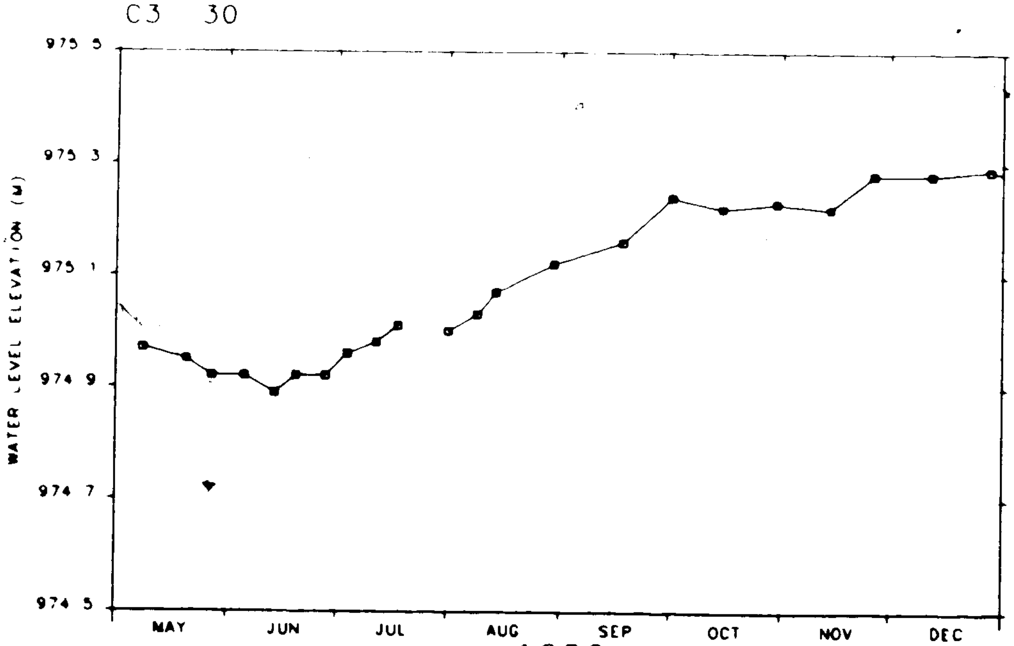

1986

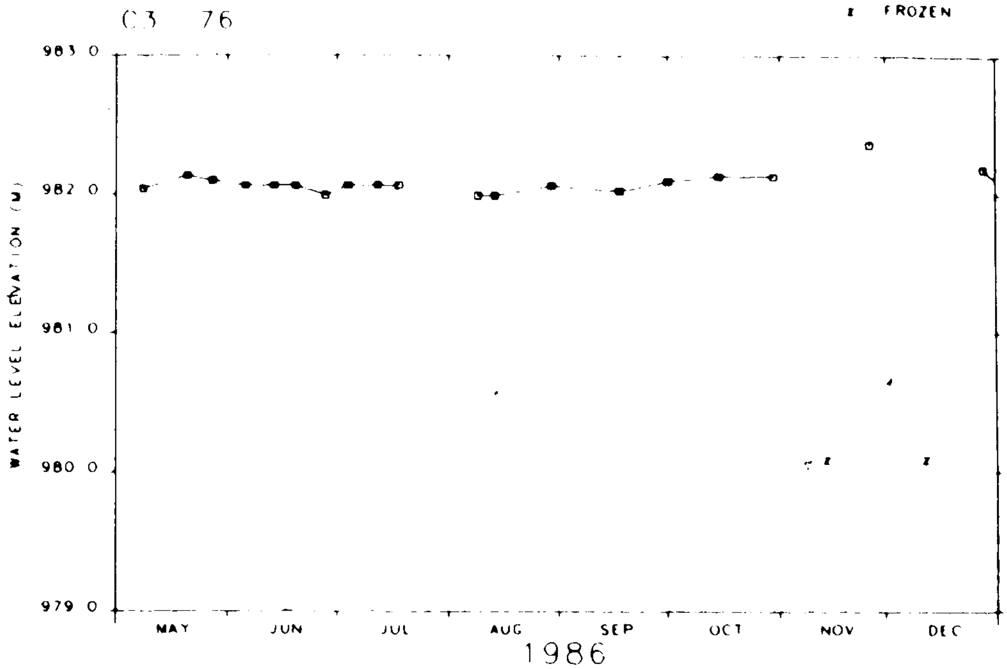
C3 76
FROZEN
983.0
982.0
981.0
980.0
979.0
WATER LEVEL ELEVATION (M)
MAY
JUN
JUL
AUG
SEP
OCT
NOV
DEC
1986

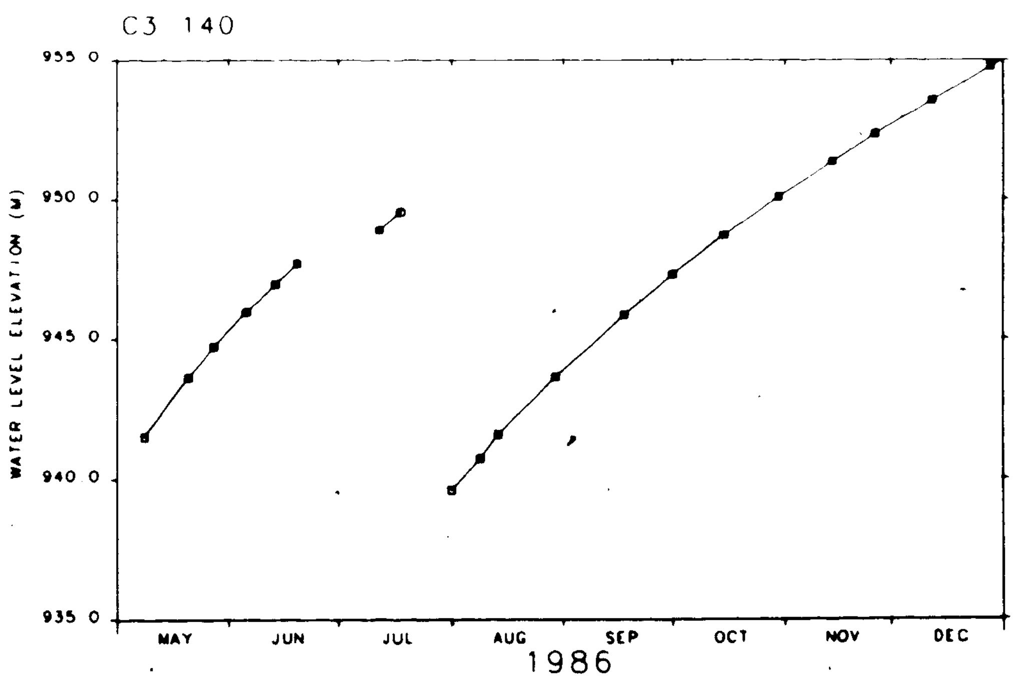
C3 140
955.0
950.0
945.0
940.0
935.0
WATER LEVEL ELEVATION (M)
MAY
JUN
JUL
AUG
SEP
OCT
NOV
DEC
1986

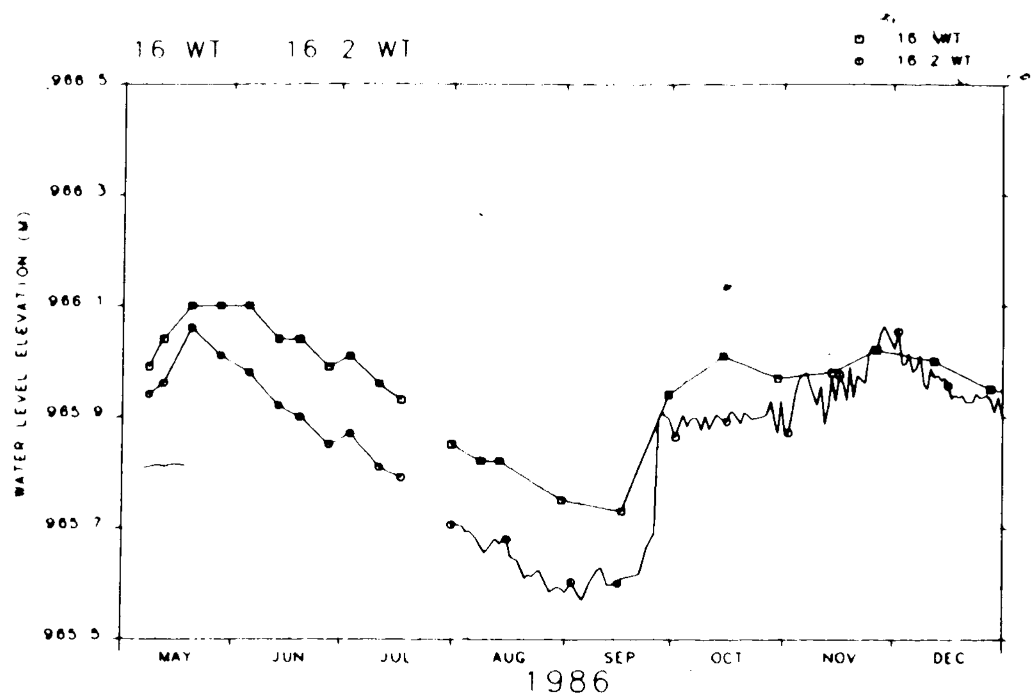
16 WT 16 2 WT
16 WT
16 2 WT
966.5
966.3
966.1
965.9
965.7
965.5
WATER LEVEL ELEVATION (M)
MAY
JUN
JUL
AUG
SEP
OCT
NOV
DEC
1986

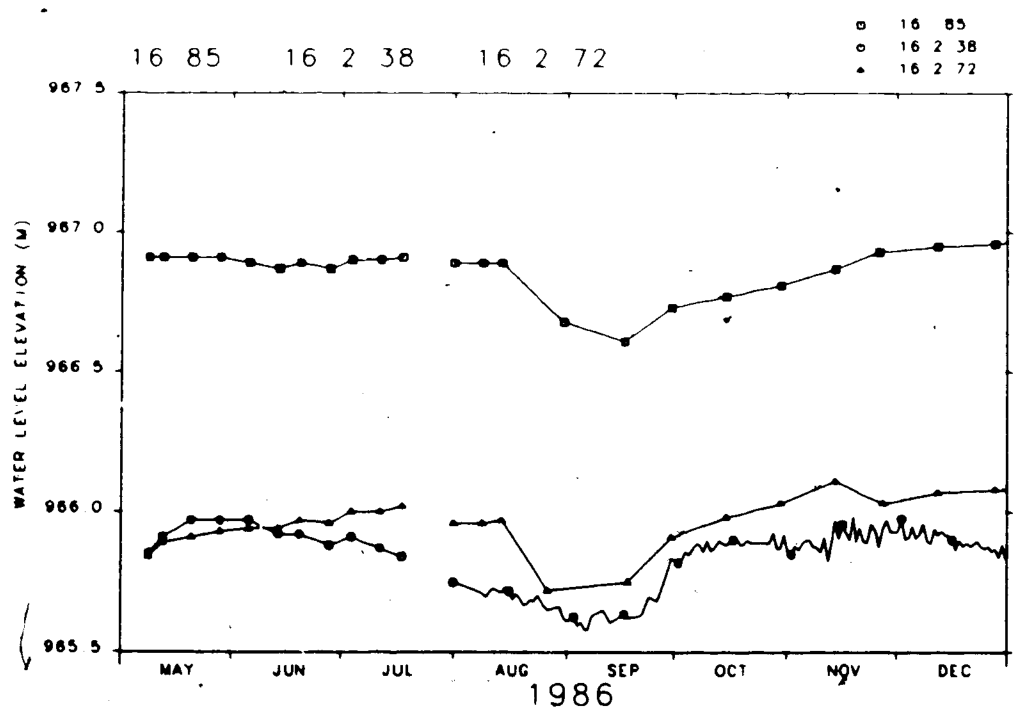
16 85 16 2 38 16 2 72
16 85
16 2 38
16 2 72
967.5
967.0
966.5
966.0
965.5
WATER LEVEL ELEVATION (M)
MAY
JUN
JUL
AUG
SEP
OCT
NOV
DEC
1986

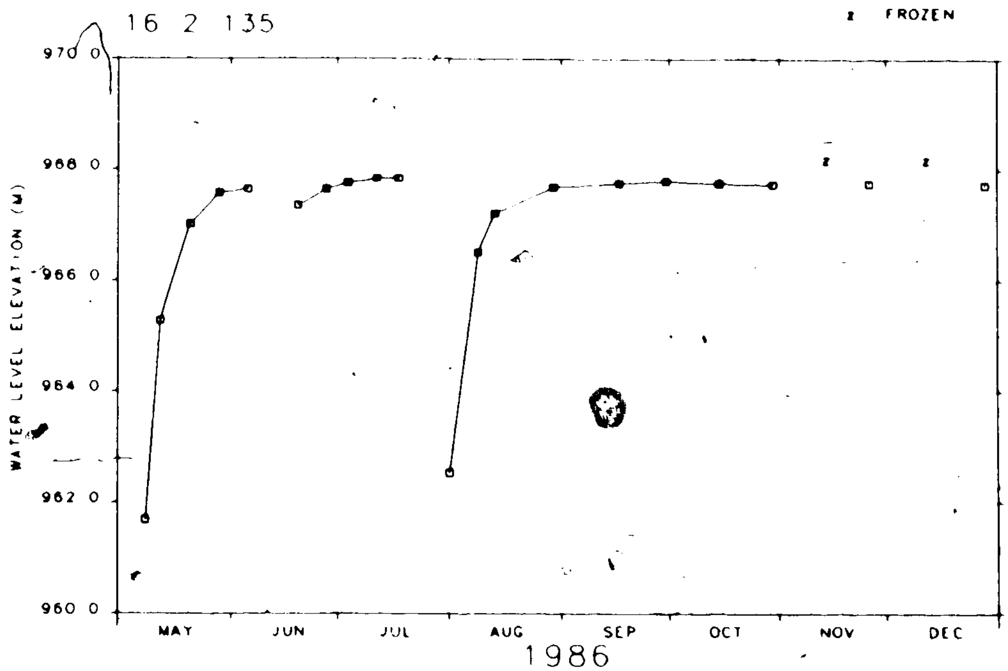
16 2 135
FROZEN
WATER LEVEL ELEVATION (M)
970.0
968.0
966.0
964.0
962.0
960.0
MAY
JUN
JUL
AUG
SEP
OCT
NOV
DEC
1986

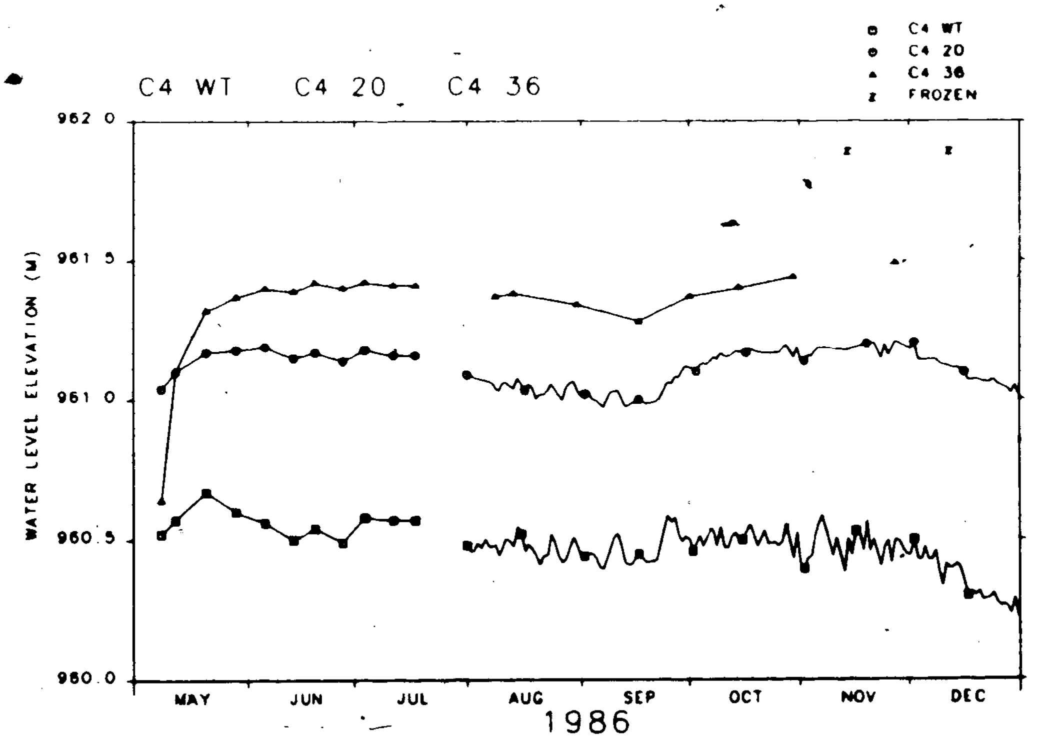
C4 WT C4 20 C4 36
C4 WT
C4 20
C4 36
FROZEN
WATER LEVEL ELEVATION (M)
962.0
961.5
961.0
960.5
960.0
MAY
JUN
JUL
AUG
SEP
OCT
NOV
DEC
1986

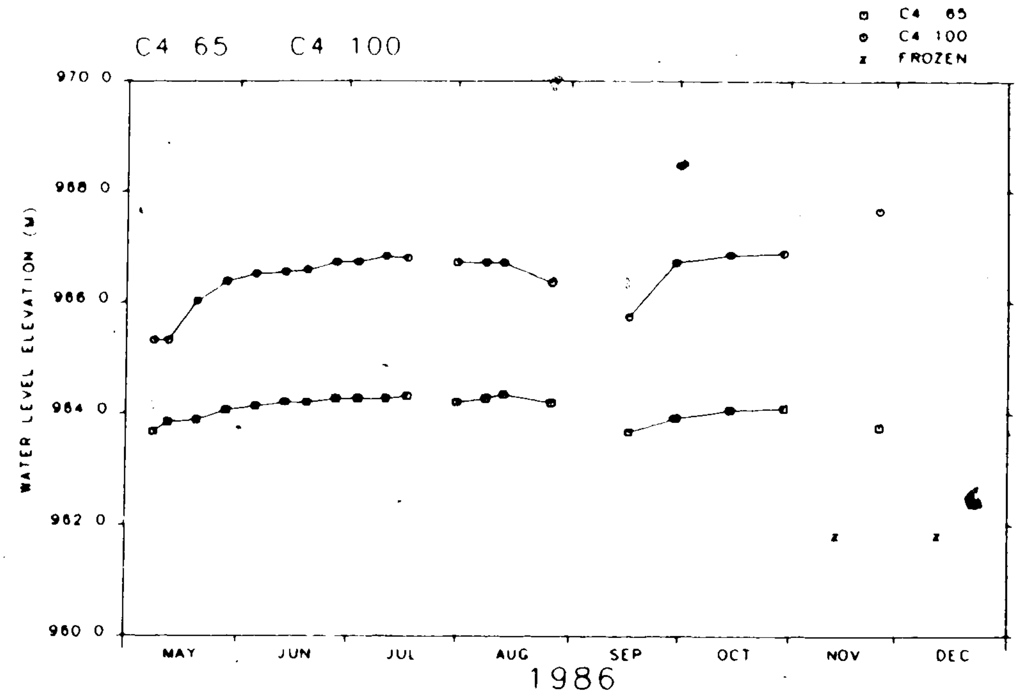
C4 65 C4 100
C4 65
C4 100
FROZEN
970.0
968.0
966.0
964.0
962.0
960.0
WATER LEVEL ELEVATION (M)
MAY
JUN
JUL
AUG
SEP
OCT
NOV
DEC
1986

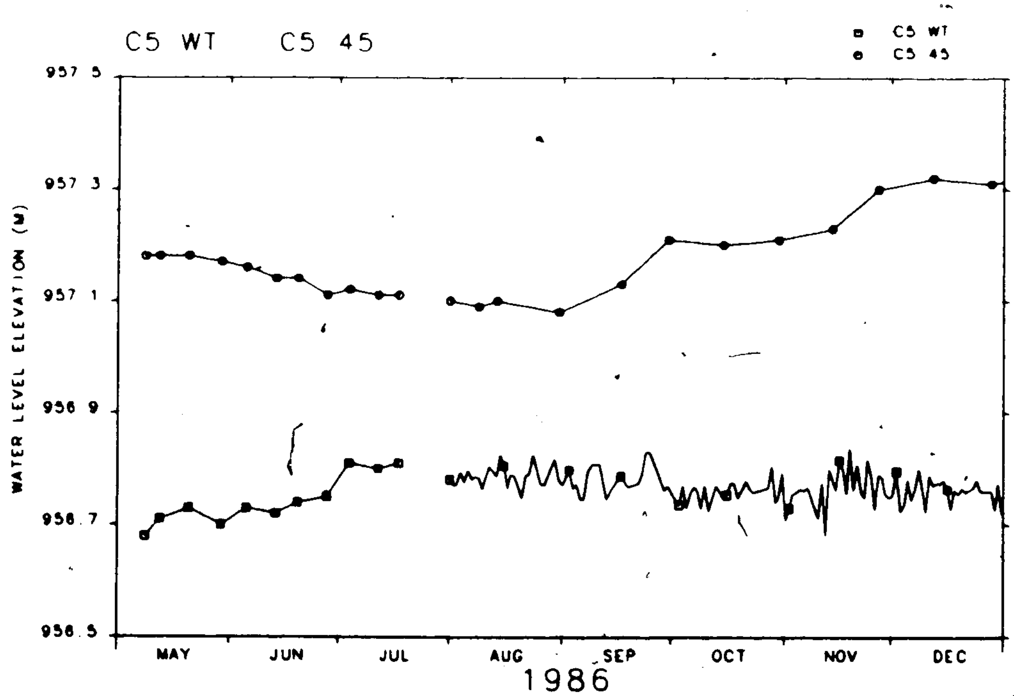
C5 WT C5 45
C5 WT
C5 45
957.5
957.3
957.1
956.9
956.7
956.5
WATER LEVEL ELEVATION (M)
MAY
JUN
JUL
AUG
SEP
OCT
NOV
DEC
1986

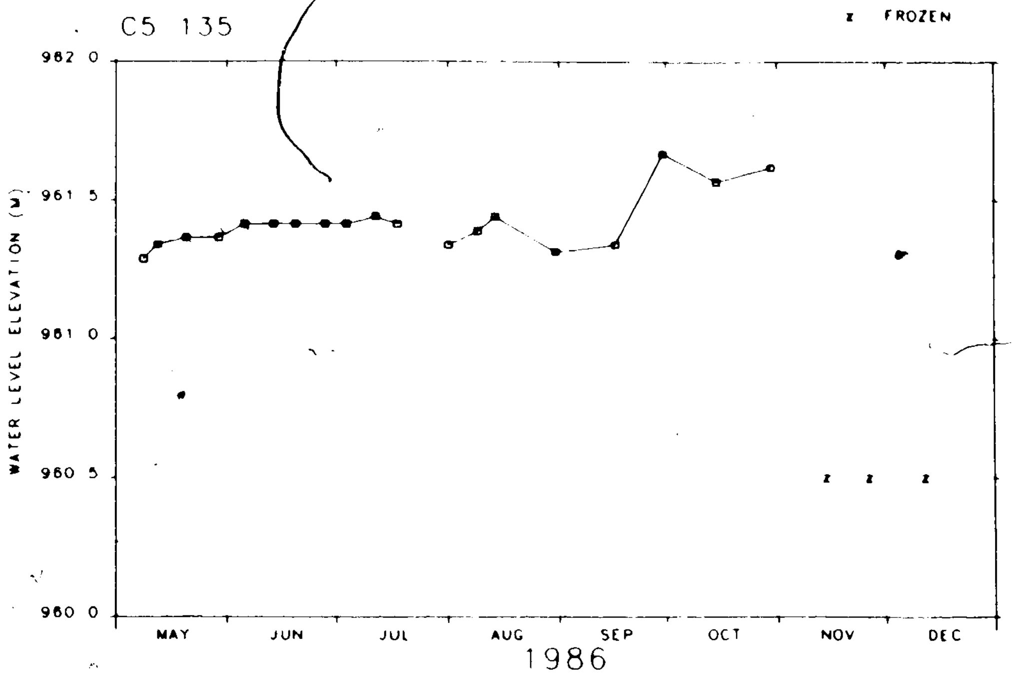
C5 135
FROZEN
WATER LEVEL ELEVATION (M)
962.0
961.5
961.0
960.5
960.0
MAY
JUN
JUL
AUG
SEP
OCT
NOV
DEC
1986

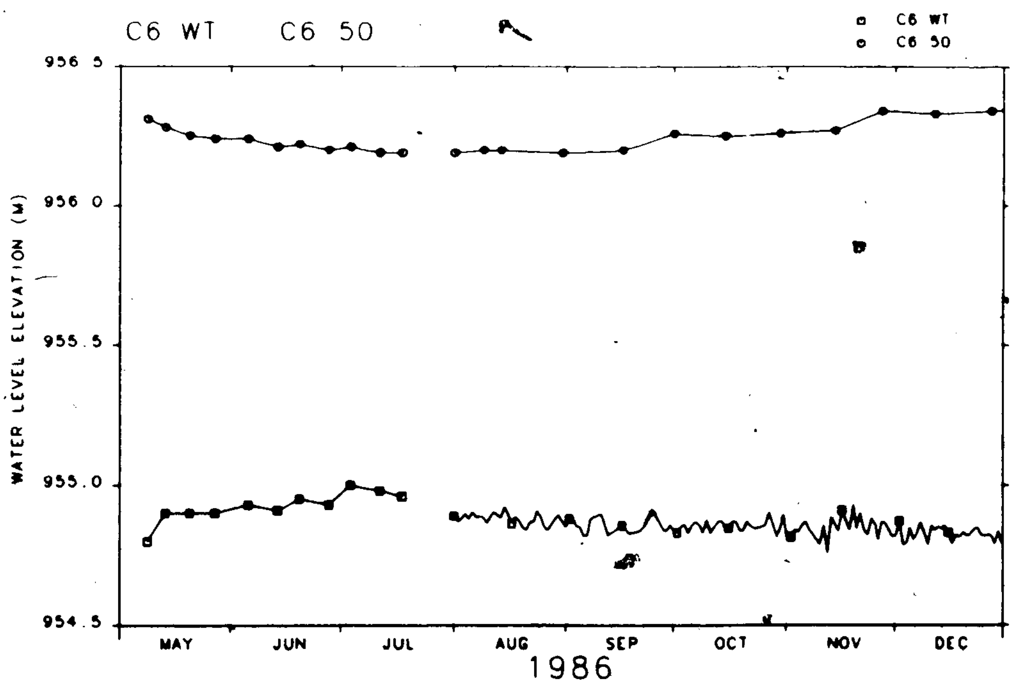
C6 WT C6 50
C6 WT
C6 50
WATER LEVEL ELEVATION (M)
956.5
956.0
955.5
955.0
954.5
MAY
JUN
JUL
AUG
SEP
OCT
NOV
DEC
1986

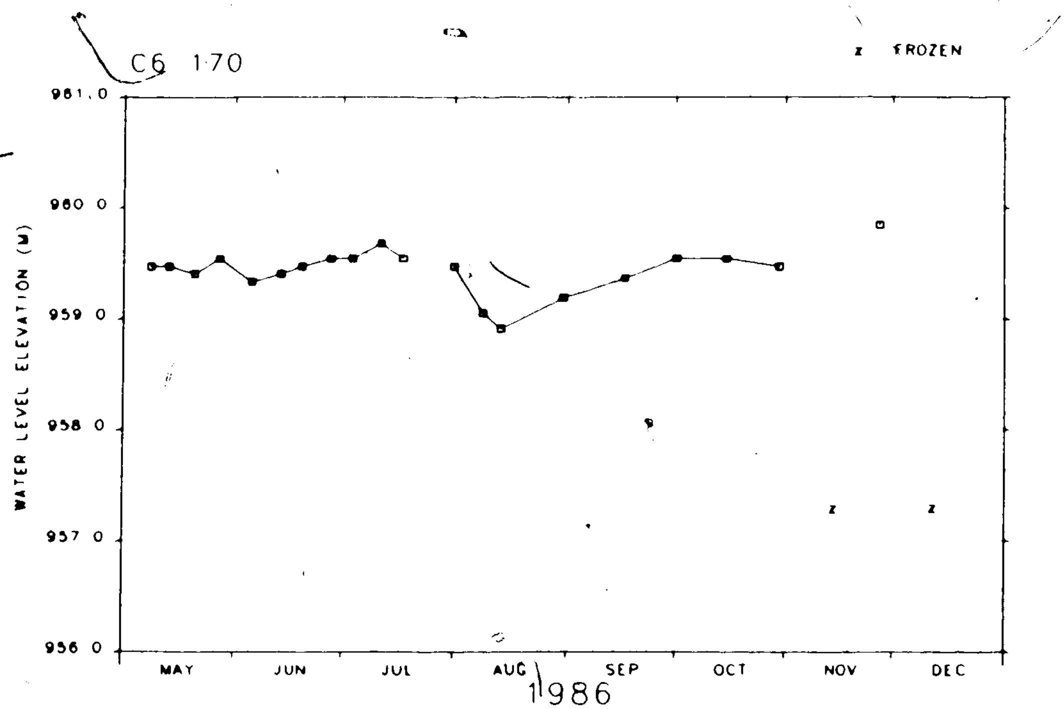
C6 170
z FROZEN
981.0
980.0
959.0
958.0
957.0
956.0
WATER LEVEL ELEVATION (M)
MAY
JUN
JUL
AUG
SEP
OCT
NOV
DEC
1986

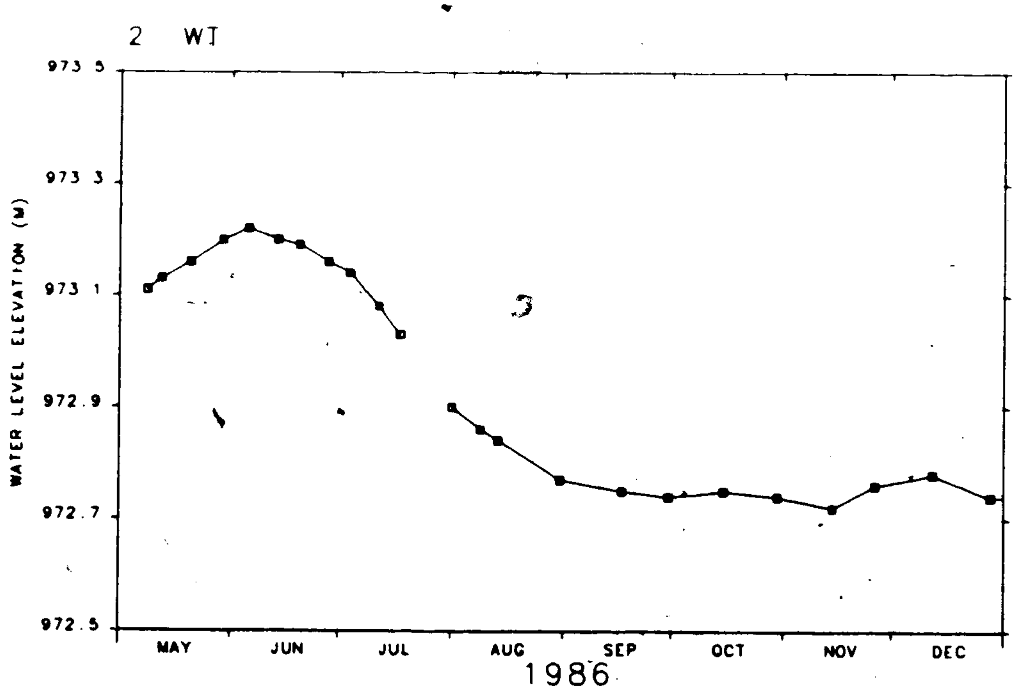
2 WT
973.5
973.3
973.1
972.9
972.7
972.5
WATER LEVEL ELEVATION (M)
MAY
JUN
JUL
AUG
SEP
OCT
NOV
DEC
1986

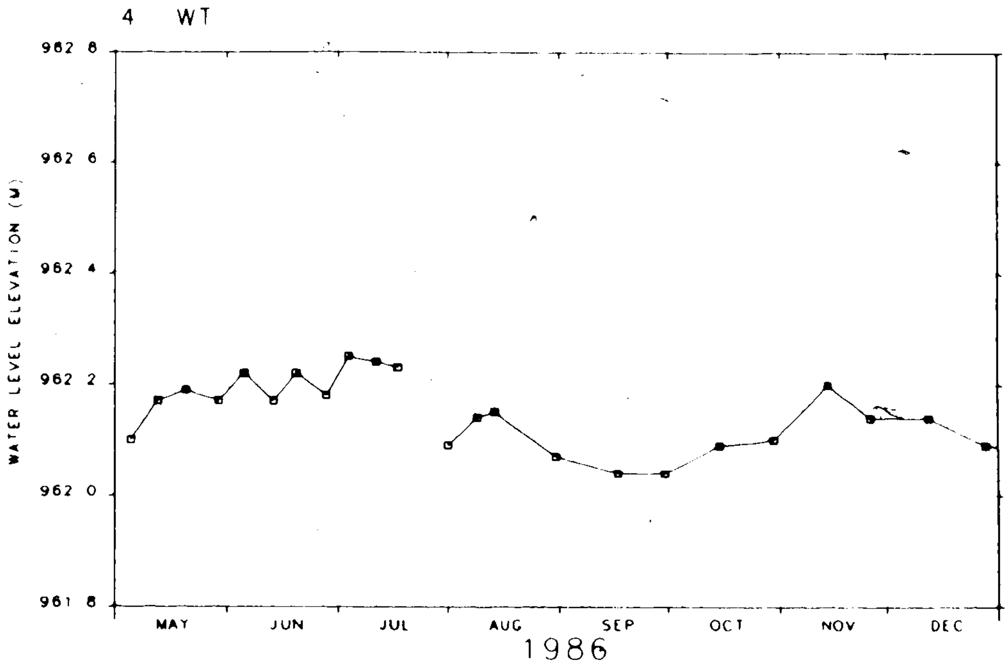
4 WT
962.8
962.6
962.4
962.2
962.0
961.8
WATER LEVEL ELEVATION (M)
MAY
JUN
JUL
AUG
SEP
OCT
NOV
DEC
1986

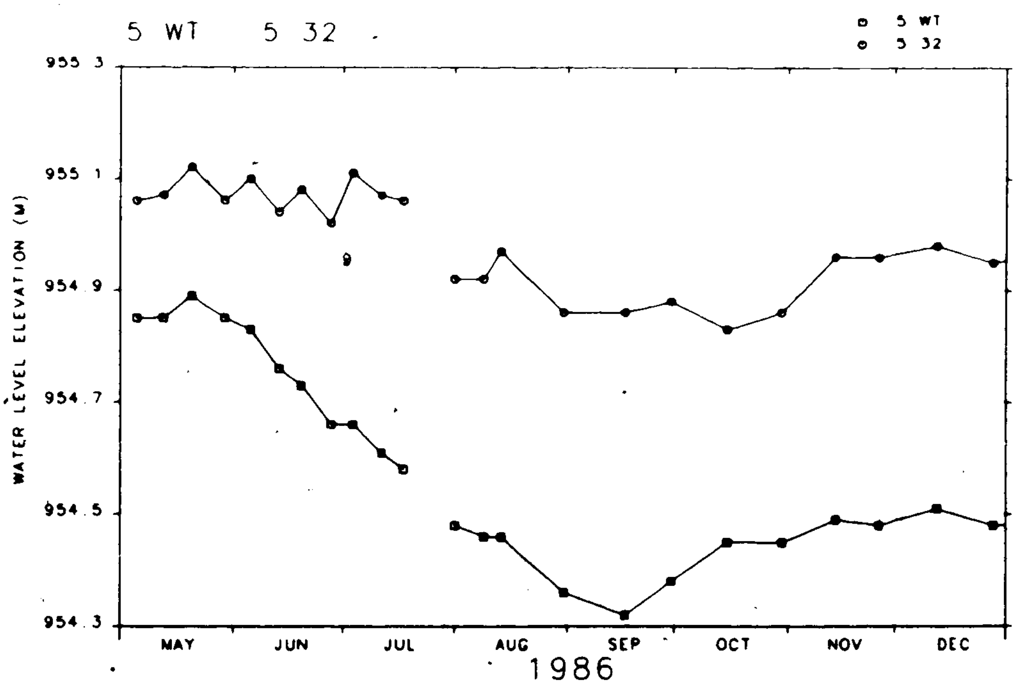
5 WT 5 32
5 WT
5 32
955.3
955.1
954.9
954.7
954.5
954.3
WATER LEVEL ELEVATION (M)
MAY
JUN
JUL
AUG
SEP
OCT
NOV
DEC
1986

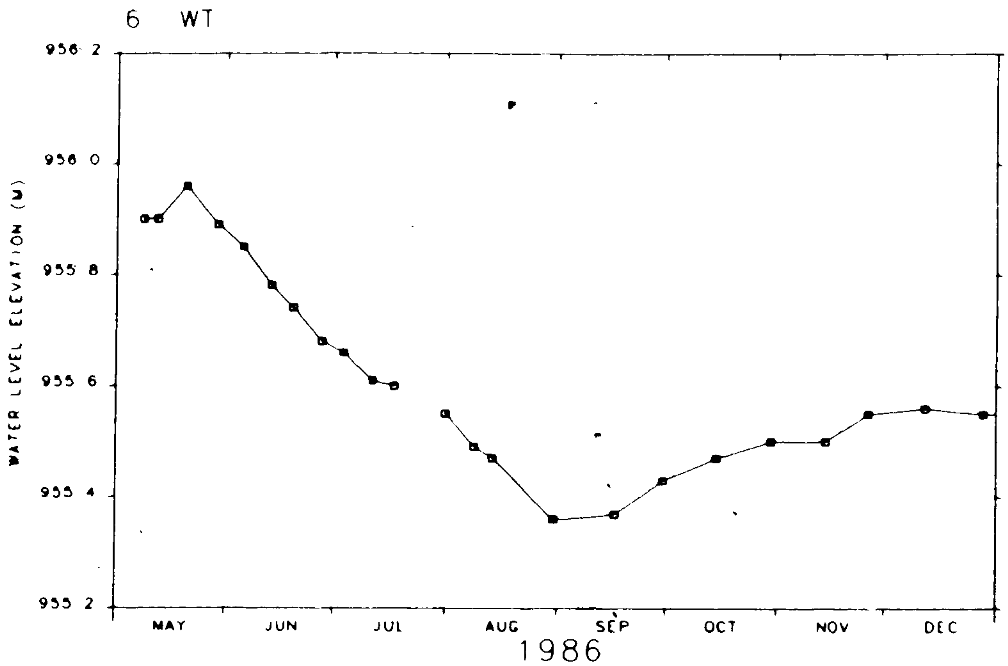
6 WT
956.2
956.0
955.8
955.6
955.4
955.2
WATER LEVEL ELEVATION (M)
MAY
JUN
JUL
AUG
SEP
OCT
NOV
DEC
1986

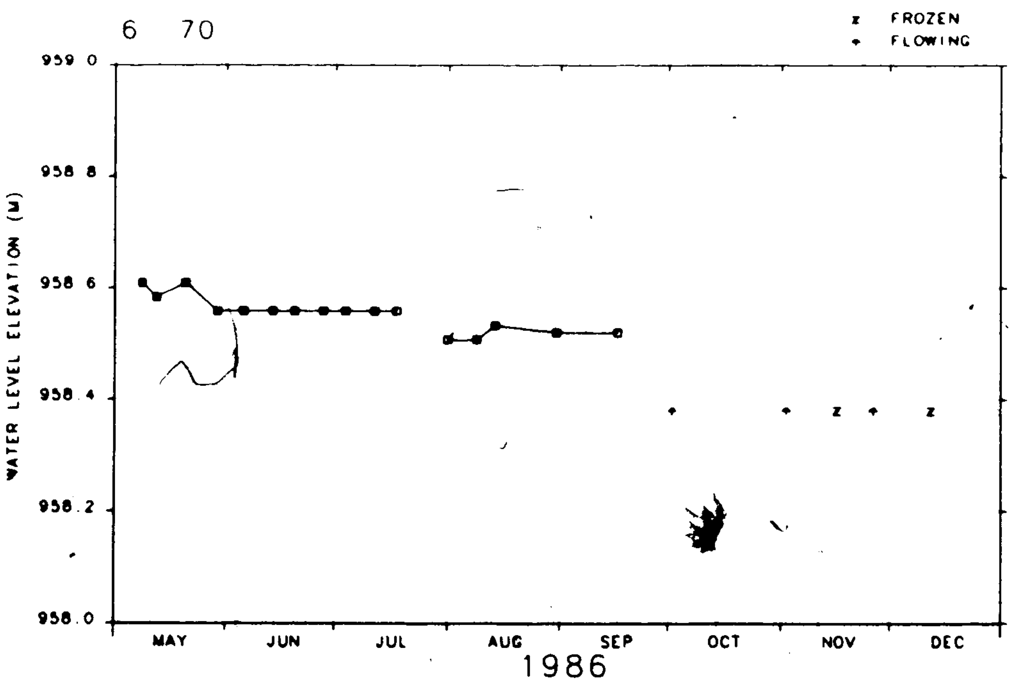
6 70
z FROZEN
+ FLOWING
959.0
958.8
958.6
958.4
958.2
958.0
WATER LEVEL ELEVATION (M)
MAY
JUN
JUL
AUG
SEP
OCT
NOV
DEC
1986

7 WT

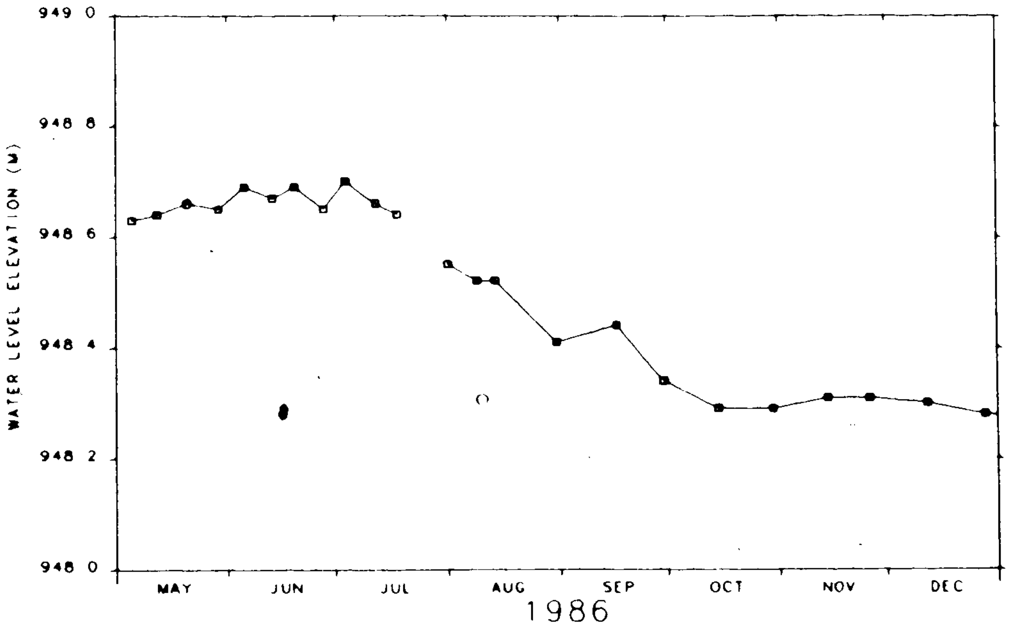
949.0
948.8
948.6
948.4
948.2
948.0
WATER LEVEL ELEVATION (M)
MAY
JUN
JUL
AUG
SEP
OCT
NOV
DEC
1986

8 WT

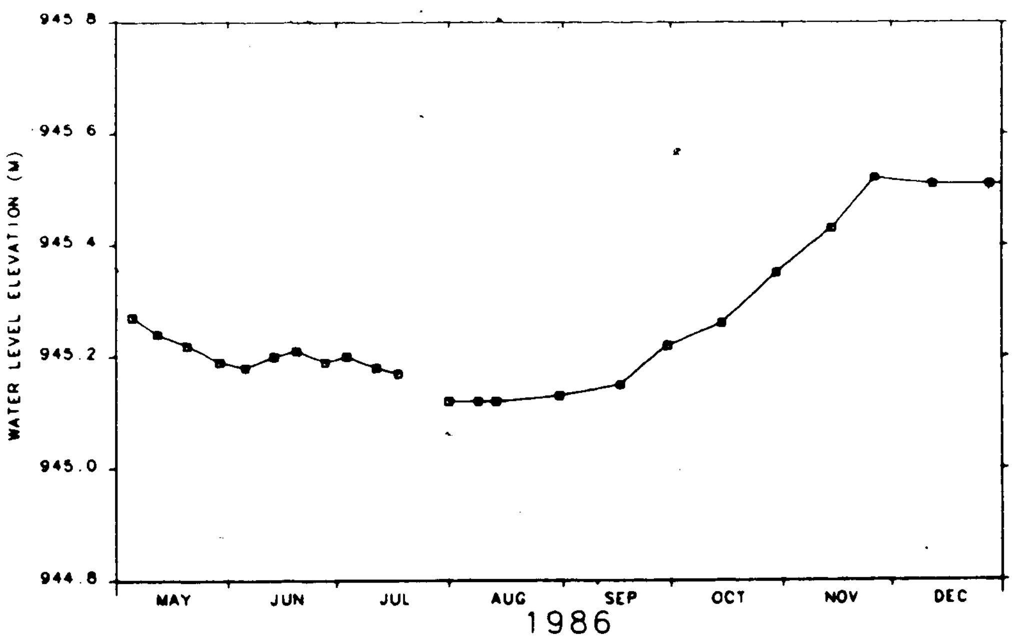
945.8
945.6
945.4
945.2
945.0
944.8
WATER LEVEL ELEVATION (M)
MAY
JUN
JUL
AUG
SEP
OCT
NOV
DEC
1986

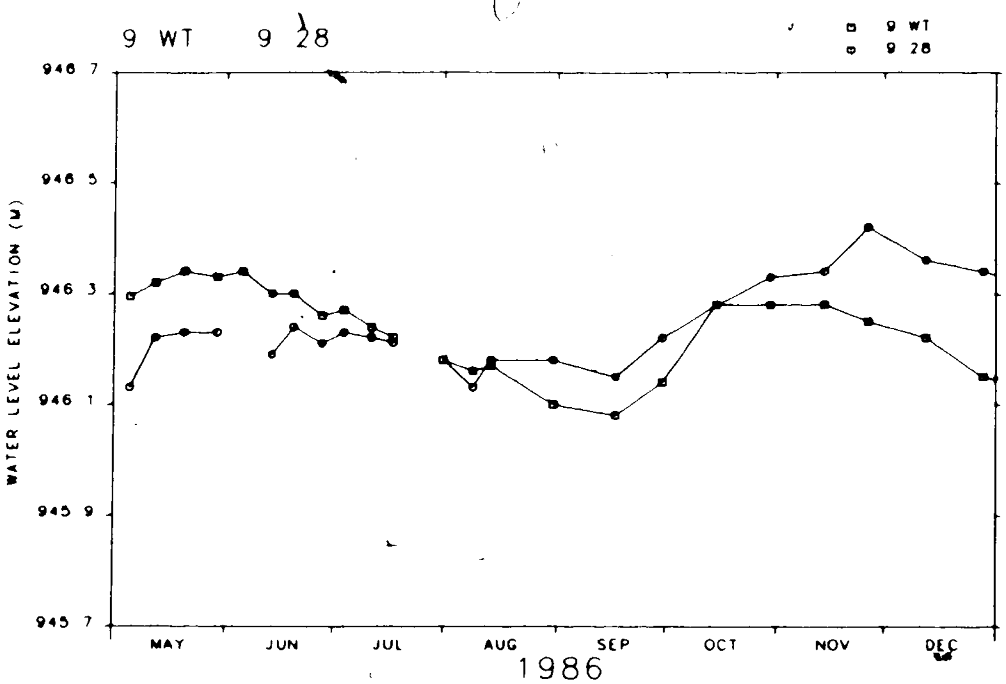
9 WT 9 28
9 WT
9 28
946.7
946.5
946.3
946.1
945.9
945.7
WATER LEVEL ELEVATION (M)
MAY
JUN
JUL
AUG
SEP
OCT
NOV
DEC
1986

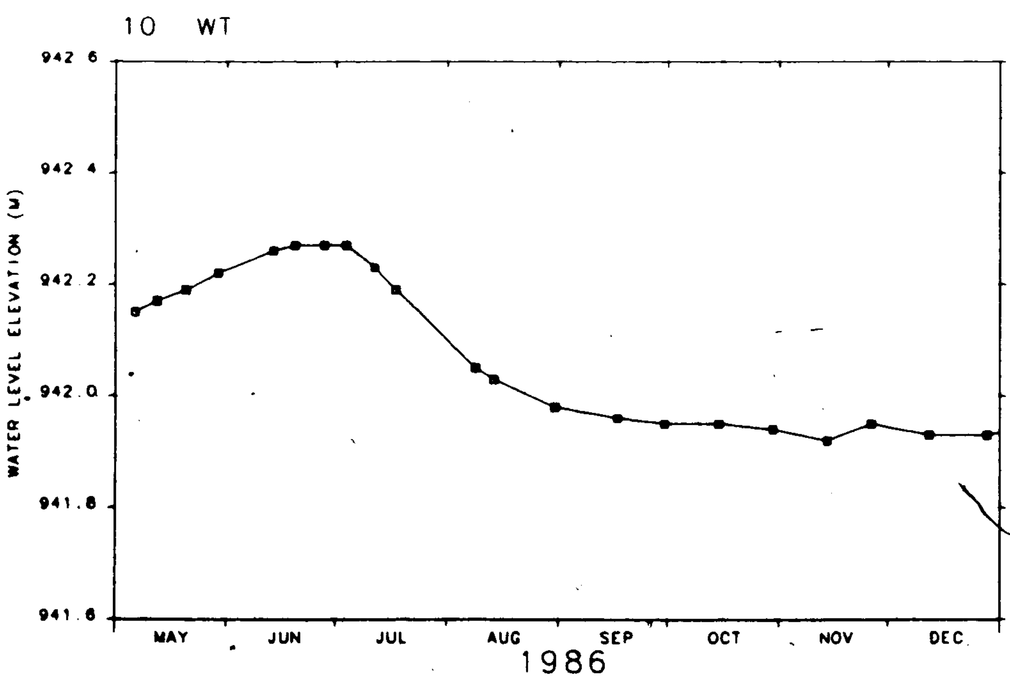
10 WT
942.6
942.4
942.2
942.0
941.8
941.6
WATER LEVEL ELEVATION (M)
MAY
JUN
JUL
AUG
SEP
OCT
NOV
DEC
1986

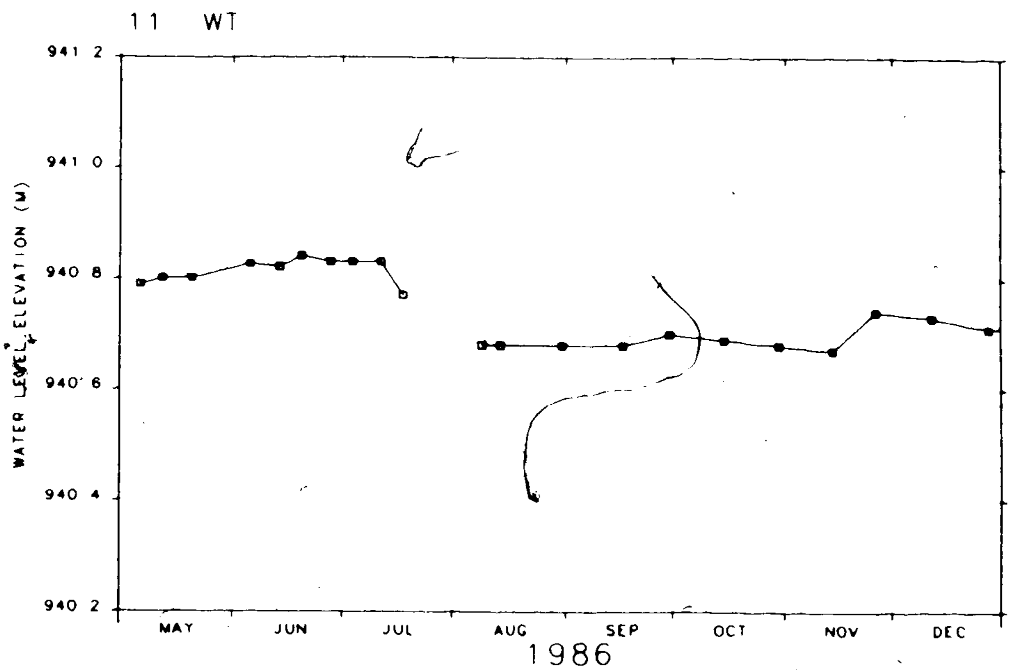
11 WT
941.2
941.0
940.8
940.6
940.4
940.2
WATER LEVEL ELEVATION (M)
MAY
JUN
JUL
AUG
SEP
OCT
NOV
DEC
1986

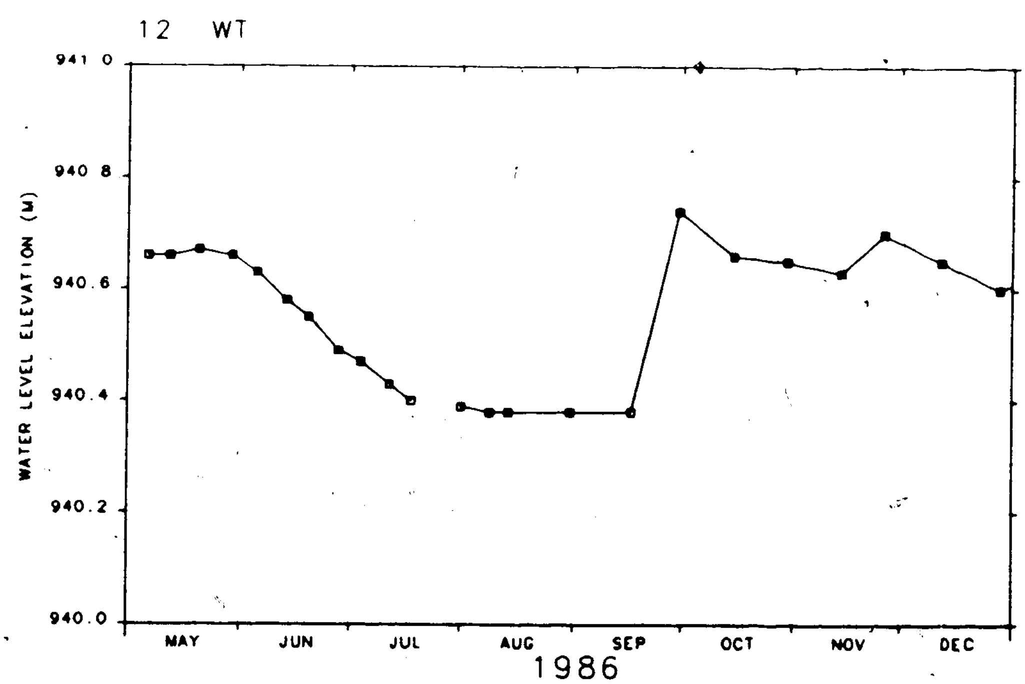
12 WT
941.0
940.8
940.6
940.4
940.2
940.0
WATER LEVEL ELEVATION (M)
MAY
JUN
JUL
AUG
SEP
OCT
NOV
DEC
1986

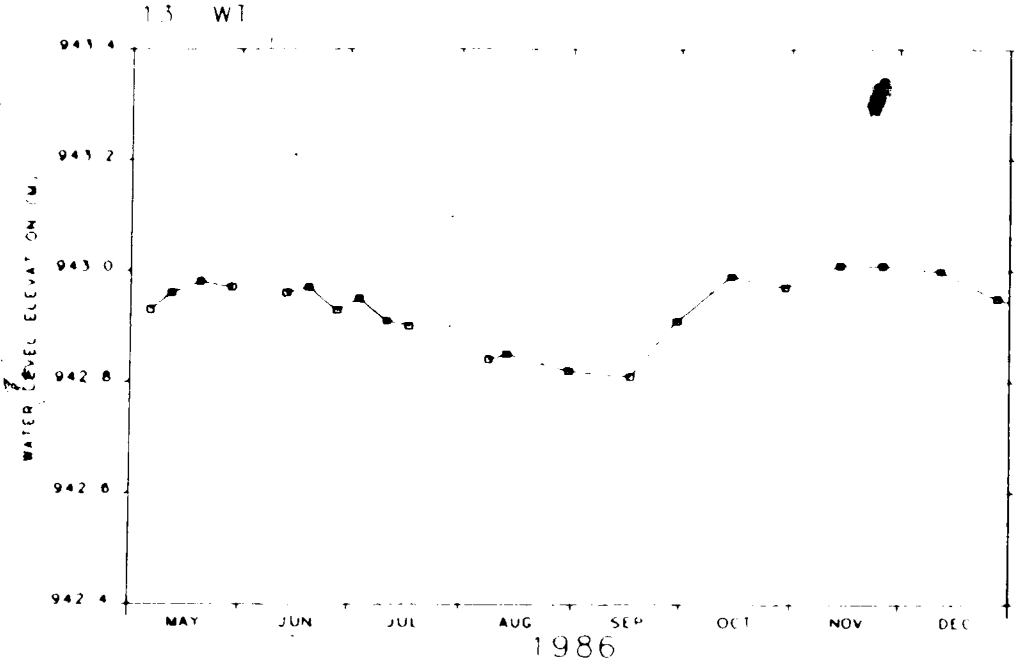
13 WT
943.4
943.2
943.0
942.8
942.6
942.4
WATER LEVEL ELEVATION (M)
MAY
JUN
JUL
AUG
SEP
OCT
NOV
DEC
1986

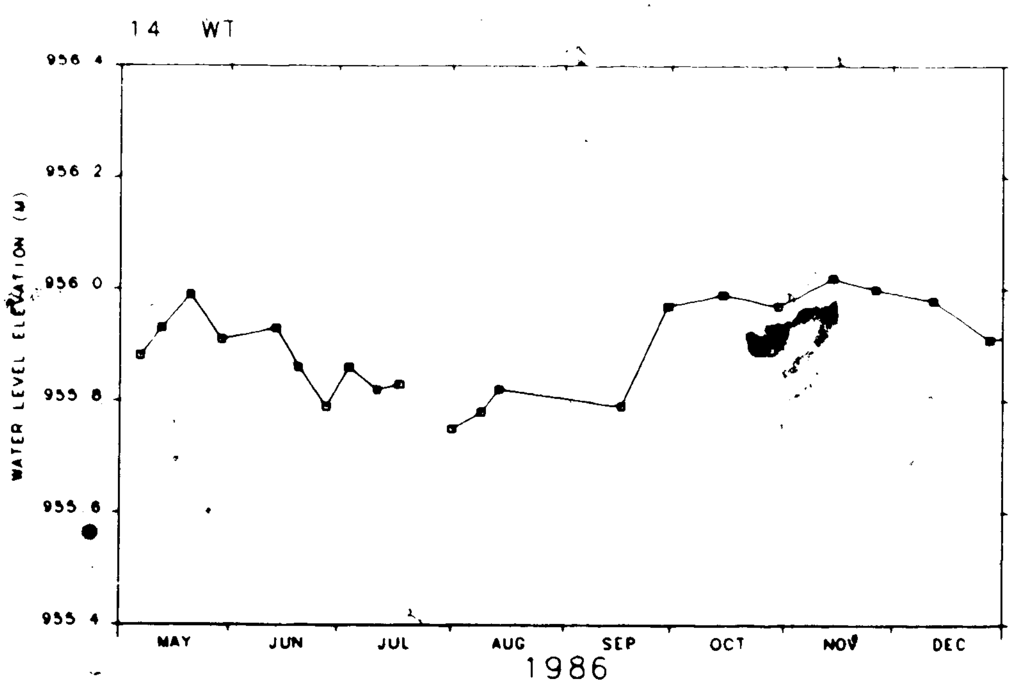
14 WT
956.4
956.2
956.0
955.8
955.6
955.4
WATER LEVEL ELEVATION (M)
MAY
JUN
JUL
AUG
SEP
OCT
NOV
DEC
1986

15 WT, 15 24

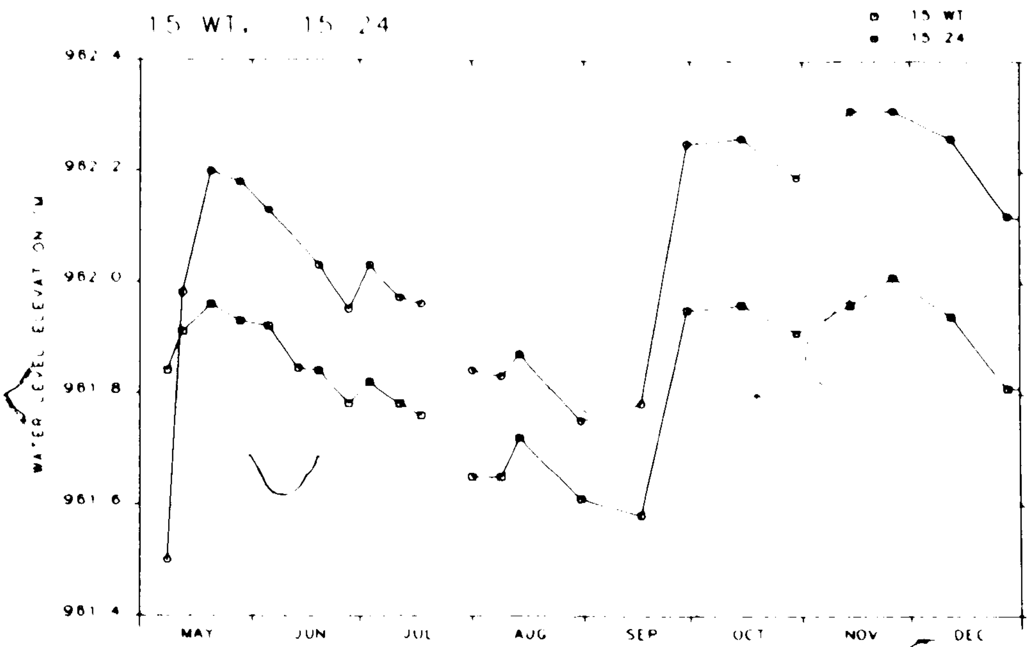

1986

17 WT

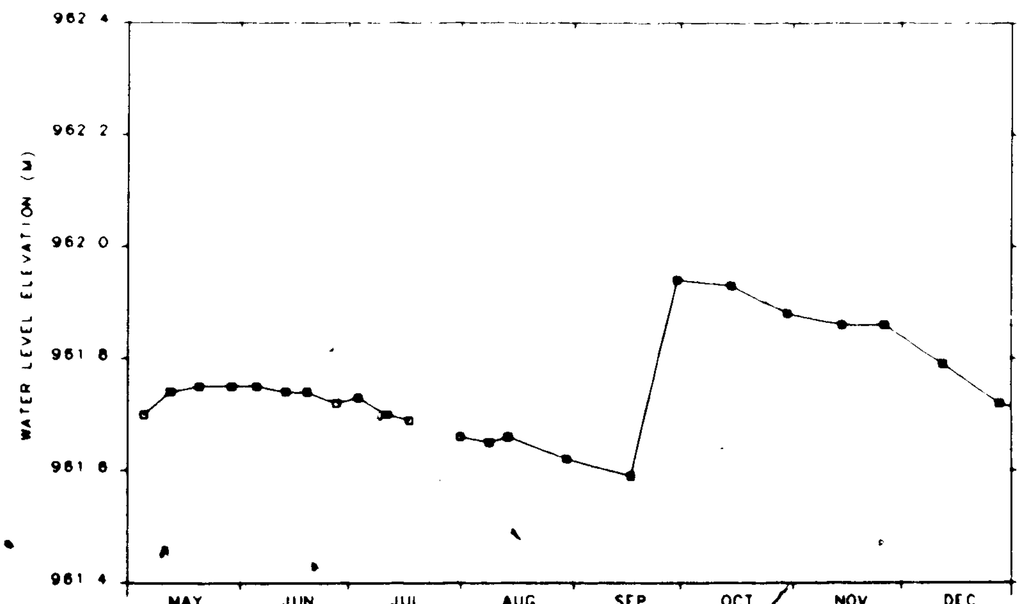

1986

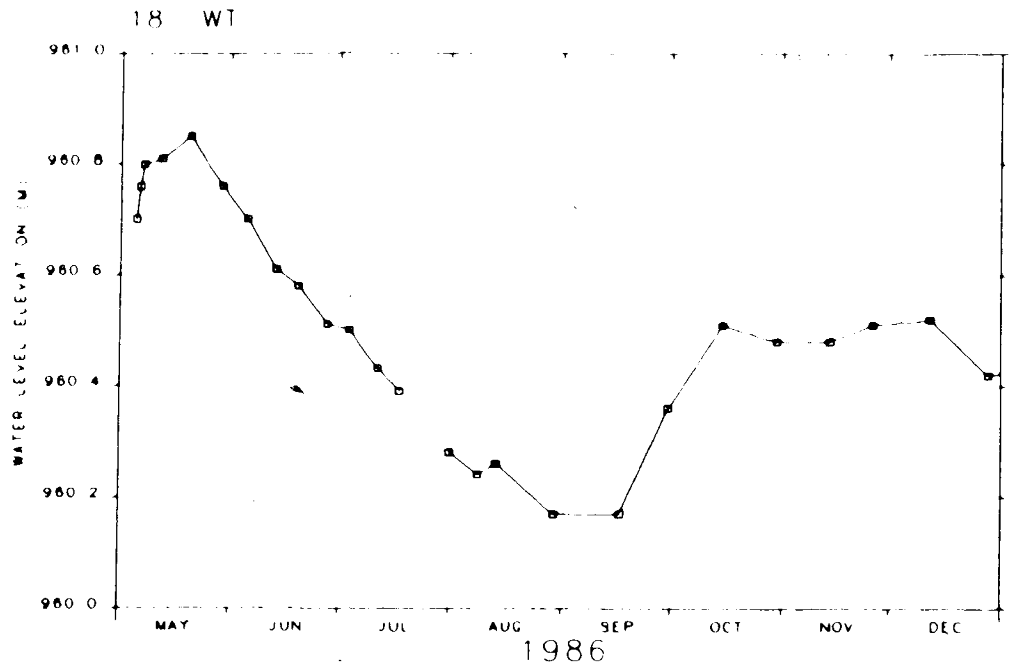
18 WT
WATER LEVEL ELEVATION (M)
961.0
960.8
960.6
960.4
960.2
960.0
MAY
JUN
JUL
AUG
SEP
OCT
NOV
DEC
1986

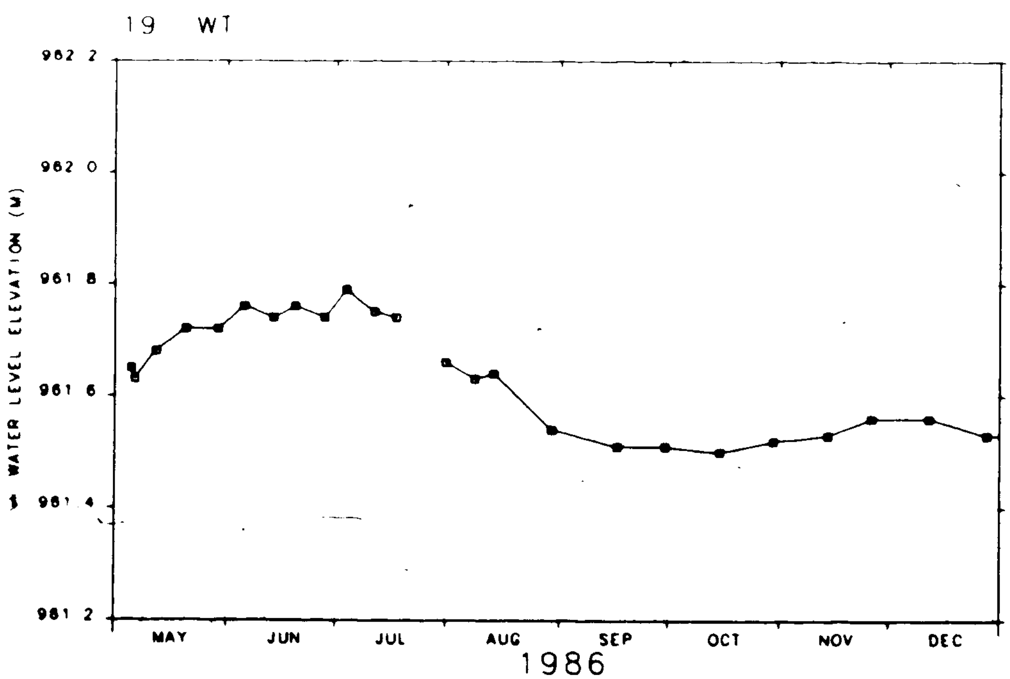
19 WT
WATER LEVEL ELEVATION (M)
962.2
962.0
961.8
961.6
961.4
961.2
MAY
JUN
JUL
AUG
SEP
OCT
NOV
DEC
1986

APPENDIX 7

Hydrochemical Determinations

SAMPLE		DEPTH m	FIELD pH	FIELD COND	LAB pH	LAB COND	Ca mg/L	Mg mg/L	Na mg/L	K mg/L	HCO3 mg/L	SO4 mg/L	Cl mg/L
A1	WT	5.5	7.1	4000			530.0	235.0	291	23.2	394	2250	71.0
	34	.4	6.7	2400			184.0	157.0	108	12.7	406	1000	33.0
	55	6.8	6.8	2200			111.0	131.0	138	8.4	330	850	24.0
	87	6.5	8.4	1500			4.4	2.1	425	2.3	889	66	3.6
	130	9.6	8.6	1800			4.6	1.4	530	2.1	1144	50	3.7
	297	60.0	8.4	1800			1.6	1.5	510	2.0	1144	14	4.4
	295	89.9	7.9	4000			27.4	8.4	1090	5.2	686	150	1330.0
A2	33	10.1	7.1	4500			334.0	207.0	1610	16.4	549	4100	65.0
	92	28.0	7.8	2700			23.2	15.1	1090	5.3	1042	1425	20.0
	107	32.6	8.7	800			6.2	2.8	515	2.4	610	560	12.0
	232	70.7	8.3	2000			3.8	1.6	500	2.5	1093	27	25.5
A3	WT	5.5	7.2	11000			244.0	344.0	3410	17.0	824	7950	65.0
	33	10.1	7.0	7000			124.0	210.0	2460	15.6	956	5500	59.0
	98	29.9	7.7	5000			27.6	13.7	1610	5.5	1179	2360	29.5
	233	71.0	8.2	1900			4.8	3.3	690	3.1	1195	34	212.0
A4	WT	4.6	7.2	10000			428.0	750.0	6500	6.7	686	16800	81.0
	50	15.2	7.1	7000			235.0	155.0	1700	16.2	585	4500	38.0
	64	19.5	7.0	6200			422.0	112.0	1510	17.7	610	4300	30.0
	90	27.4	7.1	7000			94.0	76.0	2000	8.0	712	4160	39.0
A5	WT	5.5	7.2	5500			416.0	252.0	1060	12.7	686	3800	75.0
	61	18.6	6.9	3500			189.0	95.0	620	8.3	422	1800	13.5
	90	27.4	7.1	2600			128.0	57.0	510	7.5	361	1270	11.5
	297	90.5	7.5	2000			5.7	11.5	510	3.4	1068	187	30.0
	343	104.5	8.1	2800			3.6	1.4	850	2.7	1525	11	380.0
B1	34	10.4	7.0	7000			438.0	256.0	1350	20.8	585	4300	170.0
	65	19.8	7.6	3500			27.0	31.6	880	6.9	737	1300	21.0
	176	53.6	8.3	1900			7.4	2.9	570	3.2	1159	120	40.0
B2	34	10.4	7.4	22000			280.0	308.0	6600	32.2	1322	14000	150.0
	50	15.2	7.1	14000			181.0	56.0	4500	14.0	1485	8050	90.0
	105	32.0	8.2	2000			8.2	2.7	530	2.4	1119	165	18.0
B3	WT	5.5	7.2	1850			106.0	83.0	260	3.2	369	850	12.5
	60	18.3	6.8	4200			460.0	190.0	500	14.0	585	2400	17.5
	70	51.8	7.5	4600			48.2	14.6	1150	6.4	925	1650	14.5
	198	60.3	8.2	2600			11.8	3.1	660	2.2	1220	180	41.0
	268	81.7	7.5	12000			83.0	17.4	2810	8.7	508	15	3850.0

SAMPLE		Si mg/L	F mg/L	TIC mg/L	TOC mg/L	NO3 mg/L	FIELD ALK mg/L	FIELD Fe mg/L	DO mg/L	TDS mg/L	Log SI gypsum	Ca/Mg molar
A1	WT	18.2		77.5	21.0	.2	375			3811	.27	1.37
	34	3.7		80.0	9.1	.1	624			1905	-.30	.71
	55	11.2		65.0	6.7	.1	570			1604	-.54	.51
	87	7.3		175.0	8.0	.1	831			1400	-2.78	1.27
	130	6.6		225.0	11.5	.1	1025			1742	-2.95	1.99
	197	8.5		225.0	10.8	.1	1018			1685	-3.83	.61
	295	8.7		135.0	15.6	.3	627			3306	-1.87	1.95
A2	33	9.3		108.0	25.8	30.5	665			6921	.18	.98
	92	6.2		205.0	16.5	1.3	971			3628	-1.12	.93
	107	6.3		120.0	23.8	.3	560			1715	-1.88	1.21
	232	7.9		215.0	17.0	.1	971			1561	-3.23	1.52
A3	WT	12.2		162.0	33.5	50.0	891			12915	.12	.43
	33	10.4		188.0	27.2	.9	920			9335	-.21	.36
	98	7.7		232.0	10.5	.2	1063			5233	-.96	1.21
	233	8.2		235.0	24.4	.1	1123			2150	-3.10	.92
A4	WT	9.9		135.0	50.0	1.9	671			25263	.43	.35
	50	15.9		115.0	10.5	.0	681			7244	.05	.92
	64	13.0		120.0	10.8	.0	690			7014	.30	2.29
	90	13.0		140.0	12.5	.1	757			7101	-.36	.75
A5	WT	13.4		135.0	24.0	.5	624			6315	.26	1.00
	61	12.0		83.0	7.5	.1	379			3159	-.16	1.21
	90	9.7		71.0	7.7	.1	388			2354	-.37	1.36
	297	10.1		210.0	9.8	.0	955			1825	-2.27	.30
	343	7.6		300.0	17.2	.0	1460			2781	-3.74	2.43
B1	34	9.6		115.0	21.0	.3	541			7129	.30	1.04
	65	9.7		145.0	13.0	.1	716			3013	-1.06	.51
	176	8.6		228.0	22.0	.2	1034			1911	-2.40	1.42
B2	34	12.7		260.0	154.0	.3	1219			22705	.23	.55
	50	11.5		292.0	28.0	.1	1327			14387	-.01	1.96
	105	6.3		220.0	20.3	.2	888			1851	-2.21	1.62
B3	WT	14.1		72.5	7.5	.2	350			1697	-.55	.77
	60	12.8		115.0	8.0	1.7	535			4180	.23	1.47
	170	10.6		182.0	9.6	.1	897			3819	-.78	1.94
	198	7.3		240.0	13.0	.1	1193			2125	-2.03	2.43
	268	8.3		100.0	17.0	.0	509			7300	-2.61	2.96

SAMPLE	DEPTH m	FIELD pH	FIELD COND	LAB pH	LAB COND	Ca mg/L	Mg mg/L	Na mg/L	K mg/L	HCO3 mg/L	SO4 mg/L	Cl mg/L
B4 WT	5.5	7.1	13000			403.0	2080.0	8000	25.7	824	24700	210.0
29	8.8	7.1	11000			404.0	860.0	5700	27.9	1119	15200	140.0
73	22.2	7.0	7000			363.0	200.0	1580	17.5	1078	4150	100.0
B5 WT	4.6	6.7	2200			250.0	164.0	40	2.4	249	1010	46.0
40	12.2	6.8	3500			408.0	266.0	160	12.5	569	2100	7.0
83	25.3	6.9	2900			156.0	112.0	400	16.5	496	1225	18.0
118	36.0	7.3	6000			73.0	26.5	1385	6.5	889	2290	33.0
194	59.1	8.1	3400			4.0	.8	820	3.1	1093	15	580.0
228	69.5	7.7	4800			11.1	2.7	1130	3.3	966	20	1100.0
265	82.3	7.6	5000			40.0	13.5	1580	7.5	599	110	2025.0
B6 50	15.2	6.9	750			87.0	23.2	58	3.1	277	172	21.0
80	24.4	6.9	1100			78.0	19.9	139	4.7	376	220	6.2
130	39.6	7.6	1400			54.0	14.7	250	4.7	496	225	7.2
355	108.2	7.4	4000			34.3	31.9	825	5.8	1129	850	320.0
415	126.8	7.8	6200			16.7	5.1	1500	4.4	773	35	1750.0
C1 70	21.3	8.3	3150	8.0	5500	40.0	12.0	1435	5.8	1160	2070	40.0
230	70.1	8.4	1400	8.2	2050	5.4	2.4	577	2.6	1300	61	61.0
C2 40	12.2	7.4	7500	7.5	14600	377.0	232.0	3525	21.0	1870	7785	91.0
66	20.1	6.9	6500	7.5	11000	308.0	185.0	2600	13.0	1470	5610	62.0
125	38.1	8.5	1250	8.2	2000	6.7	3.9	532	2.7	1227	112	55.0
C3 30	9.1	7.5	1700	8.2	2700	49.0	15.0	621	6.8	761	861	12.0
76	23.2	7.8	4500	7.8	6300	30.0	7.4	1645	4.4	1230	2478	30.0
16 WT	7.6	7.0	7500	8.0	11200	403.0	333.0	2540	17.0	850	6645	69.0
85	25.9	8.1	2500	8.3	3650	11.0	4.0	934	4.0	968	1161	19.0
16 2 WT	3.7	7.1	8000	7.6	12900	376.0	400.0	2920	12.0	1090	7515	67.0
38	11.6	7.1	7500	7.5	11500	412.0	310.0	2485	14.0	974	6405	69.0
72	21.9	7.2	5500	7.8	9300	149.0	51.0	2415	10.0	1122	4605	45.0
135	41.1	8.2	1550	8.2	2620	1.8	3.1	676	4.6	1510	137	105.0
C4 WT	3.7	7.5	27000	7.6	41600	418.0	1765.0	14240	10.0	1530	35220	55.0
20	6.1	7.0	12000	7.4	18500	325.0	409.0	5110	11.0	1130	11775	130.0
36	11.0	7.2	8200	7.7	13100	328.0	176.0	3175	17.0	1020	7350	96.0
65	19.8	7.3	4800	7.6	8050	61.0	17.0	2085	6.2	1260	3540	41.0
100	30.5	7.3	4850	8.0	8000	67.0	20.0	2075	6.2	1390	3555	40.0

SAMPLE		Si mg/L	F mg/L	TIC mg/L	TOC mg/L	NO3 mg/L	FIELD ALK mg/L	FIELD Fe mg/L	DO mg/L	TDS mg/L	Log SI gypsum	Ca/Mg molar
B4	WT	12.2		162.0	70.0	1.2	824			36055	.45	.12
	29	12.0		220.0	40.0	.1	1088			23462	.39	.28
	73	17.0		212.0	17.4	.1	993			7505	.21	1.10
B5	WT	13.0		49.0	7.8	3.2	216			1777	-.18	.92
	40	16.7		112.0	7.8	.3	620			2539	.15	.93
	83	17.0		97.5	9.6	.1	554			2440	-.33	.84
	118	8.0		175.0	7.5	.1	853			4711	-.54	1.64
	194	7.5		215.0	13.0	.1	1009			2523	-3.59	2.43
	228	9.4		190.0	22.0	.1	875			3242	-3.10	2.22
	265	5.8		118.0	20.0	.2	576			4382	-1.91	1.73
B6	50	11.8		54.5	6.6	.4	248			653	-1.06	2.29
	80	11.2		74.0	5.6	1.0	334			856	-1.03	2.37
	130	10.7		97.5	8.0	.2	490			1062	-1.19	2.18
	355	10.5		222.0	10.5	.2	1142			3206	-1.10	.64
	415	7.4		152.0	15.0	.1	719			4091	-2.74	2.06
C1	70	19.0	.4			.0	2135		.5	4284	-.84	2.02
	230	53.0	1.4			.0	1082	.1	8.5	1480	-2.80	1.36
C2	40	10.0	.3			11.0	1569	.1	9.5	14156	.28	.99
	66	8.6	.2			6.6	1193	.3	2.5	10100	.16	1.01
	125	33.0	2.0			.0	967		1.6	1460	-2.45	1.04
C3	30	3.8	.3			.0	620	.7	2.3	1992	-.89	1.98
	76	7.3	.9			.0	1002	.3	1.6	4880	-.94	2.46
16	WT	3.9	.3			18.0	703	.5	1.3	11564	.30	.73
	85	10.0				1.5	783	.3	4.1	2676	-1.49	1.67
16 2	WT	9.6	.3			54.0	764	.3	1.9	13270	.28	.57
	38	6.8	.3			16.0	732	.3	2.0	11390	.31	.81
	72	3.7	.3			.0	869	1.1	1.3	8152	-.16	1.77
	135	51.0	1.6			.0	1301		.0	1864	-2.99	.35
C4	WT	12.0	.3			.7	1139	.3	3.0	52800	.49	.14
	20	8.9				.0	856	.4	2.4	18660	.26	-.48
	36	9.6	.3			.0	780	1.7	1.5	12436	.23	1.13
	65	7.9	.5			.0	996	1.0	.3	6540	-.57	2.18
	100	7.5	.5			.0	983	1.0	.3	6712	-.54	2.03

SAMPLE	DEPTH m	FIELD pH	FIELD COND	LAB pH	LAB COND	Ca mg/L	Mg mg/L	Na mg/L	K mg/L	HCO3 mg/L	SO4 mg/L	Cl mg/L
C5 WT	6.1	7.6	13000	7.8	19500	334.0	489.0	5340	6.0	761	12990	56.0
45	13.7	7.3	9100	7.6	14700	178.0	218.0	3990	16.0	1122	8293	56.0
135	41.1	7.8	3500	8.0	5300	21.0	5.7	1380	3.6	1330	1791	38.0
C6 WT	5.5	7.6	14000	7.7	22400	382.0	992.0	6410	2.7	893	17100	32.0
50	15.2	7.0	4700	7.4	7000	405.0	145.0	1380	9.3	893	3750	33.0
170	51.8	8.2	1750	8.0	2650	17.5	3.2	701	3.4	1390	40	206.0
2 WT	5.5	7.3	4300	7.5	7050	437.0	396.0	1100	7.2	838	3945	73.0
4 WT	5.5	7.2	7200	7.5	12500	374.0	329.0	2870	19.0	1240	6855	98.0
5 WT	5.5	7.2	8000	7.5	13200	357.0	473.0	2905	12.0	1360	7455	160.0
32	9.8	6.8	4750	7.5	7750	455.0	162.0	1560	11.0	1280	3765	75.0
6 WT	4.6	7.4	7500			358.0	493.0	2515	1.8	937	7050	97.0
70	21.3	7.2	3400	7.6	5400	160.0	47.0	1175	2.8	886	2259	28.0
7 WT	6.4	7.0	4500	7.6	7000	468.0	466.0	1055	17.0	633	4230	265.0
8 WT	9.1	7.2	19200	7.4	32700	340.0	3075.0	5760	23.0	1260	23100	46.0
9 WT	4.6	7.4	5200	7.6	9200	340.0	420.0	1740	11.0	600	5445	39.0
28	8.5	7.2	1750	7.9	2670	88.0	35.0	480	5.4	648	750	71.0
10 WT	6.1	7.2	2850	7.8	4500	369.0	230.0	568	4.2	362	2559	39.0
11 WT	4.6	7.3	2250	7.8	3590	35.0	159.0	339	17.0	406	1926	63.0
12 WT	4.6	7.2	6200	7.8	9420	146.0	445.0	1750	4.9	476	5175	57.0
13 WT	5.5	7.3	1300	7.8	1980	221.0	92.0	117	3.9	414	777	21.0
14 WT	5.2	7.3	7000	7.5	11700	350.0	527.0	2330	15.0	809	6780	79.0
15 WT	3.7	7.6	14500	7.9	22000	343.0	775.0	5975	13.0	1168	14745	187.0
24	7.3	7.0	10000	7.4	15700	359.0	301.0	3670	21.0	1430	8670	124.0
17 WT	5.6	7.4	8500	7.8	13600	404.0	646.0	256	8.3	1050	7515	110.0
18 WT	3.5	6.9	14000	7.6	22600	415.0	2025.0	5496	20.0	1160	18420	302.0
19 WT	3.7	6.9	6000	7.6	9620	363.0	382.0	1875	14.0	1210	5175	57.0
SURFACE SAMPLES/DATE												
A1.3	11-03-85	7.5	40	6.9	82	5.6	1.6	0	9.6	24	5	1.6
A3.5	11-03-85	–	–	7.5	680	30.0	19.0	103	14.0	118	267	5.7
A5	11-03-85	–	200	7.3	660	25.0	15.0	105	14.0	104	243	5.7
A5	20-06-85	–	3400	9.2	4450	114.0	123.0	1020	26.0	772	2475	38.0
B2.5	11-03-85	–	–	7.3	335	11.0	5.7	57	13.0	99	69	10.0

SAMPLE	Si mg/L	F mg/L	TIC mg/L	TOC mg/L	NO3 mg/L	FIELD ALK mg/L	FIELD Fe mg/L	DO mg/L	TDS mg/L	Log SI gypsum	Ca/Mg molar
C5 WT	13.0	.2			8.6	601	.2	7.5	23392	.29	.41
45	7.1	.0			.0	878	.6	5.0	14092	-.03	.50
135	10.0	1.0			.0	1085	.2	2.5	3968	-1.17	2.23
C6 WT	10.0	.5			12.0	614	.6	1.5	25472	.37	.23
50	16.0	.0			.0	735	6.5	.1	6604	.29	1.95
170	58.0	2.0			.0	1193		2.6	1724	-2.28	1.42
2 WT	13.0	.4			50.0	566	1.2	6.0	7480	.26	.67
4 WT	12.0	.4			43.0	990	.9	2.0	12492	.27	.69
5 WT	15.0	.2			.0	1098	.3	4.0	13264	.25	.46
32	14.0	.0			.1	1066	.3	.8	7180	.27	1.70
6 WT	9.6	.4			2.0	700	.5	4.1	12352	.25	.44
70	12.0	.2			.0	706	.4	.4	4392	-.22	2.07
7 WT	1.3	.1			.0	601	.6	1.5	8776	.30	.61
8 WT	12.0	.2			19.0	897	.6	11.0	46148	.34	.07
9 WT	16.0	.1			.2	445	.3	6.0	9432	.21	.49
28	7.3	.0			.5	573	.4	5.5	2020	-.68	1.53
10 WT	12.0	.2			9.3	270	.6	6.0	4584	.15	.97
11 WT	9.6	.0			10.0	312	.9	5.2	3360	.16	1.66
12 WT	8.8	1.1			1.9	379	.8	6.0	10500	-.16	.20
13 WT	13.0	.2			.2	356	.3	12.0	1812	-.29	1.46
14 WT	9.4	.1			38.0	589	.5	.8	12800	.23	.40
15 WT	4.9	.2			73.0	885	.4	5.9	24900	.30	.27
24	12.0	.2			1.9	1002	.5	2.8	15600	.28	.72
17 WT	15.0	.5			62.0	827	.4	3.0	15696	.30	.38
18 WT	11.0	.9			18.0	824	1.0	1.5	29220	.39	.12
19 WT	9.2	.0			9.2	920	.7	2.0	9804	.22	.58
SURFACE SAMPLES											
A1.3	18.0	.0			1.7	-	-	-	112	-3.41	2.12
A3.5	29.0	.0			13.0	-	-	-	532	-1.30	.96
A5	25.0	.0			6.8	-	-	-	492	-1.40	1.01
A5	16.0	.3			.0	-	-	-	4000	-.38	.56
B2.5	27.0	.0			.0	-	-	-	292	-2.14	1.17

APPENDIX 8

Piper Tri-linear Diagrams for Water Samples
from Individual Piezometer-nest Sites and for Samples
from Piezometers Completed in Drift and Bedrock Sediment.

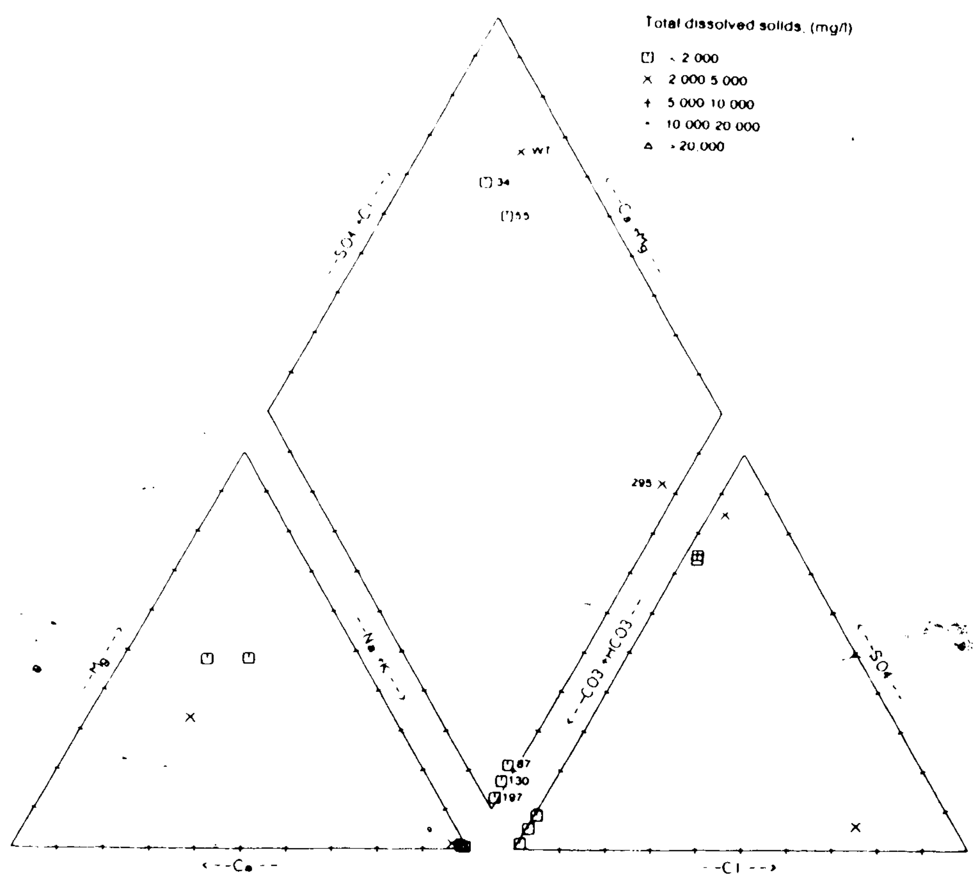
Total dissolved solids, (mg/l)
< 2 000
2 000 5 000
5 000 10 000
10 000 20 000
> 20 000
WT
34
55
295
87
130
197
Mg
Na +K
Ca
CO3 +HCO3
SO4
Cl
SO4 +Cl
Ca +Mg

Site A1

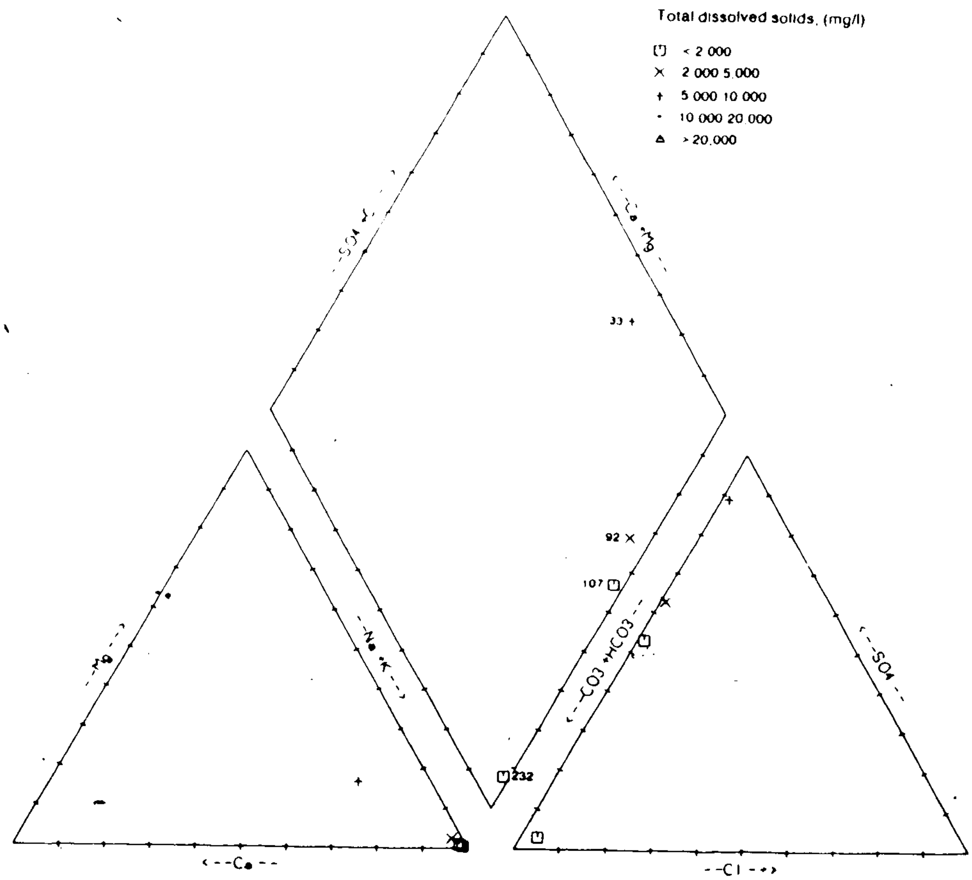
Total dissolved solids, (mg/l)
< 2 000
2 000 5 000
5 000 10 000
10 000 20 000
> 20,000
33
92
107
232
<--Ca--
--Cl-->
<--SO4--
--Na+K-->
<--CO3+HCO3--
--Mg-->
<--Ca+Mg--

Site A2

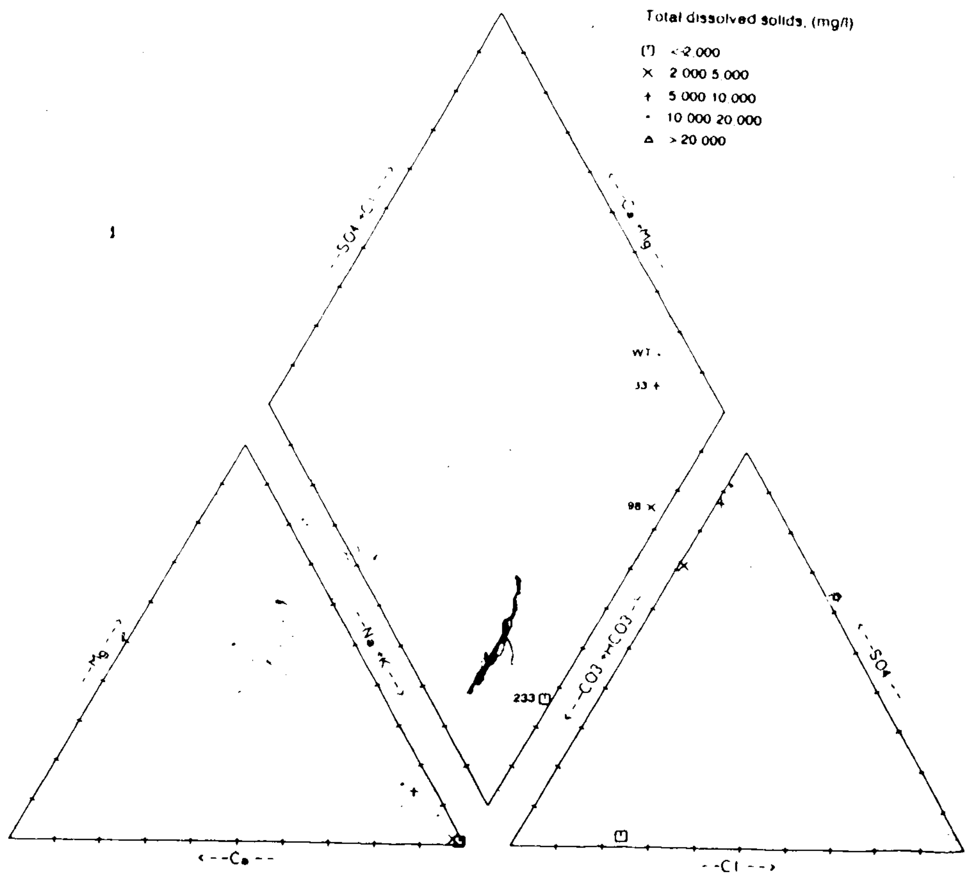
Total dissolved solids, (mg/l)
< 2 000
2 000 5 000
5 000 10 000
10 000 20 000
> 20 000
WT
33
98
233
<--Ca--
--Cl-->
--SO4-->
--Na+K-->
<--CO3+HCO3--
<--Ca+Mg--
--Mg-->
<--SO4--

Site A3

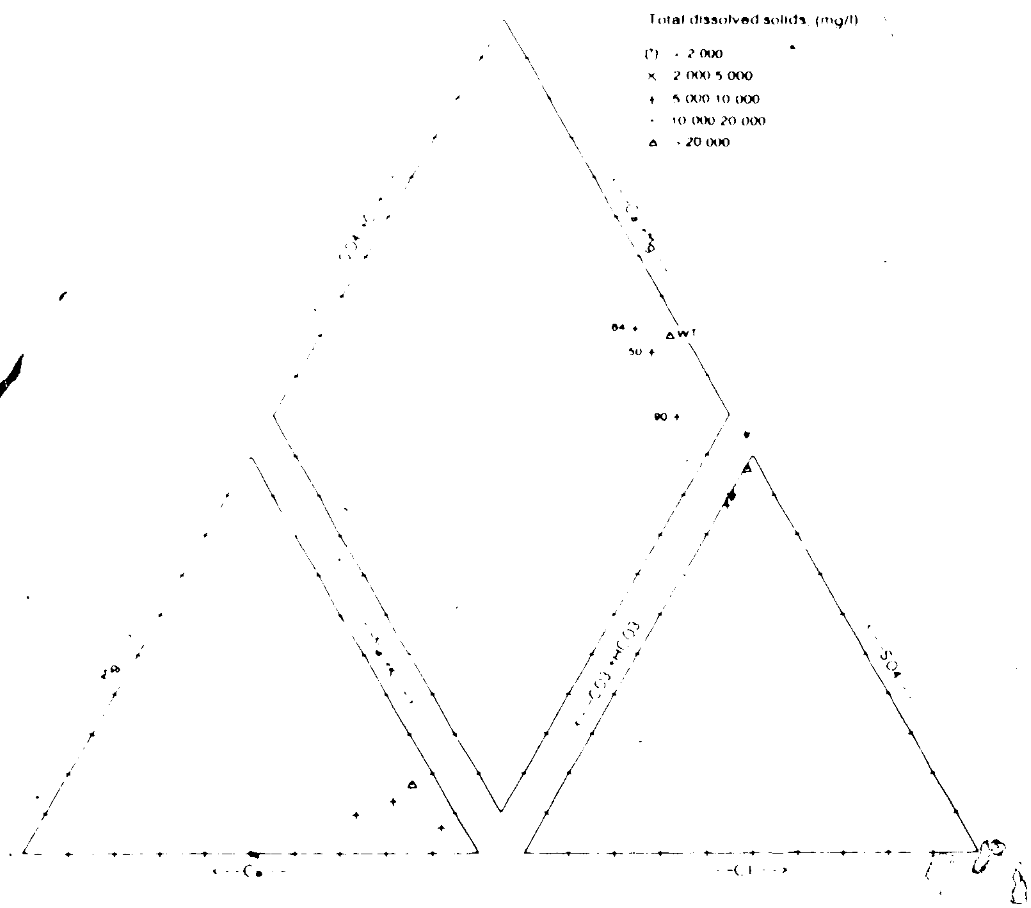
Total dissolved solids (mg/l)
< 2 000
2 000 5 000
5 000 10 000
10 000 20 000
> 20 000
64
50
90
WT
CO3+HCO3
SO4
Ca
Cl

Site A4

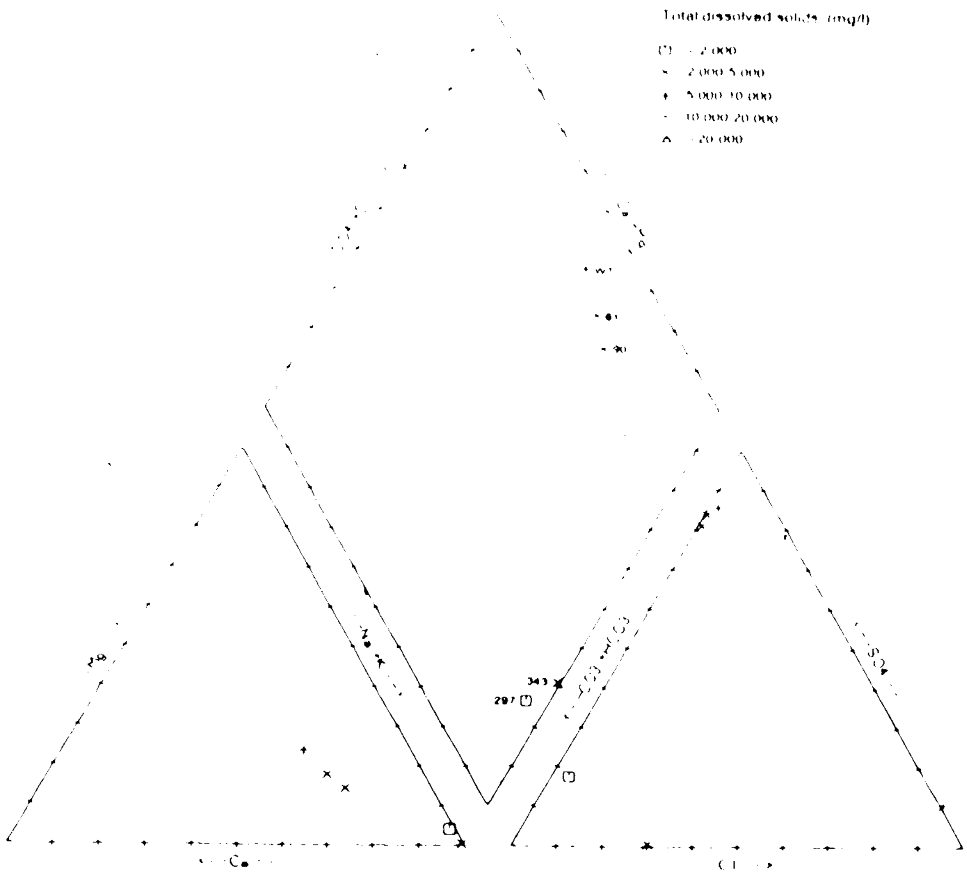

Site A5

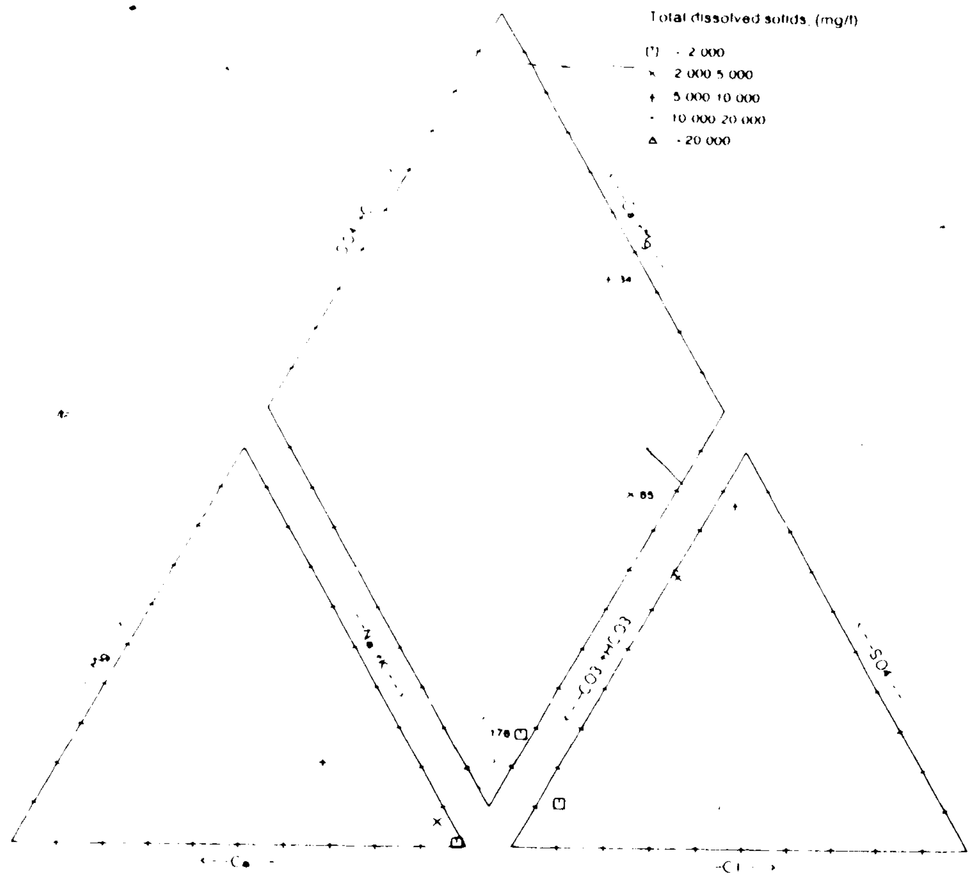
Total dissolved solids, (mg/l)
< 2 000
2 000-5 000
5 000-10 000
10 000-20 000
> 20 000
34
85
178
SO4
Cl

Site B1

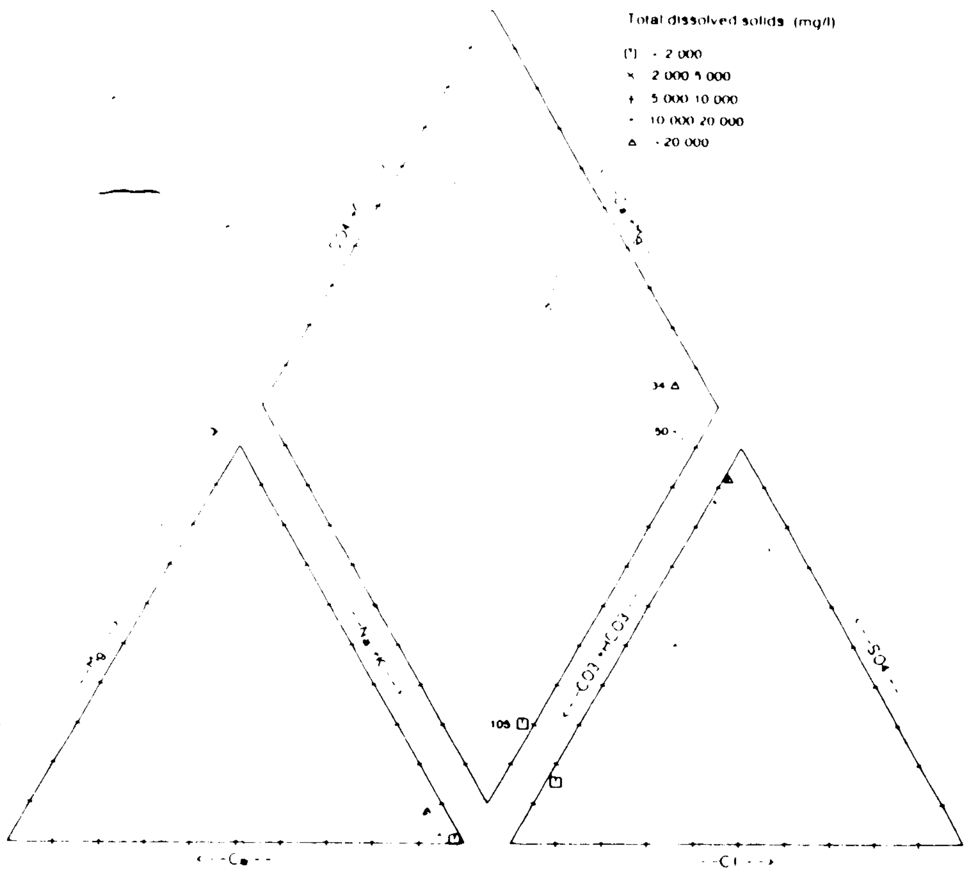

Total dissolved solids (mg/l)
· 2 000
2 000 5 000
5 000 10 000
10 000 20 000
· 20 000
34
50
109
Na+K
CO3+HCO3
SO4
Ca
Cl

Site B2

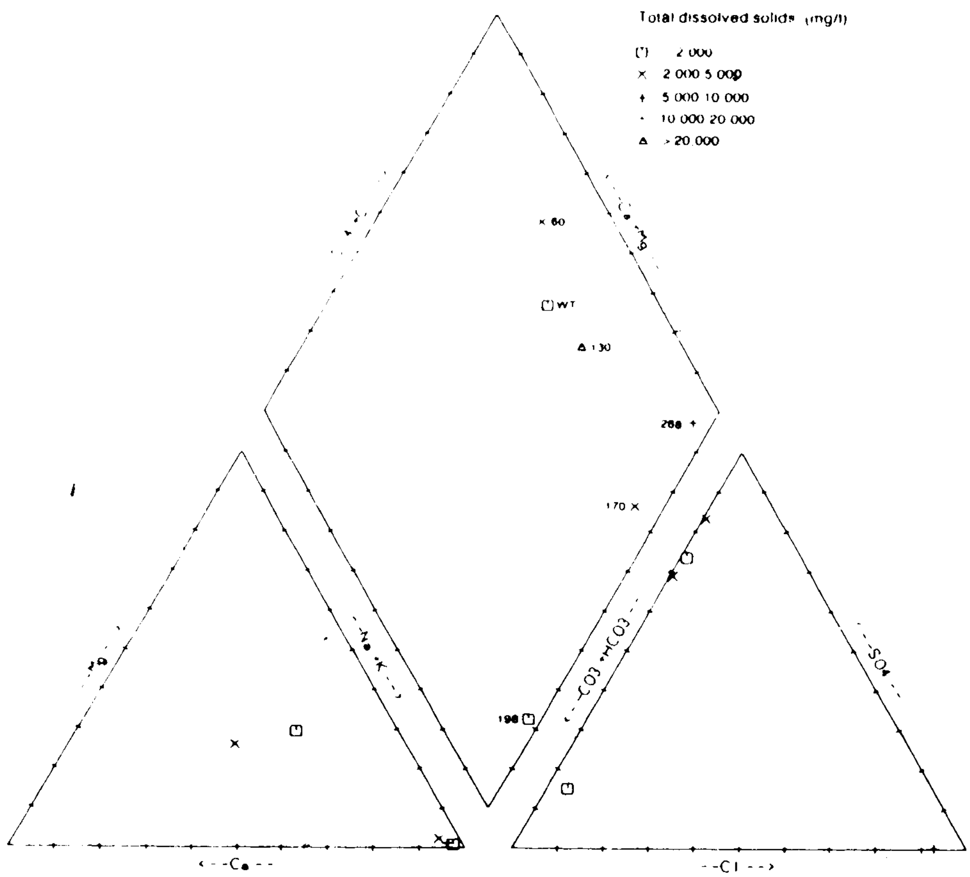
Total dissolved solids (mg/l)
2 000
2 000 5 000
5 000 10 000
10 000 20 000
> 20 000
60
WT
130
288
170
198
Na+K
CO3+HCO3
SO4
Ca
Cl

Site B3

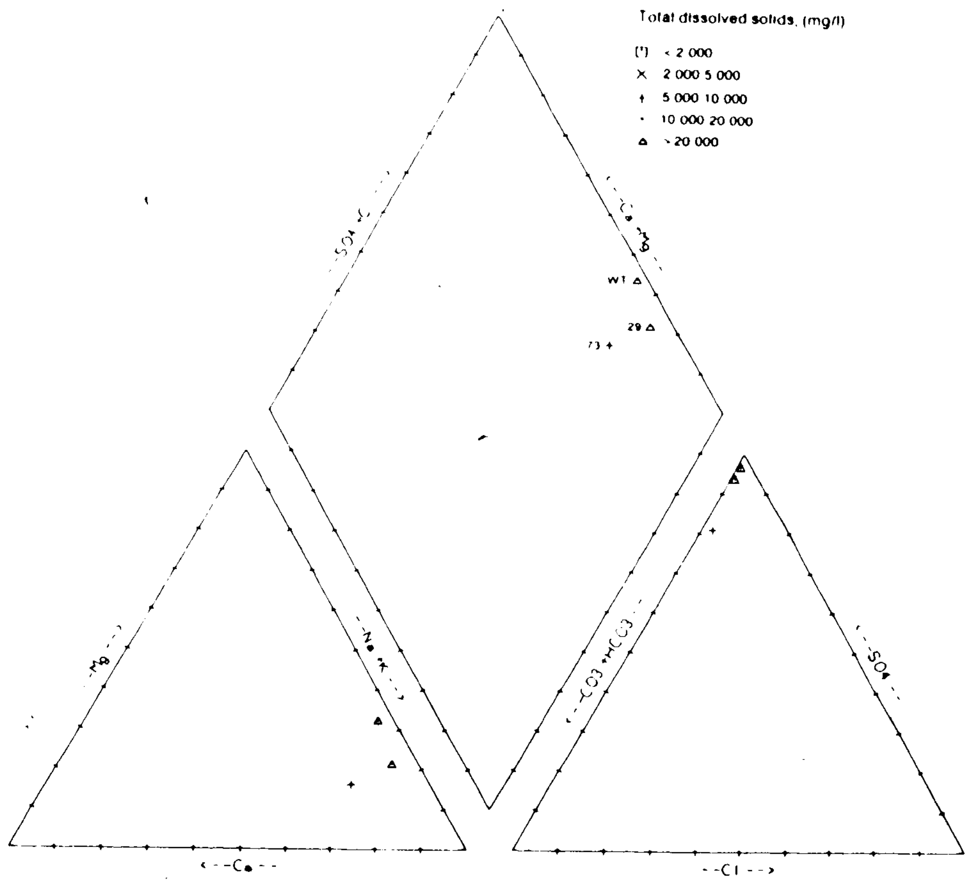
Total dissolved solids, (mg/l)
< 2 000
2 000 5 000
5 000 10 000
10 000 20 000
> 20 000
WT
29
73
Mg
Na + K
Ca
CO3 + HCO3
SO4
Cl

Site B4

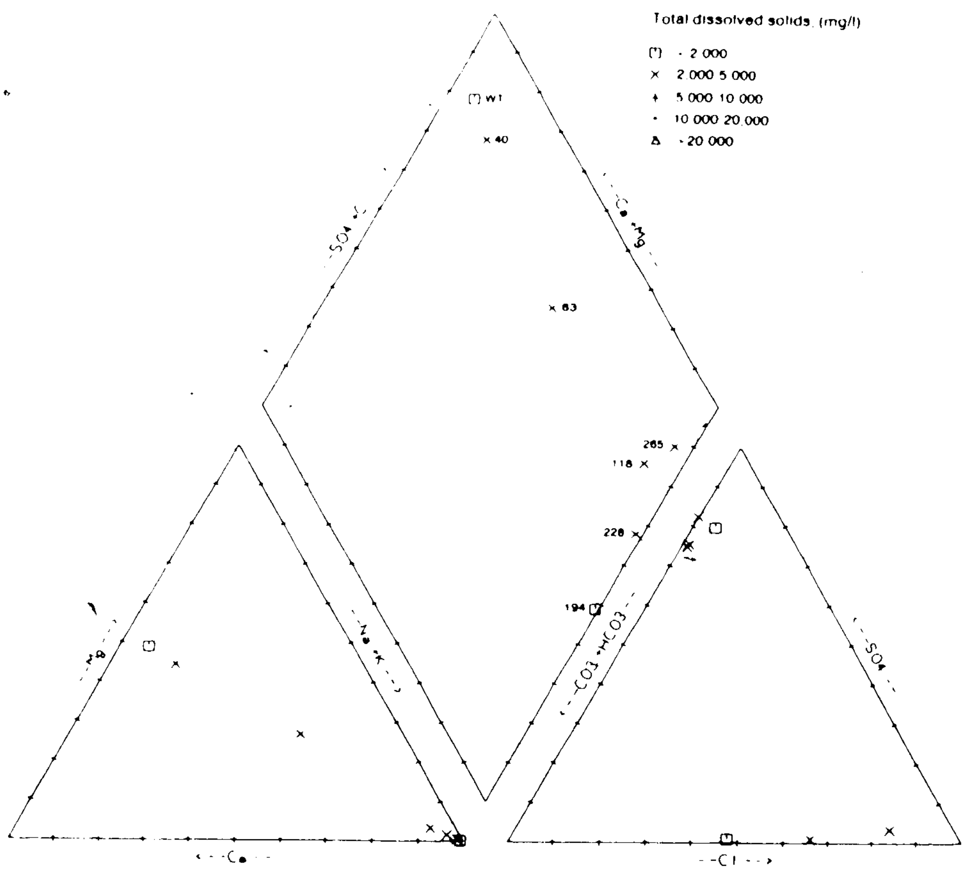
Total dissolved solids (mg/l)
< 2 000
2 000 5 000
5 000 10 000
10 000 20 000
> 20 000
W1
40
63
265
118
228
194
SO4
Ca + Mg
Na + K
CO3 + HCO3
Mg
Ca
Cl
SO4

Site B5

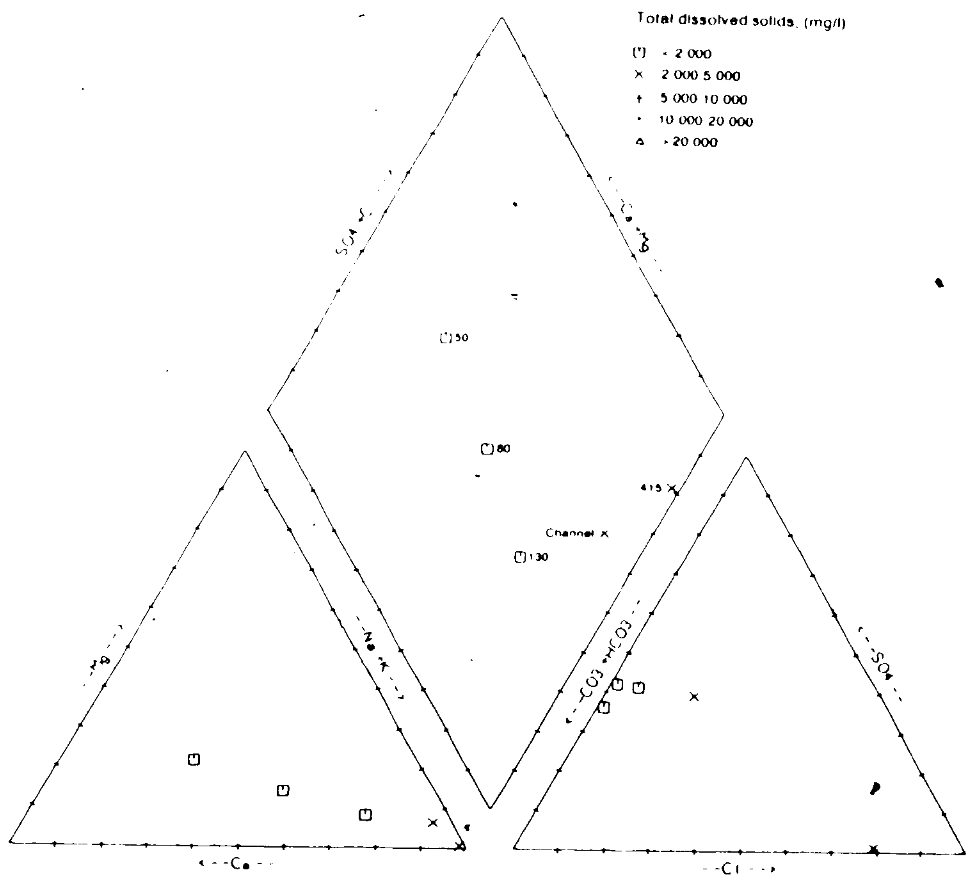
Total dissolved solids, (mg/l)
< 2 000
2 000 5 000
5 000 10 000
10 000 20 000
> 20 000
50
80
415
Channel
130
SO4
Ca+Mg
Na+K
CO3+HCO3
Mg
SO4
Ca
Cl

Site B6

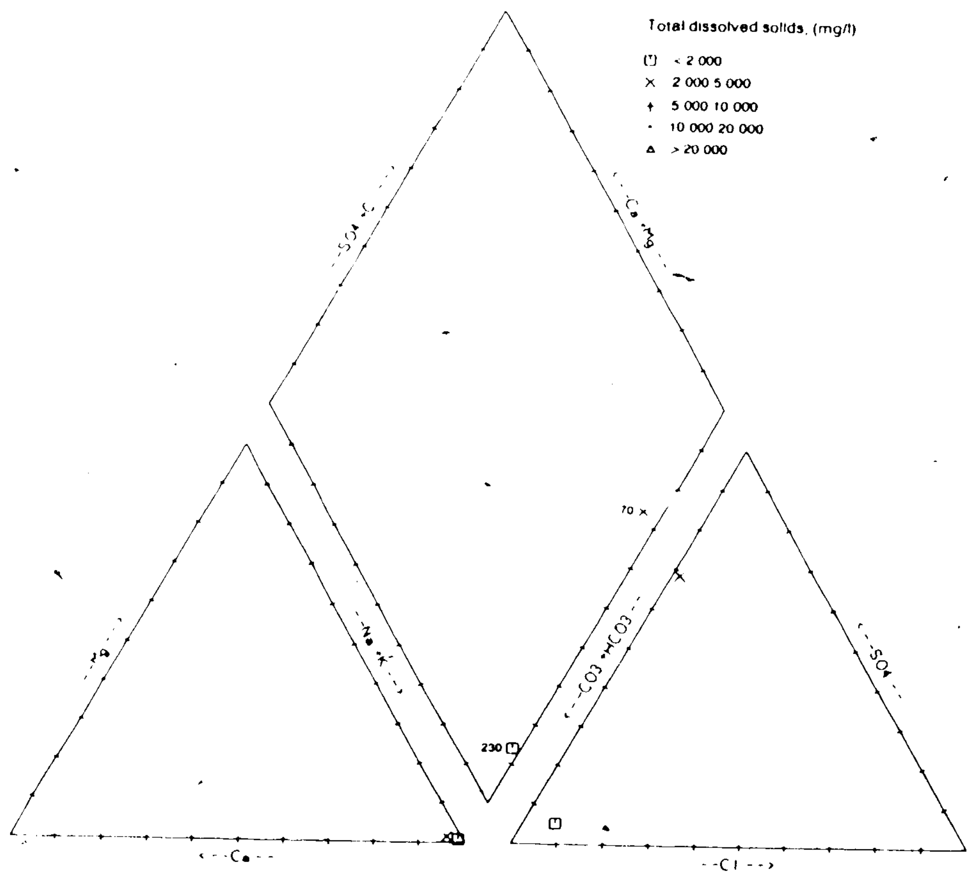
Total dissolved solids, (mg/l)
< 2 000
2 000 5 000
5 000 10 000
10 000 20 000
> 20 000
230
70

Site C1

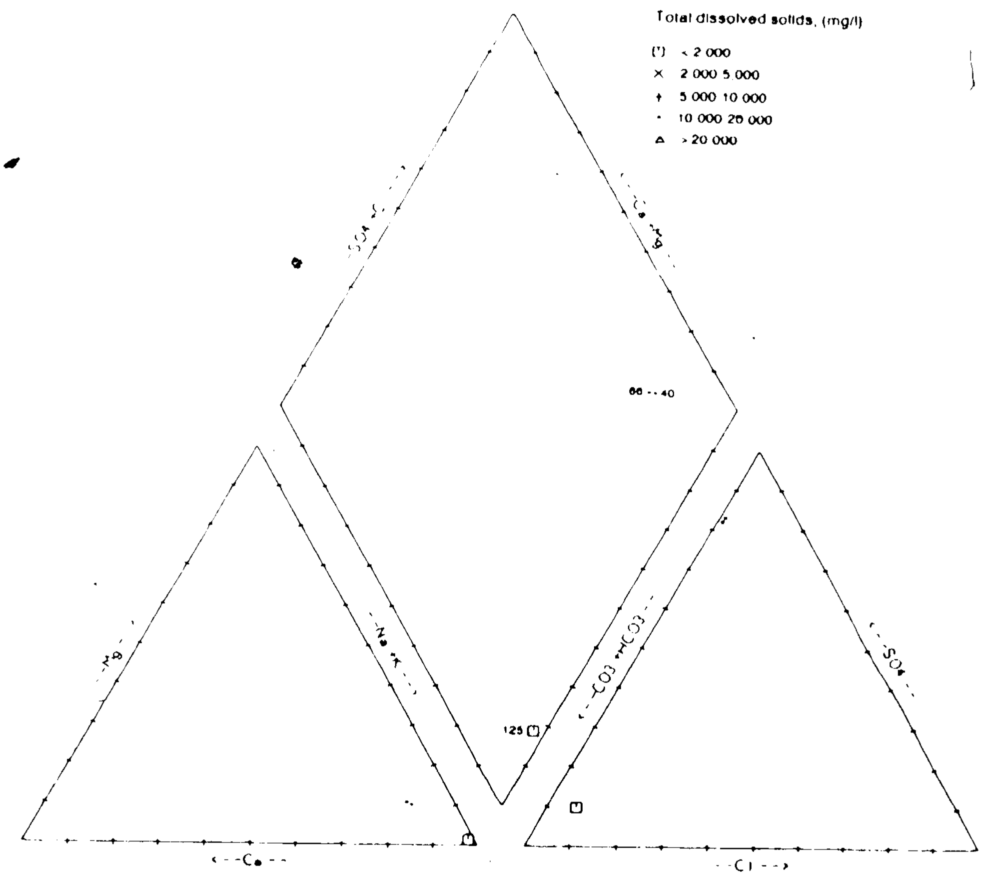
Total dissolved solids, (mg/l)
< 2 000
2 000 5 000
5 000 10 000
10 000 20 000
> 20 000
60 -- 40
125
<--Ca-->
<--Cl-->
--SO4--
CO3+HCO3
Na+K
Mg

Site C2

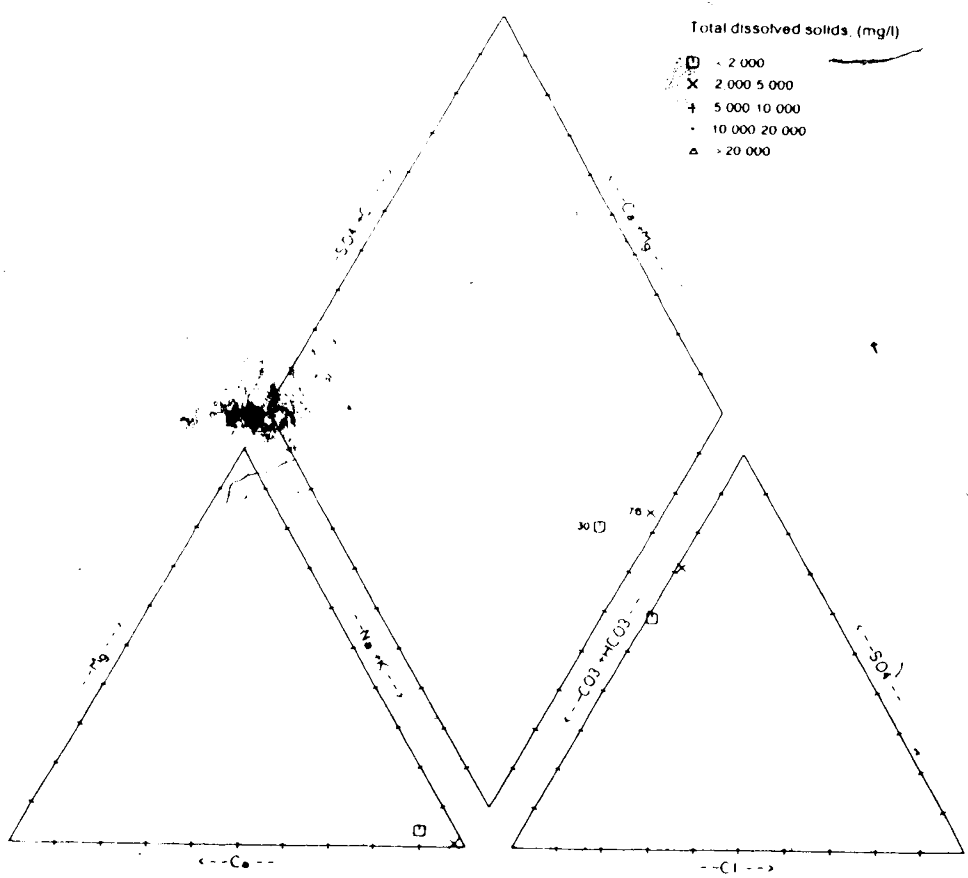
Total dissolved solids (mg/l)
< 2 000
2 000 5 000
5 000 10 000
10 000 20 000
> 20 000
Ca +Mg
Na +K
Mg
Ca
CO3 +HCO3
SO4
Cl

Site C3

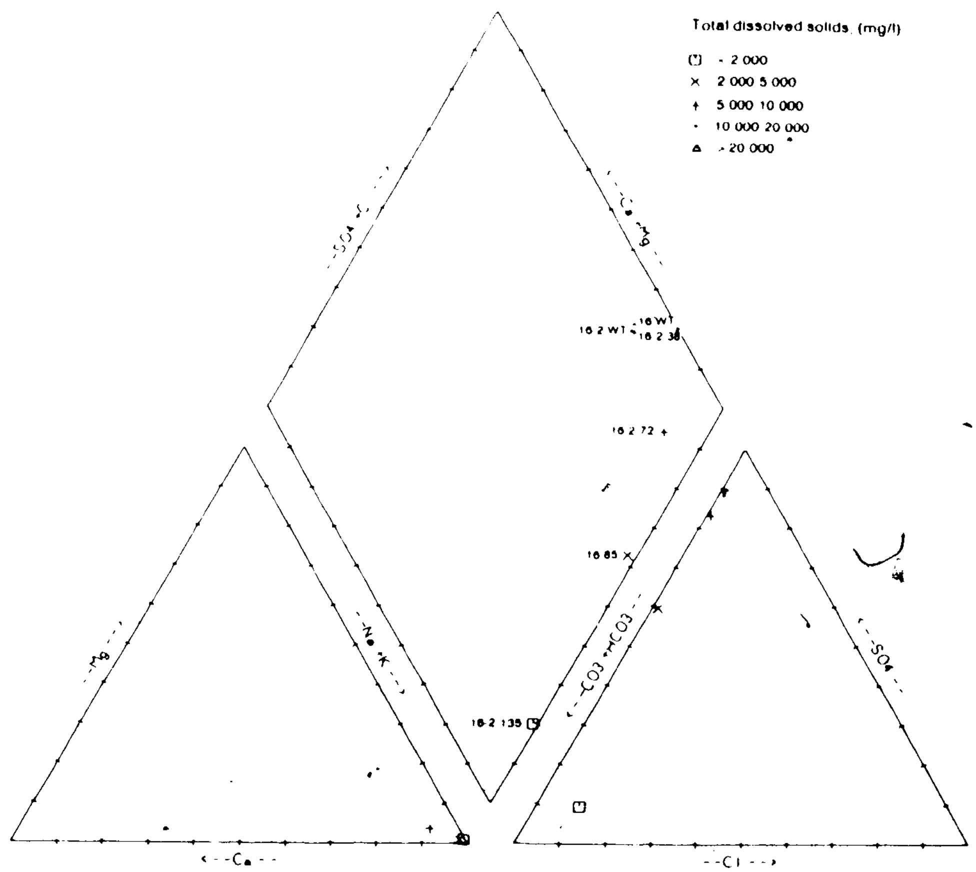
Total dissolved solids (mg/l)
- 2 000
2 000 5 000
5 000 10 000
10 000 20 000
> 20 000
--Ca+Mg--
16 WT
16 2 WT
16 2 38
16 2 72
16 85
16 2 135
--Mg--
--Na+K--
<--Ca--
<--CO3+HCO3--
<--SO4--
--Cl-->

Site 16

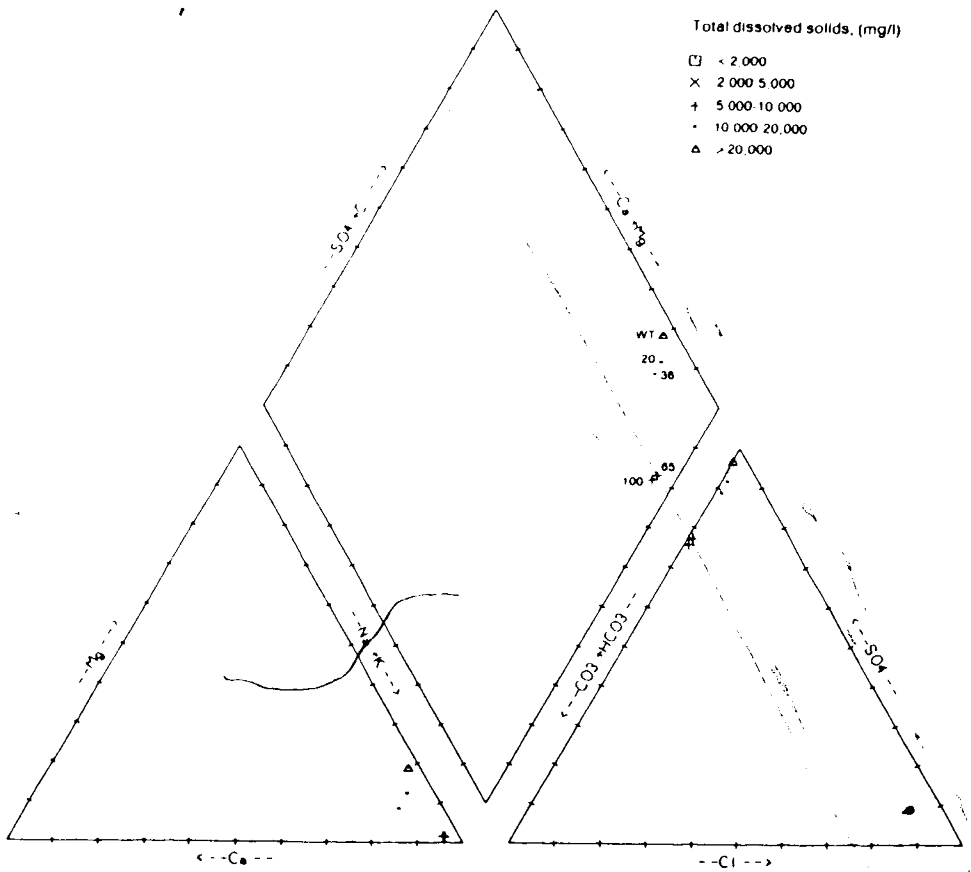
Total dissolved solids, (mg/l)
< 2,000
2,000-5,000
5,000-10,000
10,000-20,000
> 20,000
WT
20
38
100
65
Mg
Ca
Cl
SO4
CO3 + HCO3
Ca + Mg
SO4 + Cl

Site C4

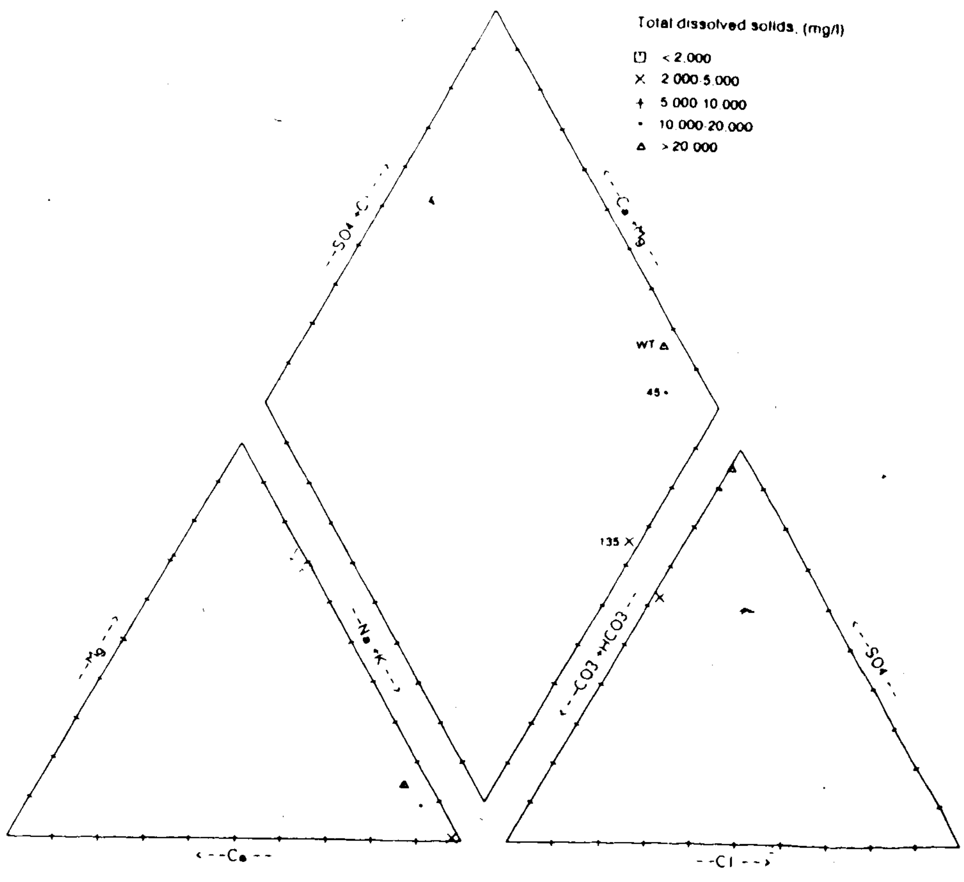
Total dissolved solids, (mg/l)
< 2,000
2,000-5,000
5,000-10,000
10,000-20,000
> 20,000
SO4 +Cl
Ca +Mg
WT
45
135
Mg
Na +K
CO3 +HCO3
SO4
Ca
Cl

Site C5

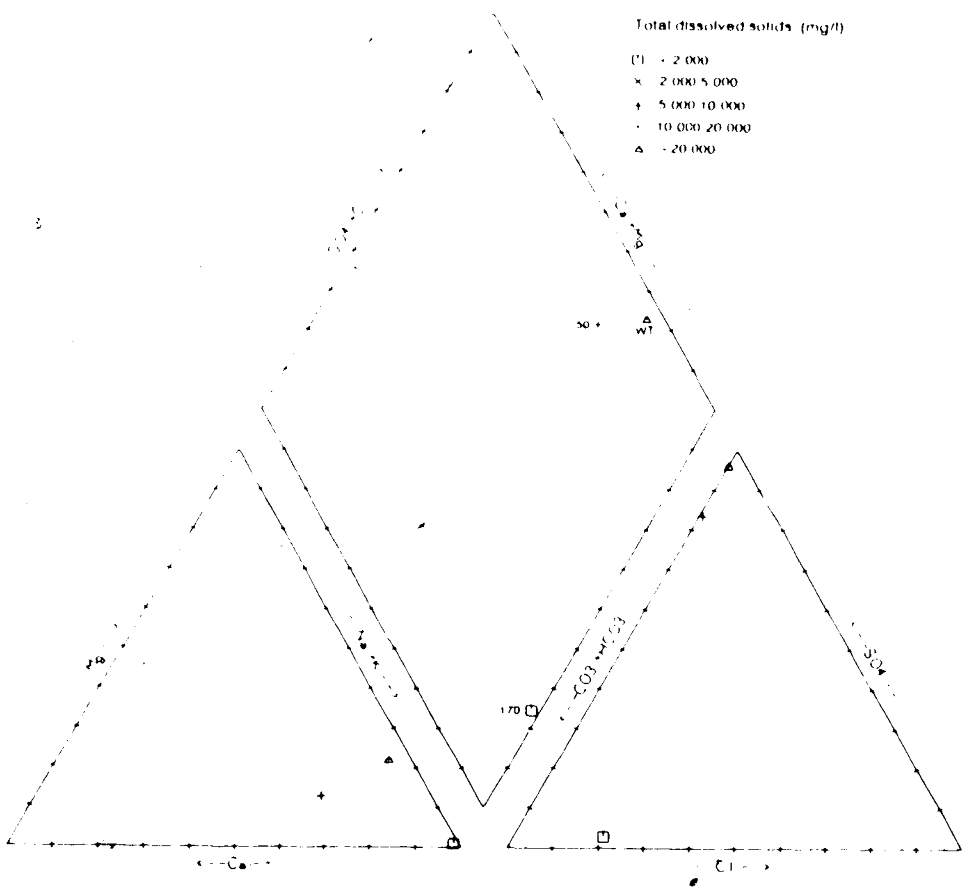
Total dissolved solids (mg/l)
2 000
2 000 5 000
5 000 10 000
10 000 20 000
20 000
50
170

Site C6

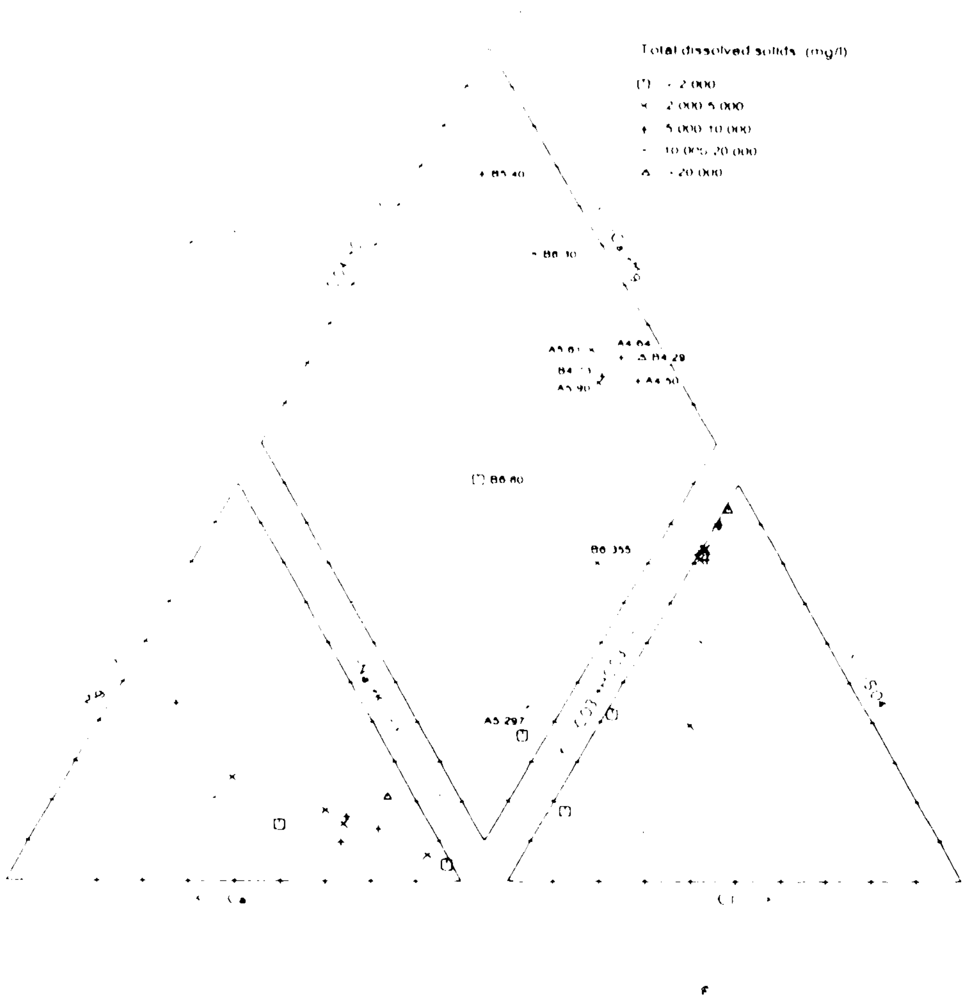

Drift-water Hydrochemistry, A and B-Lines

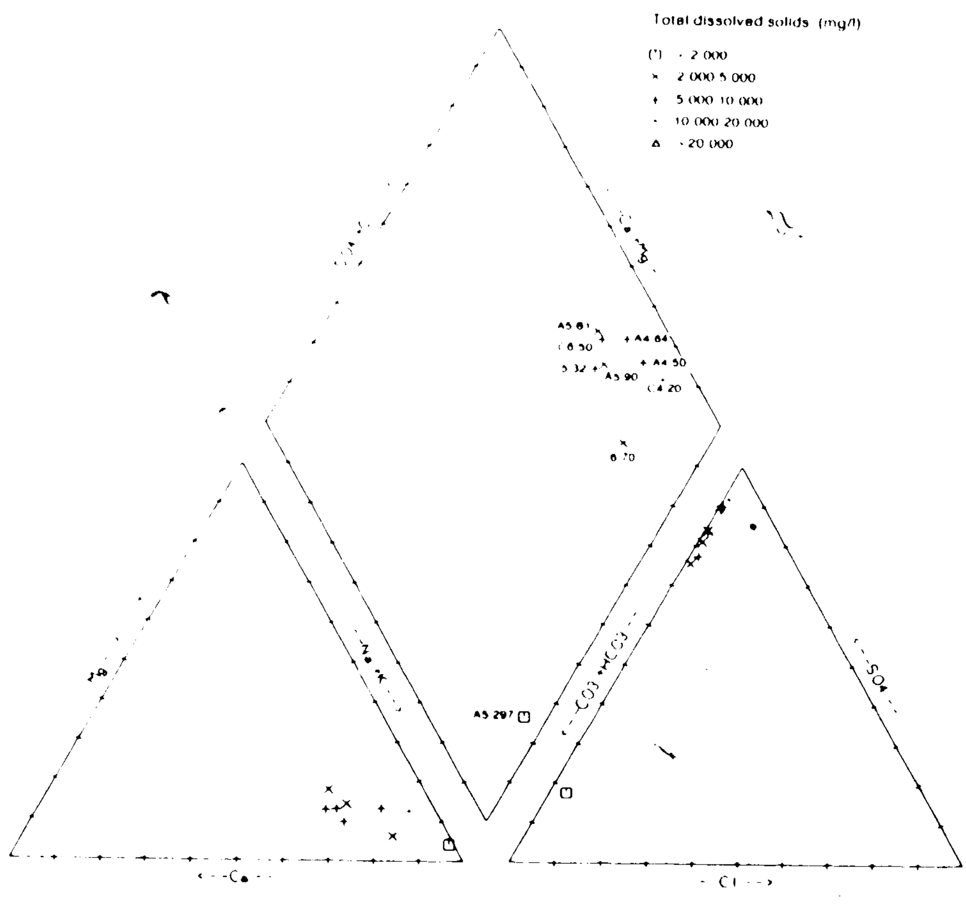

. Drift-water hydrochemistry, C-Line and vicinity

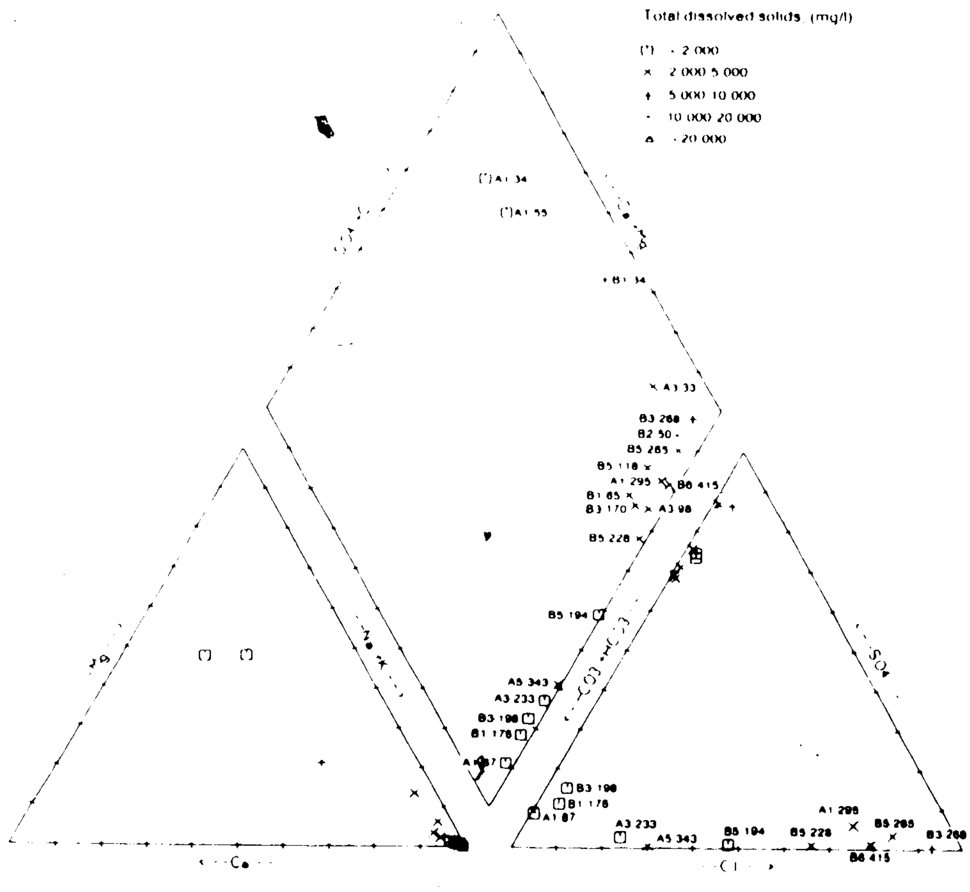

Bedrock-water Hydrochemistry, A and B-Lines

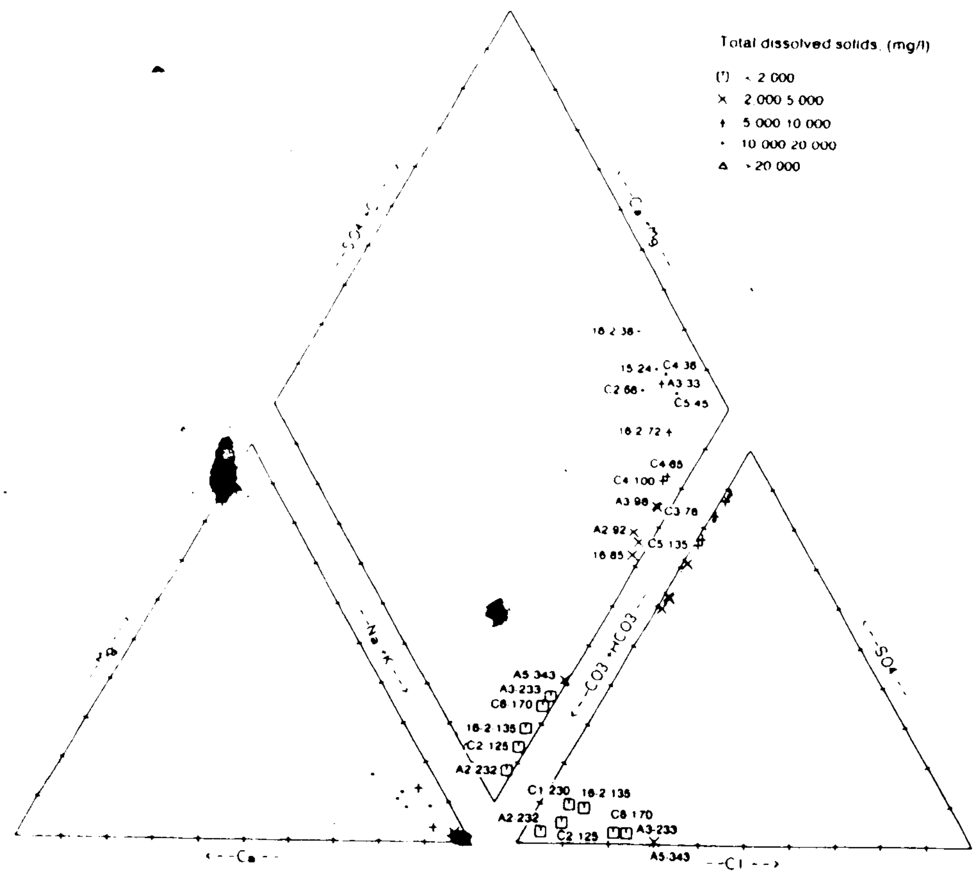

Bedrock-water hydrochemistry, C-Line and vicinity.

APPENDIX 9

Tritium Activity Determinations

Water samples from A-Line piezometers and water-table wells.

	Feb/84	Nov/84	Dec/84
A1 WT	46±18		
34	0±17		<45(0±15)
55	45±16		<42(23±20)
87	11±18		<36(0±23)
130	39±16*		<41(10±22)
197	20±16*		<41(16±22)
295	58±17*	<31(15±17)	
A2 92	61±18		<44(37±24)
232	8±15		<37(26±20)
315	70±18*	46±17*	
A3 WT	39±18		<39(18±19)
33	36±16		<37(31±24)
98	24±18		<37(21±20)
233	22±15*		<37(7±22)
357	53±15*	43±20*	
A4 WT	30±13		<14(10±12)
50	15±16		<14(7±11)
64	0±17		<14(0±12)
90	19±18		<14(10±11)
122	15±16		19±12*
260	13±16*		17±12*
A5 WT	56±19		66±12
61	15±18		17±9
90	4±19		<15(8±13)
135	0±18		<35(25±17)
297	0±20		<14(0±12)
343	0±18		<14(12±12)

* water considered contaminated with drilling mud. Piezometers recleaned before November 1984 sampling. Piezometers not resampled in December 1984 were reduced to 1.9 cm diameter by installing new pipe.

Water samples from B-Line piezometers and water-table wells.

	Feb/84	Nov/84	Dec/84
B 34	1±18		<32(2±20)
65	74±18		<32(0±19)
176	0±17		<32(0±17)
278	46±18*		
B2 50	32±17		<15(4±11)
105	35±17	<31(17±18)	
198	59±16*	<32(24±20)	
320	52±15*	55±21*	
B3 WT	81±15		44±18
60	17±14		<34(6±21)
130	49±17		<33(29±22)
170	41±21		<33(3±24)
198	18±16		<34(6±17)
268	3±15		<33(14±21)
298	55±14*	36±21*	
B4 WT	15±21		18±12
29	6±17		<15(5±11)
73	0±19		<15(9±13)
B5 WT	49±18		53±21
40	5±20		<43(0±21)
83	1±19		<33(3±19)
118	0±18		<34(0±20)
194	12±21		<37(11±20)
228	9±22		<37(2±15)
265	61±19*	<31(13±18)	
B6 50	0±20		<35(0±20)
80	15±18		<39(0±22)
130	27±17		38±20
230	51±20*	<31(25±17)*	-
355	9±19		<37(7±20)
415	9±19		<38(14±21)

* water considered contaminated with drilling mud. Piezometers recleaned before November 1984 sampling. Piezometers not resampled in December 1984 were reduced to 1.9 cm diameter by installing new pipe.

Water samples from C-Line and vicinity piezometers and water-table wells (sampled August 1986).

C1 70	<25(16±17)
125	41±17
230	<25(14±17)
C2 40	<26(4±16)
66	<27(8±18)
93	<27(4±16)
125	<27(0±18)
C3 30	<27(0±18)
76	<27(0±15)
140	<27(1±15)
C4 WT	<27(6±17)
20	<28(0±15)
36	<27(4±16)
65	<40(0±19)
100	<38(12±20)
C5 WT	<39(13±21)
45	<39(3±19)
135	<39(2±20)
C6 WT	<39(9±22)
50	<39(8±22)
170	<39(0±19)
16-2 WT	<39(29±20)
38	<39(2±22)
72	<39(12±18)
135	<39(1±21)

2 WT	<39(30±19)
4 WT	<39(6±20)
5 WT	<39(2±23)
32	<39(0±24)
6 WT	52±21
70	<39(0±25)
7 WT	<39(14±18)
8 WT	<39(15±23)
9 WT	<39(16±21)
28	<39(15±17)
10 WT	46±22
11 WT	63±19
12 WT	51±20
13 WT	67±21
14 WT	<37(22±25)
15 WT	<38(12±20)
24	<38(4±21)
16 WT	<39(17±18)
85	<38(0±21)
17 WT	<38(21±22)
18 WT	19±17
19 WT	51±21

Snow and surface water samples

Snow	Dec/83	22±12
	Mar/84	23±12
	Nov/84	<31(13±20)
	Feb/85	15±12
	Feb/85	<14(8±11)
	Mar/85	<36(0±23)
	Apr/85	<36(0±26)
Peacock Slough	Mar 29/85	<36(13±20)
	Apr 11/85	<37(19±20)
	Apr 24/85	<38(2±17)
	May 9/85	<38(17±22)
	May 16/85	<38(35±22)
	June 6/85	49±23
	June 20/85	<37(35±24)
Dugout at A1	Apr 4/85	<37(21±23)
	Apr 17/85	<39(0±21)
	May 2/85	<37(28±23)
	May 30/85	<41(23±22)
	June 6/85	43±27
	June 20/85	<37(27±23)
Little Bow River	Mar/81	81±15

A-Line: water extracted from cores

Core site and depth (metres)	Activity (TU)
A4 0.0(a)	49±25
0.0(b)	74±20
0.6	76±21
1.2(a)	91±20
1.2(b)	58±22
3.0	20±21
4.6	<19(4±21)
7.6	<22(11±20)
12.2	<38(13±27)
19.8	<25(11±22)
25.9	<23(21±22)

B-Line:

Core site and depth (metres)	Activity (TU)
B2 0.0	44±22
0.6	<39(19±25)
1.2	78±24
3.0	107±22
4.6	91±24
B3 3.0	41±21
7.6	<18(2±22)
13.7	<20(12±23)
18.3	<21(1±22)
30.5	<20(0±20)
B4 0.6(a)	44±21
0.6(b)	80±20
1.2(a)	96±21
1.2(b)	70±21
3.0	43±22
6.1	<27(12±22)
7.6	<20(14±20)
10.7	<22(6±22)
15.2	<21(10±22)
19.8	<22(10±20)

Core site and depth (metres)	Activity (TU)
B5 0.0(a)	105±22
0.0(b)	99±21
0.6	95±23
1.2	74±20
3.0	67±20
4.6	<21(9±12)
6.1	<22(8±16)
9.1	<30(15±22)
12.2	<18(8±15)
16.8	<23(10±18)
22.9	<30(10±20)
B6 4.6	133±24
9.1	34±16
15.2	<20(3±20)
21.3	<18(7±14)
24.4	<18(10±20)
27.4	<24(20±16)

C Line and Vicinity: Water extracted from cores.

Core site and depth (metres)	Activity (TU)
C4 0.3	60±21
1.8	56±23
3.4	<36(36±22)
4.9	<36(13±19)
C5 3.4	<37(22±20)
4.9	<40(23±22)
6.4	<39(26±25)
7.9	<40(27±23)
9.4	<39(28±20)
C6 0.3	<40(34±20)
0.9	80±21
1.8	67±21
2.4	<39(9±21)
3.4	<39(0±20)
4.6	<45(38±16)
6.1	<40(25±19)
7.6	<40(1±19)
2 0.3	47±19
0.8	54±18
1.4	58±22
1.8	64±22
2.4	<39(32±23)
3.0	39±22
5 1.8	47±19
3.4	<40(13±18)
4.9	<38(17±23)
5.6	<38(14±22)
10 0.3	<39(37±19)
1.8	132±21
3.4	69±20
4.9	46±20
11 0.3	<40(36±18)
1.8	54±26
3.4	72±21
4.7	<39(31±24)
12 0.3	<39(19±24)
1.7	40±22
3.2	<39(32±22)
4.8	<39(28±26)
6.5	<40(0±17)
13 0.3	<39(19±22)
1.7	<24(3±25)
3.2	180±22
4.7	63±24
6.4	<39(31±21)
14 0.3	<41(24±21)
1.8	<41(12±21)
3.4	<40(6±23)
4.8	<41(7±18)

APPENDIX 10

Stable Isotope Determinations

Snow and surface water samples.

Location	Date Sampled	$\delta^{18}O$	δD
A5	29-MAR-85	-18.93	-152.1
A5	03-APR-85	-17.59	-143.4
A5	11-APR-85	-16.68	-135.5
A1.3	04-APR-85	-18.15	-144.4
A1.3	10-APR-85	-16.25	-132.0
A1.3	17-APR-85	-11.69	-113.7
A5	17-APR-85	-11.91	-112.6
A5	24-APR-85	-15.06	-128.5
A5	02-APR-85	-13.31	-119.8
A5	09-MAY-85	-11.98	-113.3
A5	16-MAY-85	-10.03	-106.0
A5	23-MAY-85	-7.38	-91.5
A5	30-MAY-85	-8.18	-95.6
A5	06-JUNE-85	-6.99	-91.7
A5	13-JUNE-85	-6.99	-89.0
A5	26-FEB-86	-23.61	-174.4
A5	13-MAR-86	-20.95	-158.0
A5	27-MAR-86	-16.40	-136.2
A5	22-APR-86	-8.70	-98.3
A5	08-MAY-86	-8.52	-94.6
A1	02-MAY-85	-21.43	-163.2
A1	09-MAY-85	-20.77	-156.0
A1	16-MAY-85	-19.03	-153.1
A1	23-MAY-85	-18.66	-150.4
A1	30-MAY-85	-17.61	-146.1
A1	06-JUNE-85	-16.79	-141.3
A1	13-JUNE-85	-15.97	-139.5
A1	20-JUNE-85	-15.15	-134.2
SNOW	29-MAR-85	-21.19	-157.0
SNOW	04-APR-85	-22.11	-161.6
SNOW	12-FEB-86	-21.13	-151.5
SNOW	MAR-83	-19.34	-143.1
SNOW	DEC-83	-23.35	-176.2

Water samples from water table wells.

Location	Date Sampled	$\delta^{18}O$	δD
A1 WT	JULY-86	-19.42	-152.5
A3 WT	JULY-86	-18.94	-150.1
A4 WT	JULY-86	18.82	144.0
A5 WT	JULY-86	-16.04	-130.6
B1 34	JULY-86	-19.00	150.3
B2 34	JULY-86	-17.21	-139.2
B3 WT	JULY-86	-21.23	-159.7
B4 WT	JULY-86	-19.35	-151.7
B5 WT	JULY-86	-19.62	-150.3
B6 50	JULY-86	-18.43	-142.0
C1 70	JULY-86	-19.89	-152.5
C2 40	JULY-86	-19.19	-149.6
C3 30	JULY-86	-22.82	-167.5
C4 WT	JULY-86	-17.48	-137.0
C5 WT	JULY-86	-19.36	-147.4
C6 WT	JULY-86	-19.90	-148.8
16 WT	JULY-86	-18.65	-146.6
16 2 WT	JULY-86	-17.15	-140.3
2 WT	JULY-86	-19.28	-147.6
4 WT	JULY-86	-18.87	-148.1
5 WT	JULY-86	-19.22	-147.7
6 WT	JULY-86	-19.17	-149.4
7 WT	JULY-86	-20.24	-155.7
8 WT	JULY-86	-19.31	-148.9
9 WT	JULY-86	-20.97	-160.2
10 WT	JULY-86	-18.39	-141.5
11 WT	JULY-86	-17.11	-133.2
12 WT	JULY-86	-15.70	-125.0
13 WT	JULY-86	-20.20	-152.5
14 WT	JULY-86	-18.08	-140.2
15 WT	JULY-86	-18.22	-144.7
17 WT	JULY-86	-19.34	-149.5
18 WT	JULY-86	-19.49	-150.0
19 WT	JULY-86	-20.17	-153.6

Water samples from piezometers completed in drift.

Location		Date Sampled	$\delta^{18}O$	δD
A4	50	JULY 86	-20.37	-151.6
A4	64	JULY-86	-20.37	-153.5
A4	90	JULY-86	-20.78	152.6
A5	90	JULY-86	-20.74	-159.1
A5	297	JULY-86	-19.70	148.9
B3	60	JULY-86	-20.64	-154.8
B3	130	JULY-86	-20.78	-158.4
B4	29	JULY-86	-20.40	-156.3
B4	73	JULY-86	-20.51	-159.1
B5	40	JULY-86	-22.57	-169.8
B6	80	JULY-86	-19.13	-149.5
B6	355	JULY-86	-19.87	-153.4
C4	20	JULY-86	-18.56	-143.6
C6	50	JULY-86	-21.00	-159.5
5	32	JULY-86	-19.67	-153.9
6	70	JULY-86	-20.87	-159.8
A5	61	JULY-86	-18.80	-147.2

Water samples from piezometers completed in bedrock.

	Location	Date Sampled	$\delta^{18}O$	δD
Type 1	A1 34	JULY-86	-19.09	-147.8
	A1 55	JULY-86	-18.10	-145.0
	A1 87	JULY-86	-18.39	-145.3
	A2 92	JULY-86	-19.29	-150.0
	A3 33	JULY-86	-19.54	-152.8
	A3 98	JULY-86	-19.48	-155.1
	B1 34	JULY-86	-19.00	-150.3
	B1 65	JULY-86	-18.75	-148.7
	B2 50	JULY-86	-19.02	-149.8
	B2 34	JULY-86	-17.21	-139.2
	B3 170	JULY-86	-20.56	-156.7
	B5 118	JULY-86	-20.31	-153.2
	C2 66	JULY-86	-18.68	-145.1
	C3 76	JULY-86	-19.68	-151.0
	16 85	JULY-86	-21.89	-165.3
	16 2 38	JULY-86	-17.97	-145.0
	16 2 72	JULY-86	-20.78	-157.6
	C4 65	JULY-86	-20.47	-156.8
	C4 36	JULY-86	-19.46	-152.6
	C4 100	JULY-86	-20.55	-155.7
	C5 45	JULY-86	-19.95	-152.8
	C5 135	JULY-86	-19.07	-149.4
	15 24	JULY-86	-18.18	-146.4
Type 2	A2 232	JULY-86	-14.68	-125.5
	A3 233	JULY-86	-12.07	-112.0
	A5 343	JULY-86	-16.71	-132.0
	B1 176	JULY-86	-16.79	-134.1
	B3 198	JULY-86	-16.42	-134.5
	B3 268	JULY-86	-10.56	-103.5
	B5 194	JULY-86	-16.33	-132.8
	B5 228	JULY-86	-14.11	-122.1
	B6 415	JULY-86	-13.08	-114.0
	C1 230	JULY-86	-13.23	-117.0
	C2 125	JULY-86	-15.50	-128.0
	16 2 135	JULY-86	-16.13	-131.1
	C6 170	JULY-86	-16.39	-131.9

APPENDIX 11

Calculations of Salt Flux to the Water Table

Groundwater discharge and salt flux to the water table.

From Harr (1962): $k_{eq} = \dfrac{d}{\Sigma d_i/k_i}$

where k_{eq} = vertical hydraulic conductivity of an equivalent homogeneous layer (L/T)

k_i = hydraulic conductivity of each individual layer (L/T)

d = total thickness of the layered medium (L), and

d_i = thickness of each individual layer (L).

By Darcy's Law, $Q_w = kia$

where Q_w = discharge rate of water (L^3/T),

k = hydraulic conductivity (L/T),

i = hydraulic gradient, = $\Delta h/d$, (L/L),

a = cross-sectional area over which discharge occurs (L^2), and

Δh = head loss across thickness d, (L).

Substituting k_{eq} for k gives

$$Q_w = \frac{d}{\Sigma d_i/k_i} \cdot \frac{\Delta h}{d} \cdot a, \text{ which reduces to}$$

$$Q_w = \frac{a\Delta h}{\Sigma d_i/k_i}$$

For units T = sec and L = m, $Q_w = m^3/sec$. Multiplying by 3.16×10^7 sec/year and considering a cross-sectional area of discharge of 1 m^2 gives:

$$Q_w = \frac{3.16 \times 10^7 \Delta h}{\Sigma d_i/k_i} \ m^3/year/m^2 \text{ of surface area}$$

The salt flux $Q_s = Q_w \times TDS$, where

Q_s = salt flux (M/T), and

TDS = total dissolved solids (M/L^3).

For units of M = kg,

$$Q_s = \frac{3.16 \times 10^7 \Delta h \ (TDS)}{\Sigma d_i/k_i} \ kg/year/m^2 \text{ of surface area}$$

C4

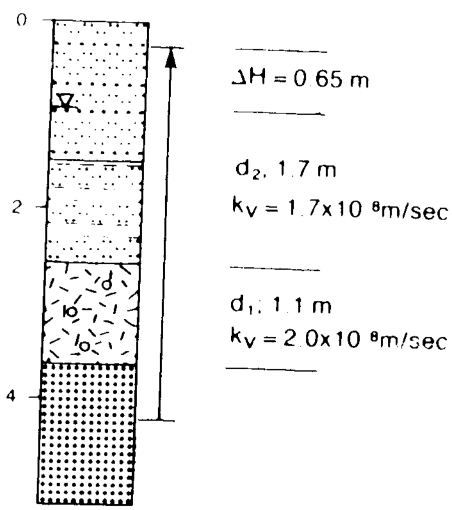

$$Q_w = \frac{(3.16 \times 10^{7})\,(0.65)}{[1.1/(2 \times 10^{-8})] + [1.7/(1.7 \times 10^{-8})]} = 0.13 \ m^3/year/m^2$$

TDS of water from sand unit = 18660 mg/L = 18.7 kg/m^3

$$Q_s = 0.13 \times 18.7 = 2.4 \ kg/year/m^2$$

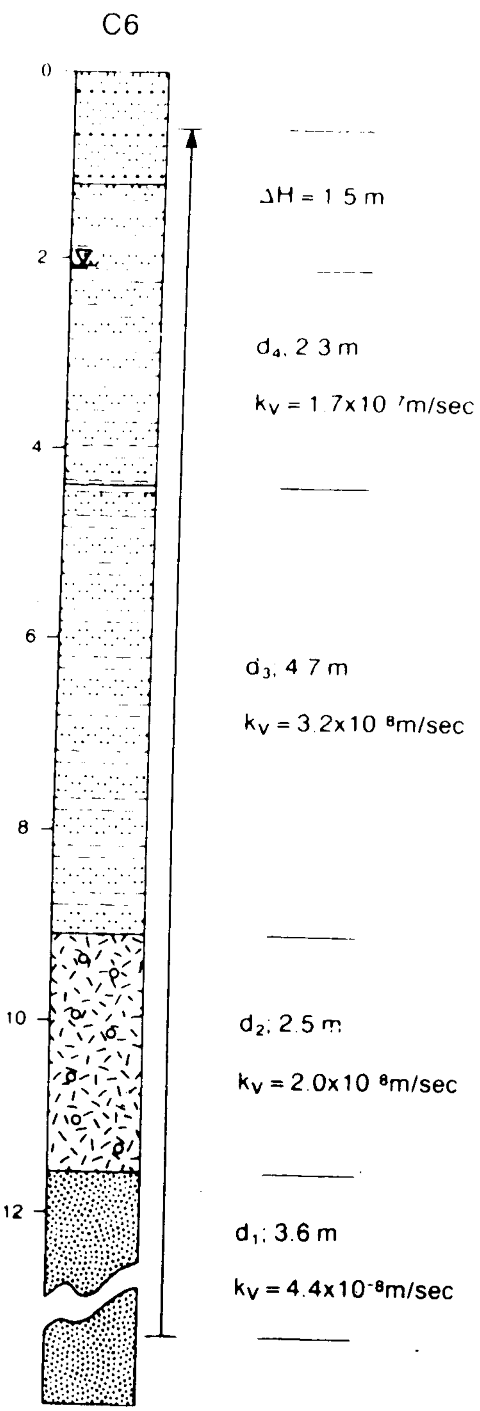

(a) assuming k_v of unit d_3 = 3.2×10^{-8} m/sec

Q_w = [(3.16 x 10^{7})(1.5)]/{[3.6/4.4 x 10^{-8}] + [2.5/(2.0 x 10^{-8})] + [4.7/(3.2 x 10^{-8})] + [2.3/1.7 x 10^{-7}]}

= 0.1[illegible] m^3/year/m^2

(b) assuming k_v of unit d_3 = 3.0×10^{-9} m/sec

Q_w = 0.026 m^3/year/m^2

(c) assuming k_v of unit d_3 = 3.0×10^{-10} m/sec

Q_w = 0.003 m^3/year/m^2

TDS of water from unit d_1 = 6604 mg/L = 6.6 kg/m^3

then, for case

(a) Q_s = 0.13 x 6.6 = 0.86 kg/year/m^2

(b) Q_s = 0.026 x 6.6 = 0.17 kg/year/m2

(c) Q_s = 0.003 x 6.6 = 0.02 kg/year/m^2

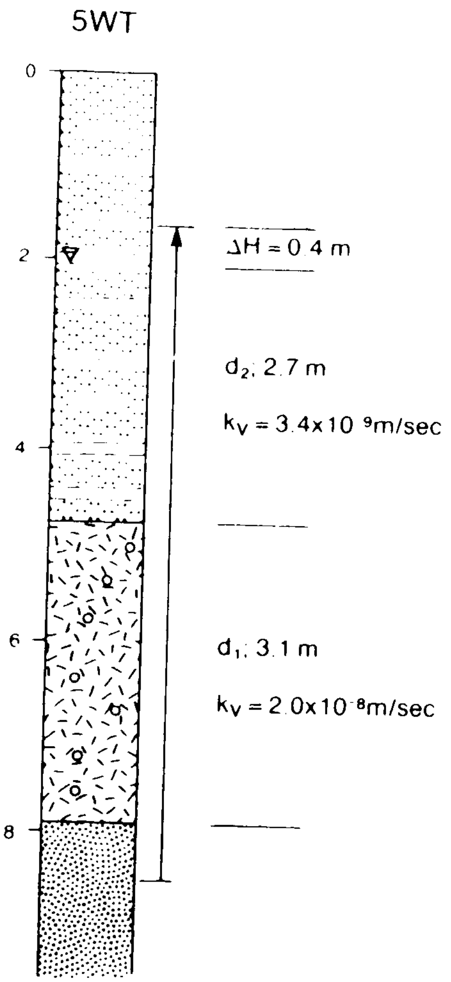

$$Q_w = \frac{(3.16 \times 10^7)\ (0.4)}{[3.1/(2.0 \times 10^{-8})] + [2.7/(3.4 \times 10^{-9})]} = 0.013\ m^3/year/m^2$$

TDS of water from sand and gravel unit = 7180 mg/L = 7.18 kg/m^3

Q_s = 0.013 x 7.18 = 0.09 kg/year/m2

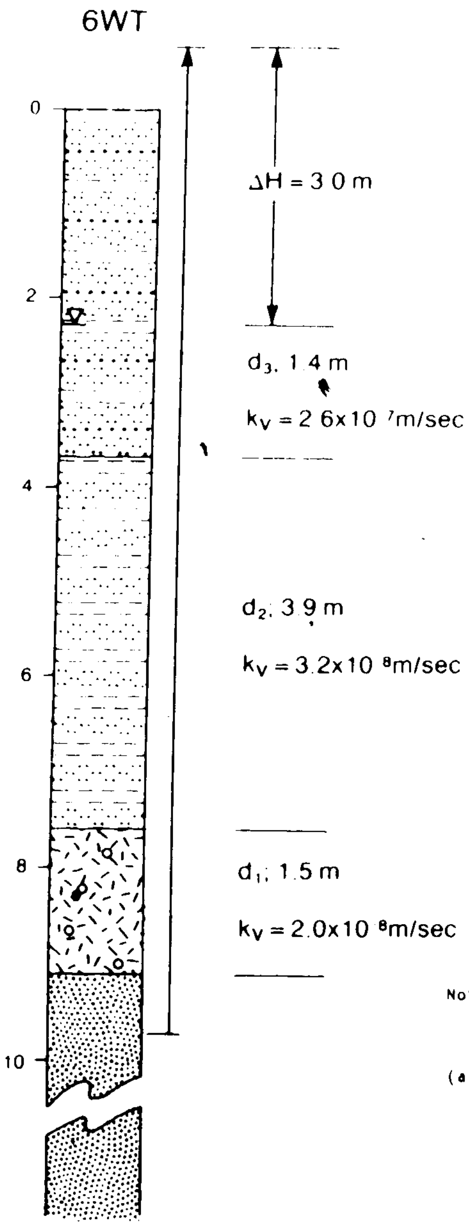

Note. Head in sand and gravel assumed equal to head at base of till because gravel pack extends to within one metre of till.

(a) assuming k_v of unit $d_2 = 3.2 \times 10^{-8}$ m/sec

$$Q_w = \frac{(3.16 \times 10^{7})\ (3.0)}{[1.5/(2.0 \times 10^{-8})] + [3.9/(3.2 \times 10^{-8})] + [1.4/(2.6 \times 10^{-7})]}$$

$= 0.47\ m^3/year/m^2$

(b) assuming k_v of unit $d_2 = 3.0 \times 10^{-9}$ m/sec

$Q_w = 0.069\ m^3/year/m^2$

(c) assuming k_v of unit $d_2 = 3.0 \times 10^{-10}$ m/sec

$Q_w = 0.007\ m^3/year/m^2$

TDS of water from sand and gravel = 4392 mg/L = 4.4 kg/m^3,

then, for case

(a) $Q_s = 0.47 \times 4.4 = 2.1$ kg/year/m^2

(b) $Q_s = 0.069 \times 4.4 = 0.3$ kg/year/m^2

(c) $Q_s = 0.007 \times 4.4 = 0.03$ kg/year/m^2.

APPENDIX 12

Piezometer and Water-table Well Completion Details

Piezometer No.	A1 WT	A1 34	A1 55	A1 87	A1 130	A1 197	A1 295
Date Completed	Oct.5/83	Oct. 6/83	Nov. 20/83	Nov. 20/83	Nov. 21/83	Nov. 22/83	Nov. 23/83
Drilling Method	hollow stem auger	solid auger	rotary	rotary	rotary	rotary	rotary
Surface Elevation (mamsl)	1035.0	1035.0	1035.0	1035.0	1035.0	1035.0	1034.9
Top Casing Elevation (mamsl)	1035.939	1035.963	1035.869	1035.846	1035.850	1035.937	1035.895
Meas. Point (m above ground level)	0.90	0.95	0.90	0.85	0.85	0.95	1.0
Total Depth (m)	5.5	10.4	16.8	26.5	39.6	60.0	89.9
Seal Type and Interval (m)	none	peltonite 8.4-8.8	peltonite 13.4-14.0	peltonite 22.6-23.5	peltonite 36.9-37.8	peltonite 57.6-58.5	peltonite 87.2-88.1
Gravel Pack Interval (m)	1.2-5.5	8.8-10.4	14.0-16.8	23.5-26.5	37.8-39.6	58.5-60.0	88.1-89.9
Screened Interval (m)	3.1-5.5	9.8-10.4	16.2-16.8	25.9-26.5	39.0-39.6	59.4-60.0	89.3-89.9
Slot Size (in. X 10^{-3})	15	20	20	20	20	20	20
Centralizer	no	yes	yes	yes	yes	yes	yes
Washdown valve	no	no	yes	yes	yes	yes	yes
Annular Backfill	cuttings	cuttings	bentonite slurry	bentonite slurry	bentonite slurry	bentonite slurry	bentonite slurry
Comments	dry on completion	dry on completion	washed in place				

Piezometer No.	A2 33	A2 92	A2 107	A2 232	A2 315	A3 WT	A3 33
Date Completed	Oct. 31/83	Nov. 14/83	Nov. 15/83	Nov. 16/83	Nov. 17/83	Oct. 6/83	Oct. 6/83
Drilling Method	solid auger	rotary	rotary	rotary	rotary	solid auger	solid auger
Surface Elevation (mamsl)	1029.3	1029.3	1029.4	1029.3	1029.3	968.2	968.2
Top Casing Elevation (mamsl)	1030.164	1030.074	1030.170	1030.139	1030.197	969.034	969.022
Meas. Point (m above ground level)	0.85	0.80	0.80	0.80	0.90	0.80	0.80
Total Depth (m)	10.1	28.0	32.6	70.7	96.0	5.5	10.1
Seal Type and Interval (m)	peltonite 6.6-7.0	peltonite 25.3-25.9	peltonite 29.9-30.8	peltonite 66.7-68.0	peltonite 92.7-93.9	peltonite 0.9-1.2	peltonite 8.2-8.5
Gravel Pack Interval (m)	7.0-10.1	25.9-28.0	30.8-32.6	68.0-70.7	93.9-96.0	1.2-5.5	8.5-10.1
Screened Interval (m)	7.6-10.1	27.4-28.0	31.7-32.3	69.5-70.1	95.1-95.7	2.4-5.5	9.4-10.1
Slot Size (in. X 10^{-3})	15	20	20	20	20	15	20
Centralizer	yes	yes	yes	yes	yes	no	yes
Washdown valve	no	yes	yes	yes	yes	no	no
Annular Backfill	cuttings	bentonite slurry	bentonite slurry	bentonite slurry	bentonite slurry	cuttings	cuttings
Comments	dry on completion	lose water when washing piezometer	washed in place		backfilled with peltonite & gravel below [illegible]	dry on completion	dry on completion

Piezometer No.	A3 98	A3 233	A3 357	A4 WT	A4 50	A4 64	A4 90
Date Completed	Nov. 17/83	Nov. 18/83	Nov. 19/83	Nov. 2/83	Nov. 1/83	Nov. 2/83	Nov. 8/83
Drilling Method	rotary	rotary	rotary	solid auger	hollow stem auger	hollow stem auger	rotary
Surface Elevation (mamsl)	968.3	968.2	968.2	952.8	952.8	952.7	952.7
Top Casing Elevation (mamsl)	968.984	968.928	969.052	953.558	953.588	953.594	953.474
Meas. Point (m above ground level)	0.70	0.75	0.90	0.80	0.90	0.80	0.80
Total Depth (m)	29.9	71.0	108.8	4.6	15.2	19.5	27.4
Seal Type and Interval (m)	peltonite 27.1-28.0	peltonite 68.3-69.2	peltonite 106.7-107.3	peltonite 0.6-0.9	peltonite 13.4-13.7	peltonite 17.5-18.0	peltonite 25.0-25.6
Gravel Pack Interval (m)	28.0-29.9	69.2-7.10	107.3-108.8	0.9-4.6	13.7-15.2	18.0-19.5	25.6-27.4
Screened Interval (m)	29.3-29.9	70.4-7.10	108.2-108.8	2.1-4.6	14.6-15.2	18.9-19.5	26.8-27.4
Slot Size (in. X 10^{-3})	20	20	20	15	20	20	20
Centralizer	yes	yes	no	yes	no	no	yes
Washdown valve	yes	yes	yes	no	no	no	yes
Annular Backfill	bentonite slurry	bentonite slurry	bentonite slurry	cuttings	cuttings	cuttings	bentonite slurry
Comments	washed in place	washed in place	backfilled with peltonite & gravel below compl. zone	dry on completion	dry on completion		some sloughing, washed in place

Piezometer No.	A4 122	A4 260	A5 WT	A5 61	A5 90	A5 135	A5 297
Date Completed	Nov. 9/83	Nov. 10/83	Oct. 6/83	Nov. 2/83	Nov. 1/83	Nov. 2/83	Nov. 5/83
Drilling Method	rotary	rotary	solid auger	rotary/ auger	rotary/ auger	rotary	rotary
Surface Elevation (mamsl)	952.7	952.7	942.9	942.9	943.0	942.9	943.0
Top Casing Elevation (mamsl)	953.677 953.602*	953.504	943.858	943.971	944.174	943.946	944.016
Meas. Point (m above ground level)	1.0 0.9	0.70	1.0	1.10	1.20	1.10	1.0
Total Depth (m)	37.2	79.2	5.5	18.6	27.4	41.1	90.5
Seal Type and Interval (m)	peltonite 34.4-35.1	peltonite 74.7-76.2	peltonite 0.9-1.2	peltonite 14.5-14.9	peltonite 24.1-25.0	peltonite 37.8-38.4	peltonite 88.1-89.0
Gravel Pack Interval (m)	35.1-37.2	76.2-79.2	1.2-5.5	14.9-18.6	25.0-27.4	38.4-41.1	89.0-90.5
Screened Interval (m)	36.6-37.2	78.6-79.2	3.0-5.5	18.0-18.6	26.8-27.4	40.5-41.1	89.9-90.5
Slot Size (in. X 10^{-3})	20	20	15	20	20	20	20
Centralizer	yes	yes	no	yes	yes	no	yes
Washdown valve	yes	yes	no	yes	yes	yes	yes
Annular Backfill	bentonite slurry	bentonite slurry	cuttings	cuttings & bentonite slurry	bentonite slurry	bentonite slurry	bentonite slurry
Comments	washed in place *new elevation after damage repair	backfilled with peltonite & gravel below completion zone	dry on completion	washed in place completed in auger hole	some sand sloughing; completed in auger hole	washed in place	washed in place

Piezometer No.	A5 343	B1 WT	B1 34	B1 65	B1 176	B1 278	B2 34
Date Completed	Nov. 6/83	Oct. 11/83	Oct. 11/83	Dec. 10/83	Dec. 11/83	Dec. 11/83	Nov 3/83
Drilling Method	rotary	hollow stem auger	solid auger	rotary	rotary	rotary	solid auger
Surface Elevation (mamsl)	943.0	1029.4	1029.4	1029.3	1029.5	1029.7	993.0
Top Casing Elevation (mamsl)	944.000	1030.154	1030.113	1030.081	1030.218	1030.269	993.930
Meas. Point (m above ground level)	1.0	0.75	0.75	0.75	0.70	0.60	0.90
Total Depth (m)	104.5	4.6	10.4	19.8	53.6	84.7	10.4
Seal Type and Interval (m)	peltonite 102.1-103.0	peltonite 0 -1.2	peltonite 8.5-8.8	peltonite 17.4-18.3	peltonite 50.9-51.8	peltonite 80.8-81.7	peltonite 8.5-8.8
Gravel Pack Interval (m)	103.0-104.5	1.2-4.6	8.8-10.1	18.3-19.8	51.8-53.6	81.7-84.7	8.8-10.4
Screened Interval (m)	103.9-104.5	1.5-4.6	9.8-10.4	19.2-19.8	53.0-53.6	84.1-84.7	9.8-10.4
Slot Size (in. X 10^{-3})	20	15	20	20	20	20	20
Centralizer	no	no	yes	yes	yes	yes	yes
Washdown valve	yes	no	no	yes	yes	yes	no
Annular Backfill	bentonite slurry	n.a.	cuttings	bentonite slurry	bentonite slurry	bentonite slurry	cuttings
Comments	backfilled & sealed with peltonite below compl. zone	dry on completion	dry on completion			backfilled with peltonite & gravel below compl. zone	dry on completion

Piezometer No.	B2 50	B2 105	B2 198	B2 320	B3 WT	B3 60	B3 130
Date Completed	Dec. 9/83	Dec. 9/83	Dec. 10/83	Dec. 9/83	Oct. 12/83	Oct. 12/83	Dec 5/83
Drilling Method	rotary	rotary	rotary	rotary	solid auger	hollow stem auger	rotary
Surface Elevation (mamsl)	993.0	993.0	993.0	993.0	994.5	994.6	994.3
Top Casing Elevation (mamsl)	994.068	993.956	993.896	993.884	955.317	955.275	954.897
Meas. Point (m above ground level)	1.10	1.0	0.90	0.90	0.80	0.70	0.50
Total Depth (m)	15.2	32.0	60.3	97.5	5.5	18.3	39.6
Seal Type and Interval (m)	peltonite 13.1-13.7	peltonite 29.6-30.5	peltonite 57.6-58.5	peltonite 94.2-95.1	peltonite 0 -1.2	peltonite 16.8-17.1	peltonite 36.9-38.1
Gravel Pack Interval (m)	13.7-15.2	30.5-32.0	58.5-60.3	95.1-97.5	1.2-5.5	17.1-18.3	38.1-39.9
Screened Interval (m)	14.6-15.2	31.4-32.0	59.7-60.3	96.9-97.5	2.4-5.5	17.7-18.3	39.0-39.6
Slot Size (in. X 10^{-3})	20	20	20	20	15	20	20
Centralizer	yes	yes	yes	yes	no	no	yes
Washdown valve	yes	yes	yes	yes	no	no	yes
Annular Backfill	bentonite slurry	bentonite slurry	bentonite slurry	bentonite slurry	n.a	cuttings	bentonite slurry
Comments					dry on completion	dry on completion	

Piezometer No.	B3 170	B3 198	B3 268	B3 298	B4 WT	B4 29	B4 73
Date Completed	Dec. 6/83	Dec. 6/83	Dec. 7/83	Dec. 7/83	Nov. 3/83	Nov. 3/83	Nov 2/83
Drilling Method	rotary	rotary	rotary	rotary	solid auger	hollow stem auger	hollow stem auger
Surface Elevation (mamsl)	994.5	994.5	994.2	994.3	994.4	994.4	994 4
Top Casing Elevation (mamsl)	955.193	955.168	954.889	955.046	945.093	945.051	945.051
Meas. Point (m above ground level)	0.70	0.70	0.70	0.70	0.70	0.70	0 70
Total Depth (m)	51.8	60.3	81.7	90.8	5.5	8.8	22 2
Seal Type and Interval (m)	peltonite 48.2-49.1	bentonite slurry 58.5 to surface	peltonite 79.2-79.9	peltonite 85.3-86.9	peltonite 1.2-1.5	peltonite 5.8-6.1	peltonite 17 7-18 0
Gravel Pack Interval (m)	49.1-51.8	58.5-60.3	79.9-81.7	86.9-90.8	1.5-5.5	6.1-8.8	18 0-22 2
Screened Interval (m)	51.2-51.8	59.7-60.3	81.1-81.7	90.2-90.8	3.0-5.5	8.2-8.8	21 6-22.2
Slot Size (in. X 10^{-3})	20	20	20	20	15	20	20
Centralizer	yes	yes	yes	yes	no	no	no
Washdown valve	yes	yes	yes	yes	no	no	no
Annular Backfill	bentonite slurry	bentonite slurry	bentonite slurry	bentonite slurry	cuttings	cuttings	cuttings as auger backed out
Comments		slurry used as seal due to boulders		shale trap used below piez. as seal below screen washed in place	dry on completion	seal set above wet sand interval	seal set above sand interval 2.5 m water on completion

Piezometer No.	B5 WT	B5 40	B5 83	B5 118	B5 194	B5 228	B5 265
Date Completed	Oct. 14/83	Oct. 14/83	Oct. 14/83	Dec. 11/83	Dec. 12/83	Dec. 13/83	Dec. 12/83
Drilling Method	solid auger	hollow stem auger	hollow stem auger	rotary	rotary	rotary	rotary
Surface Elevation (mamsl)	934.3	934.4	934.5	934.4	934.8	934.8	934.7
Top Casing Elevation (mamsl)	935.075	935.225	935.285	935.185	935.455	935.535	935.165
Meas. Point (m above ground level)	0.80	0.85	0.80	0.80	0.70	0.75	0.50
Total Depth (m)	4.6	12.2	25.3	36.0	59.1	69.5	82.3
Seal Type and Interval (m)	peltonite 1.2-1.5	peltonite 10.4-10.7	peltonite 23.5-23.8	peltonite 33.2-34.1	peltonite 56.4-57.3	peltonite 66.1-67.1	bentonite slurry 77.7 to surface
Gravel Pack Interval (m)	1.5-4.6	10.7-12.2	23.8-25.3	34.1-36.0	57.3-59.1	67.1-69.5	77.7-82.3
Screened Interval (m)	2.1-4.6	11.6-12.2	24.7-25.3	35.4-36.0	58.5-59.1	68.9-69.5	80.2-80.8
Slot Size (in. X 10^{-3})	15	20	20	20	20	20	20
Centralizer	no	no	no	yes	yes	yes	yes
Washdown valve	no	no	no	yes	yes	yes	yes
Annular Backfill	cuttings	cuttings as auger backed out	cuttings as auger backed out	bentonite slurry	bentonite slurry	bentonite slurry	bentonite slurry
Comments	dry on completion		dry on completion				backfilled with gravel & peltonite below compl. zone

Piezometer No.	B6 WL	B6 50	B6 80	B6 130	B6 230	B6 355	B6 415
Date Completed	Oct. 13/83	Oct. 13/83	Oct. 13/83	Dec. 13/83	Dec. 14/83	Jan. 6/84	Jan. 4/84
Drilling Method	solid auger	hollow stem auger	hollow stem auger	rotary	rotary	rotary	rotary
Surface Elevation (mamsl)	934.5	934.6	934.5	934.3	934.3	934.5	934.4
Top Casing Elevation (mamsl)	935.245	935.295	935.145	935.045	935.015	935.105	935.165
Meas. Point (m above ground level)	0.70	0.70	0.60	0.70	0.75	0.65	0.80
Total Depth (m)	4.9	15.2	24.4	39.6	70.1	108.2	126.8
Seal Type and Interval (m)	peltonite 0.9-1.2	peltonite 13.4-13.7	peltonite 22.9-23.2	peltonite 37.2-38.1	peltonite 66.4-67.1	bentonite slurry to 101.5 to surface	peltonite 122.5-124.0
Gravel Pack Interval (m)	1.2-4.9	13.7-15.2	23.2-24.4	38.1-39.6	67.1-70.1	101.5-108.2	124.0-126.8
Screened Interval (m)	1.8-4.9	14.6-15.2	23.8-24.4	39.0-39.6	69.5-70.1	107.6-108.2	125.9-126.8
Slot Size (in. X 10^{-3})	15	20	20	20	20	20	20
Centralizer	no	no	no	yes	yes	yes	yes
Washdown valve	no	no	no	yes	yes	yes	yes
Annular Backfill	cuttings	cuttings as auger backed out	cuttings as auger backed out	bentonite slurry	bentonite slurry	bentonite slurry	bentonite slurry
Comments	dry on completion	dry on completion			washdown failed; caved hole at 73.1 m	gravel pack entire sand & gravel interval	

Piezometer No.	C1 40	C1 70	C1 125	C1 230	C2 40	C2 66	C2 93
Date Completed	April 2/86	April 12/86	April 11/86	April 11/86	April 13/86	April 13/86	April 12/86
Drilling Method	rotary	rotary	rotary	rotary	rotary	rotary	rotary
Surface Elevation (mamsl)	1015.4	1015.4	1015.5	1015.6	995.8	995.7	995.7
Top Casing Elevation (mamsl)	1015.96	1016.04	1016.11	1016.21	996.38	996.33	996.32
Meas. Point (m above ground level)	0.56	0.54	0.54	0.58	0.54	0.52	0.52
Total Depth (m)	12.2	21.3	38.1	70.1	12.2	20.1	28.4
Seal Type and Interval (m)	peltonite 6.4 - 7.6	peltonite 17.1 - 18.0	peltonite 34.1 - 35.1	peltonite 66.1 - 67.1	peltonite 3.4 - 4.6	peltonite 16.8 - 18.0	peltonite 25.0 - 26.2
Gravel Pack Interval (m)	7.6 - 12.2	18.0 - 21.3	35.1 - 38.1	67.1 - 70.1	4.6 - 12.2	18.0 - 20.1	26.2 - 28.4
Screened Interval (m)	9.1 - 12.2	18.3 - 21.3	37.5 - 38.1	69.5 - 70.1	9.1 - 12.2	18.9 - 19.8	27.1 - 29.1
Slot Size (in. x 10^{-3})	20	20	20	20	20	20	20
Centralizer	yes	yes	yes	yes	yes	yes	yes
Washdown valve	no	no	no	no	no	no	no
Annular Backfill	bentonite	bentonite	bentonite	bentonite	bentonite	bentonite	bentonite
Comments				backfilled to 83.8 m with peltonite and gravel			

Piezometer No.	C2 125	C3 30	C3 76	C3 140	C4 WT	C4 20	C4 36
Date Completed	April 12/86	April 13/86	April 13/86	April 13/86	April 3/86	April 3/86	April 3/86
Drilling Method	rotary	rotary	rotary	rotary	solid auger	solid auger	solid auger
Surface Elevation (mamsl)	995.7	979.4	979.5	979.4	961.4	961.3	961.3
Top Casing Elevation (mamsl)	996.27	980.02	980.09	980.03	962.00	961.94	961.89
Meas. Point (m above ground level)	0.54	0.51	0.62	0.50	0.75	0.65	0.60
Total Depth (m)	38.1	9.1	23.2	42.7	3.7	6.1	11.0
Seal Type and Interval (m)	peltonite 32.3 - 33.5	peltonite 3.4 - 4.6	peltonite 18.6 - 19.8	peltonite 38.4 - 39.6	peltonite 0 - 0.6	peltonite 4.0 - 4.9	peltonite 8.5 - 9.5
Gravel Pack Interval (m)	33.5 - 38.1	4.6 - 9.1	19.8 - 23.2	39.6 - 42.7	0.6 - 3.7	4.9 - 6.1	9.5 - 11.0
Screened Interval (m)	37.5 - 38.1	6.1 - 9.1	20.1 - 23.2	42.1 - 42.7	0.6 - 3.7	5.5 - 6.1	10.4 - 11.0
Slot Size (in. x 10^{-3})	20	20	20	20	20	20	20
Centralizer	yes	yes	yes	yes	no	yes	yes
Washdown valve	yes	no	no	yes	no	no	no
Annular Backfill	bentonite	bentonite	bentonite	bentonite		cuttings	cuttings and peltonite
Comments	backfilled 38.1 to 71.6 peltonite and gravel			backfilled to 59.4 m. with peltonite and gravel			

Piezometer No.	C4 65	C4 100	C5 WT	C5 45	C5 135	C6 WT	C6 50
Date Completed	April 11/86	April 10/86	March 12/86	April 10/86	April 10/86	April 1/86	April 1/86
Drilling Method	rotary	rotary	solid auger	rotary	rotary	solid auger	hollow auger
Surface Elevation (mamsl)	961.1	961.2	960.0	959.9	959.9	956.9	956.9
Top Casing Elevation (mamsl)	961.74	961.80	960.60	960.53	960.50	957.45	957.47
Meas. Point (m above ground level)	0.50	0.62	0.58	0.52	0.58	0.56	0.66
Total Depth (m)	19.8	30.4	6.1	~~13.7~~	44.2	5.5	15.2
Seal Type and Interval (m)	peltonite 15.2 - 16.5	peltonite 23.8 - 25.0	peltonite 0.9 - 1.8	peltonite 8.8 - 10.1	peltonite 37.2 - 38.1	peltonite 0.6 - 1.5	peltonite 12.5 - 13.7
Gravel Pack Interval (m)	16.5 - 19.8	25.0 - 30.5	1.8 - 6.1	10.1 - 13.7	38.1 - 44.2	1.5 - 5.5	13.7 - 15.2
Screened Interval (m)	16.8 - 19.8	27.4 - 30.5	3.1 - 6.1	10.7 - 13.7	40.2 - 44.2	2.4 - 5.5	14.6 - 15.2
Slot Size (in. x 10^{-3})	20	20	20	20	20	20	20
Centralizer	yes	yes	no	yes	yes	no	no
Washdown valve	no	no	no	no	yes	no	no
Annular Backfill	peltonite and gravel	pelt. 19.8-22.6, bentonite and gravel to surface	cuttings	peltonite and gravel	bentonite	cuttings	cuttings, back out augers
Comments		backfilled to 89.9 with peltonite & gravel	backfilled with cuttings and peltonite to 10.7 m				

Piezometer No.	C6 170	2 WT	4 WT	5 WT	5 32	6 WT	6 70
Date Completed	April 9/86	March 11/86	March 11/86	March 12/86	March 12/86	April 2/86	April 14/86
Drilling Method	rotary	solid auger	solid auger	solid auger	hollow auger	solid auger	rotary
Surface Elevation (mamsl)	956.7	976.2	964.5	956.8	956.6	957.9	957.8
Top Casing Elevation (mamsl)	957.29	976.75	965.14	957.38	957.21	958.50	958.38
Meas. Point (m above ground level)	0.65	0.70	0.64	0.68	0.64	0.62	0.57
Total Depth (m)	53.3	5.5	5.5	5.5	9.8	4.6	22.9
Seal Type and Interval (m)	peltonite 46.3 - 47.2	peltonite 0.6 - 1.5	peltonite 0.6 - 1.5	peltonite 0.6 - 1.5	peltonite 7.3 - 7.9	peltonite 0.3 - 1.2	peltonite 7.6 - 9.8
Gravel Pack Interval (m)	47.2 - 53.3	1.5 - 5.5	1.5 - 5.5	1.5 - 5.5	7.9 - 9.8	1.2 - 4.6	pitgravel/ natural 9.8 - 22.9
Screened Interval (m)	51.2 - 51.8	2.4 - 5.5	2.4 - 5.5	2.4 - 5.5	9.1 - 9.8	1.5 - 4.6	19.8 - 20.4
Slot Size (in. x 10^{-3})	20	20	20	20	20	20	20
Centralizer	yes	no	no	no	no	no	yes
Washdown valve	yes	no	no	no	no	no	no
Annular Backfill	bentonite	cuttings	cuttings	cuttings	cuttings, back out augers	cuttings	bentonite

Piezometer No.	7 WT	8 WT	9 WT	9 28	10 WT	11 WT	12 WT
Date Completed	April 1/86	April 1/86	April 1/86	April 1/86	April 2/86	April 2/86	April 2/86
Drilling Method	solid auger	solid auger	solid auger	solid auger	solid auger	solid auger	solid auger
Surface Elevation (mamsl)	951.1	948.0	948.6	948.6	944.9	943.9	942.9
Top Casing Elevation (mamsl)	951.74	948.61	949.18	949.23	945.48	944.46	943.54
Meas. Point (m above ground level)	0.62	0.57	0.58	0.55	0.63	0.62	0.62
Total Depth (m)	6.4	9.1	4.6	8.5	6.1	4.6	4.6
Seal Type and Interval (m)	peltonite 0.9 - 1.8	peltonite 0.9 - 1.8	peltonite 0.6 - 1.5	peltonite 6.7 - 7.3	peltonite 0.9 - 1.8	peltonite 0.6 - 1.5	peltonite 0.3 - 1.2
Gravel Pack Interval (m)	1.8 - 6.4	1.8 - 9.1	1.5 - 4.6	7.3 - 8.5	1.8 - 6.1	1.5 - 4.6	1.2 - 4.6
Screened Interval (m)	3.4 - 6.4	6.1 - 9.1	1.5 - 4.6	7.9 - 8.5	3.1 - 6.1	1.5 - 4.6	1.5 - 4.6
Slot Size (in. x 10^{-3})	20	20	20	20	20	20	20
Centralizer	no	no	no	yes	no	no	no
Washdown valve	no	no	no	no	no	no	no
Annular Backfill	cuttings	cuttings	cuttings	cuttings	cuttings	cuttings	cuttings
Comments					Backfilled to 9.1 m with peltonite and sand		

Piezometer No.	13 WT	14 WT	15 WT	15 24	16 WT	16 85	16-2 WT
Date Completed	April 2/86	April 2/86	April 2/86	April 2/86	April 3/86	April 4/86	April 3/86
Drilling Method	solid auger	solid auger	solid auger	solid auger	solid auger	rotary	solid auger
Surface Elevation (mamsl)	945.4	956.9	963.1	963.2	968.2	968.2	967.6
Top Casing Elevation (mamsl)	946.01	957.48	963.71	963.84	968.83	968.76	968.21
Meas. Point (m above ground level)	0.62	0.57	0.46	0.55	0.62	0.58	0.60
Total Depth (m)	5.5	5.2	3.7	7.3	7.6	25.9	3.7
Seal Type and Interval (m)	peltonite 0.6 - 1.5	peltonite 0.6 - 1.5	peltonite 0 - 0.6	peltonite 4.6 - 5.5	peltonite 2.1 - 3.1	peltonite 23.5 - 24.7	peltonite 1.5 - 2.4
Gravel Pack Interval (m)	1.5 - 5.5	1.5 - 5.2	0.6 - 3.7	5.5 - 7.3	3.1 - 7.6	24.7 - 25.9	2.4 - 3.7
Screened Interval (m)	2.4 - 5.5	2.1 - 5.2	0.6 - 3.7	6.7 - 7.3	4.6 - 7.6	25.3 - 25.9	3.1 - 3.7
Slot Size (in. x 10^{-3})	20	20	20	20	20	20	20
Centralizer	no	no	no	yes	no	yes	no
Washdown valve	no	no	no	no	no	no	no
Annular Backfill	cuttings	cuttings		cuttings and peltonite	cuttings	bentonite	cuttings
Comments	backfilled to 6.7 m with peltonite and sand,					backfilled to 29 m with peltonite and gravel	

Piezometer No.	16-2 38	16-2 72	16-2 135	17 WT	1[illegible]	19 WT
Date Completed	April 14/86	April 14/86	April 14/86	April 3/86	April 3/86	April 3/86
Drilling Method	rotary	rotary	rotary	solid auger	solid auger	solid auger
Surface Elevation (mamsl)	967.6	967.6	967.6	963.3	962.3	963.9
Top Casing Elevation (mamsl)	968.21	968.16	968.17	963.89	962.98	964.49
Meas. Point (m above ground level)	0.57	0.57	0.59	0.62	0.60	0.60
Total Depth (m)	11.6	21.9	41.2	5.6	3.5	3.7
Seal Type and Interval (m)	peltonite 7.9 - 9.1	peltonite 17.1 - 18.3	peltonite 35.4 - 36.6	peltonite 0.3 - 1.2	peltonite 0 - 0.5	peltonite 0 - 0.6
Gravel Pack Interval (m)	9.1 - 11.6	18.3 - 21.9	36.6 - 41.2	1.2 - 4.6	0.5 - 3.5	0.6 - 3.7
Screened Interval (m)	10.4 - 11.6	18.9 - 21.9	37.5 - 40.5	1.5 - 4.6	0.5 - 3.5	0.6 - 3.7
Slot Size (in. x 10^{-3})	20	20	20	20	20	20
Centralizer	yes	yes	yes	no	no	no
Washdown valve	no	no	no	no	no	no
Annular Backfill	bentonite	bentonite	bentonite	cuttings		